The Geochemistry and Geochronology of the Eocene Absaroka Volcanic Province, Northern Wyoming and Southwest Montana, USA

by

Margaret M. Hiza

A THESIS

submitted to

Oregon State University

in partial fulfullment of
the requirements for the
degree of

Doctor of Philosophy

Presented March 30, 1999
Commencement June 2000

AN ABSTRACT OF THE THESIS OF

Margaret M. Hiza, for the degree of Doctor of Philosophy in Geology presented on March 30, 1999. Title: The Geochemistry and Geochronology of the Eocene Absaroka Volcanic Province, Northern Wyoming and Southwest Montana, USA.

Abstract approved: Anita L. Grunder

Anita L. Grunder

The Absaroka volcanic province is the largest of Eocene volcanic fields in the northern Cordillera of the western U.S., and consists of 25,000 km^2 of lava flows, shallow intrusions, ash-flow tuffs and volcaniclastic deposits. It is aligned with northwest-trending Precambrian lineaments, and includes the remains of at least ten volcanic centers. This study presents $^{40}Ar/^{39}Ar$ geochronological data, and major, trace element and isotopic compositional data which are the result of detailed mapping and field sampling of four representative volcanic centers, peripheral lava flows, intrusions, and ash-flow tuffs. Age data show that volcanism occurred between 53 and 43 Ma in a general northwest to southeast age progression, and have allowed significant revisions in regional correlations across the volcanic province. Local dike orientations from one volcanic center suggest that volcanism occurred during extensional faulting. Geochemical and Nd, Sr and Pb isotopic data show that mafic lavas are enriched in incompatible elements derived from an ancient source. Mafic rocks (<53% SiO_2, >5% MgO) are characteristically potassic, and are typical products of early eruptions at each of the Hyalite, Crandall, Ishawooa, and Rampart

volcanic centers, and not spatially restricted to any one region. Although products of volcanism are broadly similar, volcanic centers exhibit distinct mineralogic, compositional and isotopic characteristics. Least squares calculations based on mineralogical data indicate that shoshonites can be produced from mafic samples by fractionation of olivine and augite ± plagioclase. More silicic samples have petrographic features and compositions which indicate they are derived from a mixture of sources including continental crust. Changing chemical and isotopic compositions suggest that early eruptions contain a lithospheric mantle component, with an increasing melt contribution from crustal sources with time. The last eruptions include rhyolite from the southern Absaroka volcanic province and basanite with an asthenospheric isotopic composition sampled from a peripheral lava flow in the northern Absaroka volcanic province.

The Geochemistry and Geochronology of the Eocene Absaroka Volcanic Province, Northern Wyoming and Southwest Montana, USA

by

Margaret M. Hiza

A THESIS

submitted to

Oregon State University

in partial fulfullment of
the requirements for the
degree of

Doctor of Philosophy

Presented March 30, 1999
Commencement June 2000

Doctor of Philosophy thesis of Margaret M. Hiza presented on March 30, 1999

APPROVED:

Anita L. Grunder

Major professor, representing Geology

R. M. Bloomer

Chair of Department of Geosciences

Sally Francis

Dean of Graduate School

I understand that my thesis will become part of the permanant collection of Oregon State University libraries. My signature below authorizes release of my thesis to any reader upon request.

Margaret M. Hiza

Margaret M. Hiza, Author

ACKNOWLEDGMENT

I wish to express my sincere gratitude to several people, all of whom have played a major role in the completion of this thesis, to my thesis advisor, Anita Grunder, who has been both supportive and inspirational, and gave me the opportunity to feel like a member of the human race, to Lawrence Snee, who taught me that I was capable, to John David Love, who always believed in my abilities, to Dave Graham, for his sincere interest in my work and insightful discussions, and to Dan Unruh, who has always treated me as a member of the geological community. A substantial part of my success, however, is also due to my three children, Aidan, Robert, and Shondiin Redsteer, to whom I dedicate this thesis. They not only understood, and let me follow a difficult educational path, but also tolerated my working long nights and days, and became proficient at holding our small family together through it all.

CONTRIBUTION OF AUTHORS

Dr Anita L. Grunder was involved in the organization and editing of each manuscript. Dr Lawrnece Snee assisted in interpretation of $^{40}Ar/^{39}Ar$ data collected in his laboratory, and read and assisted in manuscript editing. Dr Daniel Unruh analyzed samples for Nd Sr and Pb isotopic compositions, and provided valuable discussions on the interpretation of the isotopic data and assited in data interpretation. Dr James Budahn analyzed samples for trace element composition by neutron activation, and assited in geochemical modeling.

TABLE OF CONTENTS

Page

INTRODUCTION
The Geochemistry and Geochronology of the Eocene Absaroka Volcanic Province Northern Wyoming and Southwest Montana, USA 1

CHAPTER 1
Temporal and Geochemical Variability in Eocene Alkaline Volcanism, Absaroka Volcanic Province, Greater Yellowstone: southwest Montana and northwestern Wyoming 4

INTRODUCTION 5

PREVIOUS WORK 7

METHODS 9

AGE RESULTS 11

ASH-FLOW TUFFS 17

Slough Creek Tuff 17
Lost Crrek Tuff 20
Blue Point Ash-Fall 22
Regional Correlations 23

MAJOR ELEMENT CHEMISTRY OF VOLCANIC CENTERS 25

DISCUSSION 28

The Sequence of Eruptions 28
Eruptive Volume 31
Geographic Distribution of Eocene Volcanism 31

CONCLUSIONS 37

REFERENCES CITED-1 39

CHAPTER 2
Mineralogic and Geochemical Variability in Shoshonitic Magmatism from the Type Locality: Absaroka Volcanic Province, Southwest Montana and Northern Wyoming, USA 48

INTRODUCTION 49

ANALYTICAL METHODS 52

TABLE OF CONTENTS (Continued)

Page

GEOLOGY AND MINERALOGY OF VOLCANIC CENTERS 53

The Crandall Volcanic Center 54
The Ishawooa Volcanic Center 55
The Rampart Volcanic Center 56
The Hyalite Volcanic Center 57
Peripheral Lavas 58

COMPOSITION OF VOLCANIC CENTERS 63

Sample compositions from the Crandall Volcanic Center 70
Sample compositions from the Ishawooa Volcanic Center 78
Sample compositions from the Rampart Volcanic Center 80
Sample compositions from the Hyalite Volcanic Center 82
Samples Peripheral to Volcanic Centers 85

MINERAL COMPOSITIONS 87

Olivine 87
Pyroxene 87

DISCUSSION 92

Crandall Volcanic Center 94
Ishawooa Volcanic Center 102
Hyalite Volcanic Center 105
Comparison of Fractionation Paths 105
Source Enrichment 108
Source Mineralogy 108

CONCLUSIONS 114

REFERENCES CITED-2 115

CHAPTER 3
The Petrogenesis of Mafic Potassic Magmas,
Absaroka Volcanic Province, Wyoming-Montana 120

INTRODUCTION 121

GEOLOGIC SETTING 124

Volcanic Centers 124
Samples 125

TABLE OF CONTENTS (Continued)

Page

MAJOR AND TRACE ELEMENT COMPOSTIONS 126

Major Elements 126
Trace Elements 127

ISOTOPIC COMPOSTIONS OF ABSAROKA SAMPLES 133

Nd and Sr Isotopes 133
Pb Isotopes 145

DISCUSSION 150

Mafic Lavas of the Crandall, Ishawooa, Rampart, and Sunlight Volcanic Centers 151
Lavas from the Hyalite Volcanic Center, and Other Intermediate Compositions 153
Enrichment and Metasomatism of Mafic Lavas 157
Mineralogic, Trace Element, and Isotopic Variations with Time 159

CONCLUSIONS 162

REFERENCES CITED-3 164

CHAPTER 4

Synextensional Magmatism of the White Mountain Monzogabbro and its Relationship to Regional Volcanism in the Eocene Absaroka Volcanic Province: Implications for the Heart Mountain Detachment 170

INTRODUCTION 171

FIELD RELATIONSHIPS AT WHITE MOUNTAIN 175

Fault and Intrusion Relationships 175
Evidence for Thermal Effects 177
Interpretation of Field and Petrologic Features 179

REGIONAL FAULT AND DIKE RELATIONSHIPS 182

Observations 182
Interpretation of Dike and Fault Relationships 184

AGE RELATIONSHIPS 185

Observations 185
Interpretation 186

TABLE OF CONTENTS (Continued)

	Page
DISCUSSION	188
CONCLUSIONS	190
REFERENCES CITED-4	191
SUMMARY AND CONCLUSIONS	194
BIBLIOGRAPHY	201
APPENDICES	216

LIST OF FIGURES

Figure		Page
1.1	Distribution of middle Eocene igneous rocks and volcanic fields in the North American Cordillera	6
1.2	Map showing the locations of volcanic centers and the distribution of volcanic rocks assigned to the Washburn, Sunlight, and Thorofare Creek Groups of the Absaroka volcanic province	10
1.3	Schematic map showing distribution of igneous rocks and volcanic centers of the Absaroka volcanic province	16
1.4	Schematic map showing distribution of Slough Creek Tuff, Lost Creek Tuff, and Sepulcher block and ash-flow tuff in northern Yellowstone Park and the Beartooth Wilderness	18
1.5	Graph showing the wt% BaO in feldspar core and rim versus BaO in feldspar rims	21
1.6	Correlation chart showing age relationships of volcanic centers to ash-flow tuffs, lava flows, and formations in the Absaroka volcanic province	24
1.7	Chemical classification and nomenclature for mafic volcanic rocks from the Absaroka volcanic province using subdivisions from the total alkalis versus silica diagram of Le Maitre et al. (1989)	26
1.8	MgO versus K_2O for mafic rocks from individual volcanic centers of the Absaroka volcanic province	26
1.9.	K_2O versus silica for mafic rock samples from the northeastern and southwestern belts of the Absaroka volcanic province	27
1.10	Duration of igneous activity at volcanic centers of the northeastern and southwestern belts of the Absaroka volcanic province	30
1.11	Maps showing distribution of middle Eocene igneous rocks and volcanic fields, direction of age progression in the Absaroka volcanic province, and relative motions of the Kula, Farallon, and Vancouver plates during middle Eocene time	35
2.1	Schematic map showing distribution of igneous rocks and volcanic centers of the Absaroka volcanic province	51
2.2	Photomicrographs of samples from different volcanic centers of the Absaroka province	60

LIST OF FIGURES (continued)

Figure		Page
2.3	Chemical classification and nomenclature for sampled igneous rocks from the Absaroka volcanic province, using subdivisions from the total alkalis versus silica diagram of Le Maitre et al., (1989).....	64
2.4	Harker variation diagrams for sampled igneous rocks from the Absaroka volcanic province.....	71
2.5	Trace elements versus silica variation diagrams for sampled igneous rocks from the Absaroka volcanic province.....	73
2.6	Chondrite normalized trace elements for samples from the Crandall volcanic center.....	75
2.7	La versus Cr for samples from the Crandall volcanic center.....	75
2.8a	$(La/Sm)_N$ versus Sm_N for mafic samples from volcanic centers of the Absaroka volcanic province.....	76
2.8b	$(Gd/Yb)_N$ versus Yb_N for mafic samples from volcanic centers of the Absaroka volcanic province.....	76
2.9.	Chondrite normalized REE, for high Cr, high MgO samples from the Crandall volcanic center.....	77
2.10	Zr versus P_2O_5 for mafic samples from the Absaroka volcanic province.....	77
2.11	Zr/Ta versus K/Rb for for mafic samples from the Absaroka volcanic province.....	78
2.12	Chondrite normalized trace element abundances for selected samples from the Ishawooa volcanic center.....	79
2.13	Chondrite normalized trace elements for samples from the Rampart volcanic center.....	81
2.14	Ce/Yb versus Hf/Ta for samples from the Ishawooa and Rampart volcanic centers.....	81
2.15	Chondrite normalized trace elements for samples from the Hyalite volcanic center.....	83
2.16	Trace element ratios of mafic samples from each of the volcanic centers (<54% SiO2, >4% MgO) showing subdivisions for classification of volcanic rocks by Muller and Groves (1991).....	84
2.17	Chondrite-normalized REE for mafic end-mamber samples from each of the volcanic centers and for sampled basanite.....	86

LIST OF FIGURES (continued)

Figure		Page
2.18a	Al_2O_3 versus TiO_2 for augite phenocrysts from sampled rocks of mafic, intermediate, and silicic compositions from different volcanic centers, and for sampled basanite	89
2.18b	CrO versus MgO for augite phenocrysts from sampled rocks	90
2.18c	Fe_2O_3 versus CaO+MgO for augite phenocrysts	90
2.19	CrO versus MgO for orthopyroxene phenocrysts from shoshonite of the Hyalite volcanic centers, and for a high MgO silicic sample from the Ishawooa volcanic center	91
2.20	La versus SiO_2 for samples from the Crandall volcanic center showing variation allowed by calculated 7% fractionation of augite, olivine, and plagioclase	97
2.21	Chondrite-normalized plot of REE, Sc and Cr (x100), for Crandall volcanic center samples, and source-1 composition calculated partial melts	100
2.22	Chondrite-normalized plot of REE, Sc and Cr (x100), for Crandall volcanic center samples, and source-2 composition calculated partial melts	101
2.23	Compositions from the Ishawooa volcanic center shown with those derived from fractionation calculations	104
2.24	Ba versus Sr for Hyalite volcanic center data	107
2.25	Ba/Sr versus Rb for AFC calculated compositions of sampled basanite assimilating phlogopite, and an average OIB composition assimilating phlogopite	111
3.1	Schematic map showing the Absaroka volcanic province, and sampled volcanic centers	122
3.2	Chemical classification and nomenclature of volcanic rocks showing distribution of sampled rock types from the Absaroka volcanic province	128
3.3a	Cr versus Mg# for samples <55% SiO_2 from the Absaroka volcanic province	129
3.3b	Cr versus Ni for samples <55% SiO_2 from the Absaroka volcanic province	129

LIST OF FIGURES (continued)

Figure		Page
3.4	Chondrite-normalized trace elements for mafic samples (<%55% SiO2) showing wt% MgO for each.....	131
3.5	K/Rb versus Ba/Rb for mafic samples from the Crandall, Sunlight, Rampart, Ishawooa and Hyalite volcanic centers monzogabbro from the vicinity of the Sunlight volcanic center, and a peripheral basanite flow.....	131
3.6	Rb/Sr versus Ba/Rb for samples from the Crandall, Sunlight, Rampart, Ishawooa and Hyalite volcanic centers, monzogabbro from the vicinity of the Sunlight volcanic center, and a peripheral basanite flow.....	132
3.7	Th/U versus Th/La for samples from the Crandall, Sunlight, Rampart, Ishawooa and Hyalite volcanic centers.....	132
3.8a	$^{143}Nd/^{144}Nd$ versus $^{87}Sr/^{86}Sr$ for samples from the Crandall, Ishawooa, Rampart, and Hyalite volcanic centers of the Absaroka volcanic province.....	139
3.8b	$^{143}Nd/^{144}Nd$ versus $^{87}Sr/^{86}Sr$ for samples from the Absaroka volcanic provinceand compostional fields for selected mafic alkalic and crustal rocks of the Wyoming Province.....	140
3.9	Th/U versus $^{87}Sr/^{86}Sr$ for samples from the Absaroka volcanic province.....	141
3.10	$^{87}Sr/^{86}Sr$ versus SiO2 for samples from the Absaroka volcanic province.....	142
3.11	$^{87}Sr/^{86}Sr$ versus 1/Sr for samples from the Absaroka volcanic province.....	142
3.12	$^{87}Sr/^{86}Sr$ versus Rb for samples from the Absaroka volcanic province.....	143
3.13a	$^{143}Nd/^{144}Nd$ versus 1/Nd for samples from the Absaroka volcanic province.....	144
3.13b	$^{143}Nd/^{144}Nd$ versus Sm/Nd for samples from the Absaroka volcanic province.....	144
3.14a	$^{207}Pb/^{204}Pb$ versus $^{206}Pb/^{204}Pb$, of samples from the Crandall, Ishawooa, Rampart, and Hyalite volcanic centers, and shoshonite and rhyolite of the Absaroka volcanic province.....	147

LIST OF FIGURES (continued)

Figure		Page
3.14b	$^{208}Pb/^{204}Pb$ versus $^{206}Pb/^{204}Pb$, of samples from the Crandall, Ishawooa, Rampart, and Hyalite volcanic centers, and shoshonite and rhyolite of the Absaroka volcanic province.....	148
3.15a	$^{87}Sr/^{86}Sr$ versus age for samples from the Absaroka volcanic province.....	149
3.15b	$^{143}Nd/^{144}Nd$ versus age for samples from the Absaroka volcanic province.....	149
3.15c	Th/U versus age for samples from the Absaroka volcanic province.....	150
3.16	Trace elements for mafic samples from volcanic centers normalized to estimated mafic granulite lower crust.....	155
3.17	Schematic diagram showing changing depth of melt sources with time....	161
4.1	Generalized geologic map of the northeastern Absaroka Range, including the northern Heart Mountain fault area, Crandall volcanic center, and Sunlight volcanic center.....	172
4.2	Stratigraphic column showing formations exposed in map area of Figure 4.1, and general location of detachment horizon.....	173
4.3	Idealized sketch of White Mountain, showing rotated and deformed early shoshonite dikes, sheared monzogabbro, late cross-cutting vertical dikes, and extent of exposure of the detachment horizon and cataclastic breccia.....	176
4.4	Photomicrograph of White Mountain monzogabbro.	177
4.5	Photomicrographs showing breccia within the detachment horizon.....	178
4.5	Proposed sequence of deformation and intrusion at White Mountain, based on interpretation of field and lithologic relationships.....	181
4.6	Orientation of faults and dikes of the northeastern Absaroka volcanic province, above and below the Heart Mountain detachment	183
4.7	Schematic diagram showing differential extension, rotation and orientation of faults and dikes adjacent to the southern edge of the Beartooth Plateau.....	185
4.8	$^{40}Ar/^{39}Ar$ age spectra for samples from the northeastern Absaroka volcanic province.....	187

LIST OF APPENDICES

Page

Appendix A - $^{40}Ar/^{39}Ar$ Data Table 217

Appendix B 222
$^{40}Ar/^{39}Ar$ age spectra for samples
from the Absaroka volcanic province 222
$^{40}Ar/^{36}Ar$ versus $^{40}Ar/^{36}Ar$ linear isochrons for selected age data 228

Appendix C - Electron microprobe analyses of feldspar compositions
from ash-flow tuffs 230

Appendix D - Petrographic description of analyzed samples 233

Hyalite Volcanic Center Samples 233
Ishawooa Volcanic Center Samples 234
Rampart Volcanic Center Samples 235
Crandall Volcanic Center Samples 236

Appendix E - Pyroxene compositions electron microprobe analyses 238

Appendix F - AFC Calculations 240

Basanite and Phlogopite 240
OIB and Phlogopite 241
Basanite and Lower Crustal Xenolith 242

Appendix G - Equations used in calculations 243

The Geochemistry and Geochronology of the Eocene Absaroka Volcanic Province Northern Wyoming and Southwest Montana, USA

INTRODUCTION

The Eocene Absaroka volcanic province is an enigmatic province for two reasons: 1) it is the type locality for highly alkaline rocks of the absarokite-shoshonite-banakite series, for which the processes of formation and sources are not well understood; and 2) it is part of a group of calc-alkaline and alkaline volcanic fields for which the tectonic setting has long been a puzzle. The 25,000 km^2 Absaroka volcanic province is the largest of middle Eocene volcanic fields in the northern Cordillera, which are distributed in a broad diffuse belt from Oregon northward into Canada, and eastward to the Black Hills of South Dakota. Because of the association of calc-alkaline and alkaline rock types with subduction, popular tectonic reconstructions of the northern Cordillera have modeled these volcanic fields as the product of subduction-related magmatism (Armstrong, 1988; Armstrong and Ward, 1991). However, the extreme distance of the Absaroka volcanic province and adjacent volcanic fields from the nearest possible subduction zone to the west ($\geq$ 1500 km) requires extreme processes to allow a subduction driven origin for these igneous rocks. Examination of the tectonic setting and source of magmatism for the Absaroka volcanic province is the goal of this study.

Within the Absaroka volcanic province are the remains of at least ten well-preserved volcanic centers, which have been dissected by subsequent glacial erosion. Chadwick (1970) assigned volcanic centers in the Absaroka volcanic province to two subparallel northwest-trending belts, a younger southwestern calc-alkaline, and an older northeastern alkaline belt, postulated to represent petrologic zonation of a subduction-related volcanic arc. The Hyalite and Crandall volcanic centers from the northeastern volcanic belt, and the Ishawooa and Rampart volcanic centers from the southwestern volcanic belt were chosen for detailed study. These volcanic centers

also represent the regional map units of the Washburn, Sunlight and Thorofare Creek Groups, respectively. Samples peripheral to volcanic centers are also included in order to represent the entire compositional spectrum of rock types within the province. In addition, the selection of volcanic centers was made based upon availability of fresh samples, which is critical to the preservation of original alkali content. The Crandall, Rampart, Ishawooa, and Hyalite volcanic centers lack mineralization which occurs elsewhere, especially in the South Fork, Kirwin, and Sunlight volcanic centers, and in the New World-Cooke City area (Hausel, 1982).

In order to reconstruct the tectonic setting, it is necessary to establish the ages of the volcanic centers and province-wide age relationships, and to compare these regionally to other Eocene volcanic fields (Chapter 1). To examine how and why magmatism evolved in the Absaroka volcanic province, the goals of my work have been to study individual volcanic centers and identify local igneous processes at each of them, and to compare these volcanic centers regionally. This includes an examination of field relationships and rocks types, and a detailed study of mineralogy and composition at each of the volcanic centers (Chapter 2). These chapters are in the form of manuscripts to be submitted for publication.

The first chapter is a comprehensive study of the age of the rocks within the Absaroka volcanic province. This work includes $^{40}Ar/^{39}Ar$ geochronology of selected ash-flow tuffs and intrusions from individual volcanic centers. These new data are combined with published paleomagnetic and $^{40}Ar/^{39}Ar$ dates to define province-wide age-relationships and to correlate of regional ash-flow tuff units and unconformities. These data provide a comprehensive understanding of the duration of volcanic activity at each volcanic center, as well as province-wide relationships. Both types of constraints provide insight on changing eruption style, dynamics and composition.

Defining the potential sources of enrichment for this unusual suite of rocks has important implications for the world-wide occurrence of shoshonitic rock types. Therefore, this study outlines the igneous processes and evaluates potential crust and mantle contributions to the magma source (Chapter 3). The sources of distinct trace element enrichment for each of the volcanic centers are defined through examination

of Nd, Sr and Pb isotopes. Characterization of the age and type of source enrichment, combined with an age comparison of changing sources with time are used to evaluate how, and in what type of tectonic setting, melting was generated.

Another important aspect to evaluating the tectonic setting is the documentation of field relationships between local structural features and volcanic deposits. Field relationships in the vicinity of the Crandall volcanic center include fault and dike orientations which are combined with geochronological data in order to outline the relationship and timing of volcanism to the structural setting (Chapter 4).

CHAPTER 1

Temporal and Geochemical Variability in Eocene Alkaline Volcanism, Absaroka Volcanic Province, Greater Yellowstone: Southwest Montana and Northwestern Wyoming

Margaret M. Hiza, Anita L. Grunder, and Lawrence W. Snee

To be submitted to the *Geological Society of America Bulletin*, Boulder Colorado
43 pages

INTRODUCTION

Broadly scattered Eocene volcanic fields and associated plutonic rocks exist throughout the Cordillera of western North America, from Wyoming, to Oregon (Figure 1.1). The 53 to 43 Ma Absaroka volcanic province of southwest Montana and northwest Wyoming is the largest of these middle Eocene volcanic fields, consisting of 25,000 km^2 (9,000 mi^2) of shallow intrusions, lava flows, ash-flow tuffs, and volcaniclastic deposits. Previous workers have subdivided the Absaroka province into the alkaline and calc-alkaline Washburn Group, the mafic potassic Sunlight Group, and the more silicic calc-alkaline Thorofare Creek Group (Smedes and Prostka, 1972). A northwest to southeast age progression within the Absaroka volcanic province, coincident with a shift from calc-alkaline to alkaline volcanism has often been cited as evidence of Andean-style flat-slab subduction (Baker, 1987; Chadwick, 1981; Lipman, 1980; Dickinson 1979; Hamilton, 1969). A north to south age progression within the province is evident, but refined based on new $^{40}Ar/^{39}Ar$ analyses of mineral separates from sampled volcanic centers and province-wide correlation of ash-flow tuffs. In light of new data presented herein, we demonstrate that the previously defined compositional distribution of alkaline igneous rocks does not bear up. Consequently, the tectonic interpretation warrants re-examination.

Although popular models link calc-alkaline magmatism to subduction, a growing number of isotopic and trace element geochemical studies in the Cordillera have rejected the flat-slab subduction model as a mechanism for producing middle Eocene magmatism (Morris and Hooper, 1997; Hooper et. al., 1995; Carlson and others, 1991; Dudas, 1991; Norman and Mertzman, 1991; Hooper et. al., 1990; Holder and Holder, 1988). In addition, the formation of arc-like magmas under extensional conditions has been acclaimed by numerous recent studies in the Basin and Range province (Christiansen, 1989; Gans et al., 1989.; Smith et al., 1990; Best and Christiansen, 1991; Feeley and Grunder, 1991; Davis and Hawkesworth, 1994).

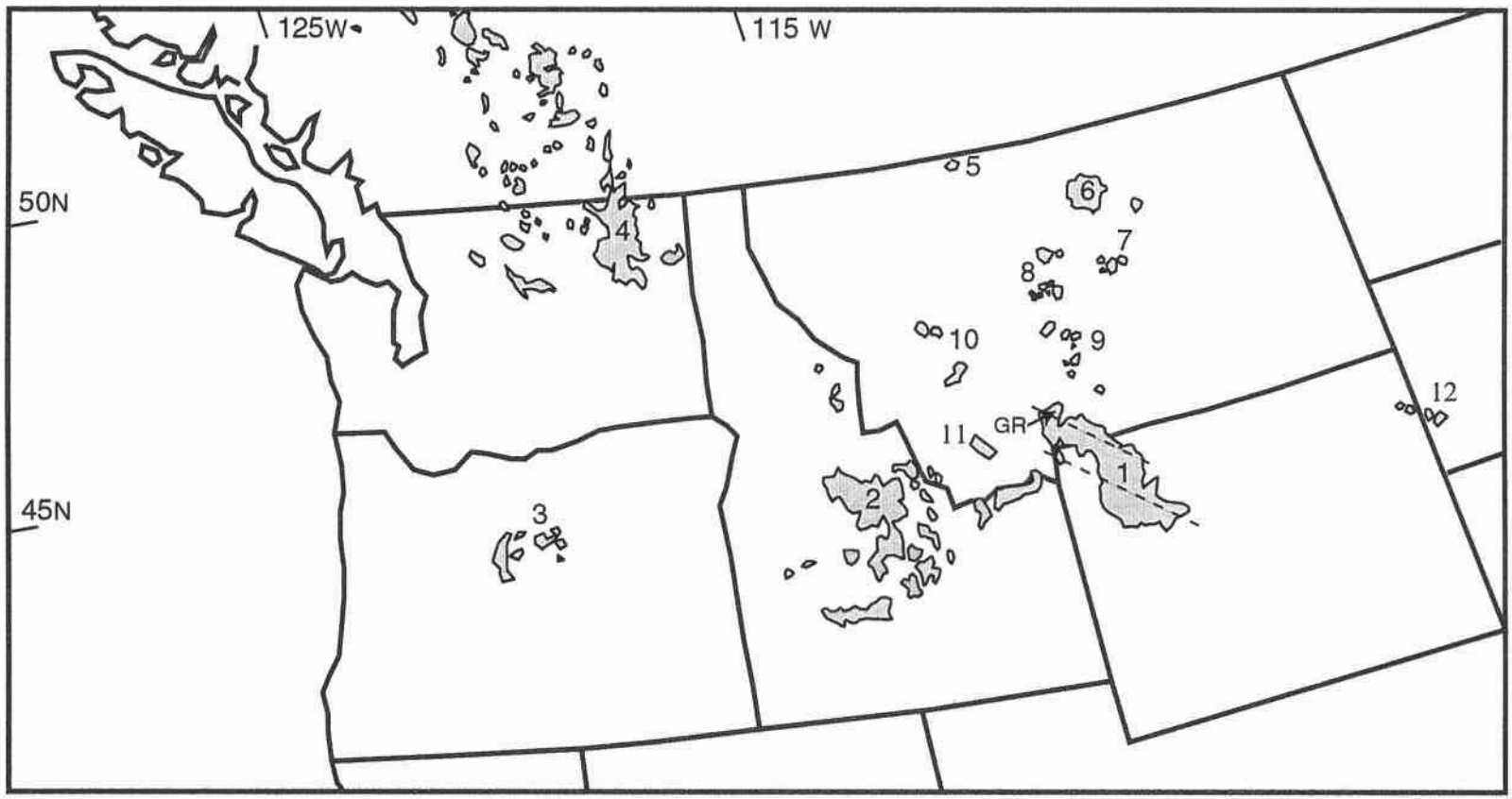

Figure 1.1. Distribution of middle Eocene igneous rocks and volcanic fields in the North American Cordillera, showing location of the 1) Absaroka volcanic province, 2) Challis volcanic field, 3) Clarno volcanic field 4) Colville igneous complex, 5) Sweet Grass Hills, 6) Bearpaw Mountains 7) Missouri Breaks diatremes, 8) Highwood and Castle Mountains, 9) Crazy Mountains, 10) Garnet Range and Lowland Creek volcanic field 11) Pioneer Mountains 12) Devils Tower and Black Hills. GR-denotes location of Gallatin Range, Montana. (Modified after Chadwick, 1972, 1985; and Snoke, 1993)

The largest volcanic field associated with this puzzling episode of middle Eocene magmatism is the Absaroka volcanic province. Previous to this study, most of the province had not been investigated by modern analytical methods. In this paper, we summarize the major-element characteristics of mafic rocks from individual volcanic centers, and revise the stratigraphy of the Absaroka volcanic province with new $^{40}Ar/^{39}Ar$ age data, and improve stratigraphic relationships based on the correlation of three major ash-flow tuffs. Mafic (<55% SiO_2) potassic volcanism occurred early at each of the volcanic centers, was especially voluminous early in the history of the province, and has no spatial trend in the province as a whole.

PREVIOUS WORK

The first description of igneous rocks from the Absaroka volcanic province was by Joseph P. Iddings (1895, 1899) as part of a regional study of Yellowstone National Park. This historic study describes the occurrence of potassic igneous rocks which he classified as the absarokite-shoshonite-banakite series. He noted that rocks of the region exhibited mineralogical and geochemical diversity, and that this "peculiar" series was found together with "normal" basalts and andesites. He also noted that rocks within Yellowstone were similar in composition and mineralogy to those of the northern Gallatin Range described by George Merrill (1895). Subsequent studies have consisted primarily of mapping and petrologic work in separate parts of the southern Absaroka volcanic province, most notably by Love (1939), Wilson (1960), Dunrud (1962), Fisher (1966), Sundell (1980), Barnes (1985), and in parts of the northern Absaroka province by Shultz (1962), Rubel (1971), Wedow et al. (1975), Pierce (1978), Simons et al. (1979), and Hickenlooper and Gutman (1982). Among work conducted in the northern part of the Absaroka province, mapping, petrologic, and geochemical studies were done by Chadwick (1968a, 1969, 1970, 1981, 1985) who observed that volcanic centers within the province are aligned as belts along two northwest-southeast- trending subparallel Precambrian lineaments (Figure 1.1). He proposed the addition of igneous rocks in

the northern Gallatin Range to the Absaroka volcanic province, as an extension of volcanic centers located along the northeastern lineament. Chadwick (1972, 1981) also suggested that these belts of volcanic centers exhibit arc-like geochemical affinities with calc-alkaline rocks located in the southwestern belt, and potassic alkaline rocks found within the northeastern belt.

Additional modern petrologic and geochemical studies include work by Nicholls and Carmichael (1969), and Geist and McBirney (1979) who debated derivation of the absarokite-shoshonite-banakite series by fractionation. These studies provide whole rock and microprobe analyses of regional samples. Isotopic data from samples of the Absaroka volcanic province are limited, and from widely scattered outcrops of variable composition (Peterman et al., 1970). Work on the Independence volcano by Meen (1987, 1988, 1990), and Meen and Eggler (1987) includes major, trace element, isotopic analyses, and experimental work on samples from a single volcanic center within the northwestern belt of Absaroka province. $^{40}Ar/^{39}Ar$ data from this volcanic center by Harlan and Snee (1996) give ages from 51.57 ± 0.14 Ma to 48.50 ± 0.12 Ma, indicating that Independence volcano is middle Eocene in age.

K/Ar age data from twelve mineral separates at seven sample localities from Rohrer and Obradovich (1969) and Smedes and Prostka (1972) range from 44.4 ± 1.4 Ma to 49.3 ± 1.4 Ma, and establish a middle Eocene age for volcanism in the remainder of the Absaroka volcanic province. This work subdivided the province into the calc-alkaline Washburn Group, the mafic alkaline Sunlight Group, and the intermediate to silicic Thorofare Creek Group. Stratigraphic work and lithologic descriptions by Smedes and Prostka (1972) and Sundell (1993) characterize deposits within the Absaroka volcanic province as dominantly consisting of calc-alkaline andesites and related epiclastic sediments. In this study, we find that diverse rock types are common, and encompass the entire compositional spectrum, from basanite to rhyolite. Large, well-preserved volcanic centers are exposed in a dissected terrain of considerable relief, and are defined by radially and structurally influenced dike swarms which surround central hypabyssal plutons. Mafic to felsic end-member rock types are often associated with a single volcanic center.

METHODS

Samples in this study were selected to encompass the geochemical and temporal trends across the entire Absaroka volcanic province. This study is based on detailed mapping at individual volcanic centers, namely the Hyalite, Crandall, and Ishawooa and Rampart volcanic centers, which were chosen to represent regional map units of the Washburn, Sunlight and Thorofare Creek Groups, respectively (Figure 1.2). These volcanic centers lack alteration, which is important for the preservation and comparison of alkali compositions. Additionally, the Kirwin volcanic center of the Thorofare Creek Group, and peripheral lava flows were sampled to give a more complete comparison of rock types from the northeast and southwest belts of the province. Samples of regionally extensive ash-flow tuffs are also included in order to link temporal and geochemical relationships of individual volcanic centers to the eruptive history of the entire volcanic field.

Province-wide age relationships are based on ash-flow tuff correlations, new $^{40}Ar/^{39}Ar$ and field data, and age and paleomagnetic data from the literature. Ash-flow tuff samples were analyzed by Cameca SX50 electron microprobe, at Oregon State University, in order to compare mineralogic composition of samples with altered glass. Composition of whole rock powders for other samples were obtained by X-ray fluorescence at the analytical laboratories of the U.S. Geological Survey in Denver, Colorado. New samples analyzed for this study are compared to published analytical data from Iddings (1895) from the Ishawooa and Crandall volcanic centers, Nicholls and Carmichael (1962) from northeast and southeast Yellowstone Park, Nelson and Pierce (1968) from the Sunlight and Rampart volcanic center, and Rubel (1971) and Meen (1987), from the Independence volcanic center.

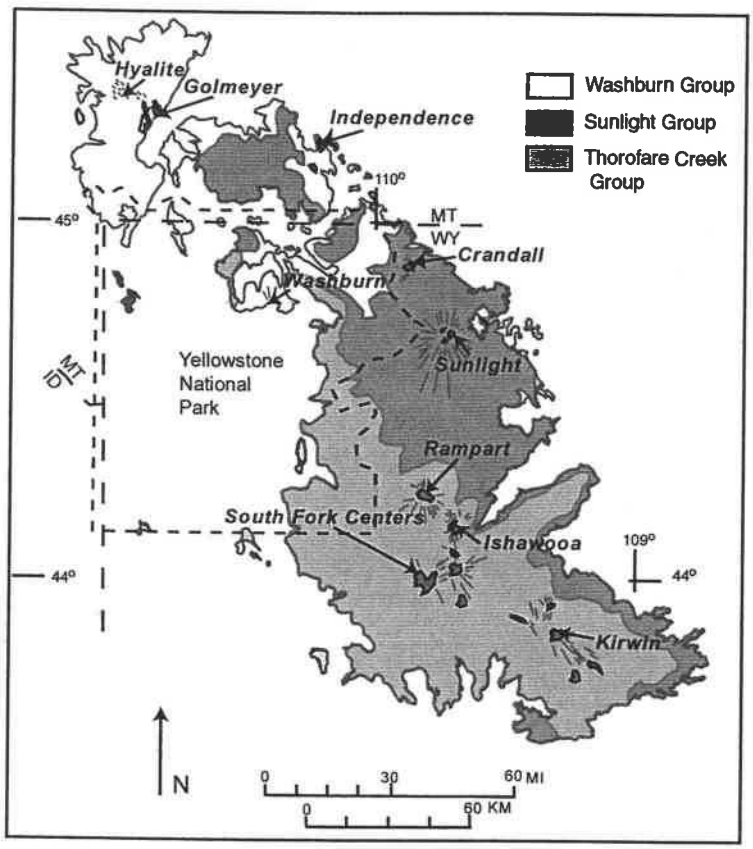

Figure 1.2 Map showing the locations of volcanic centers and the distribution of volcanic rocks assigned to the Washburn, Sunlight, and Thorofare Creek Groups of the Absaroka volcanic province. (Modified from Smedes and Prostka, 1972).

New $^{40}Ar/^{39}Ar$ data are from mineral separates prepared from twenty-one sample localities (Table 1.1). Samples were crushed and sieved to 40-100 mesh size, and rinsed free of dust. Sanidine, biotite, and hornblende were separated by heavy liquids, magnetic separator, and hand picked to greater than 99% purity. Minerals were cleaned with reagent grade acetone and deionized water in an ultrasonic bath, then oven-dried. Clean mineral separates were weighed, wrapped in aluminum foil capsules, and sealed in silica vials with neutron fluence monitors prior to irradiation. Monitors of both Fish Canyon Tuff sanidine with an age of 27.84 Ma ± 1.0 Ma, and Minnesota hornblende (MMhb-1) with a K-Ar age of 520.4 ± 1.7 Ma were used to calculate *J*-values for the analyses (Samson and Alexander, 1987). Sample separates and monitors were irradiated in the TRIGA reactor at the U.S. Geological Survey in Denver, Colorado. Each sample was heated in a double

vacuum low-blank resistance furnace for 20 minutes, in a series of 10 to 15 steps, to a maximum temperature of 1450°C, and analyzed using the standard stepwise heating technique described by Snee (1982). All samples were analyzed in the Argon Laboratory, U.S. Geological Survey in Denver, Colorado using a Mass Analyzer Products 215 rare gas mass spectrometer with a Faraday cup. Five isotopes of argon were measured at each temperature step. The detection limit at the time the measurements were made was 3.5×10^{-17} moles Ar. Abundances of "Radiogenic ^{40}Ar and "K-derived ^{39}Ar" are measured in volts, with a conversion to moles made using 1.160×10^{-12} moles argon per volt signal. Apparent ages were calculated using decay constants of Steiger and Jager (1977). Mass discrimination was determined by measuring a $^{40}Ar/^{36}Ar$ ratio of 298.9 for atmospheric argon during the analyses. Abundances of interfering isotopes of argon from K and Ca were calculated from reactor production ratios, determined by irradiating CaF_2 and K_2SO_4 simultaneously with these samples.

AGE RESULTS

$^{40}Ar/^{39}Ar$ dates from volcanic and intrusive rocks of the Absaroka volcanic province yield apparent ages from 53.64 ± 0.3 to 43.68 ± 0.09 Ma (Table 1.1). $^{40}Ar/^{39}Ar$ data include fifteen plateau ages which consist of three or more contiguous temperature steps whose apparent ages overlap within analytical uncertainty (Appendix A). Errors given for individual analyses are estimates of the analytical precision at the 1-sigma (67%) confidence level. These plateau ages span from 50.01 ± 0.14 Ma to 44.84 ± 0.08 Ma. The data also include one "near-plateau age" that does not fit the strict definition of a plateau, which requires that more than 50% of cumulate $^{39}Ar_K$ be released during plateau temperature steps (Dalrymple and Lanphere, 1969; Fleck et al., 1977; McGrew and Snee, 1994). This sample is a sanidine separate from rhyolite (AR76-121) sampled at the southern margin of the Absaroka volcanic province. It has an isochron age of 44.08 ± 0.14 Ma and total gas age of 44.13 ± 0.24 which are both within analytical uncertainty at the 2-sigma

confidence level of the "near-plateau" age of 43.68 ± 0.18 Ma (Appendix A). This sample has the youngest age reported from the Absaroka volcanic province.

Additional age data presented here are from four mineral separates which produced complicated age spectra. These samples are from dacite and andesite of the Sepulcher Formation and Golmeyer Creek Volcanics of the northern Absaroka volcanic province, with apparent ages from 51.56 ± 0.20 to 53.64 ±0.30 Ma, and from a shallow dacite intrusion on Mt. Burwell, in the southeastern Absaroka volcanic province, with an apparent age of 44.82 ± 0.85 Ma. Ages reported from these samples are based on isochrons derived from linear regression of $^{40}Ar/^{36}Ar$ and $^{39}Ar/^{36}Ar$ of individual temperature steps. Biotite separates from dacite ash-flow tuff (YRL1-93), and andesite dike (PR2-93), and hornblende from dacite (AR76-120) have $^{40}Ar/^{36}Ar_i$ >300 (initial values derived from linear regression). Because $^{40}Ar/^{36}Ar_i$ for these samples are higher than measured values for atmospheric Ar, these reported ages represent maximum estimates resulting from excess Ar (Appendix A). Samples with well-defined plateaus have straight line regressions with an $^{40}Ar/^{36}Ar$ intercept equal to the atmospheric ratio (for examples see Appendix B).

New data and fieldwork from this study corroborate field work and analytical data from previous workers that show the oldest intrusions and related volcanic deposits occur in the northern Absaroka volcanic province, and the youngest volcanism, which is primarily silicic, occurs in the south (Smedes and Prostka, 1972; Love, 1972). A northwest to southeast decrease in $^{40}Ar/^{39}Ar$ ages is exhibited separately in both the northeast and southwest belts of volcanic centers and related intrusions (Figure 1.3). Biotite from a shallow intrusion on Greys Peak in the southern Gallatin Range has a plateau age of 50.00 ± 0.09 Ma, which establishes a middle Eocene age for these igneous and volcanic rocks, located at the northern end of the southwestern volcanic belt. $^{40}Ar/^{39}Ar$ age data indicate that ash-flow tuffs also exhibit a north to south age progression from 49.62 ± 0.08 to 46.97 ± 0.09 Ma. Two ash-flow tuffs with identical ages, were previously assigned as members of formations from separate established groups (Smedes and Prostka, 1972). Total gas ages from the Pacific Creek Tuff (biotite) and Lost Creek Tuff (sanidine) are 48.81 ± 0.17 Ma and 48.81 ± 0.13 Ma, respectively. Plateau ages for these samples of

48.89 ± 0.12 and 48.78 ± 0.08 Ma, from simple age spectra, are also remarkably similar, and identical within 1-sigma analytical uncertainty. A feldspar separate from an ash-fall sampled on Two-Ocean Plateau in southern Yellowstone National Park has a "near plateau" age of 47.8 ±0.07 Ma. Similarly, a hornblende separate of the Blue Point ash-fall, sampled at Irish Rock in the southern Absaroka volcanic province, yielded a plateau age of 47.7 ± 0.10 Ma. 98.7 % $^{39}Ar_K$ is included in the plateau temperature steps for this sample, making this age a precise estimate for a locality which is known for the preserved remains of vertebrate Eocene fauna (Bown, 1982a). The ages of mineral separates from the ash-fall sampled from southern Yellowstone Park and Irish rock are identical, within 1-sigma analytical uncertainty. Sanidine from rhyolite ash-flow tuff sampled at Pinnacle Buttes, another well- known fossil locality at the southern margin of the Absaroka province, yielded a plateau age of 46.97 ± 0.09 Ma.

$^{40}Ar/^{39}Ar$ age data from the Crandall volcanic center are from a trachyte ash-flow tuff which overlies shoshonitic flows sampled at this volcanic center. Biotite from this sample yields a plateau age of 50.01 ± 0.14, giving a minimum estimate for the age of eruptive activity at the Crandall volcanic center. Hornblende from a cross-cutting shallow latite intrusion gives an age of 49.12 ± 0.09 Ma. These ages indicate that potassic lavas erupted very early in the history of the Absaroka volcanic province. Biotite from a banakite dike sampled on Ishawooa Mesa yields a plateau age of 46.75 ± 0.11 Ma. This dike cross-cuts flows of absarokite and shoshonite from the Ishawooa volcanic center, and gives a minimum age estimate for eruptive activity at this volcanic center. Similarly, biotite from a shallow banakite intrusion at the Rampart volcanic center yields a plateau age of 46.55 ± 0.11 Ma. Although neither of these ages provide a maximum age for eruptive activity, lava flows at Ishawooa Mesa overlie avalanche deposits which have been correlated to the Sunlight volcanic center by Malone (1997). These deposits have been interpreted as predating fault movement of the Heart Mountain detachment (Malone, 1997). Biotite sampled from a monzogabbro intrusion in the vicinity of the Sunlight volcanic center is deformed by the Heart Mountain detachment faulting, and yields a plateau age of 48.21 ± 0.10 Ma (Chapter 4). This age indirectly provides a minimum estimate for the age of avalanche deposits. This constrains the age of mafic lava flows from the Ishawooa volcanic center, which overlie avalanche deposits, from 48.2 to 46.6 Ma.

Table 1.1. Summary of $^{40}Ar/^{39}Ar$ analyses and apparent ages used for stratigraphic revisions of the Absaroka Volcanic Province.

Area	Sample no.	Rock type	Mineral	Age (Ma) and error	Character of age spectrum
NW YNP *Sepulcher Mtn*	YRL1-93	dacite block and ash-flow	biotite	53.36±0.3	Preferred date for disturbed spectrum, excess Ar, maximum estimate
NW YNP *Bighorn Peak*	YGDC1-96	dacite	hornblende	53.64±0.3	Preferred date for disturbed spectrum, , maximum estimate
N AVP *Golmeyer Cr Volcanics*	PR2-93	andesite dike	biotite	51.56±0.2	Preferred date for disturbed spectrum, excess Ar, maximum estimate
N YNP *Slough Cr.*	YSC-5-95	rhyolite ash-flow tuff	sanidine	49.62±0.08	Plateau date; 60.7% $^{39}Ar_K$
N YNP *Slough Cr.*	YSC-3-95	rhyolite ash-flow tuff	biotite	49.79±0.1	Preferred date for disturbed spectrum, excess Ar, maximum estimate
NW YNP *S Gallatin R.*	YFP7-93	dacite, shallow intr.	biotite	50.00±0.09	Plateau date; 51.3% $^{39}Ar_K$
N YNP *Lost Cr.*	P-348	rhyodacite ash-flow tuff	sanidine	48.78±0.08	Plateau date; 71.8% $^{39}Ar_K$
E YNP *Pacific Cr.*	P-306	rhyodacite ash-flow tuff	biotite	48.89±0.12	Plateau date; 55.8% $^{39}Ar_K$
SE YNP *Two Ocean*	3497	Blue Pt. ash-flow tuff	feldspar	47.8±0.07	Plateau date; 46.8% $^{39}Ar_K$
SE AVP *Irish Rock*	68-0-51	Blue Pt. ash-flow tuff	hornblende	47.7±0.1	Plateau date; 94.9% $^{39}Ar_K$
NE AVP Crandall	HHM17B-95	trachyte ash-flow tuff	biotite	50.01±0.14	Plateau date; 80.6% $^{39}Ar_K$
NE AVP *Crandall*	HM1-94	banakite, shallow intr.	hornblende	49.12±0.09	Plateau date; 76.6% $^{39}Ar_K$
NE AVP *Sunlight*	HMD4-96	monzogabbro shallow intr.	biotite	48.21±0.08	Plateau date; 64.8% $^{39}Ar_K$
NE AVP *Sunlight*	HMD4-96	monzogabbro shallow intr.	hornblende	48.8±0.1	Preferred date for disturbed spectrum, excess Ar, maximum estimate
S AVP *Ishawooa*	71-0-4	banakite dike	biotite	46.75±0.11	Plateau date; 90.2% $^{39}Ar_K$
S AVP *Rampart*	AR77-184	banakite intr.	biotite	46.55±0.11	Plateau date; 98.7% $^{39}Ar_K$
S AVP Pinnacle B.	70-0-13	rhyolite Ash-flow tuff	sanidine	46.97±0.09	Plateau date; 63.3% $^{39}Ar_K$
SE AVP *Mt Burwell (Kirwin)*	AR76-120	dacite shallow intr.	hornblende	44.82±0.85	Preferred date for disturbed spectrum, excess Ar, maximum estimate
SE AVP	AR76-115	dacite shallow intr.	biotite	44.84±0.08	Plateau date; 74.4% $^{39}Ar_K$
SE AVP	AR76-115	dacite shallow intr.	hornblende	44.92±0.14	Plateau date; 53.0% $^{39}Ar_K$
S AVP *Dunrud Peak*	AR76-121	rhyolite shallow intr.	sanidine	43.68±0.09	Near Plateau date; 46.4% $^{39}Ar_K$

Sample separates from dacite intrusions in the Kirwin area of the southern Absaroka volcanic province have young ages which are analytically identical, from 44.92 ± 0.14 to 44.82 ± 0.85. These ages are slightly older than Dunrud Peak rhyolite, which provides a minimum age for eruptive activity at both the Kirwin volcanic center, and for the entire volcanic province.

Detailed examination of age relationships reveals that magmatic activity at many of the volcanic centers overlaps temporally. Mafic lavas sampled in this study, began erupting prior to 50 Ma at the Crandall volcanic center. The youngest ages (from 46.5 to 43.7 Ma) are limited to samples from intermediate to silicic dacite and rhyolite.

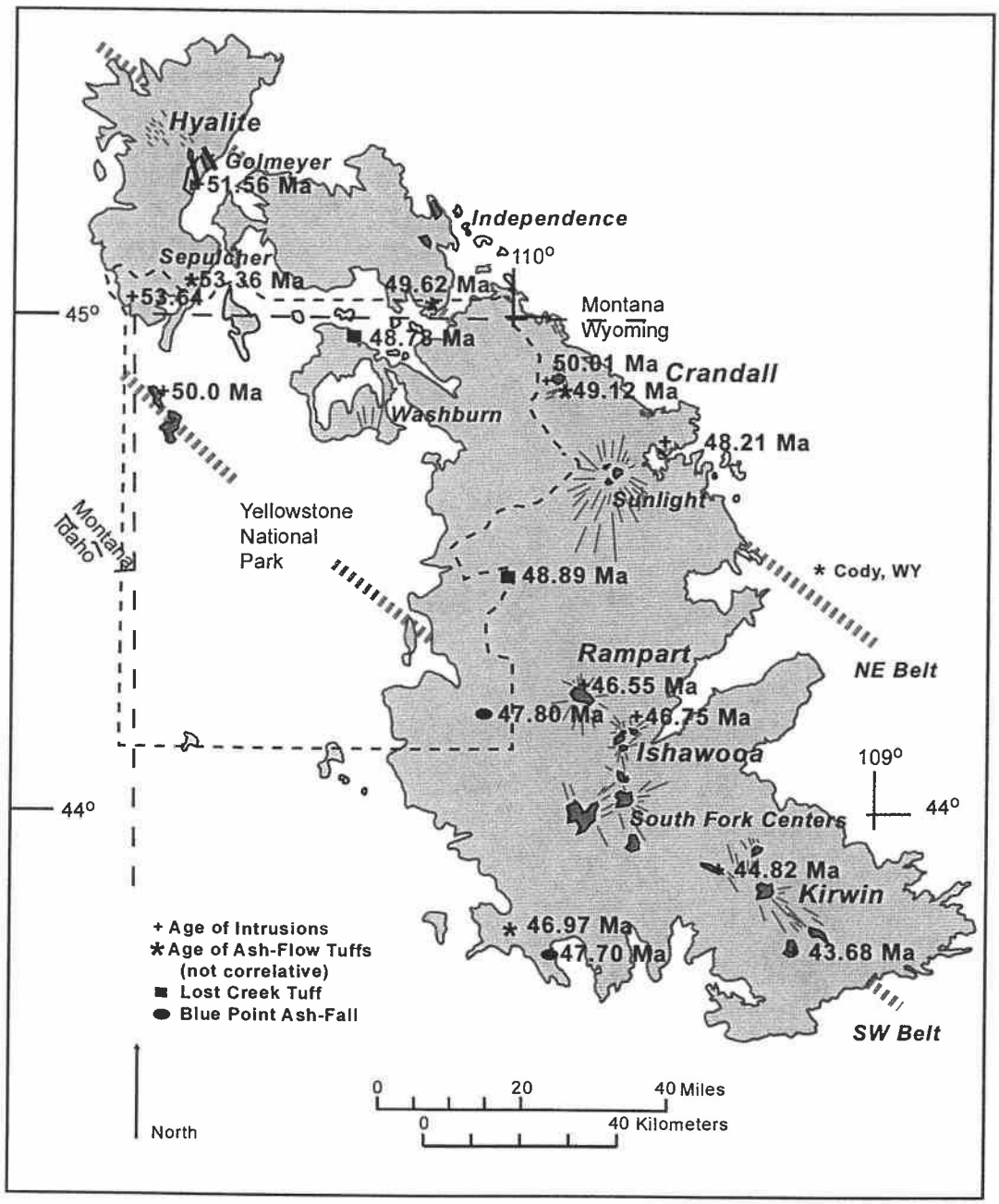

Figure 1.3. Schematic map showing distribution of igneous rocks and volcanic centers of the Absaroka volcanic province. Sample localities for $^{40}Ar/^{39}Ar$ analyses and ages used for stratigraphic correlation are shown by separate symbols (Modified after Smedes and Prostka, 1972; R.A. Chadwick, 1972).

ASH-FLOW TUFFS

Regionally extensive tuffs are essential to establishing a regional geochronologic framework for the Absaroka volcanic province. Using field relationships and petrographic features, $^{40}Ar/^{39}Ar$ age data, and mineralogical data obtained by electron microprobe, we have established that there are three regionally extensive units: the Slough Creek Tuff, with an age of 49.7 Ma, the Lost Creek Tuff which includes the Pacific Creek Tuff, with an age of 48.8 Ma and the Blue Point ash-fall, which includes the Two Ocean ash-fall, with an age of 47.7 Ma.

Slough Creek Tuff

Sixteen samples of rhyodacite and rhyolite of the Slough Creek Tuff from northern Yellowstone Park and the Beartooth Wilderness are included in this study (Figure 1.4). Field relationships, chemical composition and mineralogy indicate that the Slough Creek Tuff consists of two units. The lower unit is a single cooling unit as thick as 300 m, and is a welded to densely-welded, normally-zoned rhyodacite. The upper unit is a rhyolitic ash-flow tuff that is typically 3 to 15 m thick, and directly overlies the irregular, densely welded surface of the lower unit at the type section of Slough Creek Tuff. This densely welded portion of the lower unit which is vitrophyric, was previously unrecognized and mapped as lava flows of the Mount Wallace Formation (U.S. Geological Survey, 1972; Smedes and Prostka, 1972).

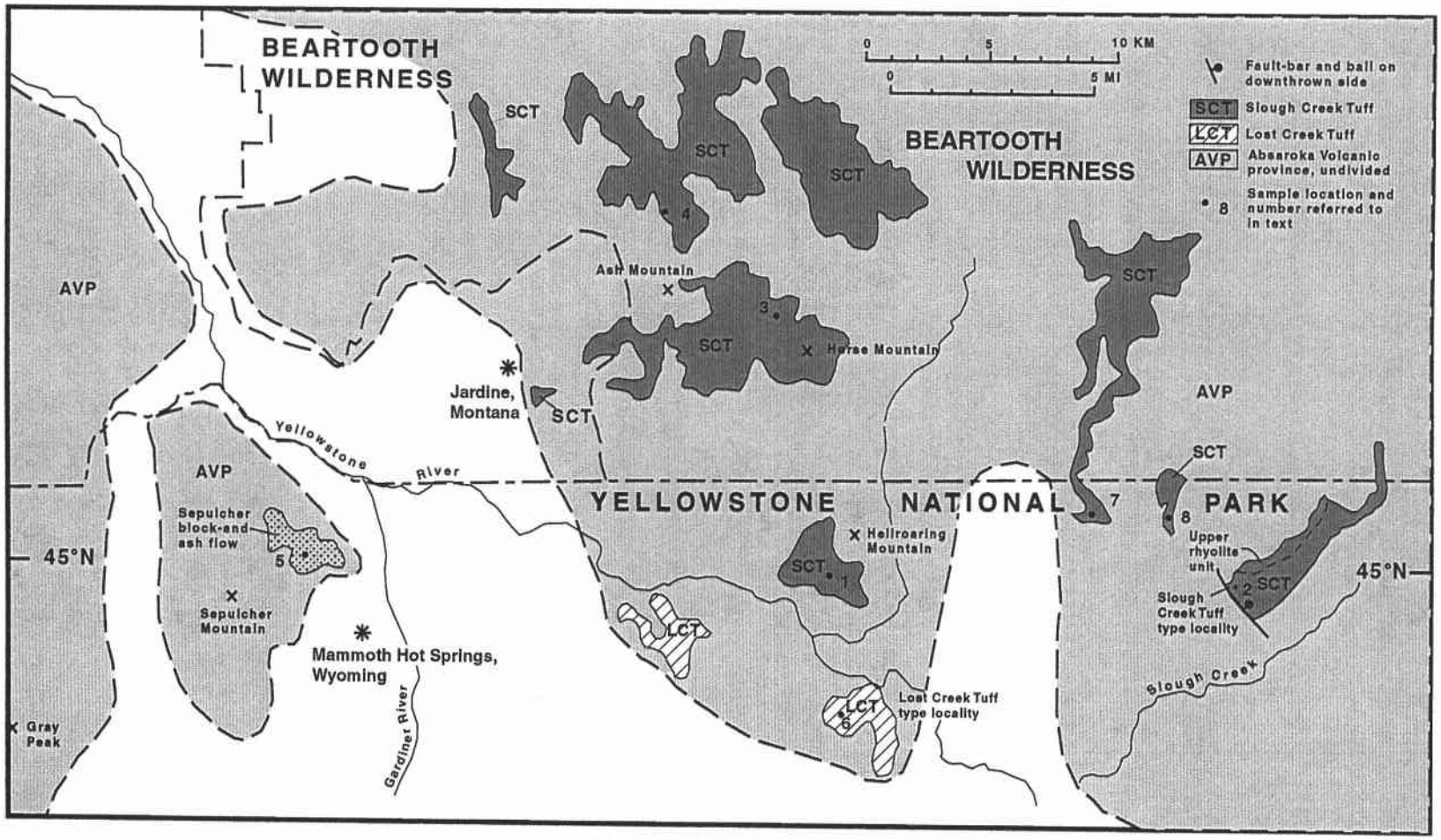

Figure 1.4. Schematic map showing distribution of Slough Creek Tuff, Lost Creek Tuff, and Sepulcher block and ash-flow tuff in northern Yellowstone Park and the Beartooth Wilderness. Sample localities are indicated by numbers.

The upper rhyolite unit of Slough Creek Tuff has a more southerly distribution. Outcrops of the lower Slough Creek Tuff thicken substantially northward and are rich in accidental lithic fragments at the base. In northern Yellowstone Park, it has a lower zone rich in grus derived from outcrops of Precambrian granitic gneiss, indicating uplift and exposure of the Beartooth block prior to eruption (Location 1, Figure 1.4). This field evidence also suggests that the source of the Slough Creek Tuff was to the north, where granitic gneiss outcrops occur beneath volcanic strata.

The lower unit of Slough Creek Tuff has been subdivided into the Hildan and Aslan members (Hickenlooper and Gutman, 1982). Samples of these members from Yellowstone Park and the Beartooth Wilderness were analyzed by electron microprobe (Locations 3 and 4, Figure 1.4). Three additional tuff samples from the Slough Creek type locality were also analyzed by electron microprobe, and selected for $^{40}Ar/^{39}Ar$ analyses. These include a sample from the lower sanidine-rich unit recognized as part of the Aslan member of the Slough Creek Tuff, a sample from the densely welded vitrophyre, and the separate upper biotite-rich rhyolitic unit (Location 2, Figure 1.4).

The Aslan and Hildan members of the Slough Creek Tuff are distinguishable in thin section because the latter contains an appreciably higher percentage of hypersthene and augite. However, uniform feldspar compositions between the two members, together with observed petrographic and field relationships suggest the two members are a single cooling unit. The Hildan Tuff contains glomerocrysts of An_{50} plagioclase, hypersthene and augite, together with a mixture of equal proportions of fragmented, embayed and corroded sanidine, An_{30} plagioclase phenocrysts (0.5-2.0 mm) with calcic rims, and smaller (<0.2 mm) euhedral An_{45-35} plagioclase with normal zonation. The Aslan tuff at both sample localities is especially phenocryst-rich at the base (>75% phenocrysts) with much more abundant sanidine than plagioclase (4:1). Aslan and Hildan member ash-flow tuffs both have sanidine and plagioclase phenocrysts with embayed and non-embayed populations. Feldspars from the central welded portion of the type locality are of similar composition, but less abundant (30-40%) and more fragmented. Although the presence of pyroxene glomerocrysts in the Hildan tuff has been used to distinguish

these members, the vitrophyric portion of the Aslan tuff at the type section also contains pyroxene glomerocrysts in greater abundance than samples of welded tuff lower in the section. Therefore, stratigraphic revisions in this study treat the two members as a single zoned ash-flow tuff.

In contrast to the lower densely welded Slough Creek Tuff, the upper rhyolitic unit at the type section is pumiceous, moderately welded, and has biotite as the dominant phase (10%-15%), with phenocrysts of quartz (5%) and plagioclase (5%) with normal to oscillatory zonation (An_{30-40}) and sparse sanidine (<2%). Ages of the upper rhyolitic unit of Slough Creek tuff and the lower rhyodacite Slough Creek Tuff are indistinguishable within analytical error (Table 1.1). The upper unit has a maximum age estimate of 49.79 ± 0.10 Ma (biotite) and the lower unit has an age of 49.62 ±0.08 Ma (sanidine). Despite the similarity in age, the upper unit is mineralogically and chemically distinctive from the rhyodacite tuff. It is distributed over a different area, and should be considered a separate member. We recommend designating this upper unit of Slough Creek Tuff as the Lamar River member, because it is interbedded with volcaniclastic deposits of the Lamar River Formation in Yellowstone Park.

Lost Creek Tuff

A second, younger rhyodacite ash-flow tuff has been used to correlate across the Absaroka volcanic province. We correlate Lost Creek Tuff and Pacific Creek Tuff based upon age data, shared mineralogy and compositional similarity. $^{40}Ar/^{39}Ar$ data from sanidine and biotite separates yield plateau ages of 48.78 ± 0.08 and 48.89 ± 0.12, respectively (Table 1.1, Appendix A). Lost Creek Tuff at the type section is welded, has 20% sanidine, minor anorthoclase (1-2%) and 10% biotite (replaced by opaque oxides), devitrified fiamme, and also contains fragmented inclusions of volcanic glass with small An_{45-50} plagioclase phenocrysts. The Pacific Creek Tuff has variable amounts of anorthoclase or sanidine, biotite, and minor amounts of small broken crystals of An_{50} plagioclase and augite. Correlation has been further

substantiated by microprobe analysis of phenocrysts which suggests that the tuff is a single unit that exhibits zonation from sanidine to anorthoclase. Microprobe analyses of alkali feldspars from ash-flow tuff samples of Lost Creek Tuff and the Pacific Creek member show that they are characteristically zoned, with Ba-rich rims. Alkali Feldspars in Lost Creek and Pacific Creek tuffs are distinctive and exhibit more pronounced zonation than those from the Slough Creek tuff (Figure 1.5).

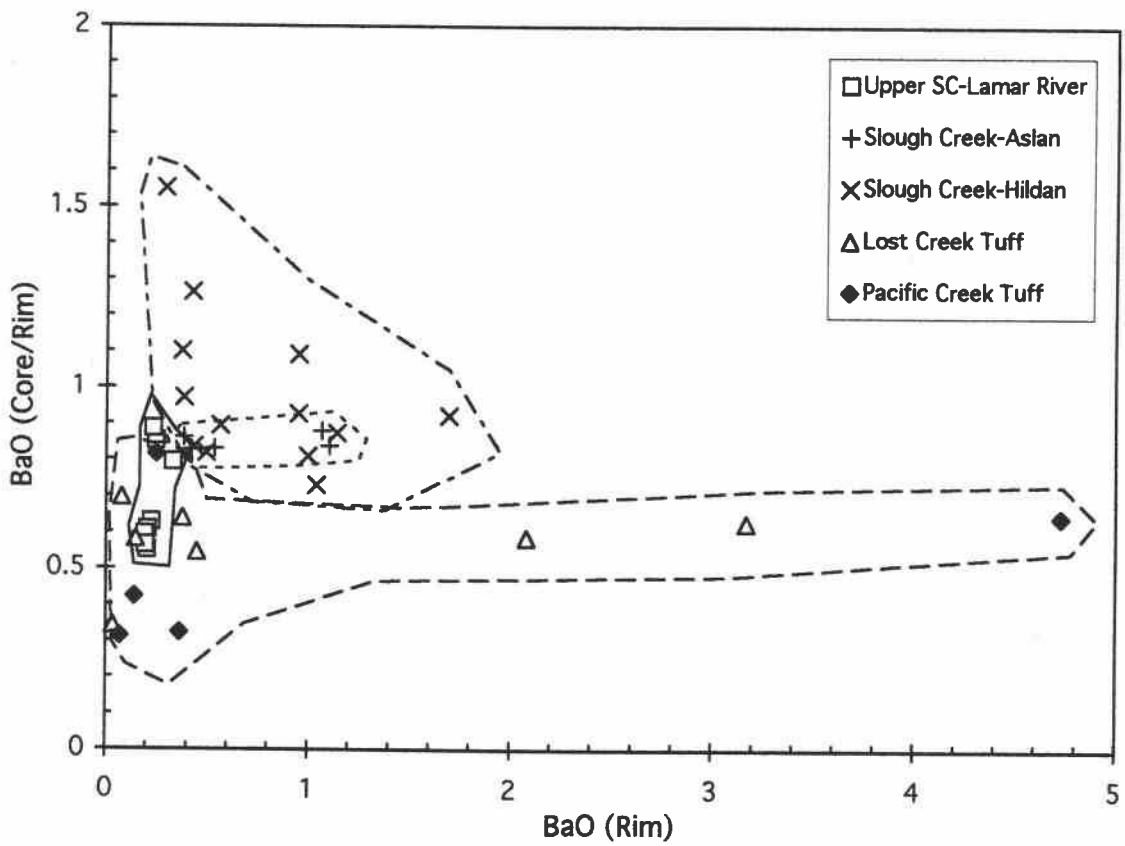

Figure 1.5. Graph showing the ratio of wt% BaO in feldspar core and rim versus BaO in feldspar rims (from electron microprobe analyses).

Outcrops mapped as Lost Creek Tuff at the base of Sepulcher Mountain are from a dacitic block and ash flow which is biotite-, hornblende- and plagioclase-rich, and lacks phenocrysts of sanidine or anorthoclase (Location 5, Figure 1.4). We explicitly exclude these outcrops from the Lost Creek Tuff and call this unit the Sepulcher block and ash-flow tuff. Age data from this pyroclastic deposit provide a maximum age estimate of 53.36 ± 0.3 Ma, which is significantly older than Lost Creek Tuff at the type locality (Location 6, Figure 1.4). An outcrop north of the Yellowstone River is also excluded from the Lost Creek Tuff and included with the Slough Creek Tuff because it has abundant sanidine and plagioclase of the same composition as those in the Slough Creek Tuff, and lacks biotite (Location 1, Figure 1.4). Other localities of welded ash-flow tuff sampled north of the Yellowstone River (Location 7 and 8, Figure 1.4) previously mapped Mount Wallace Formation lava flows, are recognized by this study as Slough Creek Tuff (U.S. Geological Survey, 1972; Smedes and Prostka, 1972).

Blue Point Ash-Fall

Samples of ash-fall from the southern Absaroka volcanic province, at Irish Rock and Two Ocean Pass in southern Yellowstone Park were sampled, described and analyzed by $^{40}Ar/^{39}Ar$ in this study. These units are age correlative and are tentatively considered the same unit, based on age and sample mineralogy. The ash-fall unit at Irish Rock has been identified by previous studies as the Blue Point Marker (Wilson, 1963; Bown, 1982; Sundell and Eaton, 1982). Both units are of intermediate composition, light gray, and variable in thickness, typically from 3 to 5 m thick. The ash-fall in the area of southern Yellowstone thickens slightly southward and contains accidental lithic fragments. Samples from both localities are pumiceous, with phenocrysts of biotite, hornblende, and plagioclase with sanidine rims. The ages from these two units, of 47.8 ± 0.07 and 47.7 ± 0.10 Ma are identical within analytical error.

Regional Correlations

The regional framework provided by tuff correlation, in addition to ages of volcanic centers, supports interpretations of Hague et al. (1899), Smedes and Prostka (1972), Love et al. (1976), and Sundell (1993) that volcanic rocks in the Absaroka volcanic province are younger southward. However, tuff correlations include members from separate formations and groups and subdivide the Trout Peak Trachyandesite Formation of the Sunlight Group (Smedes and Prostka, 1972). Paleomagnetic data of Shive and Pruss (1977) corroborate these findings, and indicate that units of Trout Peak Trachyandesite in the Shoshone River valley are not correlative. Because flows of the Trout Peak Trachyandesite are stratigraphically separate, produced as eruptive products of local volcanic centers and cannot be mapped at a single stratigraphic horizon, we recommend that the formation name of Trout Peak Trachyandesite be abandoned. Instead, these flows are assigned to local volcanic centers (Figure 1.6). Ages of volcanic centers are established by the age of central intrusions and tuffs interbedded with flows, and then correlated regionally with ash-flow tuff deposits, $^{40}Ar/^{39}Ar$ ages, and published paleomagnetic data (Shive and Pruss, 1977; French and Van der Voo, 1978; Lee and Shive, 1983; Sundell et. al., 1984; Sundell, 1993; and Harlan et al., 1996). In some areas of the Absaroka volcanic province, age relationships have also been established by well-developed and laterally extensive unconformities (Figure 1.6).

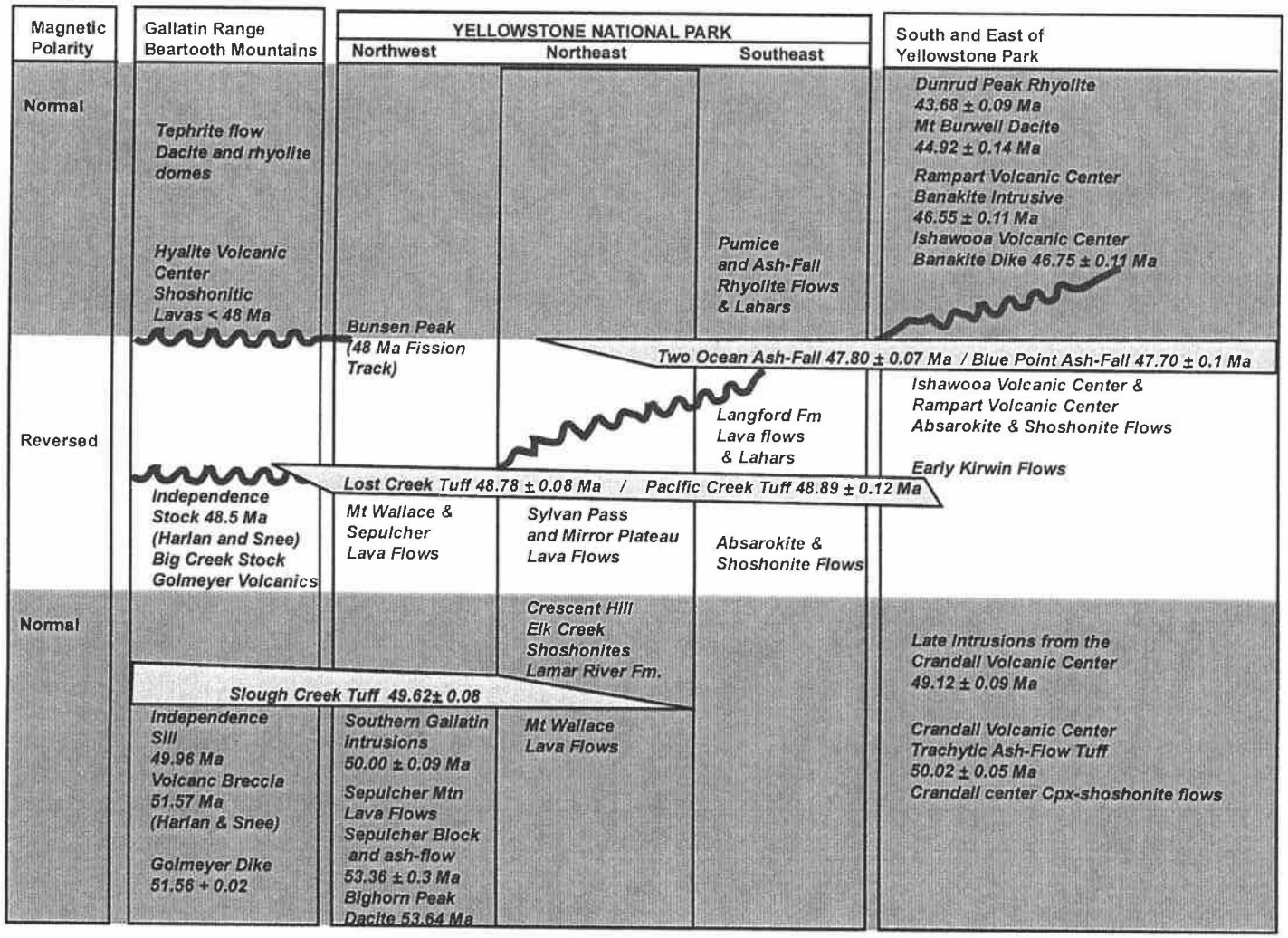

Figure 1.6. Correlation chart showing age relationships of volcanic centers to ash-flow tuffs, lava flows, and formations in the Absaroka volcanic province. (Bold wavy lines indicate location of unconformities.)

MAJOR ELEMENT CHEMISTRY OF VOLCANIC CENTERS

In order to examine the calc-alkaline versus alkaline character of eruptions in space and time, we here compare analyses of mafic rocks, because they most closely represent parental compositions. Analyses are from seven different volcanic centers, four northeastern belt centers and three southwestern belt centers, plus additional peripheral lava flows. Comparison of analyses with >4 wt% MgO and <55 wt% SiO_2 (recalculated to 100% volatile-free) at each respective volcanic center minimizes problems imposed by localized fractionation and crustal assimilation. Data with >3% LOI were rejected with the exception of sample 225 (southeast Yellowstone) from Nicholls and Carmichael (1962), which was included to represent the most extreme southwest portion of the Absaroka volcanic province.

Mafic samples range from basanite, to absarokite and shoshonite with MgO variation from 4.1 to 16.1 wt% (Figure 1.7 and 1.8). There is no province-wide trend in the distribution of mafic alkalic lava, and a diversity of compositions erupted from individual volcanic centers. All samples are K-rich, according to the original subdivision of the province by Chadwick (1972), except a few samples from the northeastern belt (Figure 1.9). The original notion of a northeast potassic and a southwest calc-alkaline belt is no longer tenable.

Mafic alkaline lava flows are found at the base of the stratigraphic sequence at each of the volcanic centers sampled in this study. Those sampled at the Crandall volcanic center erupted prior to 50 Ma. Absarokites and shoshonites which exhibit the most pronounced enrichment in K_2O erupt before 46.5 Ma, in the southwestern volcanic belt.

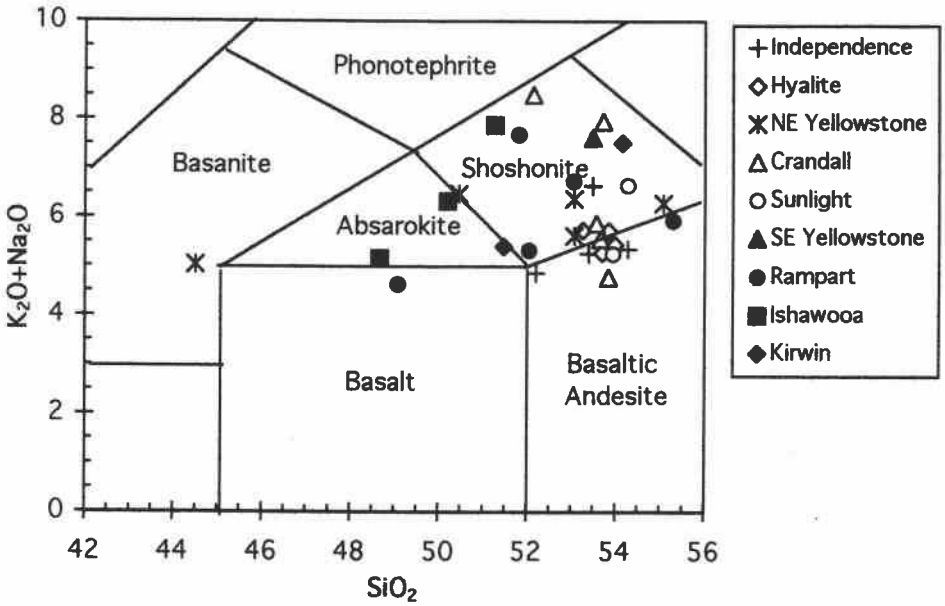

Figure 1.7. Chemical classification and nomenclature for mafic volcanic rocks from the Absaroka volcanic province using subdivisions from the total alkalis versus silica diagram of Le Maitre et al. (1989). All samples recalculated to 100% volatile-free. References for analyses from different volcanic centers given in text.

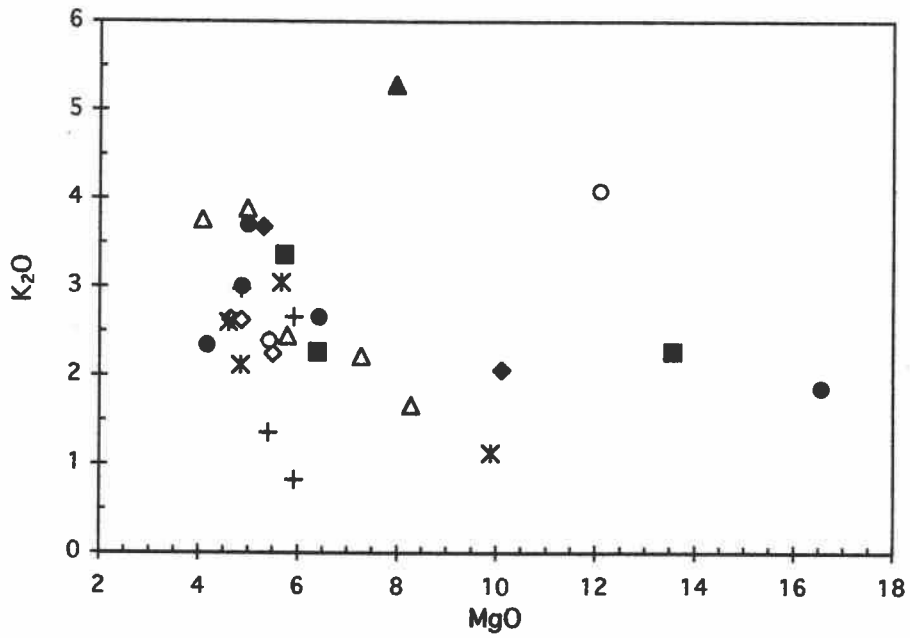

Figure 1.8. MgO vs. K_2O for mafic rocks from individual volcanic centers of the Absaroka volcanic province. (Samples and symbols the same as in Figure 1.7.)

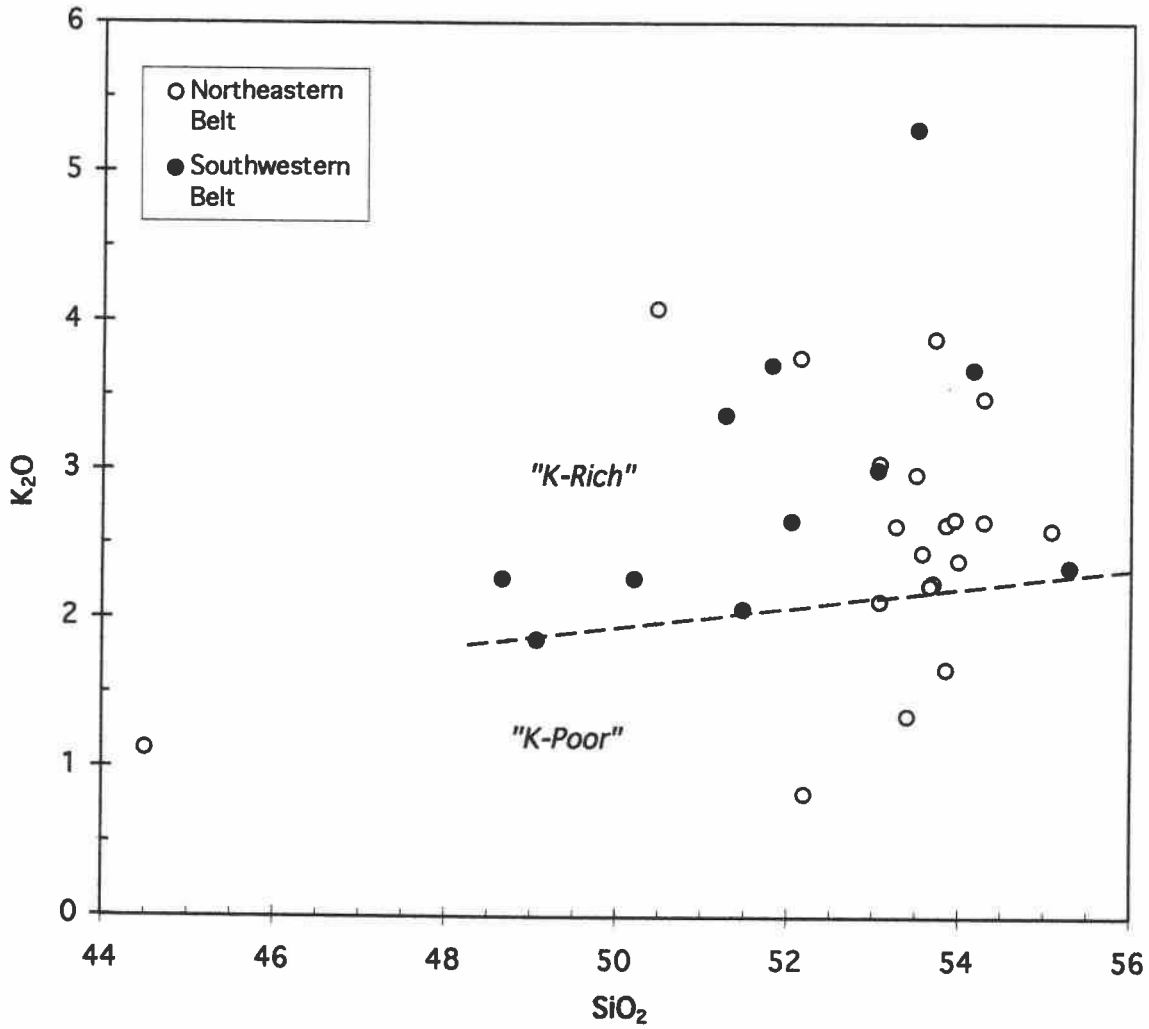

Figure 1.9. K_2O versus silica for mafic rock samples from the northeastern and southwestern belts of the Absaroka volcanic province. An arbitrary line from Chadwick (1972) separates "K-rich" from "K-poor" compositions. Note that mafic compositions fall in the "K-rich" field, and no clear distinction can be made between data from different volcanic belts.

DISCUSSION

The Sequence of Eruptions

The earliest documented eruptive activity includes a dacitic block and ash-flow tuff in the northern Absaroka volcanic province, with a maximum age estimate of 53.36 ± 0.3 Ma. Also early in the history of magmatic activity, prior to 50 Ma, is the eruption of mafic-alkaline lava flows at the Crandall volcanic center, which is synchronous with volcanism in both volcanic belts, including the formation of laccoliths in the southern Gallatin Range, as well as South Fork Centers, Independence, and Point of Rocks volcanic centers. The Slough Creek tuff, the first and northernmost of three extensive ash-flow tuffs, erupted 49.6 Ma. Following eruption of the Slough Creek Tuff, the last magmatism at Crandall and Independence volcanic centers of the northeastern belt occurred. The second ash-flow, the Lost Creek Tuff erupted 48.8 Ma. After which early fissure-fed eruptions of the Rampart, Ishawooa and Kirwin volcanic centers formed broad plateaus of high-K lavas in the southwestern volcanic belt. These plateau forming eruptions are similar in age to intrusions at the Sunlight volcanic center, based on the age of 48.2 Ma for a monzogabbro intrusion. The southernmost of ash-flow tuffs used as stratigraphic markers in this study, the Blue Point ash-fall, erupted 47.7 Ma. Its eruption marks the end of widespread activity.

Uplift and erosion followed eruption of the Blue Point ash-fall in the southern AVP, and preceded deposition of Hyalite Peak Volcanics in the northern AVP, producing a major unconformity which separates older and younger volcanic strata. Shoshonitic lavas also overlie this unconformity south of the Sunlight volcanic center. In the southern portion of the AVP this unconformity is a prominent

feature, and is well developed in the Washakie Wilderness and southeast Yellowstone National Park.

Eruptions from 47 to 43 Ma in the southern portion of the province consist primarily of dacite and rhyolite. These include intrusions at Mt. Burwell and Dunrud Peak in the vicinity of the Kirwin volcanic center, which also erupted minor mafic dike fed lavas. The last eruptions at the Rampart volcanic center and Ishawooa volcanic centers, two adjacent loci of igneous activity, occurred between 46.5 and 47 Ma. Late eruptions in the northern part of the Absaroka volcanic province consist primarily of fissure fed shoshonitic lava flows of the Hyalite volcanic center (approximately $\leq$48 Ma), and also include flows and dikes in the southern Beartooths, silicic dome eruptions, and a volumetrically minor eruption of basanite.

Samples from volcanic centers and peripheral lava flows of the northeastern and southwestern belts of eruptive centers demonstrate that mafic potassic rock types occur throughout the Absaroka volcanic province. Age relationships show that potassic magmatism is not restricted temporally, although it occurred very early in the history of each volcanic center and comprises a volumetrically significant proportion of eruptive products prior to 47 Ma. A simplified diagram of ages for volcanic centers represented in this study is shown in Figure 1.10. Early eruptions from the Crandall volcanic center consist of shoshonitic rock types, as do the eruptions from the Hyalite volcanic center. Southwestern volcanic centers erupt later and exhibit greater temporal overlap. From 49 to 48 Ma, eruptions of mafic potassic lavas occurred throughout the Absaroka volcanic province, in both the northeastern and southwestern volcanic belts. Eruptions in the region surrounding Kirwin volcanic center continue until almost 43 Ma, but with the exception of early mafic potassic eruptions, they consist primarily of intermediate to silicic compositions (See Figure 1.4).

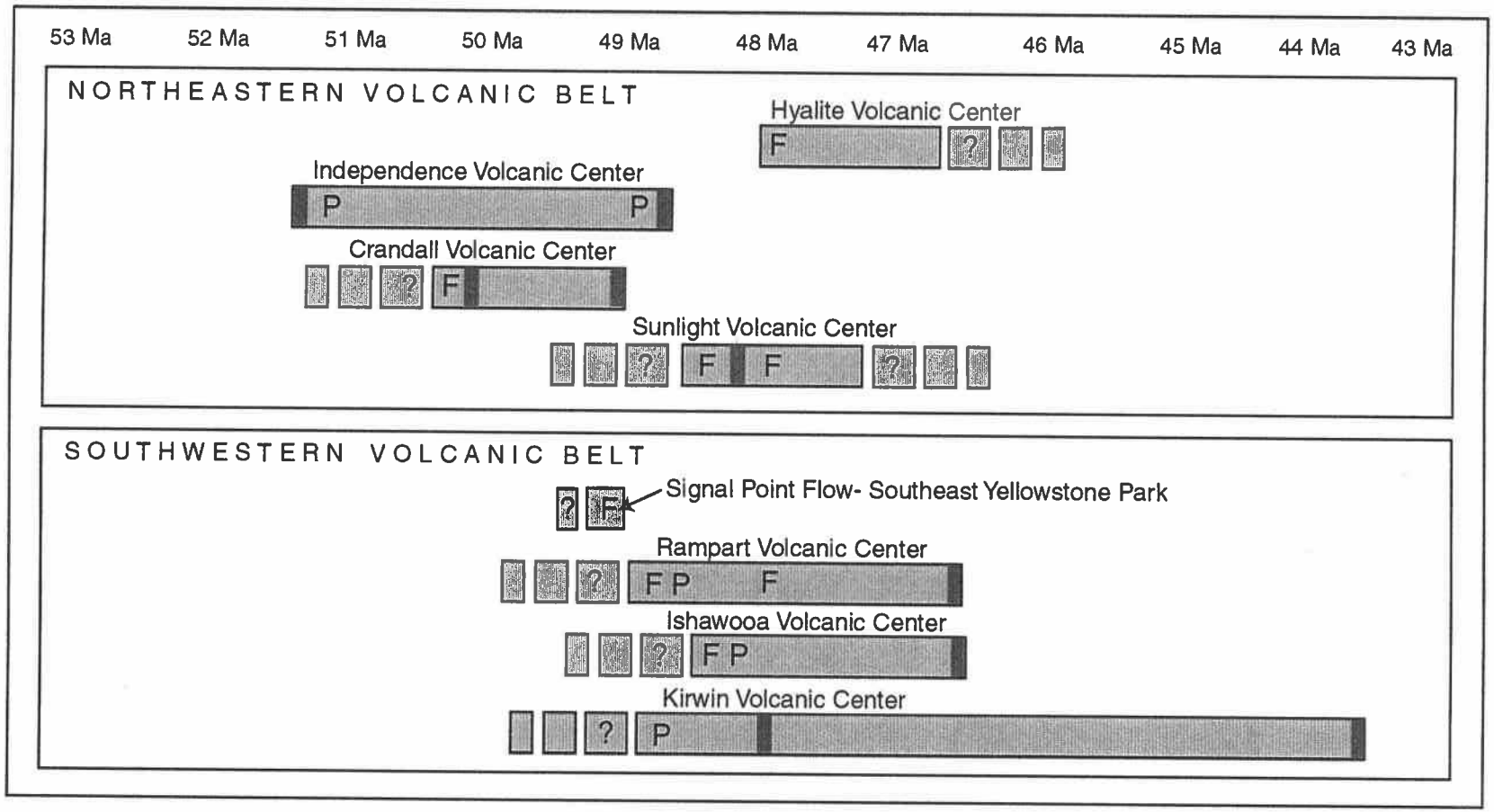

Figure 1.10. Duration of igneous activity at volcanic centers of the northeastern and southwestern volcanic belts of the Absaroka volcanic province. Dark bands indicate age constraint by $^{40}Ar/^{39}Ar$ age data; P- indicates age constraint based on published paleomagnetic data; F- indicates relative age constraint based on field data.

Eruptive Volume

The Absaroka volcanic province presently covers 25,000 km^2 with deposits as much as 1-2 km thick (Hague, 1899; Love, 1939; McMannis and Chadwick, 1984; Sundell, 1993). The estimated volume of preserved deposits in the Absaroka volcanic province is approximately 23,000 km^3. Based on geochronological data from this study, approximately 85% of this material was produced during eruptive activity from 52 to 47 Ma, and 60% of the estimated volume erupted between 49 and 47 Ma. Age data indicates that the duration of eruptive activity at individual volcanic centers may last a maximum of 2 to 3 Ma. Late volcanism, such as in the Kirwin area, is represented by scattered dome eruptions. The volume of material produced during the brief period of intense eruptive activity is therefore approximately 6,900 km^3/m.y. The average output, however, is 2,500 km^3/Ma, or 2.5 $x10^{-3}$ km^3/yr., which is essentially the same approximate output of magma as the present Yellowstone-Snake River Plain system (Crisp, 1984). The average estimated magma output rate is an order of magnitude greater than, and the duration of magmatic activity is less than half that of the central Andes. This estimate does not include the probable extent of deposition into the Bighorn and Green River basins, where isolated remnants of middle Eocene volcanic ash and detritus are preserved (Love, 1964). Nor does it include the deposits which were likely destroyed during recent volcanism of the Yellowstone Caldera.

Geographic Distribution of Eocene Volcanism

Age data from this study highlight the short-lived nature of volcanic activity of the Absaroka volcanic province. Although brief, volcanic activity within the Absaroka province, coincides with igneous activity that occurs over a broad region of the northern Cordillera, which includes the Clarno volcanic field in Oregon, consisting of calc-alkaline rocks and highly alkaline lamprophyres (Taylor; oral

commun., 1999), with kimberlite intrusions of the Missouri Breaks (Scambos, 1991), carbonatite volcanism of the Black Hills of South Dakota (Jenner, 1989), silicic to calc-alkaline andesitic volcanism of the Lowland Creek volcanics (Ispolatov, 1996) and silicic, calc-alkaline and alkaline volcanism of the Challis volcanic field (Norman and Mertzman, 1991; Janecke and Snee, 1993; M'Gonigle and Dalrymple, 1996) as well as other intrusive rocks and volcanic fields (Figure 1.1 and Table 1.2). This diffuse belt of igneous rocks extends from the margin of the North American plate to more than 1500 km inland from the possible site of a coeval trench, more than twice the distance of the broadest part of the Andes (Dudas, 1991). The process of subduction fails to provide an adequate heat source for magmatism to occur synchronously over such a broad region, and does not explain the brevity of its duration.

Igneous activity of the northern Cordillera during the middle Eocene is diverse in character, but includes mafic potassic rocks in the early part of the magmatic episode, with a change in character of later volcanism to predominantly intermediate and rhyolitic compositions (Table 1.2). Early eruptive activity of the Absaroka volcanic province from 53 to 50 Ma coincides with intrusion of highly alkaline mafic rocks of Eagle Buttes, Sweetgrass Hills, Highwood and Bearpaw Mountains from 54 to 50 Ma, eruption of rhyolitic tuff of the Lowland Creek volcanics and intrusion of rhyolitic dikes in the Challis volcanic field (Marvin et. al, 1980; Ispolatov, 1996; M'Gonigle and Dalrymple, 1996). Most of the volume of eruptive products produced from Absaroka volcanic province was erupted from 50 to 48 Ma, after which the volume of eruptive products decreases significantly. Similar observations were made by Janecke and Snee (1993) who noted an abrupt decline of Challis volcanism after 48 Ma. By this time, magmatism had ceased in many volcanic fields of the northern Cordillera, with the exception of the Challis volcanic Field, Crazy Mountains, Garnet Range, and Absaroka volcanic province. Late intermediate to silicic magmatism of the Absaroka volcanic province coincides with eruption of intermediate rock types of the Challis volcanic field at 48 Ma, and rhyolite dominated bimodal volcanism of the Garnet Range and Challis volcanic fields from 47 to 44.5 Ma (Williams and others, 1976; Janecke and Snee, 1993). These regional age comparisons indicate that voluminous eruptive activity from east to west is not diachronous in the Cordillera, as would be expected if the hinge of subducting

oceanic crust migrated. Furthermore, the majority of potassic magmatism occurred prior to 47 Ma, during the first half of erutpive activity, not only within the Absaroka volcanic province, but also regionally within the northern Cordillera.

Plate motion reconstructions from Stock and Molnar (1988) and Engebretson et. al. (1985) highlight the difficulty in constraining the position of the Kula, Farallon and Vancouver plates and resolving the location of the Kula-Farallon ridge relative to the western margin of North America during the middle Eocene. However, Stock and Molnar (1988) and Londsdale (1988) show that significant changes in plate motion occurred between 56 and 42 Ma. At the beginning of this period, Kula plate motion rotated counterclockwise from from northeast to north. This change in plate motion is constrained by plate reconstruction models and tectonic events to have occurred between 56 and 55 Ma (Londsdale, 1988; Goldfarb et. al, 1991). Between 56 and 50 Ma, Farallon plate motion also changed, from rapid northeast motion relative to the North American plate, to a slower, more oblique and northerly direction. During this period, the Vancouver plate split from the Farallon plate, so that the speed and azimuth of plate motions varied along the western edge of the north American plate (Stock and Molnar, 1988). If oblique northern directed subduction occurred during this period, then the necessary lateral length of transport for a subducted slab to travel, in order to induce middle Eocene magmatism is increased during a period when plate convergence rates were slower. In addition, an age progression resulting from the changing angle of a descending slab as suggested by models of Armstrong (1974), Lipman (1980), and Snoke (1993) should occur in a northeast to southwest direction. No east to west age progression is evident from regional age comparisons of Eocene volcanic fields (Table 1.2). The age progression exhibited by data from the Absaroka volcanic province is coeval in both the northwest to southeast belts of eruptive centers, and perpendicular to plate motion vectors (Figure 1.11). A decrease in relative plate motions suggests that the angle of the subducting oceanic slab may have steepened between 55-50 Ma. Although back-arc extension has been postulated by some authors to explain the general variation in composition from potassic alkaline rocks in the east to calc-alkaline rock in the west (Lipman et al., 1971; Armstrong and Ward, 1991; O'Brien et al., 1991), the diverse middle Eocene rock types present in the northern Cordillera are not spatially restricted.

Table 1.2 Reported ages for Middle Eocene volcanic fields and igneous rocks of the northern Cordillera.

Occurrence	Age	Method	Reference
Bearpaw Mountains, Minnette, Phonolite	54 to 50 Ma	K-Ar	Marvin et. al, 1980
Highwood Mountains Minnette, Phonolite	53 to 50 Ma	K-Ar	Marvin et. al, 1980
Eagle Buttes shonkinite and phonolite	53.1 to 50.4 Ma	K-Ar	Marvin et. al, 1980
Missouri Breaks Kimberlite	52.0 to 47 Ma	K-Ar	Scambos, 1991
Lowland Creek volcanics, Rhyolite, Qtz Latite	51.7 to 48.4 Ma	$^{40}Ar/^{39}Ar$	Ispolatov, 1996
Clarno volcanic field Lamprophyre	51.5 to 48 Ma	$^{40}Ar/^{39}Ar$	Dilles, oral commun., 1999
Sweetgrass Hills Minette	51.2 Ma	K-Ar	Marvin et. al, 1980
Crazy Mountains, Theralite, Syenite	50.4 to 43.8	K-Ar	Harlan et. al, 1991
Yogo Peak Lamprophyre	50 Ma	K-Ar	Marvin et. al, 1973
Norris Rhyolite Vitrophyre	49.3 Ma	$^{40}Ar/^{39}Ar$	Kellogg, written commun.
Challis volcanic Field Rhyolite,	49 to 45.4 Ma	$^{40}Ar/^{39}Ar$	Janecke and Snee, 1993
Challis volcanic Field	53.4 to 45 Ma	$^{40}Ar/^{39}Ar$	M'Gonigle and Dalrymple, 1996
Colville Igneous Complex (Sanpoil Formation)	53 to 51.3	U-Pb Zircon	Morris and Hooper, 1997
Colville Igneous Complex (Klondike Mountain Fm.)	48.8 Ma	$^{40}Ar/^{39}Ar$	Berger and Snee, 1992
Bearmouth Rhyolite, Garnet Range	44.5 Ma	K-Ar	Williams et. al, 1976

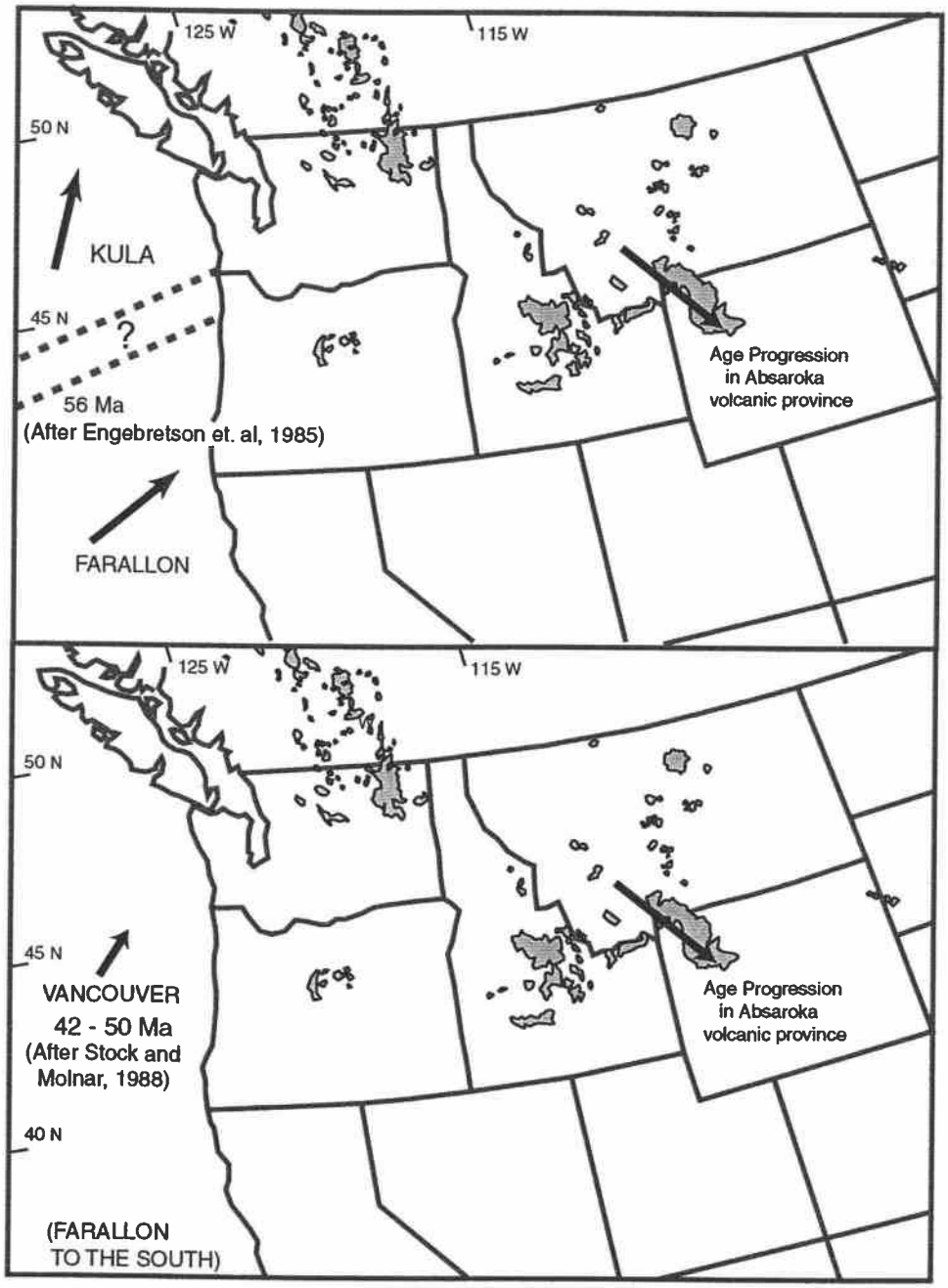

Figure 1.11. Maps showing distribution of middle Eocene igneous rocks and volcanic fields, direction of age progression in the Absaroka volcanic province, and relative motion of the Kula, Farallon, and Vancouver plates during midlle Eocene time. Vector length is proportional to relative speed of plate motion. (After Engebretson et. al, 1985; and Stock and Molnar, 1988).

Regional middle Eocene extension in the northern Cordillera is well documented by many studies, these include graben formation coeval with volcanism as early as 54 Ma in the Pacific Northwest (Hooper et al., 1995), and as early as 49 Ma in Idaho, coeval with Challis volcanism (Janecke, 1992, 1994). Extension is also documented to have occurred in deep-seated features by 48 to 50 Ma in Montana, Idaho and Wyoming, and by 54 Ma in British Columbia. It includes extensional reactivation of thrust faults deep in the subsurface of northwest Montana, British Columbia, and southwest Wyoming (Harms and Price, 1992; Costensius, 1996) and extension in the Bitterroot, Pioneer and Valhalla metamorphic core complexes of Idaho and Montana, and southeastern British Columbia (Carr et. al, 1987; Silverberg, 1990; Hodges and Applegate, 1993). Magmatism began at about 53 Ma in the northern Cordillera, prior to the majority of development of extensional features. Gans and Bohrson (1998) document a similar relationship of magmatism to extension later and to the south, in the Basin and Range Province. They observe that the inception and peak of volcanism typically predates the peak of extension, and suggest that during peak extension, volcanism may be supressed as magma becomes dispersed into smaller bodies at mid-crustal levels.

Igneous activity in the Cordillera, north of the Snake River plain, although less voluminous after 47 Ma, continues until 43 Ma. After 43 Ma, the eruption of calc-alkaline and silicic magmas and extension coincident with uplift of metamorphic core complexes occur in the northern Basin and Range, south of the Snake River Plain (Cross and Pilger, 1982; Armstrong and Ward, 1991, Hurlow et. al, 1991; McGrew and Snee, 1994; Humphreys, 1995; Brooks et. al, 1995). Volcanism and extension begins earlier in British Columbia (54 Ma), than in Montana and Idaho (53-43 Ma), and occurs later in the Northern Basin and Range of Nevada (42.6 Ma), exhibiting a southward continuance which may be reflected locally in the age progression from north to south in volcanism within the Absaroka volcanic province. The regional shift to south of the Snake River Plain also coincides with, and may be related to, a change in motion of the Pacific plate relative to North America (Engebretson et al., 1985; Stock and Molnar, 1988).

CONCLUSIONS

Age data from the Absaroka volcanic province and other Cordilleran Eocene volcanic fields do not show regional progressions as suggested by subduction-related models of Lipman (1980), and Armstrong (1988). Instead, new data emphasize the contemporaneity and brief duration of middle Eocene volcanism from northwestern Washington to Montana and Wyoming, most of which occurred between 53 and 47 Ma (Table 1.2).

The evolution of magmatism, from calc-alkaline to alkaline compositions, postulated by some authors to indicate a subduction origin for middle Eocene magmatism, does not exist within the Absaroka volcanic province. Instead, a general trend to more silicic volcanism with time occurs at individual volcanic centers. New $^{40}Ar/^{39}Ar$ data, and correlation of ash-flow tuffs substantiate a northwest to southeast age progression of eruptive activity. Age relationships demonstrate temporal overlap to most igneous activity in both the northeastern and southwestern volcanic belts. This age progression is not linked to changing alkalinity of eruptive products. Mafic rocks throughout the province are characteristically potassic, and are the products of early eruptions of individual volcanic centers. They are *NOT RESTRICTED* to a northeastern volcanic belt. Therefore, this study finds no evidence of the distribution of volcanic rocks with characteristics suggesting arc-like petrologic zonation. Instead, magmatism is more likely related to middle Eocene extension, which has been well documented by many authors (i.e. Constensius, 1996).

The widespread distribution of middle Eocene igneous rocks, and the brevity of the duration of volcanic activity, which includes mafic potassic volcanism from 53-48 Ma across the northern Cordillera, suggests that this episode of magmatism is related to the onset of extension. Middle Eocene extension is well documented in the northern Cordillera, and began as early as 54 Ma in British Columbia, and as early as 48 to 50 Ma in Montana and Idaho. Volcanism, which began as early as 53 Ma in in

Washington, Idaho and Montana, predates the development of extensional features, showing a temporal relationship between magmatism and extension similar to that which has been documented in the Basin and Range province (Gans and Bohrson, 1998). Extension began during widespread and voluminous igneous activity in the Absaroka volcanic province, between 48 and 49 Ma, which is comparable to the period of peak magma output in the Challis volcanic field (Janecke and Snee, 1993). After 47 to 48 Ma, magmatism in the Cordillera is restricted to fewer volcanic fields, eruptive activity in the Absaroka volcanic province is less voluminous, and primarily intermediate to silicic in composition. By 43 Ma, widespread volcanism in the northern Cordillera and the Absaroka volcanic province ended, and the locus of magmatism shifts to a region south of the Snake River Plain.

REFERENCES CITED-1

Armstrong, R.L. (1974) Geochronometry of the Eocene volcanic-plutonic episode in Idaho: Northwest Geology, vol. 3, p.1-15.

Armstrong, R.L. (1988) Mesozoic and Cenozoic magmatic evolution of the Canadian Cordillera: *in* Processes in Continental Lithospheric Deformation, S.P. Clark, B.C.Burchfiel, and J. Suppe, eds., GSA Special Paper 218, p. 55-91.

Armstrong, R.L., and Ward, P. (1991) Evolving geographic patterns of Cenozoic magmatism in the North American Cordillera: The temporal and spatial association of magmatism and metamorphic core complexes: Journal of Geophysical Research, vol. 96, p.13201-13224.

Baker, D.W. (1987) Central Montana Alkalic Province: Critcal review of Laramide Plate Tectonic models that extract alkalic magmas from abnormally thick Precambrian lithospheric mantle: Northwest Geology, vol.20, p.71-95.

Barnes, B.K. (1985) Stratigraphy of Eocene volcaniclastic rocks, Dick Creek Lakes quadrangle, Wyoming: M.S. Thesis, Iowa State University, Ames, 221p.

Berger, B.R., and Snee, L.W. (1992) Thermochronologic constraints on mylonite and detachment fault development, Kettle Highlands, northeastern Washington and southern British Columbia: (abs.) Geological Society of America Annual Meeting Abstracts with Programs, p.A65.

Best, M.G., and Christiansen, E. H. (1991) Limited extension during peak Tertiary volcanism, Great Basin of Nevada and Utah: Journal of Geophysical Research, vol. 96, p. 13509-13528.

Bown, T.M. (1982) Geology, paleontology, and correlation of Eocene volcaniclastic rocks, southeast Absaroka Range, Hot Springs County, Wyoming: US Geological Survey Professional Paper 1201-A, 75 p.

Brooks, W.E., Thorman, C.H., and Snee, L.W. (1995) The $^{40}Ar/^{39}Ar$ ages and tectonic setting of the middle Eocene northeast Nevada volcanic field; Journal of Geophysical Research, vol. 100, p.10403-10416.

Carlson, D.H., Fleck, R., Moye, F.J., and Fox, K.F. (1991) Geology, geochemistry, and isotopic character of the Colville Igneous Complex, northeastern Washington: Journal of Geophysical Research, vol. 96, p.13313-13333.

Carr, S.D., Parrish, R.R., Brown, R.L. (1987) Eocene structural development of the Valhalla complex, southeastern British Columbia: Tectonics, vol. 6, p. 175-196.

Chadwick, R.A. (1968) Structural and chemical relationships in the Eocene Absaroka-Gallatin volcanic province, Wyoming-Montana: (abs.) Geological Society of America Annual Meeting Abstracts with Programs, p. A50-A51.

Chadwick, R.A. (1969) The northern Gallatin Range, Montana: northwestern part of the Absaroka-Gallatin volcanic field: University of Wyoming Contributions to Geology, vol. 8, no. 2, pt. 2, p.150-166.

Chadwick, R.A. (1970) Belts of eruptive centers in the Absaroka-Gallatin volcanic province, Wyoming-Montana: Geological Society of America Bulletin, vol. 81, p.267-273.

Chadwick, R.A. (1981) Chronology and Structural Setting of Volcanism in Southwestern and Central Montana: Southwest Montana Guidebook, Montana Geological Society Field Conference and Symposium, p.301-310.

Chadwick, R.A. (1985) Overview of Cenezoic volcanism in the west-central United States, in Kaplan, S.S., and Flores, R.M., eds.: Rocky Mountain Section S. E.P.M. Cenezoic Paleogeography of the west-central United States, Symposium 3, p. 359-381.

Christiansen, R.L. (1989) Volcanism associated with post-Laramide tectonic extension in the western U.S., Abs in IAVCEI meeting on Continental Magmatism, Santa Fe, New Mexico: New Mexico Bureau of Mines and Mineral Resources Bulletin 131, p. 51.

Constensius, K.N. (1996) Late Paleogene extensional collapse of the Cordilleran fold and thrust belt; Geological Society of America Bulletin, vol. 108, p. 20-39.

Crisp, J.A. (1984) Rates of magma emplacement and volcanic output: Journal of Volcanology and Geothermal Research, vol. 20, p. 177-211.

Cross, T.A., and Pilger, R.H., Jr. (1982) Controls on subduction geometry, location of magmatic arcs, and tectonics of arc and back-arc regions: Geological Society of America Bulletin, vol. 93, p.545-562.

Dalrymple, G.B., and Lanphere, M.A. (1969) Potassium-Argon dating. W.H. Freeman, San Fransisco, California, 251 p.

Davis J., and Hawkesworth, C.J. (1993) The petrogenesis of 30-20 Ma basic and intermediate volcanics from the Mogollon Datil volcanic field, New Mexico, USA: Conrtibutions to Mineralogy and Petrology, vol. 115, p. 165-183.

Dickinson, W.R. (1979) Cenozoic plate tectonic setting of the Cordilleran region in the United States, in J.M. Armentrout, M.R. Cole, and Terbest, eds., Cenozoic paleogeography of the western United States, Society of Economic Paleontology and Mineralogy, Pacific Section, p. 1-13.

Dudas, F.O. (1991) Geochemistry of igneous rocks from the Crazy Mountains, Montana, and tectonic models for the Montana alkalic province: Journal of Geophysical Research, vol. 96, p.13,261-13,278.

Dunrud. C.R. (1962) Volcanic rocks of the Jack Creek area, southeastern Absaroka Range, Park County, Wyoming: M.S. Thesis, University of Wyoming, Laramie, 92p.

Engebetson, D.C., Cox, A., and Gordon, R.G. (1985) Relative motions between oceanic and continental plates of the Pacific Basin: Geological Society of America Special Paper 206, 59p.

Feeley, T.C., and Grunder, A. L. (1991) Mantle contribution to the Middle Teritiary silicic magmatism during the early stages of extension: the Egan Range volcanic complex, east-central Nevada: Contributions to Mineralogy and Petrology, vol. 106, p.154-169.

Fisher, F.S. (1972) Tertiary mineralization and hydrothermal alteration in the Stinkingwater mining region, Park County, Wyoming: US Geological Survey Bulletin 1332-C, 33 p.

Fleck, R.J., Sutter, J.F., and Elliot, D.H. (1977) Interpretation of discordant $^{40}Ar/^{39}Ar$ age spectra of Mesozoic tholeiites from Antarctica: Geochimica et Cosmochimica Acta, vol. 41, p.15-32.

French, A.N., and Vander Voo, R. (1978) A Summary Report of a Paleomagnetic Study of Lower Eocene Volcanics: Yellowstone National Park Library Report, 12 p.

Furlong, K.P., Chapman, D.S., and Alfeld, P.W. (1982) Thermal modeling of the geometry of subduction and implications for the tectonics of the overriding plate: Journal of Geophysical Research, vol. 87, p. 1786-1802.

Gans, P.B., and Bohrson, W.A. (1998) Supression of Volcanism During Rapid Extension in the Basin and Range Province, United States: Science, vol. 279, p. 66-68.

Gans, P.B., Mahood, G.A., and Schermer, E. (1989) Synextensional magmatism in the Basin and Range province; A case study from the eastern Basin and Range: G.S.A. Special Paper 233, 53 p.

Gest D.E., and McBirney, A.R. (1979) Genetic relations of shoshonitic and absarokitic magmas, Absaroka Mountains, Wyoming: Journal of Volcanology and Geothermal Research, vol. 6, p. 85-104.

Goldfarb, R.J., Snee, L.W., Miller, L.D., and Newberry, R.J. (1991) Rapid dewatering of the crust deduced from ages of mesothermal gold deposits; Nature, vol. 354, p.296-298.

Hague, A. (1899) Absaroka folio: U.S. Geological Survey Geol. Atlas of the United States, Folio no. 52

Hague, A., Iddings, J.P., and Weed, W.H., (1899) Geology of Yellowstone National Park: Pt II, Descriptive geology, petrography, and paleontology: U.S. Geological Survey Monograph 32, 439 p.

Hamilton, W.B., (1969) The volcanic central Andes: A modern model for the Cretaceous batholiths and tectonics of western North America, in Proceedings of the Andesite Conference, Bulletin for Oregon Department of Geology, Mineralogy and Industry, vol. 65, p.175-184.

Harlan, S.S., Mehnert, H.H., Snee, L.W., and Meen, J.K. (1991) Preliminary isotopic (K-Ar and $^{40}Ar/^{39}Ar$) age determinations from selected Late Cretaceous and Tertiary rocks in Montana: *In* Guidebook of the Central Montana Alkalic Province, D.W. Baker and R.B. Berg, eds., Montana Bureau of Mines Special Publication 100, p. 136-137.

Harlan, S.S., Snee, L.W., and Geissman, J. W. (1996) $^{40}Ar/^{39}Ar$ geochronology and paleomagnetism of Independence Volcano, Absaroka Volcanic Supergroup, Beartooth Mountains, Montana: Canadian Journal of Earth Sciences, vol. 33, p.1648-1654

Harms, T.A., and Price, R.A. (1992) The Newport fault: Eocene listric faulting, mylonitization, and crustal extension in northeast Washington and northwest Idaho; Geological Society of America Bulletin, vol. 104, p. 745-761.

Hickenlooper J.W., and Gutman, J.T. (1982) Geology of the Slough Creek Tuff, northern Absaroka volcanic field, Park County, Montana: Wyoming Geol. Assoc. 33rd Annual Field Conference Guidebook, p. 55-63.

Hodges, K.V., and Applegate, J.D. (1993) Age of Tertiary extension in the Bitterroot metamorphic core complex, Montana and Idaho; Geology, vol. 21, p.161-164.

Holder, R.W., and Holder, G.M. (1988) The Colville batholith: Tertiary plutonism in northeast Washington associated with graben and core-complex (gneiss dome) formation: Geological Society of America Bulletin, vol. 100, p.1971-1980.

Holder, G.M. , Holder, R.W., and Carlson, D.H. (1990) Middle Eocene dike swarms and their relation to contemporaneous plutonism, volcanism, core-complex mylonitization, and graben subsidence, Okanagan Highlands, Washington : Geology, vol. 18, p.1082-1085.

Hooper, P.R., Bailey, D.G., and McCarley-Holder, G.A. (1995) Tertiary calc-alkaline magmatism associated with lithospheric extension in the Pacific Northwest: Journal of Geophysical Research, vol. 100, p.10303-10319.

Humphreys, E.D. (1995) Post-Laramide removal of the Farallon slab, western United States: Geology, vol. 23, p. 987-990.

Hurlow, H.A., Snoke, A.W., Hodges, K.V. (1991) Temperature and pressure of mylonitization in a Tertiary extensional shear zone, Ruby Mountains-East Humbolt Range, Nevada: Tectonic Implications: Geology, vol. 19, p. 82-86.

Iddings, J.P. (1895) Absarokite-shoshonite-banakite series: Journal of Geology, vol.3, p.935-959.

Iddings, J.P. (1899) The igneous rocks of Electric Peak and Sepulchre Mountain: U.S. Geological Survey Monograph 32, pt. 2, p. 89-148.

Ispolatov, V.O., Dudas, F.O., Snee, L.W., and Harlan, S.S. (1996) Precise dating of the Lowland Creek volcanics, west-central Montana: (abs.) Geological Society of America Abstracts with Programs, vol. 28, p. A484.

Janecke, S.U., and Snee, L.W. (1993) Timing and Episodicity of Middle Eocene Volcanism and Onset of Conglomerate Deposition, Idaho: The Journal of Geology, vol. 101, p.603-621.

Janecke, S.U. (1994) Sedimentation and paleogeography of an Eocene to Oligocene rift zone, Idaho and Montana: Geological Society of America Bulletin, vol. 106, p. 1083-1095.

Jenner, G.A. (1989) Eocene igneous activity and related metasomatic and hydrothermal events, Bear Lodge Mountains, Crook County, Wyoming: in F.R. Karner, ed., Devils Tower-Black Hills alkalic igneous rocks and general geology: 28th International Geological Congress Field Trip Guidebook T131, p. 50-66.

Lee, T.Q., and Shive, P.N. (1983) Paleomagnetic study of the volcanic and volcaniclastic rocks from the southestern Absaroka, Wyoming: Bulletin of the Institute of Earth Sciences, Academia Sinica, vol.3, p.155-172.

Le Maitre, R.W., Bateman, P., Dudek, A., Keller, J. Lameyre Le Bas, M.J., Sabine, P.A., Schmid, R., Sorensen, H., Streckeisen, A., Woolley, A.R., and Zanettin, B. (1989) A classification of igneous rocks and glossary of terms, Blackwell, Oxford, 193p.

Lipman, P.W. (1980) Cenezoic volcanism in the western United States: Implications for continental tectonics: *in* Contnental Tectonics, Studies in Geophysisc., U.S. National Academy of Sciences, p.161-174.

Lipman, P.W., and Glazner, A.F. (1991) Introduction to middle Tertiary Cordilleran volcanism: Magma sources and relations to regional tectonics: Journal of Geophysical Research, vol. 96, p.13193- 13199.

Love, J.D. (1939) Geology along the southern margin of the Absaroka Range, Wyoming: Geological Society of America Special Paper 20, 134 p.

Love, J.D. (1964) Uraniferous phosphatic lake beds of Eocene age in intermontane basins of Wyoming and Utah: U.S. Geological Survey Professional Paper 474-E, p.E4-E40.

Love, L.L., Kudo, A.M., and Love, D.W. (1976) Dacites of Bunsen Peak, the Birch Hills, and the Washakie Needles, and their relationship to the Absaroka volcanic field, Wyoming and Montana: Geological Society of America Bulletin, vol. 87, p. 1455-1462.

Malone, David H. (1995) Very large debris-avalanche deposit within the Eocene volcanic succession of the northeatsrn Absaroka Range, Wyoming: Geology, vol. 23, no. 7, p. 661-664.

Marvin, R.F., Hearn, B.C.Jr., Mehnert, H.H., Naeser, C.W., Zartman, R.E. and Linsey, D.A. (1980) Late Cretaceous-Paleocene-Eocene igneous activity in north central Montana: Isochron West, vol.29, p.5-25.

Mitchell R.H. and Bergman, S.C. (1991) Petrology of Lamproites, Plenum, 447 p.

McGrew, A.J., and Snee, L.W. (1994) $^{40}Ar/^{39}Ar$ thermochronologic constraints on the tectonothermal evolution of the northern East Humboldt Range metamorphic core complex, Nevada: Tectonophysiscs, vol. 238, p.425-450.

McMannis, W.J., and Chadwick, R.A. (1964) Geology of the Garnet Mountain quadrangle, Gallatin County Montana: Montana Bur. Mines and Geol. Bull. 43, 47 p.

Meen, J.K. (1987) Formation of shoshonites from calcalkaline basalt magmas: geochemical and experimental constraints from the type locality: Contributions to Mineralogy and Petrology, vol. 97, p. 333-351.

Meen, J.K. (1990) Elevation of potassium content of basalt magma by fractional crystallization: the effect of pressure: Contributions to Mineralogy and Petrology, vol. 104, p. 309-331.

Meen, J.K., and Eggler, D.H. (1987) Petrology and geochemistry of the Cretaceous Independence volcanic suite, Absaroka Mountains, Montana: clues to the composition of the Archean sub-Montanan mantle, Geological Society of America Bulletin, vol. 98, p. 238-247.

Merrill, G.P. (1895) Notes on some Eruptive Rocks from the Gallatin, Jefferson, and Madison Counties Montana, Proc, U.S. National Museum, Washington, vol. 17, p.637-673

M'Gonigle, J.W.M., and Dalrymple, G.B. (1996) $^{40}Ar/^{39}Ar$ ages of some Challis Volcanic Group Rocks and Initiation of Tertiary Sedimentary Basins in Southwestern Montana; U.S. Geological Survey Bulletin 2132, 17 p.

Morris, G.A., and Hooper, P.R. (1997) Petrogenisis of the Colville Igneous Complex, northeast Washington: Implications for Eocene tectonics in the northern U.S. Cordillera: Geology, vol. 25, p.831-834.

Nelson , W.H., and Pierce, W.G. (1968) Wapiti Formation and Trout Peak Trachyandesite, northwestern Wyoming, U.S.Geological Survey Bulletin 1254-H, 11p.

Nicholls J., and Carmichael, I.S.E. (1969) Commentary on the absarokite-shoshonite-banakite series of Wyoming, U.S.A. Schweiz. Mineralgische und Petrographische Mitteilungen, vol. 49, p.47-64.

Norman, M.D., and Mertzman, S.A. (1991) Petrogenesis of Challis Volcanics from central and southwestern Idaho: trace element and Pb isotopic evidence: Journal of Geophysical Research, vol. 96, p.13279-13294.

O'Brien, H.E., Irving, A.J., McCallum, I.S. (1991) Eocene potassic magmatism in the Highwood mountains, Montana: petrology, geochemistry, and tectonic implications: Journal of Geophysical Research, vol. 96, p.13237-13260.

Parsons, W.H. (1939) Volcanic centers of the Sunlight area, Park County Wyoming: Journal of Geology, vol. 47, p. 1-26.

Peterman, Z.E., Doe, B.R., and Protska, H.J. (1970) Lead and strontium isotopes in rocks of the Absaroka volcanic field, Wyoming: Contributions to Mineralogy and Petrology, vol. 27, p.121-130.

Pierce, W.G. (1978) Geologic Map of the Cody 1° x 2° Quadrangle, Wyoming:U.S. Geological Survey Miscellaneous Field Studies Map MF-963.

Rohrer, W.L. and Obradovich, J.D. (1969) Age and stratigraphic relations of the Tepee Trail and Wiggins Formations, northwestern Wyoming: US Geological Survey Professional Paper 650-B, p.B57-B62.

Rouse, J.T. (1940) Structural and volcanic problems in the southern Absaroka Mountains, Wyoming, Geological Society of America Bulletin, vol. 51, p.1413-1428.

Royden, L. (1988) Flexure of the continental lithosphere in Italy, constraints imposed by gravity and deflection data: Journal of Geophysical Research, vol. 93, p. 7747-7766.

Royden, L. (1993) Tectonic expression of slab-pull at continental convergent boundaries: Tectonics, vol. 12, p. 303-325.

Rubel , D.N. (1971) Independence volcano, a major Eocene eruptive center, northern Absaroka volcanic province: Geological Society of America Bulletin, vol. 82, p.2473-2494.

Samson S.D., and Alexander, E.C. Jr. (1987) Calibration of interlaboratory ^{40}Ar-^{39}Ar dating standard, Mmhb-1: Chemical Geology, vol.66, p.27-34.

Scambos, T.A. (1991) Isotopic and Trace-Element Characteristics of the Central Montana Alkalic Province Kimberlite-Alnoite Suite: Montana Bureau of Mines Special Publication 100, p.93-109.

Silverberg, D.S. (1990) Denudation rates and timing of diachronous Paleogene extension in south central Idaho; Geological Society of America Abstracts with Programs, vol. 22, p.A330.

Simons, F.S., Armbrustmacher, T.J., Zilka, N.T., Federspiel, F.E., and Ridenour, J. (1979) Mineral resources of the Beartooth Primitive area and vicinity, Carbon, Park, and Sweetgrass Counties, Montana: US Geological Survey Bulletin 1391-F, 125p.

Shive, P.N., and Pruss, E.F. (1977) A paleomagnetic study of basalt flows from the Absaroka Mountains, Wyoming: Journal of Geophysical Research, vol. 82, p.3039-3048.

Shultz, C.H. (1962) Petrology of Mt. Washburn, Yellowstone National Park, Wyoming: Ph.D. dissertation, Ohio State University, Columbus, 267 p.

Smedes H.W., and Prostka, H.J. (1972) Stratigraphic framework of the Absaroka Volcanic Supergroup in the Yellowsone Park region: U.S. Geological Survey Professional Paper 729-C, 33 p.

Smith, E.I., Feuerbach, D.L., Nauman, T.R., and Mills, J.G. (1990) Mid-Miocene volcanic and plutonic rocks in the Lake Mead area of Nevada and Arizona, Geological Society of America Memoir 174, p.169-194.

Snee, L.W. (1982) Emplacement and cooling of the Pioneer batholith: Ph.D. dissertation, Ohio State University, Columbus, 320 p.

Snoke. A.W. (1993) Geologic history of Wyoming within the tectonic framework of the North America Cordillera: *In* Snoke , A.W. Steidman, J.R., and Roberst, S.M., (eds.) Geology of Wyoming: Geological Survey of Wyoming Memoir No. 5, p.2-56.

Stock, J., and Molnar, P. (1988) Uncertainties and implications of the Late Cretaceous and Tertiary positions of North America relative to the Farallon, Kula and Pacific plates: Tectonics, vol. 7, p.1339-1384.

Sundell, K.A., (1980) Geology of the North Fork of Owl Creek, Hot Springs County, Wyoming: M.S. Thesis, University of Wyoming, Laramie, 158 p.

Sundell, K.A. (1993) A geologic overview of the Absaroka volcanic province: *In* Snoke, A.W., Steidman, J.R., and Roberts, S.M., (eds.) Geological Survey of Wyoming Memoir No. 5, p. 480-506.

Sundell, K.A., and Eaton, J.G. (1982) Stratigraphic relations within the southeastern Absaroka volcanic sequence, northwestern Wyoming: Wyoming Geological Association Guidebook, Thirty-Third Annual Field Conference, p.65-70.

Sundell, K.A., Shive, P.N., and Eaton, J.G. (1984) Measured sections , magnetic polarity, and biostratigraphy of the Eocene Wiggins, Tepee Trail, and Aycross Formations within the southeastern Absaroka Range, Wyoming: Wyoming Geological Association Earth Science Bulletin, vol. 17, 1984.

U.S. Geological Survey (1975) Geologic Map of Yellowstone National Park: Miscellaneous Investigation Series Map I-711.

Wedow, H.Jr., Gaskill, D.L., Bannister, P.D., Pattee, E.C. (1975) Absaroka Primitive Area, Montana: U.S. Geological Survey Bulletin 1391-B, 115 p.

Wilson, W.H. (1963) Correlation of volcanic rock units in the southern Absaroka Mountains, northwest Wyoming: University of Wyoming Contributions to Geology, vol.2, p.13-20.

Williams, T.R., Harakal, J.E., and Armstrong, R.L. (1976) K-Ar dating of Eocene volcanic rocks near Drummond, Montana: Northwest Geology, vol. 5, p. 21-25.

CHAPTER 2

Mineralogic and Geochemical Variability in Shoshonitic Magmatism from the Type Locality: Absaroka Volcanic Province, Southwest Montana and Northern Wyoming, USA

Margaret M. Hiza and Anita L. Grunder

To be submitted to the *Journal of Petrology*, Oxford University Press

71 pages

INTRODUCTION

The middle Eocene Absaroka volcanic province contains the remains of more than ten well-preserved volcanic centers, and consists of 25,000 km^2 of mafic alkaline lava flows and dikes, intermediate and felsic hypabyssal intrusive and volcanic rocks, and intercalated volcaniclastic sediments. Individual eruptive centers roughly coincide with Precambrian zones of structural weakness that extend more than 250 kilometers (150 miles), from southwestern Montana through northwestern Wyoming (Chadwick 1970; Reid, 1957). $^{40}Ar/^{39}Ar$ age data from intrusions and ash-flow tuff deposits exhibit a northwest to southeast age progression from 53 to 43 Ma (Figure 2.1). Volcanic eruptions within the Absaroka volcanic province were voluminous from 49 to 47 Ma, and broadly synchronous throughout the Absaroka volcanic province during this brief period (Chapter 1).

Mafic lavas (<55% SiO2) are characteristically potassic throughout the Absaroka Volcanic Province, which is known for the type occurrence of the absarokite-shoshonite-banakite series (Iddings, 1895; See Chapter 1). These rocks are described by Iddings (1895), Nicholls and Carmichael (1969), and Geist and McBirney (1979) as volcanic rocks containing olivine and augite, with groundmass pyroxene, sanidine, and plagioclase, ± apatite, groundmass leucite, and phlogopite. Although famous for the occurrence of alkaline igneous rocks, the few existing modern petrologic and geochemical studies in this volcanic province have produced disparate results. Nicholls and Carmichael (1969) examined shoshonites which contained phenocrysts of both orthopyroxene and clinonopyroxene, and recognized that some shoshonites may have a tholeiitic aspect. Work by Geist and McBirney (1979) used major- and trace- element whole rock analyses and microprobe data, to demonstrate that shoshonite can be produced as a fractionation product of absarokite by the removal of olivine and augite. No orthopyroxene-bearing shoshonites were described in this study. However, petrographic evidence suggested additional plagioclase fractionation in shoshonites. Geochemical and experimental work by

Meen (1985, 1987, 1990) on samples from the Independence volcanic center of the northeastern Absaroka province did not include any absarokite. In contrast to earlier studies, Meen (1990) suggested that shoshonite is a fractionation product of olivine-free anhydrous basaltic-andesite under conditions of elevated pressure.

In order to characterize the processes involved in producing this diverse group of shoshonitic rocks, this study seeks to compare province-wide petrological and geochemical aspects of the Absaroka province magmatism through detailed mapping and sampling from four representative volcanic centers. Because the Absaroka volcanic province had been subdivided into subparallel belts of eruptive centers by Chadwick (1970), representative volcanic centers chosen for study are the Hyalite and Crandall volcanic centers from the northeastern volcanic belt, and the Ishawooa and Rampart volcanic centers of the southwestern volcanic belt. These volcanic centers were also chosen to represent regional map groups of Smedes and Prostka (1972), with the Hyalite volcanic center representing the Washburn Group, the Crandall volcanic center representing the Sunlight Group, and the Ishawooa and Rampart volcanic centers representing the Thorofare Creek Group (See Chapter 1, Figures 1.1 and 1.2). Samples from peripheral lava flows, dikes, and ash-flow tuffs are also included, in order to portray the compositional spectrum of rock types present in the Absaroka volcanic province. Age and geochemical relationships which defined volcanic belts and group subdivisions were revised in Chapter 1, but are retained herein for reference and comparison to previous studies. This study finds that although eruptive products of volcanic centers have characteristics which are broadly similar, that each volcanic center exhibits unique mineralogical and trace element characteristics. Investigating the conditions responsible for generating characteristically potassic Absaroka volcanism contributes to a broader understanding of the mechanisms which produce shoshonitic lavas, at the type locality.

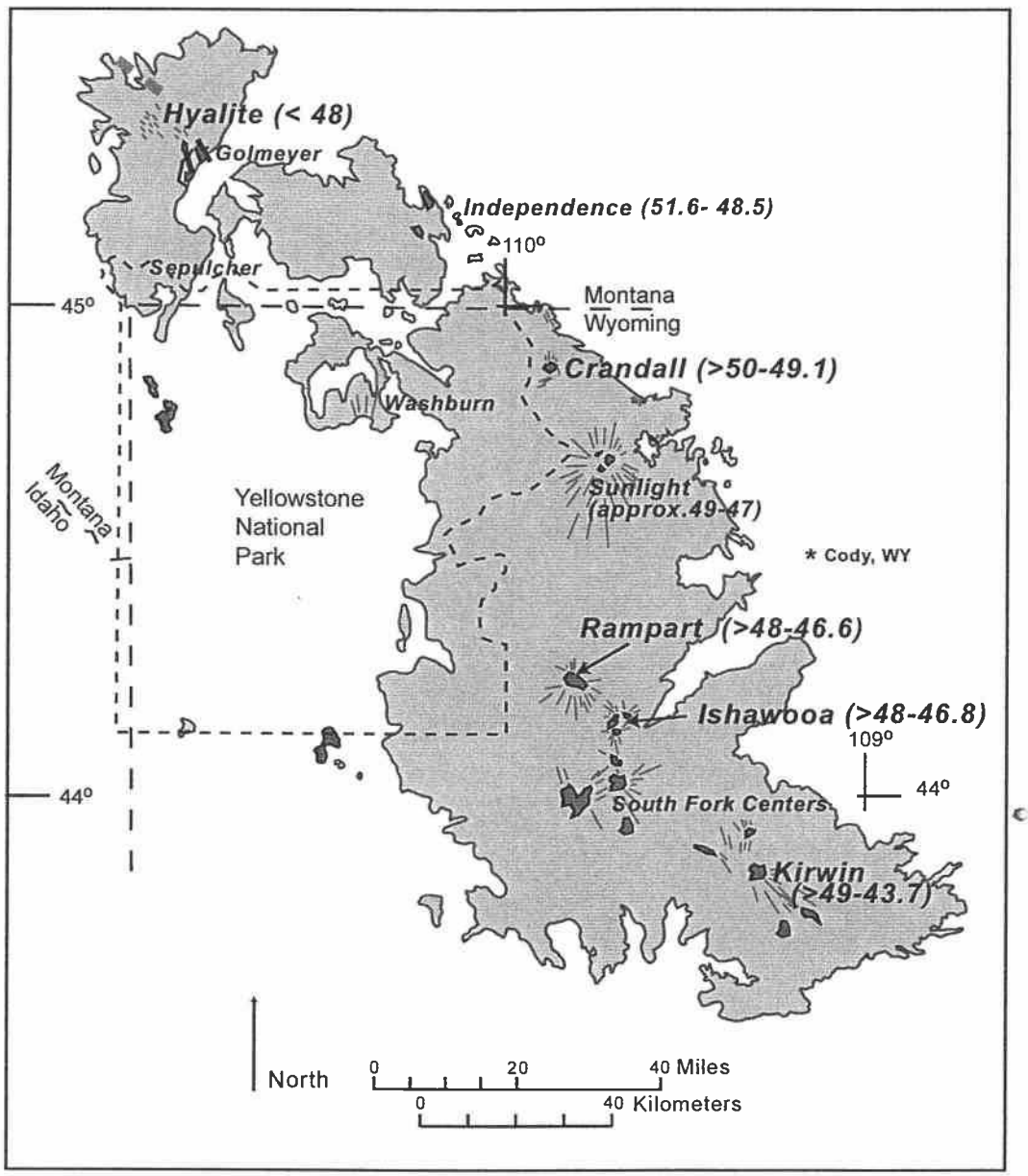

Figure 2.1. Schematic map showing distribution of igneous rocks and volcanic centers of the Absaroka volcanic province. Large intrusions and dikes are shown in gray and black. Estimated age and duration of eruptions at volcanic centers are shown in Ma, based on stratigraphic correlations in Chapter 1. (Modified after Chadwick, 1970)

ANALYTICAL METHODS

A minimum of 50 hand specimens from separate units were sampled from each of the Crandall, Hyalite, and Ishawooa volcanic centers, and supplemented by seven additional samples from the Rampart volcanic center. These units were mapped and described, with 20 or more specimens from each of the larger sample suites selected for geochemical analyses, based on the degree of weathering and alteration. Twenty additional samples of lava flows, dikes, and ash-flow tuff peripheral to volcanic centers were also analyzed. Major element analyses, presented here in oxide weight percent, were obtained by X-ray flourescence techniques (XRF); analytical procedure, accuracy and precision are described by Taggart et al, (1987). Trace element concentrations, in parts per million, were determined by neutron activation (INAA) according to the procedures outlined by Baedecker and McKown (1987). Sample powders prepared for XRF analyses were fused and molded into smooth, flat-surfaced glass discs. XRF analyses were perfomed on a Phillips PW 1600 simultaneous X-ray spectrometer with 26 fixed channels and 2 sequential scanning channels, at the analytical laboratories of the U.S. Geological Survey, Denver, Colorado. LOI were obtained from a 0.8 g portion of each sample powder which were ignited and tared in a Pt-Au crucible sample, at 925°C for 45 minutes, cooled in a dessicator and reweighed. INAA analyses were obtained from sample powders together with standard aliquants which were weighed (0.5-1.0g) and sealed in polyethelene vials and irradiated in packages of 33-37 samples and irradiated for three separate time intervals in the TRIGA reactor of the U.S. Geological Survey in Denver, Colorado.

Major elements, Sr and Cr concentrations of individual phenocrysts were analyzed using the Cameca SX50 electron microprobe at Oregon State University. Olivine, pyroxene, feldspar and groundmass phenocrysts from selected samples of the Crandall, Hyalite, Ishawooa, and Rampart volcanic centers, and peripheral basanite were examined using carbon-coated polished thin sections. Measurements were calibrated using laboratory standards of similar mineralogy, and repeated ten times to measure reproducibility. Analyses were conducted with 15 kV accelerating

voltage and a 30 nA beam current. The ZAF correction procedure was used for all quantitative analyses. Three to five points were analyzed on each phenocryst from core to rim depending on phenocryst size, with additional single point analyses of groundmass phases.

GEOLOGY AND MINERALOGY OF VOLCANIC CENTERS

All four volcanic centers, Crandall, Hyalite, Ishawooa and Rampart, are built upon broad platforms of fissure-fed shoshonite, trachyandesite, and absarokite. Although shoshonites at each volcanic center exhibit distinct textures, basal flows tend to be fine grained and sparsely porphyritic to aphanitic, with phenocrysts of olivine and clinopyroxene. Lava flows and interbedded volcaniclastic sediments characteristically exhibit primary dips away from volcanic centers, especially at Rampart and Ishawooa. These two volcanic centers exhibit the characteristics of dissected stratovolcanoes, or large summit cones, built upon earlier mafic flows; whereas Crandall and Hyalite volcanic centers have a broader morphology and exhibit greater similarities to shield volcanoes. At the Rampart and Ishawooa volcanic centers, late-stage dikes, most of which are felsic to intermediate in composition, cross-cut fissure fed lavas, and exhibit a radial pattern around central hypabyssal intrusions. At the Hyalite and Crandall volcanic centers associated dikes exhibit strong preferred linear orientations, and tend to be more mafic. Late dome- and sill-forming dacitic intrusions are associated with the Ishawooa, Rampart, and Hyalite volcanic centers, although they are less common and not centralized features at Hyalite. These dacites are crystal-rich, medium-grained porphyritic rocks with phenocrysts of plagioclase, hornblende, biotite and quartz. Many contain primary epidote phenocrysts which occur in the groundmass, and are enclosed within phenocrysts of plagioclase. In addition, dacites commonly have pyroxenite and amphibolite xenoliths, which are especially numerous at the Ishawooa volcanic center. Rock types which are peripheral to volcanic centers include basanite, absarokite, and shoshonite flows, rhyolite, rhyodacite and trachyte ash-flow tuffs.

The Crandall Volcanic Center

The Crandall volcanic center of the Sunlight Group in the northeastern belt of the Absaroka volcanic province consists of early fissure-fed shoshonitic lava flows which erupted prior to 50 Ma (Figure 2.1). Early eruptions are constrained by the 50.2 ± 0.05 Ma age of a trachyte ash-flow tuff deposited at the top of the stratigraphic sequence. Subsequent eruptions filled a central volcanic depression with minor shoshonite flows, cross-cut by a latite intrusion with an age of 48.9±0.05 Ma. These flows are also intruded by a complexly-zoned central ring dike and numerous plagioclase-phyric dikes and sills within the central depression. Early lavas are shoshonites, whereas late eruptions and cross-cutting intrusions have a broader range in chemical composition from absarokite, high-K basaltic andesite, to banakite.

Mafic lavas have phenocrysts of augite and olivine, with plagioclase phenocrysts becoming more prominent in later intrusions. Early shoshonites (>50 Ma) are fine grained, with 10-15% augite phenocrysts in a granular groundmass of plagioclase (Figure 2.2). Trachyte ash-flow tuff of variable thickness, deposited above these early flows, is crystal-poor, with 5-10 % plagioclase, biotite and amphibole phenocrysts (HM1795). The upper surface of this unit is uneven, with small-scale (≤10 cm) cross-bedding. Sills and dikes which invade these flows exhibit variable textures, and typically include plagioclase phenocrysts. Many dikes have anhedral to skeletal plagioclase (2-4 mm) in a microlitic groundmass of feldspars and magnetite. Late cross-cutting intrusions are mafic, and vary from fine-grained cryptocrystalline rocks, to coarse-grained granular porphyritic rocks with phenocrysts of plagioclase, augite, and olivine. The central ring dike consists of a fine-grained mafic outer zone, and inner silicic porphyritic portion with calcic-plagioclase phenocrysts. A prominent mafic sill (HM1995) within the volcanic center contains large calcic-plagioclase phenocrysts (up to 3 cm) which enclose phenocrysts of augite, together with olivine and augite glomerocrysts in a pilotaxitic groundmass of plagioclase and spinel.

The Ishawooa Volcanic Center

The Ishawooa volcanic center of the Thorofare Creek Group, has been considered part of the southwestern belt of Absaroka volcanic province (Chadwich, 1970; Smedes and Prostka, 1972). At this volcanic center, early plateau forming absarokite and shoshonite flows overly volcaniclastic strata interpreted as landslide deposits (Malone, 1995) or as deposits deformed by seismic liquefaction (Decker, 1990). The center itself is defined by cross-cutting dikes of shoshonite, banakite, and dacite composition, oriented in a radial pattern surrounding a central cluster of dacite domes. A biotite mineral separate from a banakite dike which cross cuts the sampled flow sequence on Ishawooa Mesa has an age of 46.74 ± 0.11, which provides a minimum age for eruptive activity at the Ishawooa volcanic center (Figure 2.1).

Lava flows at the Ishawooa volcanic center have petrographic and mineralogic features described by Iddings (1899) as typical of the absarokite-shoshonite-banakite series. The lowest flow in the sequence of sampled strata (ISH5095) is an absarokite with 10% Fo_{75} olivine which in some cases completely surrounds euhedral crystals of apatite, together with 10-15% augite phenocrysts in a holocrystalline groundmass of sanidine and plagioclase (Figure 2.2). Overlying shoshonite flows become increasingly aphyric, with olivine disappearing from the assemblage and ≤ 5% aegerine-augite in lavas at the top of the sequence (ISH4695). Early eruptions at Ishawooa are followed by more diverse magmatism, which includes synchronous eruption of absarokite (ISH995) and rhyolite, together with a larger volume of dacite(ISH695). Several fine-grained silicic flows and dikes which occur late in the sequence have 1-3 mm orthopyroxene with augite rims, smaller zoned augite phenocrysts (<1 mm), together with sparse (<5%) olivine and biotite in a cryptocrystalline to hypocrystalline groundmass (ISH795, ISH2995). Silicic rocks with similar characteristics also occur as lava flows at the Rampart volcanic center (HPt496). The general petrographic features of these samples are broadly similar to previous sample descriptions of banakite (Iddings, 1895: Nicholls and Carmichael,

1969). Similar olivine- and pyroxene-rich silicic lavas have also been found in other parts of the province, including flow breccia associated with the Lamar River Formation in Yellowstone National Park.

Rampart Volcanic Center

Rampart volcanic center of the Thorofare Creek Group is one of the most spectacularly exposed and least studied of volcanic centers in the Absaroka province, because of its remote location (Figure 2.1). More than 16 km across at the base, it consists of extensive absarokite and shoshonite lava flows interfingered with volcaniclastic strata with primary 10° dips to the north, south, east and west, away from a central banakite intrusion. A biotite separate from this intrusion gives an age of 46.55 ± 0.11 Ma, which indicates that eruptions from the Rampart and Ishawooa volcanic centers were coeval. Dikes radial to the central intrusion are primarily intermediate to felsic, but of variable composition. A limited number of samples of lava flows from the Rampart center were analyzed for this study, these lie between and include ash-flow tuff deposits and are between 48.8 and 47.7 Ma (Chapter 1). Geochemical analyses from Rampart samples are intended to supplement data from the adjacent Ishawooa volcanic center, in order to compare overall geochemical trends of the northeastern and southwestern volcanic belts.

Mafic lavas at Rampart exhibit similarities to those of the Ishawooa volcanic center. One exception is a mafic vitrophyre with rounded, skeletal 2- 3 mm An_{60} plagioclase phenocrysts, and $\leq$1 mm phenocrysts of olivine, augite, and sanidine (HPt196). This flow occurs at the base of a stratigraphic sequence that contains shoshonites, banakite and dacite that show striking similarity to flows and dikes at Ishawooa (Figure 1.2). A crystal-rich dacitic tuff from the top of the stratigraphic sequence, with >85% phenocrysts of amphibole, biotite, plagioclase and quartz is also included (HPt696). The upper portion of this tuff is less crystal-rich, but was not sampled for geochemistry because it was cross-bedded with ripple laminae, and contained a large percentage of rounded rock fragments.

The Hyalite Volcanic Center

The Hyalite volcanic center of the Washburn Group, in the northeastern belt of the Absaroka volcanic province, is composed of moderately alkaline trachyandesite flows and dikes and interbedded volcaniclastic strata. Dacite domes also are within this sequence, but were considered too altered to include in geochemical analyses. The sequence of flows sampled from the Hyalite volcanic center overlie a well developed unconformity in the Golmeyer Creek volcanics of the Point of Rocks volcanic center, making the Hyalite Peak center younger than other igneous centers in the northeastern volcanic belt. The eruption of these lavas occurred after igneous activity at the Crandall volcanic center had ceased and during late igneous activity at the Ishawooa and Rampart volcanic centers (Figure 2.1).

A vertical sequence, 1000 m thick, consisting of twenty stacked lava flows and related dikes was analyzed in this study. Flows sampled at the Hyalite volcanic center consist of a bimodal assemblage, and do not have the mineralogy or petrographic features of the absarokite-shoshonite-banakite series described by Iddings (1899). The base of the stratigraphic sequence consists of aphyric to sparsely porphyritic trachyandesite (HGB1395) with < 5% augite phenocrysts in a microlitic groundmass of plagioclase and Fo_{60-65} olivine. Flows higher in the sequence are fine grained, porphyritic trachyandesite with augite, hypersthene and plagioclase phenocrysts with either an intersertal texture (HGB795), or a glomerophyric and hypocrystalline texture (HGB1995) (Figure 2.2).

Peripheral Lavas

Additional samples from the northern Absaroka volcanic province include basanite and shoshonite flows, a monzogabbro intrusion, an andesite dike, dacite and rhyolite intrusives. A basanite flow (BHM195) sampled from the northern Absaroka volcanic province overlies the upper erosional surface of Slough Creek Tuff, and is considered part of the younger post-unconformity eruptive sequence <48 Ma (Chapter 1). The basanite is extremely fine grained with 10% phenocrysts ≤ 0.5 mm of olivine (Fo_{80}) and augite, with groundmass spinel and nepheline, and alkali feldspar replacing leucite. Other peripheral rocks sampled for geochemistry include intermediate to silicic intrusions and Slough Creek Tuff rhyodacite (YSC495, YSC595). Dacites are generally metaluminous, with plagioclase, amphibole, biotite and quartz. However, some of these intermediate rock types are fine grained and exhibit mineralogic diversity which generally includes clinopyroxene and orthopyroxene in a fine-grained trachytic groundmass of plagioclase and chromite ± sanidine, biotite and amphibole. Rhyolite from late eruptions, which are more numerous in the southern Absaroka volcanic province are generally stony felsites (WR1694). Rhyolites with visible phenocrysts commonly have 5-15% biotite, 5-10% plagioclase, and lesser amounts of sanidine and quartz. Samples of silicic intrusions include the Dunrud Peak rhyolite (WR1394) in the extreme southeastern AVP, which has an age of 43.68 ± 0.09 Ma (sanidine), and is the youngest known eruption of this volcanic province (Figure 2.1).

Samples from the northwestern part of the Absaroka Volcanic Province include two shallow intrusions. One sample from the Golmeyer Creek volcanics, which crops out north of Yellowstone Park, while the second is from the Sunlight Valley, south of the Crandall volcanic center (Figure 2.1). The Sunlight Valley intrusion, sampled at White Mountain, is a porphyritic monzogabbro, with 1-3 cm phenocrysts of plagioclase with sanidine rims, biotite, augite, and minor olivine, in a fine-grained holocrystalline groundmass of sanidine, hornblende and Ti-magnetite

(Smg496). This hypabyssal intrusive, of the Sunlight volcanic center, has an age of 48.21±0.08 (biotite), which is similar in age to early flows from the Ishawooa and Rampart volcanic centers, and younger than late intrusions from the Crandall volcanic center (Chapter 1).

The dike sampled from the Golmeyer Creek volcanics (PR295) precedes eruption of the overlying Hyalite Peak volcanics, and is separated from them by an angular unconformity. The Golmeyer dike has a maximum age of 51.56 ± 0.2 Ma, and is andesitic in composition with phenocrysts of biotite, hornblende and plagioclase.

Studied samples also include absarokite and shoshonite from the Kirwin area in the southern Absaroka volcanic province, and shoshonite from Yellowstone Park, mapped as Elk Creek basalt (Prostka et al., 1975). Shoshonites in the Kirwin area erupted later than those at the Crandall center, and probably erupted before or during the first magmatic activity at Ishawooa and Rampart (Chapter 1). They are typically medium- to fine-grained porphyritic flows with 10-15% plagioclase (An_{50-60}), 10% augite phenocrysts and olivine commonly replaced by iddingsite or bowlingite, in a pilotaxitic holocrystalline groundmass of sanidine, plagioclase and magnetite (WR1094). In contrast to shoshonites, absarokites from the Kirwin volcanic center lack plagioclase phenocrysts and have a greater proportion of olivine and clinopyroxene (WR1494). Overall, absarokites are finer-grained with up to 25% augite and olivine phenocrysts. Shoshonites exhibit more diversity and may be fine-grained and aphyric to coarse-grained and porphyritic. Fine-grained varieties typically have augite ± olivine in a holocrystalline groundmass of plagioclase, sanidine and Fe-Ti oxides. Porphyritic varieties, such as the Elk Creek basalt, tend to have granular textures with large plagioclase phenocrysts, subordinate augite ± hypersthene, and <5% olivine which is commonly replaced by bowlingite (YT194).

1a)

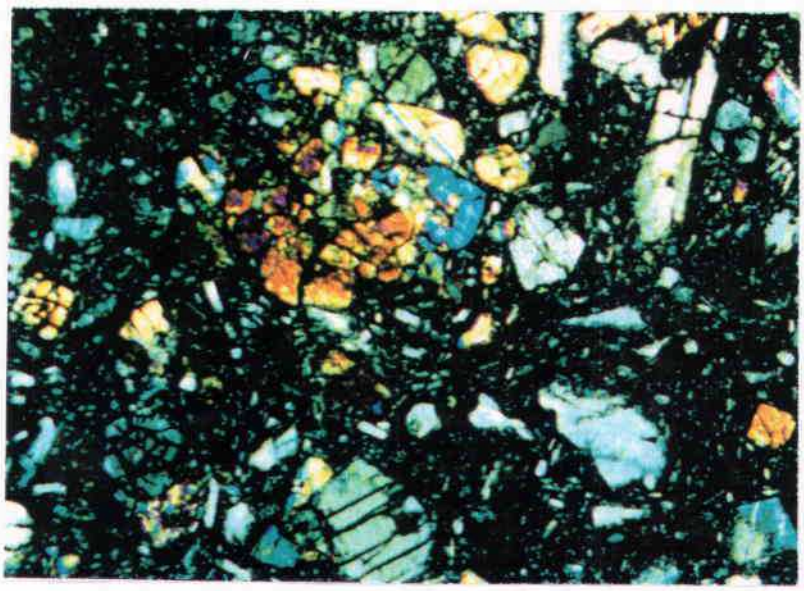

1b)

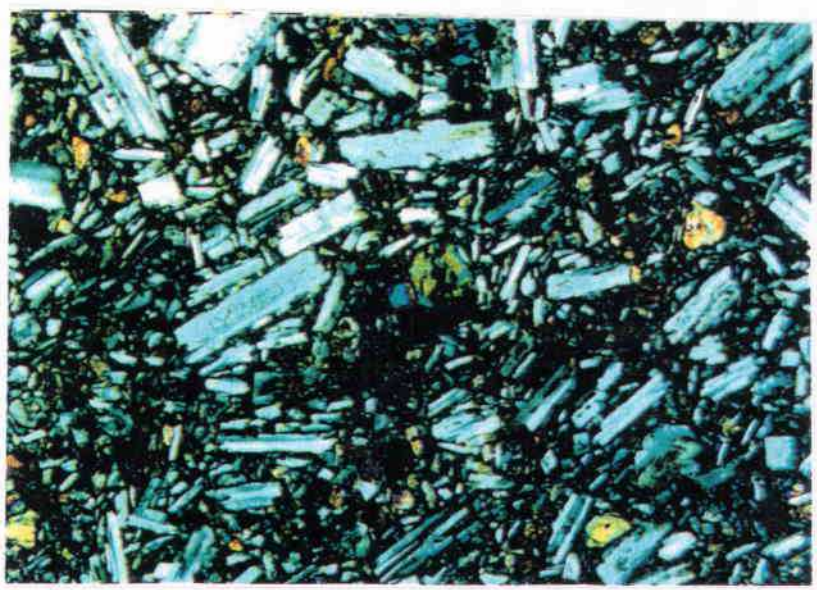

Figure 2.2 Photomicrographs of samples from different volcanic centers of the Absaroka province: 1) Samples from the Crandall volcanic center showing a) Augite-phyric sample HM895 from flow lower in the stratigraphic sequence, and b) granular texture of plagioclase-bearing porphyritic sample HM1195, typical of later dikes and intrusions; (Crossed polarized light for all photos; field of view = 4 mm across.)

2)

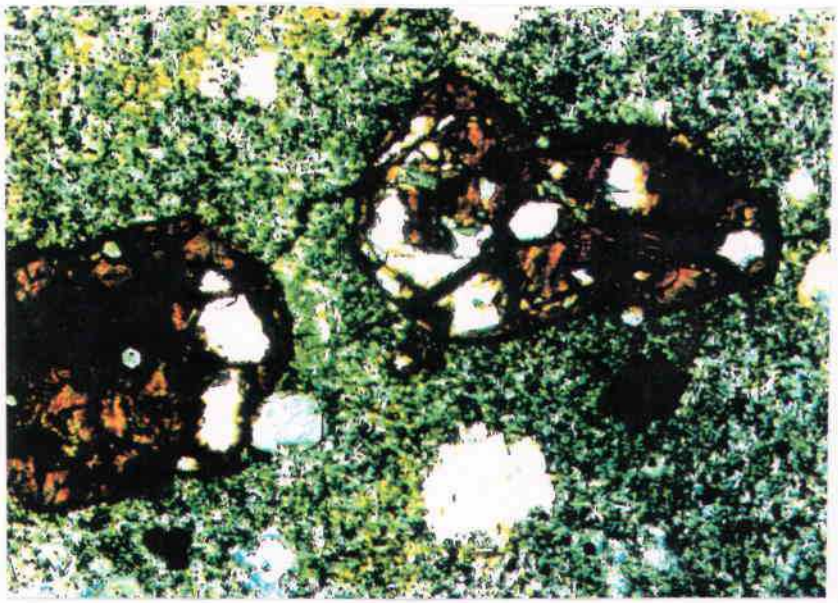

3)

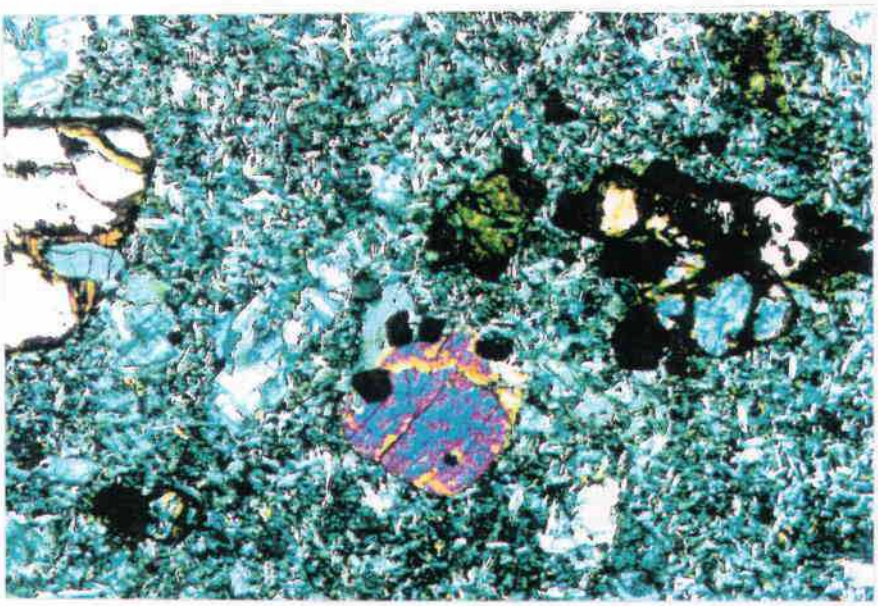

Figure 2.2 (continued). 2) Absarokite ISH5095 from the Ishawooa volcanic center showing olivine (altered to bowlingite) surrounding phenocrysts of apatite in a groundmass of sanidine and plagioclase; 3) Absarokite HPt296 from the Rampart volcanic center. Phenocrysts include olivine surrounding apatite (on the right), augite and Ti-magnetite in a groundmass of sanidine and plagioclase. (Crossed polarized light for all photos; field of view = 4 mm across.)

4a)

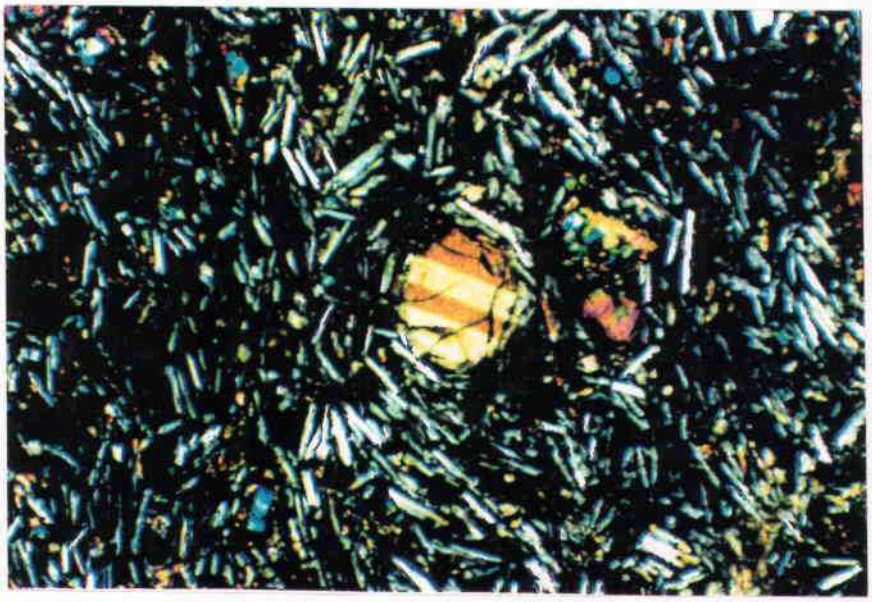

4b)

Figure 2.2 (continued). 4) Photomicrographs from the Hyalite volcanic center samples: a) Sample HGB1395 from the base of the flow sequence with a fine grained microlitic texture with small phenocrysts of augite (center), with groundmass olivine and plagioclase, and b) Sample HGB395 from the top of the sequence with plagioclase, augite and magnetite in hyaline groundmass. (Crossed polarized light for all photos; field of view = 4 mm across.)

COMPOSITION OF VOLCANIC CENTERS

The composition of mafic samples range from basanite and absarokite to shoshonite and banakite (Figure 2.3). Shoshonite (or trachyandesite) is the predominant rock type at each of the four volcanic centers, although shoshonitic lava flows from separate regions of the volcanic province exhibit different geochemical trends. More silicic rock types are less potassic and include calc-alkaline andesite, trachyte, metaluminous dacite, rhyodacite and rhyolite (Table 2.1). Mafic samples exhibit enrichment in LREE (rare earth elements, La through Sm) and most are depleted in HFSE (high field strength elements) particularly Ti and Ta, similar to subduction-arc magmas. Despite these overall similarities, each volcanic center or group of volcanic centers has distinctive composition and mineralogy.

Mafic compositions for each volcanic center show important contrasts: 1) Mafic samples from the Ishawooa and Rampart volcanic centers, as well as an intrusion in the vicinity of the Sunlight volcanic center have nepheline-normative compositions. 2) Mafic end-member samples from Crandall, are olivine and hypersthene normative. 3) Mafic samples from the Hyalite volcanic center are quartz- and hypersthene-normative trachybasalt to trachyandesite (Table 2.2). 4) Mafic flows and dikes sampled from peripheral areas are olivine normative, and include basanite from the northeastern belt of the Absaroka volcanic province, and samples from the Kirwin area of the southwestern belt.

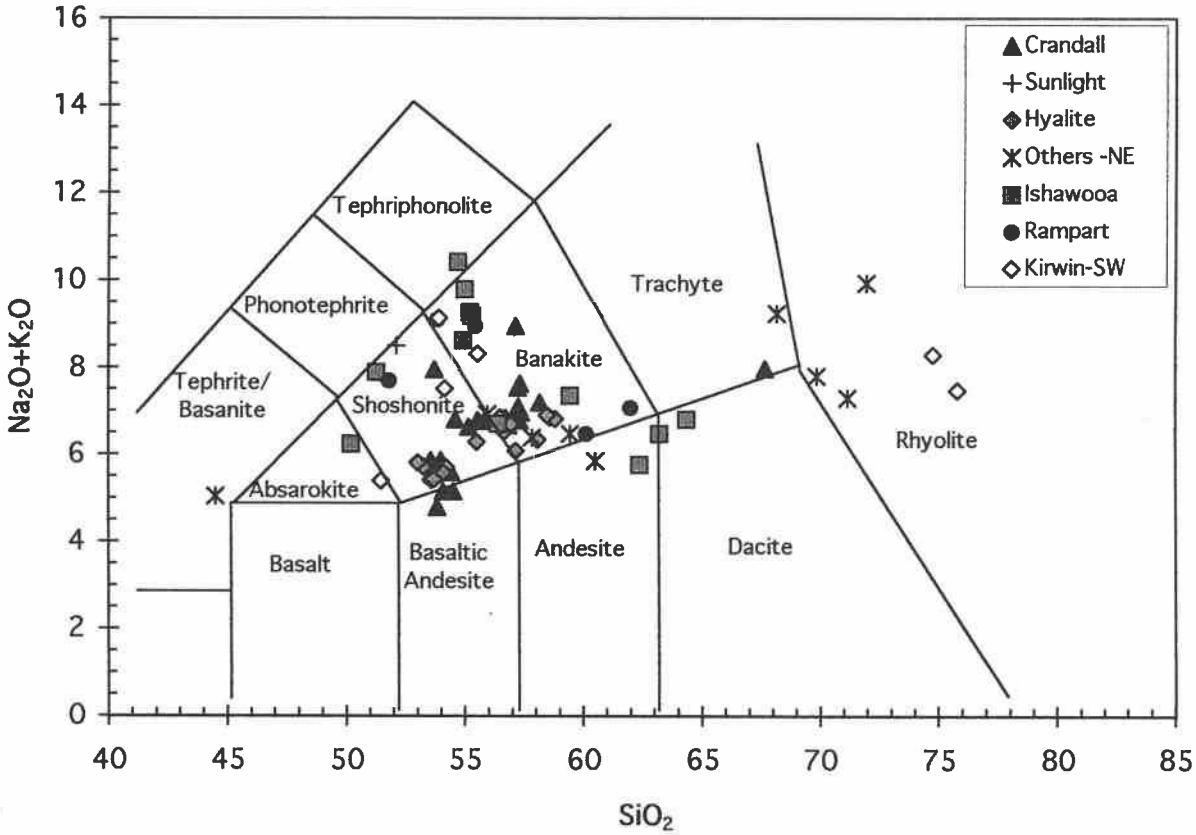

Figure 2.3. Chemical classification and nomenclature of volcanic rocks showing distribution of sampled rock types from the Absaroka volcanic province using the total alkalis versus silica diagram (subdivisions from Le Maitre et al., 1989). Samples recalculated to 100% on an H_2O- and CO_2- free basis. Samples from each volcanic center and region in the Absaroka volcanic province specified with separate symbols.

Table 2.1. Compositions of Selected Igneous Rocks, Absaroka Volcanic Province, Wyoming and Montana

	Crandall Volcanic Center												*Sunlight Center*
wt%	**HMf 895**	**HMf 294**	**HMf 1894**	**HMaf 1795**	**HMs 1995**	**HMd 2195**	**HMd 2295**	**HMd 1195**	**HMi 594**	**HMi 6A94**	**HMi 694**	**HMi 794**	**Smg 496**
SiO_2	52.79	53.07	53.64	65.56	52.56	52.77	54.02	55.6	53.48	53.83	57.77	56.67	51.1
Al_2O_3	15.92	15.66	16.01	15.56	16.65	15.98	15.78	16.37	16.54	14.22	16.68	16.78	17.92
Fe_2O_3*	9.28	8.17	8.81	3.09	7.86	7.98	8.28	6.59	8.29	8.96	6.72	7.17	8.07
MgO	5.69	7.15	6.20	1.29	4.77	4.51	4.59	3.93	5.9	8.27	3.84	3.78	3.96
CaO	7.61	7.83	7.91	2.82	5.92	6.38	6.79	5.12	7.82	8.60	5.50	5.65	6.27
Na_2O	3.33	3.28	3.52	3.55	3.93	3.36	3.47	3.63	3.26	3.11	3.85	4.07	4.61
K_2O	2.2	2.13	1.56	4.09	3.70	3.06	2.86	3.55	2.29	1.66	3.17	3.29	3.57
TiO_2	0.86	0.79	0.78	0.36	1.05	1.00	0.93	0.94	0.81	0.80	0.78	0.78	0.99
P_2O_5	0.36	0.36	0.33	0.21	0.83	0.56	0.52	0.50	0.39	0.33	0.45	0.46	1.12
MnO	0.13	0.10	0.14	0.07	0.11	0.12	0.15	0.12	0.12	0.15	0.11	0.13	0.11
LOI	1.48	0.38	0.44	2.40	1.86	2.46	1.75	2.93	0.21	-0.04	0.20	0.10	1.25
Total	99.65	98.92	99.34	99.00	99.24	99.18	99.14	99.28	99.11	99.89	99.07	98.88	99.00
						Parts Per Million							
Ni	55	187	62	3.7	69	74	33	68	75	90	31	42	47
Cr	101	425	220	17	181	130	80	119	207	345	66	54	81
Sr	1140	1050	947	770	1670	851	1310	967	1220	805	1200	1260	1430
Rb	48	49	31	99	109	67	86	85	33	29	75	75	140
Ba	1160	1080	918	1860	1480	1340	1720	1620	1690	844	1780	1860	1270
Th	4.63	4.13	2.27	11.8	12.0	7.8	11.5	8.28	3.12	2.17	10.5	10.1	14.5
La	38.0	35.3	24.6	56.6	74.9	52.7	72.2	54.5	44.6	21.8	55.1	56.6	87.8
Nd	31.8	30.3	23.5	32.7	49.8	44.6	56.5	44.5	37.3	21.6	41.8	41.9	60.9
Sm	5.86	5.35	4.74	4.58	7.65	7.62	9.06	7.3	6.23	4.33	6.76	6.86	8.8
Yb	1.48	1.29	1.44	0.986	1.40	1.77	1.82	1.52	1.41	1.36	1.47	1.50	1.55
Lu	0.217	0.186	0.211	0.152	0.201	0.257	0.257	0.218	0.201	0.195	0.207	0.216	0.229
Zr	119	93.7	90.7	152	160	150	166	184	108	95.9	164	118	215
Hf	2.56	2.75	2.37	4.4	3.84	4.04	4.33	4.24	2.52	2.17	3.85	3.69	4.48
Ta	0.28	0.31	0.20	0.72	0.69	0.67	0.69	0.73	0.22	0.24	0.56	0.34	0.95
Sc	23	21	23.7	5.2	15	17	16	13	23	28	15	69	11

Table 2.1. (Continued) Compositions of Selected Igneous Rocks, Absaroka Volcanic Province, Wyoming and Montana

	Oldest to Youngest from the Ishawooa Volcanic Center											*Kirwin Area Samples*		
wt%	**ISH 5095**	**ISH 4995**	**ISH 4695**	**ISH 895**	**ISH 995**	**ISH 695**	**ISH 795**	**ISH 3695**	**ISH* C95**	**ISH 2995**	**WRf 1094**	**WRd 1494**	**WR 1694**	**WRi 1394**
SiO_2	50.2	53.1	53.0	53.4	49.5	63.1	55.2	58.5	43.8	61.4	52.5	50.1	74.0	73.1
Al_2O_3	16.99	19.5	19.1	18.2	15.1	16.5	15.2	17.6	12.2	16.0	16.82	14.3	15.4	14.3
Fe_2O_3*	8.56	5.76	4.89	6.95	11.2	3.86	6.7	4.81	9.57	4.79	6.94	8.20	0.69	0.64
MgO	5.41	1.79	2.19	2.91	6.27	2.51	5.71	3.43	13.3	4.39	5.04	9.80	0.24	0.20
CaO	6.65	4.90	4.89	5.12	8.18	4.21	6.55	5.6	12.0	5.26	6.35	7.8	1.21	1.20
Na_2O	4.33	4.32	4.82	5.51	3.93	4.29	3.32	4.14	2.23	4.58	3.63	3.2	3.41	3.70
K_2O	3.09	5.49	3.78	2.68	1.95	2.16	3.04	2.78	1.04	1.00	3.46	1.9	3.87	4.40
TiO_2	0.95	0.79	0.81	0.89	1.08	0.44	0.90	0.51	1.80	0.51	0.85	1.3	0.07	0.05
P_2O_5	0.95	0.60	0.64	0.97	0.77	0.26	0.49	0.38	0.13	0.21	0.58	0.67	0.08	0.04
MnO	0.15	0.12	0.13	0.11	0.19	0.06	0.10	0.10	0.12	0.10	0.11	0.11	0.08	0.11
LOI	2.67	2.42	3.31	1.95	1.18	2.06	2.08	1.09	2.50	1.61	2.46	1.9	2.0	0.89
Total	100	98.79	98.9	98.7	99.35	99.45	99.3	98.9	98.69	99.85	98.70	99.28	99.6	98.63
	Parts Per Million													
Ni	32.7	3.9	4.9	31	43	33	111	50	296	99	79	200	6.4	4.6
Cr	87	1	3	52	83	56	22	61	352	190	240	488	0.2	0.9
Sr	1680	2100	2240	1820	1300	1020	1050	1810	572	998	1720	960	306	160
Rb	85.5	123	79	116	95	41	93	65	11	87	92	42	94	110
Ba	2390	2960	2930	3900	2110	1800	1750	3150	768	1290	2790	960	1630	1540
Th	6.76	8.27	8.24	9.01	5.76	8.19	17.7	17.7	1.34	3.94	8.57	8.00	5.44	6.00
La	48.5	53.2	53.1	59.5	43.3	49.9	76.4	14.5	23.7	29.8	63.2	43.0	12.7	14.5
Nd	40.8	41.7	41.2	44.3	38.8	32.5	58.4	65.0	37.3	21.9	47.1	46.0	10.3	12.0
Sm	7.01	6.55	6.65	6.69	6.91	4.31	8.35	7.67	7.78	3.21	6.95	6.40	1.90	2.01
Yb	1.58	1.52	1.61	1.28	1.6	0.794	1.33	1.17	1.49	0.755	1.29	1.30	0.85	0.98
Lu	0.23	0.21	0.21	0.18	0.23	0.12	0.18	0.16	0.21	0.10	0.178	0.183	0.118	0.110
Zr	156	146	136	156	123	128	232	227	131	92	149	147	30	32
Hf	3.07	3.38	3.34	3.51	2.75	3.63	6.27	5.80	2.64	2.49	3.28	3.66	2.29	2.54
Ta	.52	0.62	0.62	0.58	0.42	0.53	0.88	0.69	0.34	0.25	0.53	0.32	2.27	2.44
Sc	17.6	7.1	7.8	9.5	26.7	7.4	17.1	8.5	68.5	11.1	15	22	2	2

Table 2.1. (Continued) Compositions of Selected Igneous Rocks, Absaroka Volcanic Province, Wyoming and Montana

	Rampart Volcanic Center: oldest to youngest					*Slough Creek Tuff*		*Elk Creek basalt*			*Golmeyer*
wt%	**HPt**	**HPt**	**HPt**	**HPt**	**HPaf**	**YSC**	**YSC**	**YT**	**YEC**	**YCC**	**PRd**
	196	**296**	**396**	**496**	**696**	**g495**	**595**	**194**	**f 193**	**1a96**	**295**
SiO_2	51.9	50.2	52.67	61.04	59.1	68.02	70.7	54.95	55.00	59.62	55.78
Al_2O_3	20.17	16.81	19.29	15.18	16.84	15.7	13.63	16.23	15.79	14.0	14.8
Fe_2O_3*	5.57	8.61	5.7	4.37	5.04	3.8	2.71	8.25	7.04	5.71	5.96
MgO	1.69	4.43	2.15	4.67	3.91	0.26	0.07	3.54	3.09	5.75	3.72
CaO	5.57	6.80	4.82	4.66	6.04	1.94	0.79	6.10	6.29	5.37	6.07
Na_2O	4.73	3.77	4.3	3.79	4.22	4.51	2.69	3.00	3.04	4.00	3.62
K_2O	3.67	3.48	4.02	2.97	2.03	2.72	7.05	3.61	2.83	1.46	2.26
TiO_2	0.77	0.91	0.79	0.62	0.57	0.21	0.39	1.20	0.97	0.57	0.63
P_2O_5	0.59	0.74	0.60	0.31	0.33	0.15	0.18	0.56	0.43	0.19	0.30
MnO	0.12	0.15	0.12	0.06	0.08	0.03	0.01	0.12	0.09	0.09	0.06
LOI	3.16	3.09	2.95	1.25	1.64	1.50	0.82	2.00	5.15	1.39	5.82
Total	98.50	99.0	98.49	98.90	99.8	99.18	99.0	99.60	99.70	99.10	99.00
						Parts Per Million					
Ni	7.1	42.2	9.46	134	159	7.9	8.8	35.0	33.8	81.2	93.6
Cr	2	77	1	218	298	5	9	72	91	106	185
Sr	594.0	1518	2050	1250	970.0	193	155	540.0	818.0	1200	1060
Rb	147	144	49	45	46	230	175	101	77	30.3	42
Ba	3010	2280	3070	1850	1600	2260	1970	1480	1580	1440	1830
Th	7.84	6.86	8.72	6.47	3.79	15.4	14.0	9.55	10.8	6.71	7.65
La	49.8	49	55.4	49.7	34.5	55.5	48.9	49.6	47.7	38.6	48.4
Nd	37.5	41.2	42	36.7	27.3	41.2	37.9	40.0	37.4	29.4	33.7
Sm	6.2	6.93	6.87	4.77	4.12	7.39	6.93	7.83	7.08	4.08	5.37
Yb	1.46	1.62	1.58	0.60	0.967	2.83	2.52	2.48	2.31	0.843	1.21
Lu	0.209	0.234	0.235	0.09	0.148	0.404	0.359	0.348	0.314	0.123	0.174
Zr	164	138	157	173	106	377	349	237	233	27.9	134
Hf	3.20	3.06	3.63	5.13	2.94	8.94	7.77	5.61	5.65	3.1	3.43
Ta	0.57	0.51	0.64	0.38	0.24	1.19	1.12	0.85	0.85	0.399	0.55
Sc	6.8	18	7.3	9.7	13	14	11.8	16	15	9.83	13

Table 2.1. (Continued) Compositions of Selected Igneous Rocks, Absaroka Volcanic Province, Wyoming and Montana

Oldest to Youngest from the Hyalite Volcanic Center									*Northwest Belt Basanite and Rhyodacite*		
wt%	**HGB 1395**	**HGB 1595**	**HGB 2195**	**HGB 1995**	**HGB 395**	**HGB 795**	**HGS 1195**	**HGS 795**	**wt%**	**BHM 195**	**BHM 295**
SiO_2	52.9	52.2	51.6	56.4	55.8	58.1	53.4	55.1	**SiO_2**	43.78	68.52
Al_2O_3	15.6	16.2	16.1	15.9	16.1	17.0	15.8	16.7	**Al_2O_3**	13.51	14.1
Fe_2O_3*	9.62	9.94	9.89	8.08	8.46	7.36	9.63	8.96	**Fe_2O_3***	12.91	3.36
MgO	5.42	4.77	4.59	4.09	3.43	2.55	5.12	4.18	**MgO**	9.62	0.7
CaO	7.93	7.57	7.64	6.20	6.14	5.44	7.5	6.39	**CaO**	9.44	2.69
Na_2O	2.96	3.03	2.98	3.28	3.29	3.26	2.89	3.35	**Na_2O**	3.81	4.12
K_2O	2.24	2.37	2.48	3.04	3.18	3.27	2.41	2.79	**K_2O**	1.03	3.52
TiO_2	1.04	1.14	1.15	0.99	1.02	0.92	1.05	1.10	**TiO_2**	2.91	0.63
P_2O_5	0.40	0.42	0.41	0.44	0.52	0.46	0.42	0.44	**P_2O_5**	0.78	0.38
MnO	0.15	0.15	0.15	0.14	0.12	0.11	0.15	0.13	**MnO**	0.18	0.04
LOI	1.75	2.04	2.63	0.82	1.23	1.17	1.59	0.94	**LOI**	1.65	2.00
Total	100.0	99.80	99.62	99.38	99.29	99.70	99.9	100.0	**Total**	99.60	99.56
						Parts Per Million					
Ni	38.4	31.1	28.2	50.5	34.5	9.71	24.7	26.4	**Ni**	218	5
Cr	113	51	47	173	90	27	92	98	**Cr**	255	26
Sr	594	625	661	616	686	650	649	600	**Sr**	996	940
Rb	40	54	58	84	90	85	59	71	**Rb**	31	69
Ba	1360	1460	1510	1630	1690	1550	1510	1470	**Ba**	594	2330
Th	4.47	4.76	4.92	7.93	7.03	7.72	4.88	6.28	**Th**	5.19	12.8
La	31.5	33	33.3	42.8	42.2	42.8	33.8	33.8	**La**	49.3	79.9
Nd	27.5	27.5	29	36.4	35.6	34.9	29.6	31.5	**Nd**	43.6	42.5
Sm	5.8	6.13	6.28	7.00	7.09	6.89	6.17	6.44	**Sm**	8.85	5.17
Yb	2.08	2.37	2.34	2.59	2.51	2.57	2.30	2.47	**Yb**	1.81	0.52
Lu	0.29	0.32	0.33	0.37	0.38	0.36	0.32	0.36	**Lu**	0.24	0.08
Zr	168	180	157	224	214	208	185	205	**Zr**	286	180
Hf	3.62	3.87	3.86	5.35	5.0	5.08	4.0	4.7	**Hf**	5.93	5.04
Ta	0.50	0.53	0.53	0.82	0.69	0.75	0.53	0.66	**Ta**	4.73	0.85
Sc	24	22	23	17	16	12	24	17	**Sc**	22	4

Table 2.2. Calculated Normative Compositions of Selected Mafic and Intermediate Members of Sampled Volcanic Centers of the Absaroka Volcanic Province, Wyoming and Montana.

	Hyalite Volcanic Center		
	HGB 1395	**HGB 1595**	**HGB 2195**
SiO_2	52.9	52.2	51.6
Q	2.51	1.95	1.94
Or	13.24	14.01	18.08
Ab	25.05	25.64	28.43
An	22.61	23.69	19.49
Di	11.49	9.10	6.89
Hy	16.06	15.68	13.60
Mt	3.68	3.83	3.62
Il	1.98	2.17	1.77
Ap	0.93	0.97	1.30

	Ishawooa Volcanic Center		
	ISH 5095	**ISH 4995**	**ISH 995**
SiO_2	50.2	53.1	49.5
Or	18.26	32.00	11.52
Ab	31.41	29.85	30.31
An	17.80	17.17	17.72
Ne	2.83	3.63	1.59
Di	7.14	1.61	14.57
Ol	10.32	4.66	13.95
Mt	5.51	3.33	3.74
Il	1.80	1.53	2.05
Ap	2.20	1.83	1.78

	Rampart Volcanic Center			
	HPt 196	**HPt 296**		**HPt 396**
SiO_2	51.9	50.2		52.67
Or	21.69	20.57	**Or**	23.76
Ab	35.46	29.00	**Ab**	36.39
An	22.97	18.67	**An**	19.99
Ne	2.47	1.57	**C**	0.54
Di	0.66	8.34	**Hy**	5.18
Ol	4.67	10.20	**Ol**	2.06
Mt	3.29	3.49	**Mt**	3.32
Il	1.46	1.73	**Il**	1.50
Ap	1.37	1.71	**Ap**	1.39

	Crandall Volcanic Center	
	HMf 294	**HMs 1995**
SiO_2	53.07	52.56
Or	12.59	21.87
Ab	27.75	33.25
An	21.72	16.86
Di	11.88	5.79
Hy	17.22	4.44
Ol	1.14	7.09
Mt	3.32	3.70
Il	1.50	1.99
Ap	0.83	1.92

	Sunlight Intrusion
	Smg 496
SiO_2	51.1
Or	21.10
Ab	31.92
An	17.66
Ne	3.84
Di	4.98
Ol	9.57
Mt	3.61
Il	1.88
Ap	2.59

	Kirwin Flow and dike	
	HWR 1094	**HWR 1494**
SiO_2	52.5	50.1
Or	20.45	11.23
Ab	30.72	27.08
An	19.38	19.05
Di	6.68	13.55
Hy	7.03	6.76
Ol	4.14	11.86
Mt	3.41	4.20
Il	7.09	2.47
Ap	2.51	0.86

	Basanite Flow
	BHM 195
SiO_2	43.8
Or	6.50
Ab	18.24
An	16.51
Ne	7.59
Di	20.09
Ol	14.59
Mt	6.39
Il	5.53
Ap	1.81

Sample Compositions from Crandall Volcanic Center

Compositions from the Crandall center cover a triangular field from calc-alkaline basaltic andesite to shoshonite, banakite and trachyte (Figure 2.3). Major element variation in rocks from the Crandall volcanic center do not show a simple linear trend (Figure 2.4). Sampled lava flows and dikes tend to be higher in MgO, lower in Ba, and exhibit variable enrichment of K, Rb, Sr, and Th, with low concentrations of HFSE (Figure 2.5). Trace element plots of Crandall samples do not exhibit simple linear element-element trends. Samples from early pyroxene-phyric flows exhibit greater enrichment in Sr than later plagioclase-bearing intrusions. The most silicic sample from Crandall, a trachyte ash-flow tuff, has high concentrations of incompatible trace elements, and low TiO_2 (Figure 2.6). Samples have high but variable Cr (up to 425 ppm). As with Harker diagrams, a plot of Cr versus La for Crandall samples does not exhibit a single trend line, even for samples with Cr >100 ppm (Figure 2.7).

Mafic samples (>5% MgO,<54% SiO_2), which are olivine and hypersthene normative, exhibit an increase in La/Sm with increasing Sm, and increasing Gd/Yb with increasing Yb, and have lower HREE concentrations compared to mafic rocks from other volcanic centers (Figure 2.8a and 2.8b). The samples from this group with highest MgO and Cr show an inverse relationship of LREE enrichment relative to MgO (Figure 2.9). They can also be distinguished from mafic compositions of other volcanic centers by lower Zr and P_2O_5, higher Zr/Ta, and K/Rb (Figures 2.10 and 2.11).

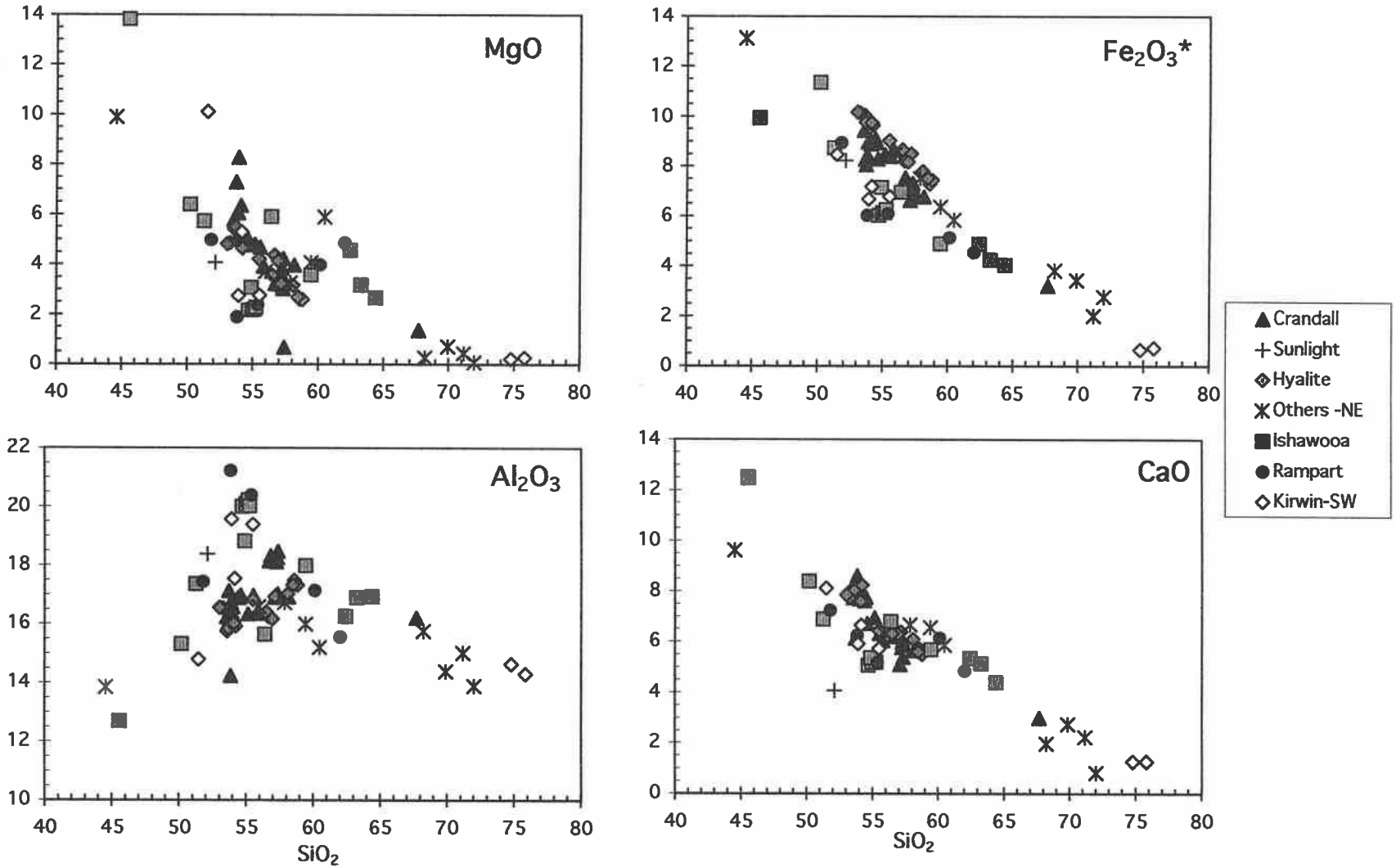

Figure 2.4. Harker variation diagrams for sampled igneous rocks from the Absaroka Volcanic Province.

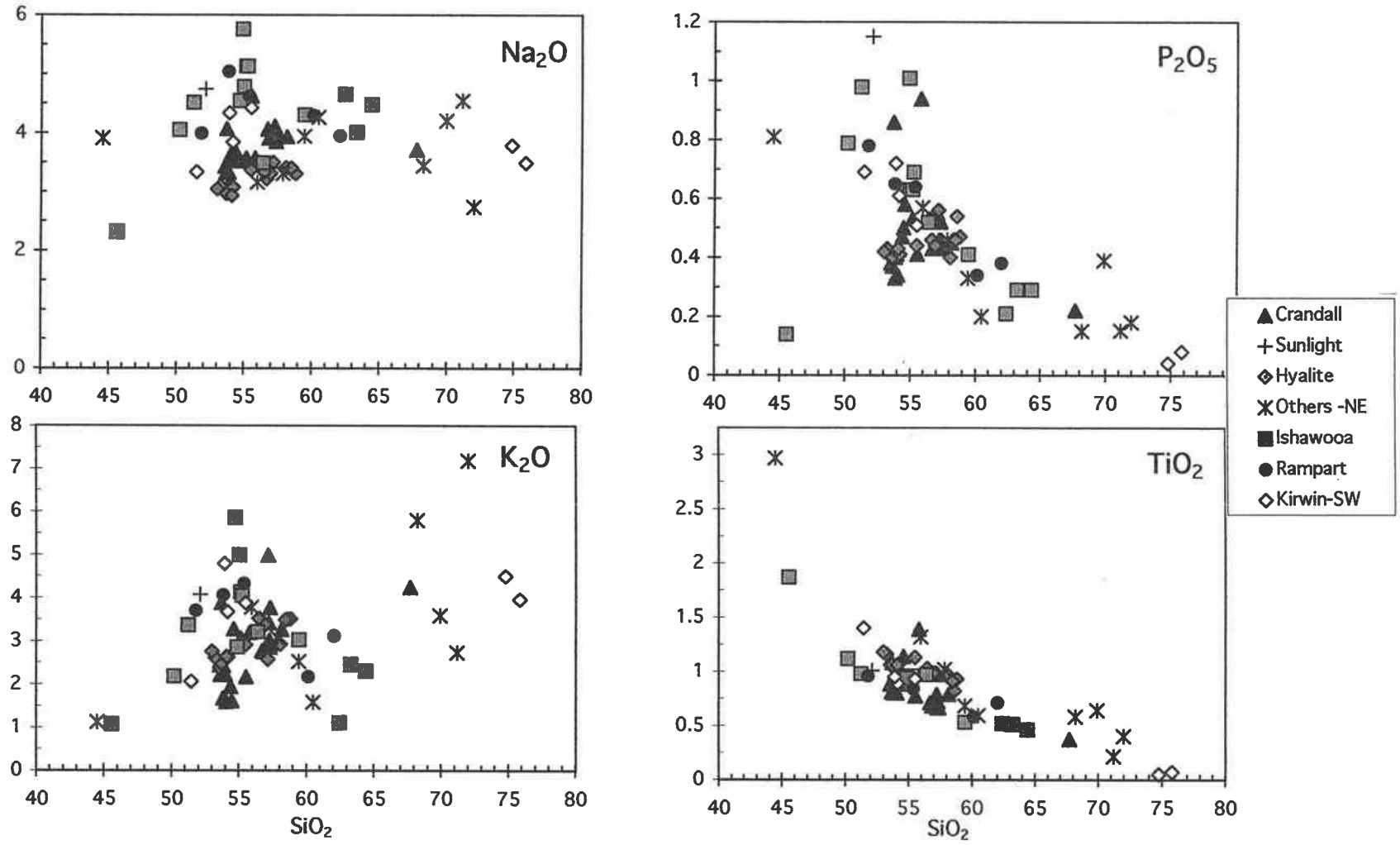

Figure 2.4.(Continued) Harker variation diagrams for sampled igneous rocks from the Absaroka Volcanic Province.

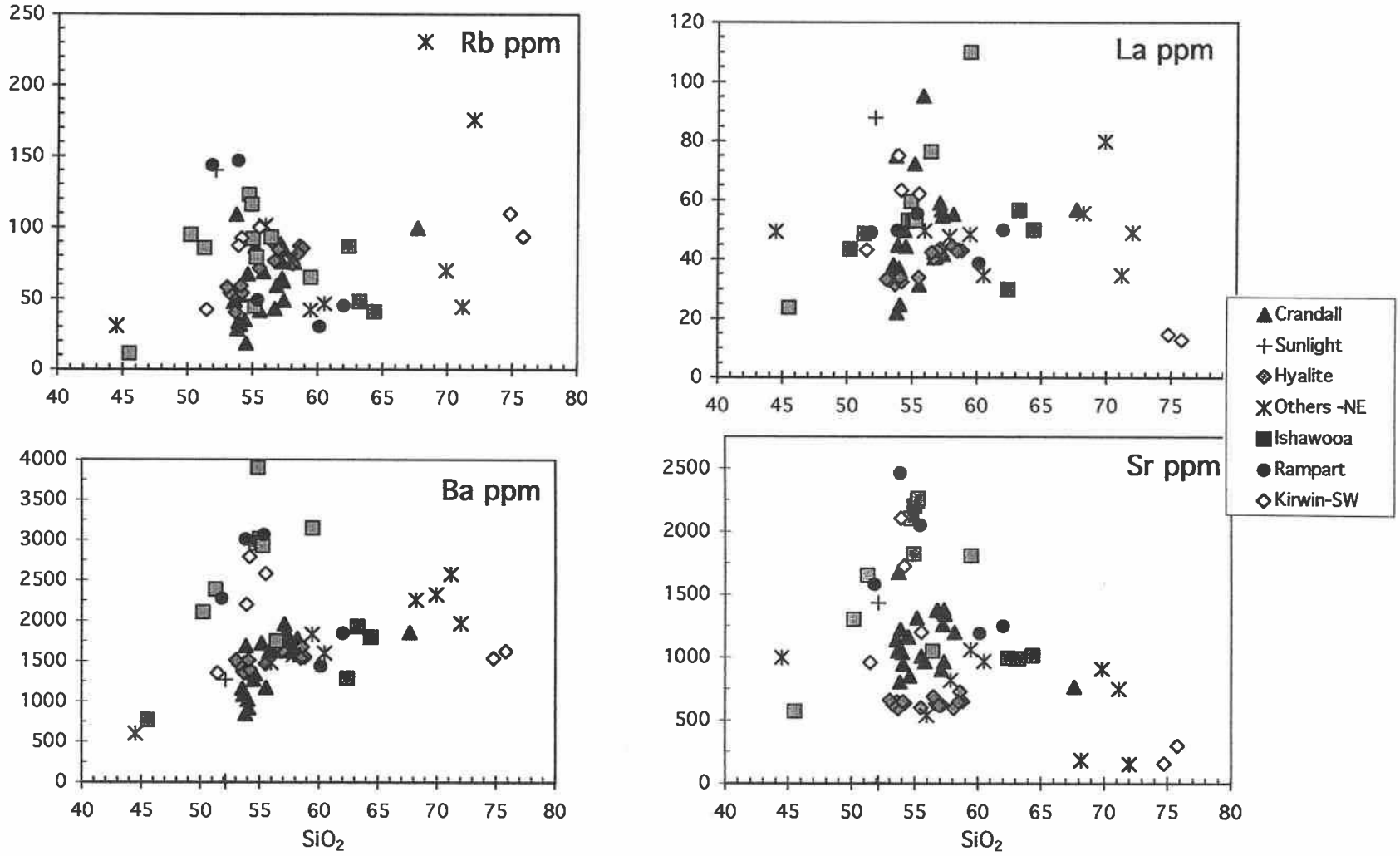

Figure 2.5. Trace element versus silica variation diagrams for sampled igneous rocks from the Absaroka Volcanic Province.

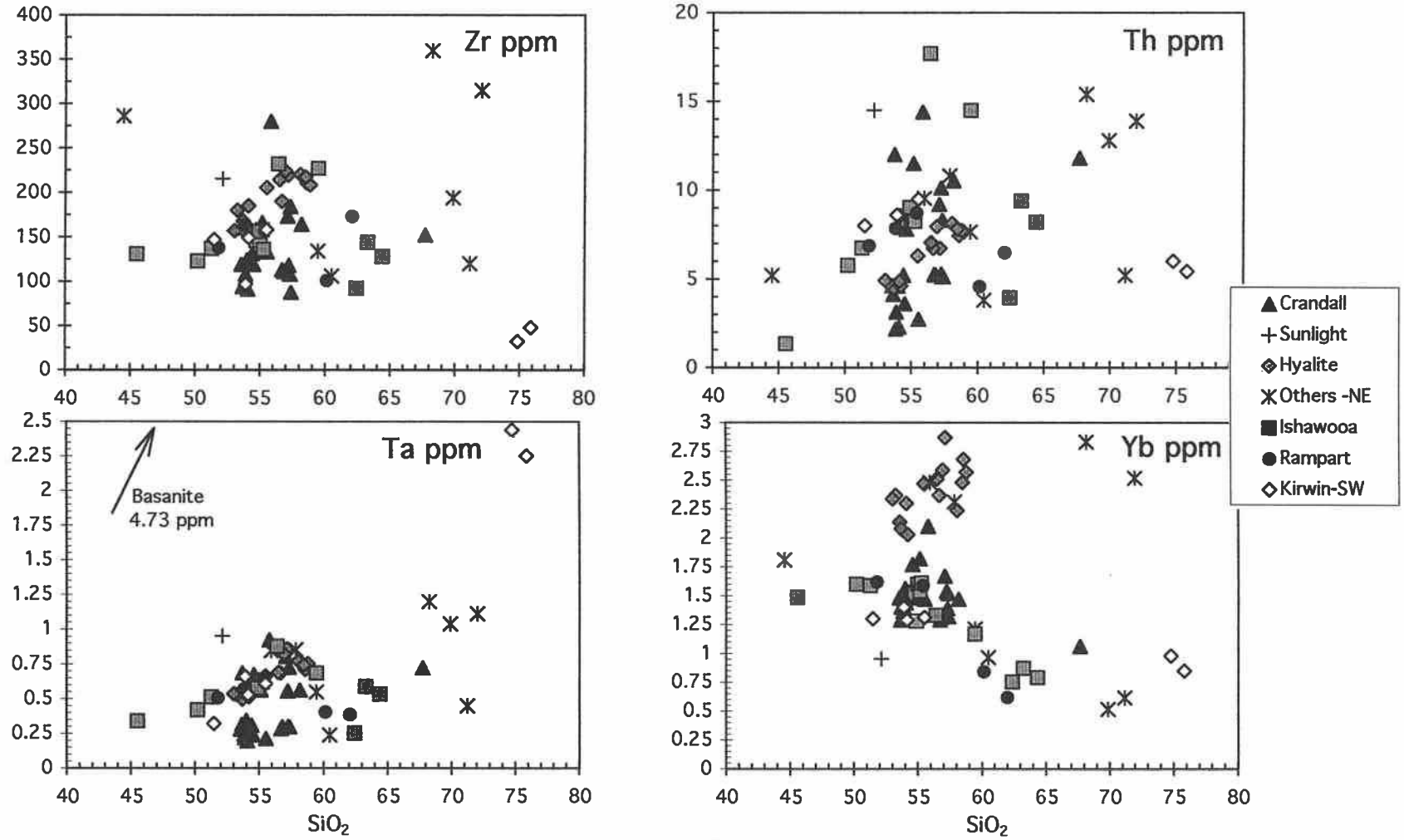

Figure 2.5. (Continued) Trace element versus silica variation diagrams for igneous rocks from the Absaroka Volcanic Province.

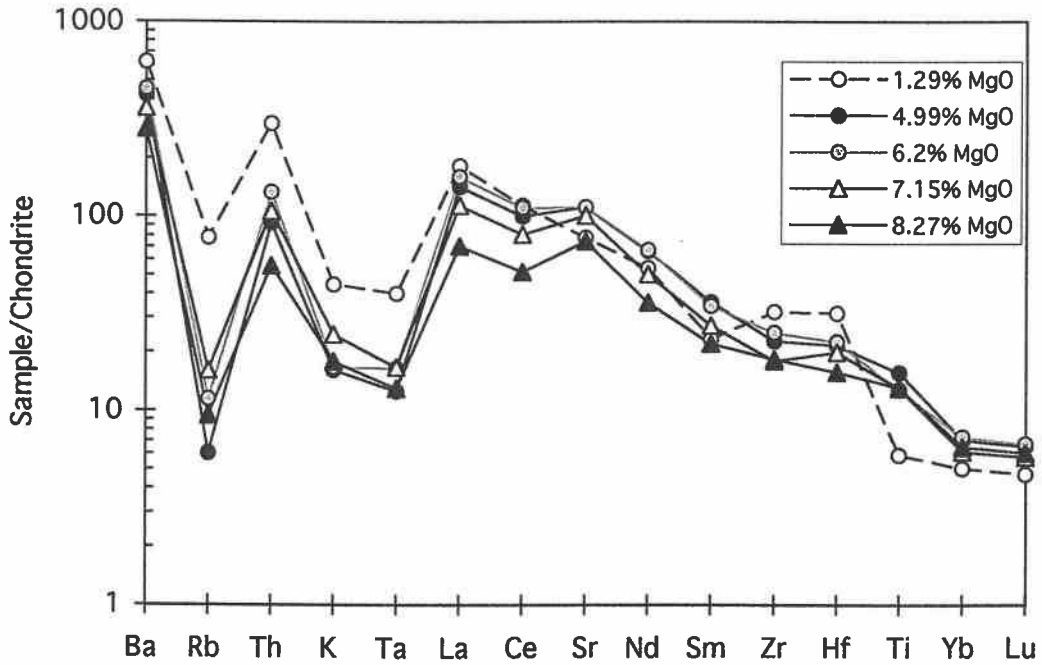

Figure 2.6. Chondrite-normalized trace elements for samples from the Crandall volcanic center. Circles indicate samples with plagioclase phenocrysts. The trachyte ash-flow tuff is represented with a dashed line.

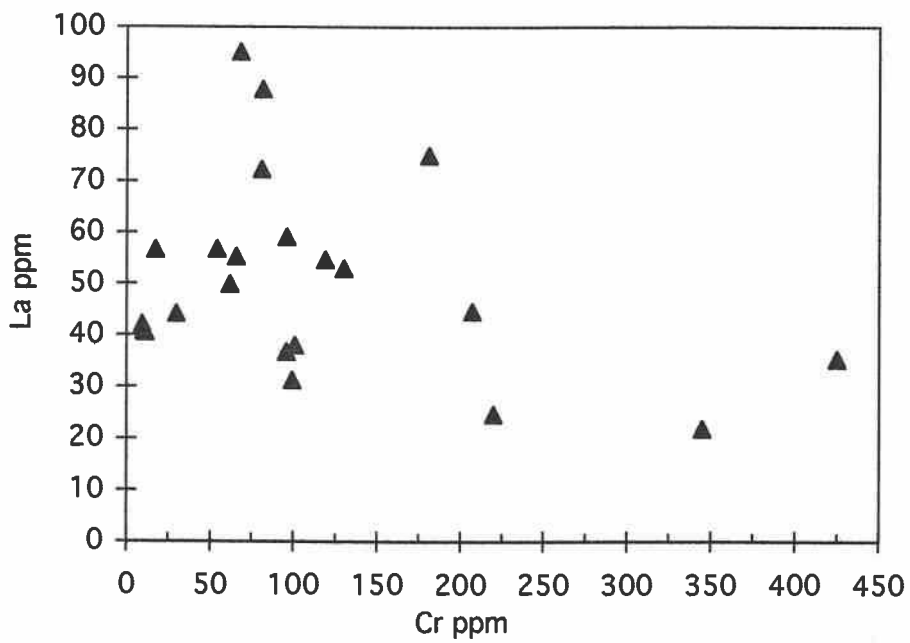

Figure 2.7. La versus Cr for samples from the Crandall volcanic center.

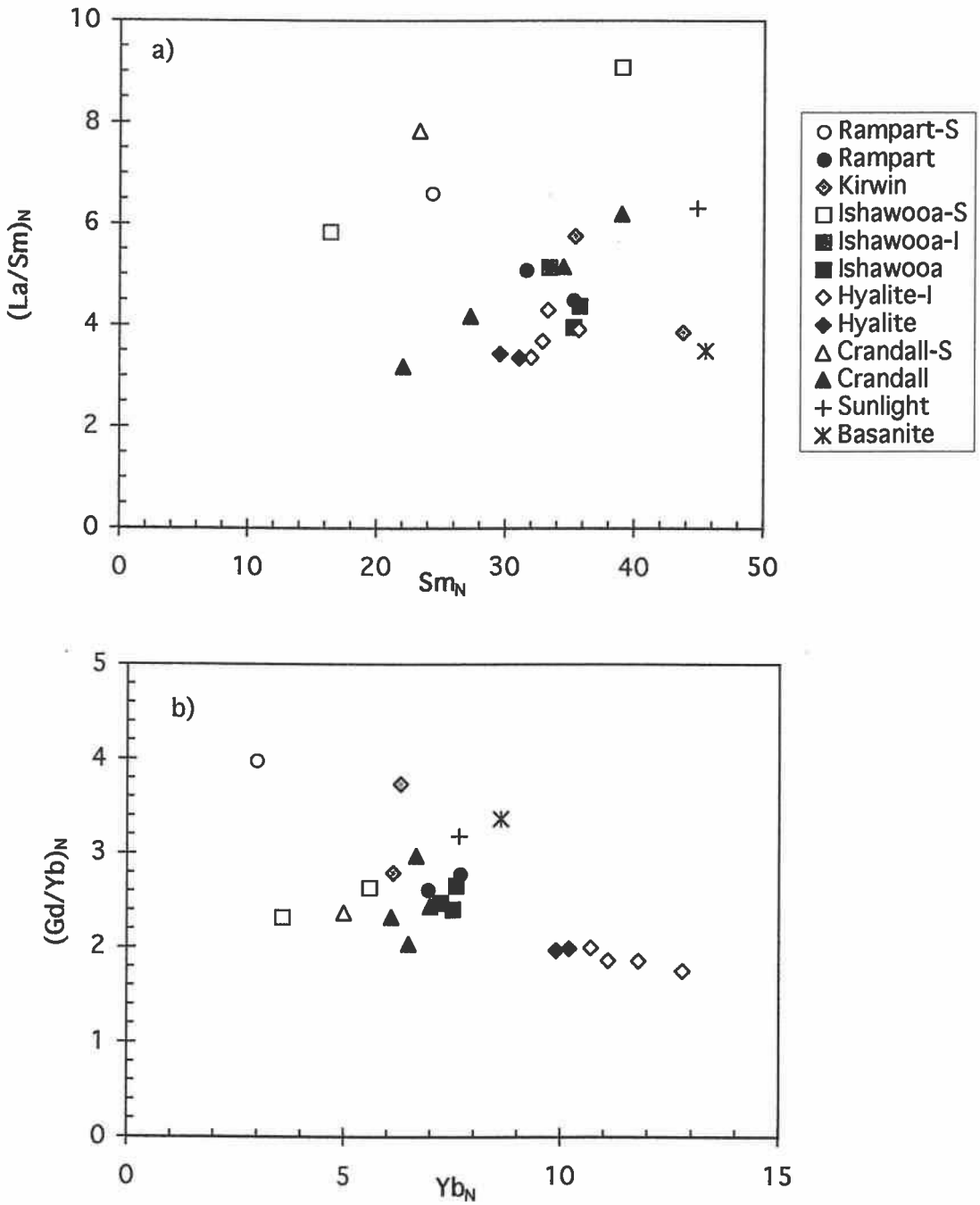

Figure 2.8.a) Chondrite normalized La/Sm versus Sm for samples from volcanic centers in the Absaroka Volcanic Province. b) Chondrite normalized Gd/Yb versus Yb for samples from volcanic centers in the Absaroka Volcanic Province. Solid symbols denote samples from specific volcanic centers with <54% SiO_2 and >5% MgO; I- indicates intermediate composition samples with <54% SiO_2, and <5%MgO; S-indicates samples with >60% SiO_2.

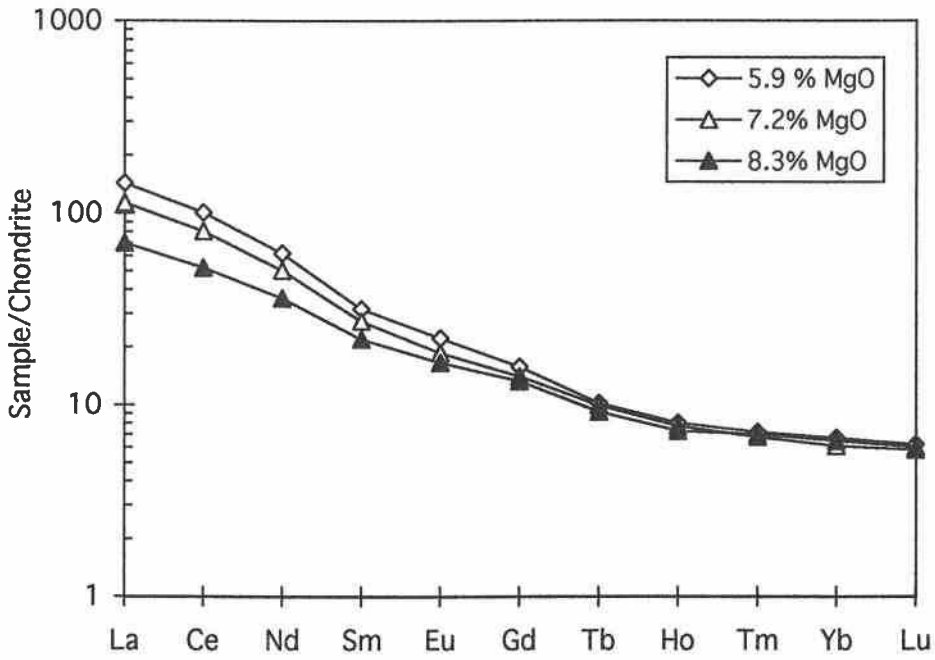

Figure 2.9. Chondrite normalized REE for high Cr, high MgO samples from the Crandall volcanic center.

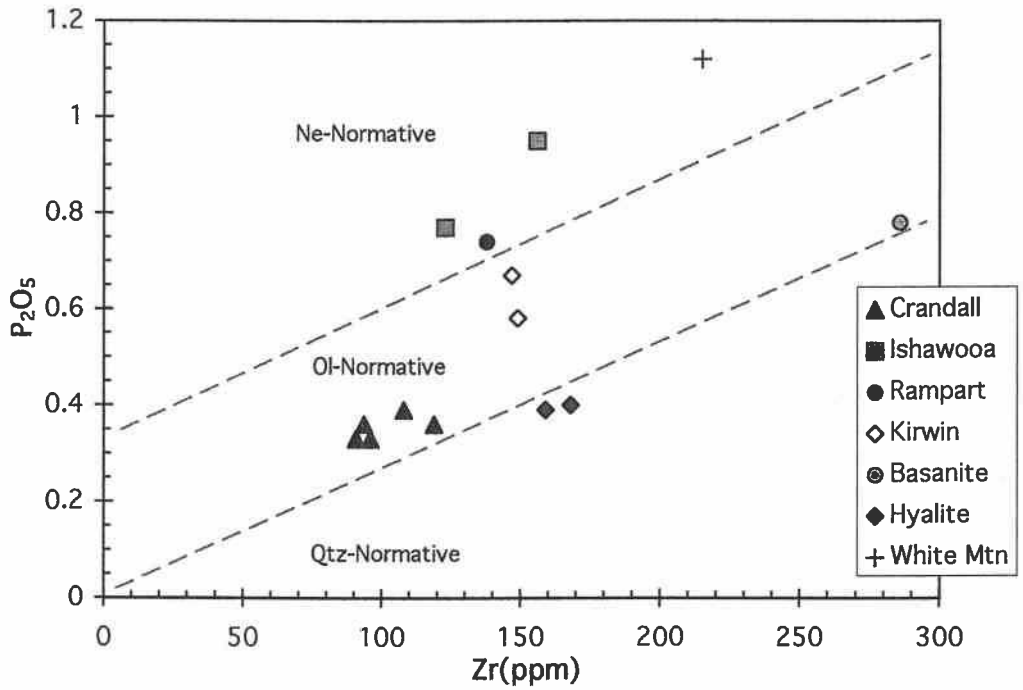

Figure 2.10. Zr versus P_2O_5 for mafic samples from the Absaroka volcanic province. Samples shown have >5% MgO and <54% SiO_2, except for Sunlight (White Mtn) monzogabbro which has 4% MgO.

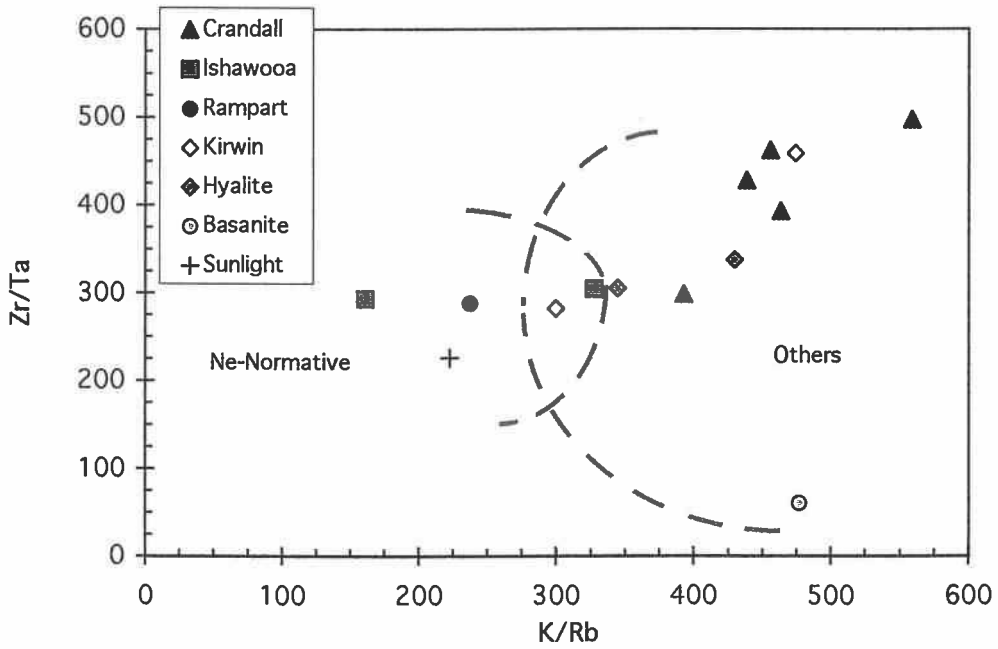

Figure 2.11. Zr/Ta versus K/Rb for mafic samples from the Absaroka volcanic province. Samples shown have >4% MgO and <54% SiO_2.

Sample Compositions from the Ishawooa Volcanic Center

Samples with < 60% SiO_2 from the Ishawooa volcanic center have higher K_2O than other volcanic centers, and range in composition from absarokite and shoshonite to banakite and tephriphonolite (Figure 2.3). Variation in major element composition does not show a simple linear trend for samples from the Ishawooa volcanic center, with the greatest disparity occurring between 55 and 57% SiO_2 (Figure 2.4). Similarly, an abrupt change in mineralogy and trace element composition also occurs within this intermediate composition interval (Figure 2.5). Amphibole-bearing samples that are higher in SiO_2 (>60%) have higher La/Sm than mafic compositions (Figure 2.8a). Intermediate to mafic olivine and augite bearing compositions show a progressive increase in La/Sm with decreasing Sm, and increasing Gd/Yb with increasing Yb (Figure 2.8a and 2.8b).

Absarokite and shoshonite from the Ishawooa volcanic center are nepheline normative, and exhibit extreme enrichment of K, Ba, Rb and Sr, with higher P_2O_5 and lower K/Rb (Figures 2.10 and 2.11). Early shoshonite lavas at Ishawooa have fairly uniform trace element concentrations and show little variation in relative concentrations of REE. La/Sm, Ba, Rb, Th, K and Sr are higher in shoshonitic samples which lack olivine and are the most depleted in MgO, Cr and Sc (Figure 2.12). Compositions with >60% SiO_2 are significantly lower in K_2O, Rb, Ba, La, Th, and HREE than mafic samples. Silicic rocks can be subdivided into two groups: medium-grained metaluminous dacites and fine-grained to glassy silicic rocks, some of which contain augite, orthopyroxene and olivine. Silicic rocks (≥60% SiO_2) with olivine and pyroxene have high MgO (>4 %), Cr (>150-200 ppm) and Ni (≥100 ppm) (See Table 2.1). These samples also exhibit lower trace element concentrations, and can be distinguished by higher Hf/Ta (Figure 2.12). Metaluminous dacites (medium-grained porphyritic rocks containing amphibole and plagioclase) have lower HREE and higher Zr than the high MgO, high Cr intermediate to silicic rocks.

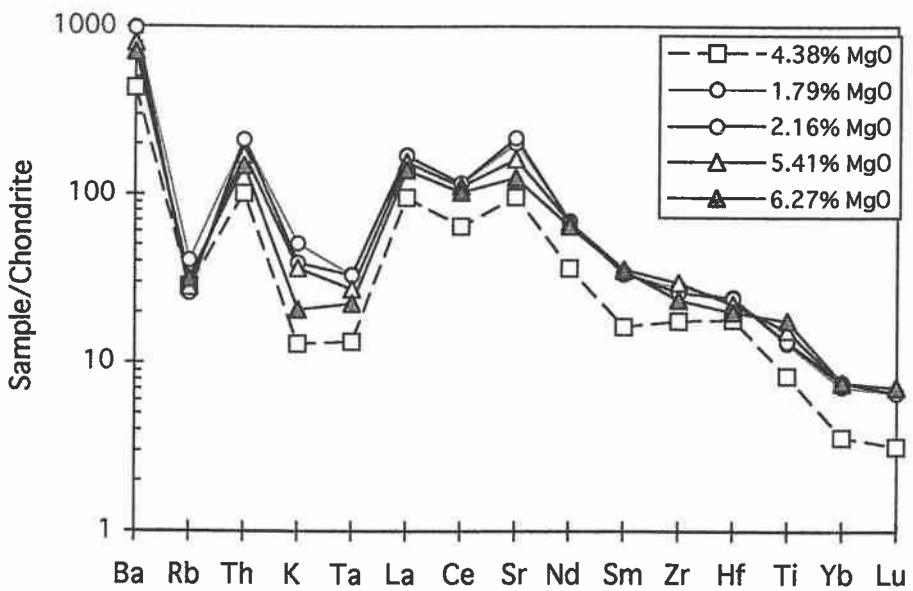

Figure 2.12. Chondrite-normalized trace element abundances for selected samples from the Ishawooa volcanic center. Samples from olivine- and pyroxene-bearing flows are represented by triangles; sparsely porphyritic augite-bearing samples are represented with circles; trace elements for a fine-grained silicic intrusion (>60 % SiO_2) containing augite, orthopyroxene with augite rims, and sparse olivine are shown with square symbols and a dashed line.

Composition of samples from the Rampart Volcanic Center

Samples from the Rampart volcanic center are potassic and do not exhibit linear trends on Harker diagrams (Figures 2.3 and 2.4). The most mafic sample (<55% SiO2, >4% MgO) has high P_2O_5, Rb, Ba, and Sr (Figure 2.5). Sampled compositions show many similarites to those from the Ishawooa volcanic center, including a similar marked change and divergence in alkalinity between 55 and 60% SiO_2. They also exhibit trace element enrichment comparable to the Ishawooa volcanic center (Figure 2.13).

Intermediate olivine-phyric rocks sampled from the Rampart volcanic center are also similar to the high Cr, high MgO samples from Ishawooa. They are fine-grained to glassy, and contain sparse phenocrysts of biotite (<5%), olivine (5%) and variable amounts of clinopyroxene and orthopyroxene. One sample has >60% SiO_2 , >4.5 % MgO, with high Cr (218 ppm) and Ni (134 ppm). In comparison to mafic samples, it exhibits less pronounced enrichment in incompatible elements. In comparison to mafic rocks and other samples with comparable SiO_2, these high MgO, high Cr rocks from both the Ishawooa and Rampart volcanic centers have higher Hf/Ta and Ce/Yb (Figure 2.14).

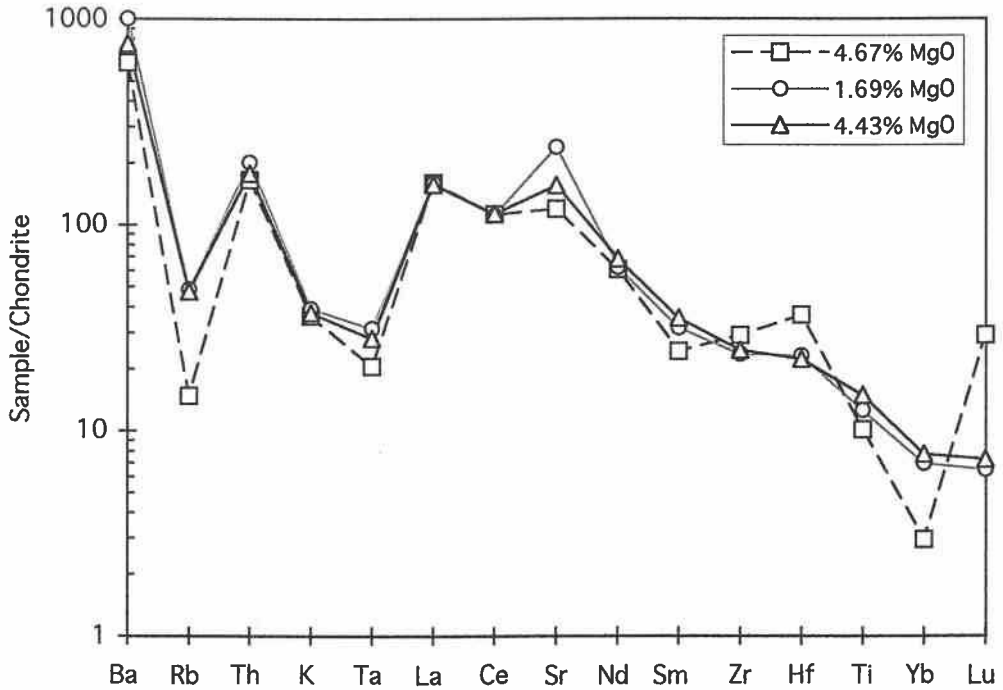

Figure 2.13. Chondrite-normalized trace elements for samples from the Rampart volcanic center. The mafic end-member olivine-phyric sample is represented with triangles. The high Cr silicic sample is represented with square symbols and a dashed line.

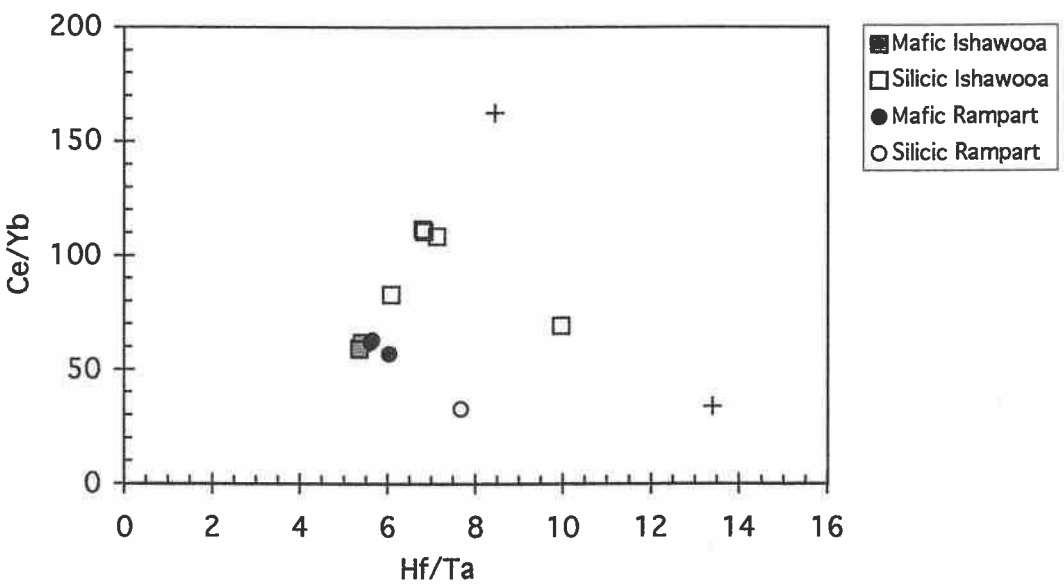

Figure 2.14. Ce/Yb versus Hf/Ta for samples from the Ishawooa and Rampart volcanic centers. Mafic samples have < 54% SiO_2. Samples with olivine and two pyroxenes, >4% MgO and >60% SiO2 are represented by crosses.

Composition of samples from the Hyalite Volcanic Center

Lava flows of the Hyalite volcanic center define a bimodal assemblage both mineralogically and geochemically. They have a limited range of chemical compositions from trachybasalt to trachyandesite, with a pronounced gap between 55 and 56 wt % SiO_2 (Figure 2.3). Unlike the other volcanic centers, compositions from the Hyalite volcanic center exhibit a linear trend on major element variation diagrams (Figure 2.4). Sampled flows and dikes have less pronounced enrichment in K_2O, and are much less enriched in Rb and Sr than other volcanic centers (Figure 2.15). Shoshonitic lavas with >56% SiO_2 exhibit an increase in K_2O and trace element concentrations, except for Sr, Eu and TiO_2 which remain fairly constant or decrease slightly. Mafic rocks with < 55% SiO_2 are relatively homogenous, with MgO≥ 4.5% and high Cr (≈ 100 ppm). They exhibit lower La/Sm and Gd/Yb, which remains constant for both mafic and intermediate compositions (Figure 2.8a and 2.8b).

Although mafic samples from the Hyalite volcanic center exhibit less pronounced enrichment in K_2O, they plot in the shoshonitic fields defined by Muller and Groves (1991) by comparing relative concentrations of Ce/Yb and Ta/Yb, as well as Th/Yb and Ta/Yb (Figure 2.16a and 2.16b). In comparison to other shoshonites from the Absaroka province, samples from the Hyalite volcanic center can be distinguished by relatively low and constant Ce/Yb, Ta/Yb and Th/Yb.

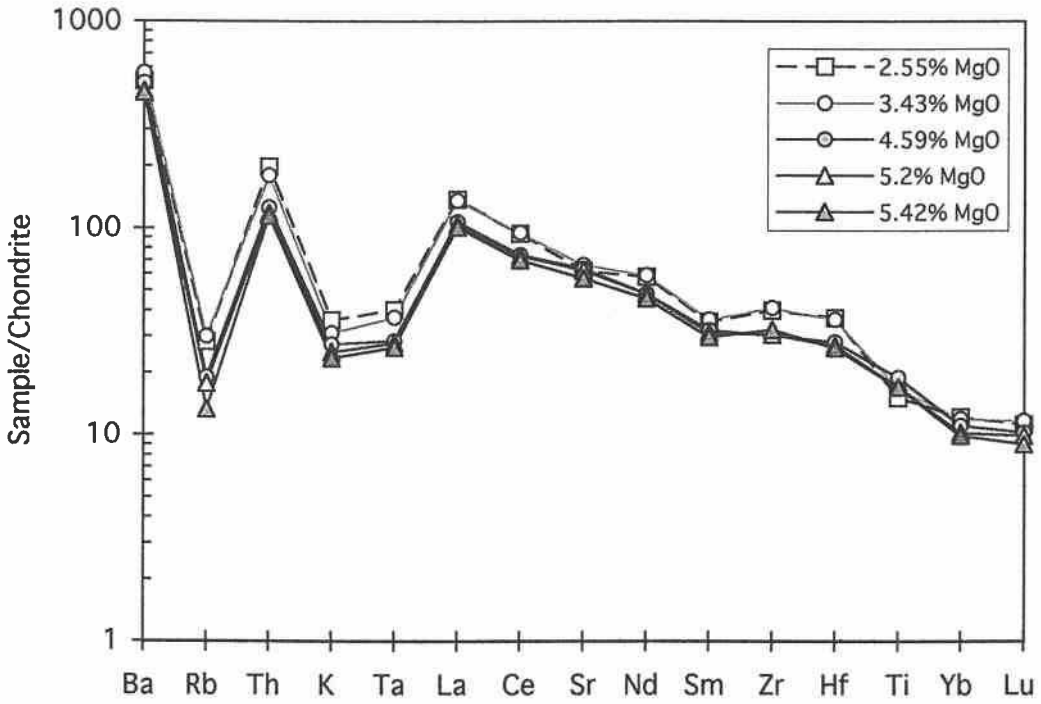

Figure 2.15. Chondrite-normalized trace elements for samples from the Hyalite volcanic center. Samples with augite and groundmass olivine (<53% SiO_2) are represented with triangles, those with plagioclase and augite phenocrysts are represented with circles (<56% SiO_2), and a sample with augite, hypersthene and plagioclase is represented with square symbols and a dashed line.

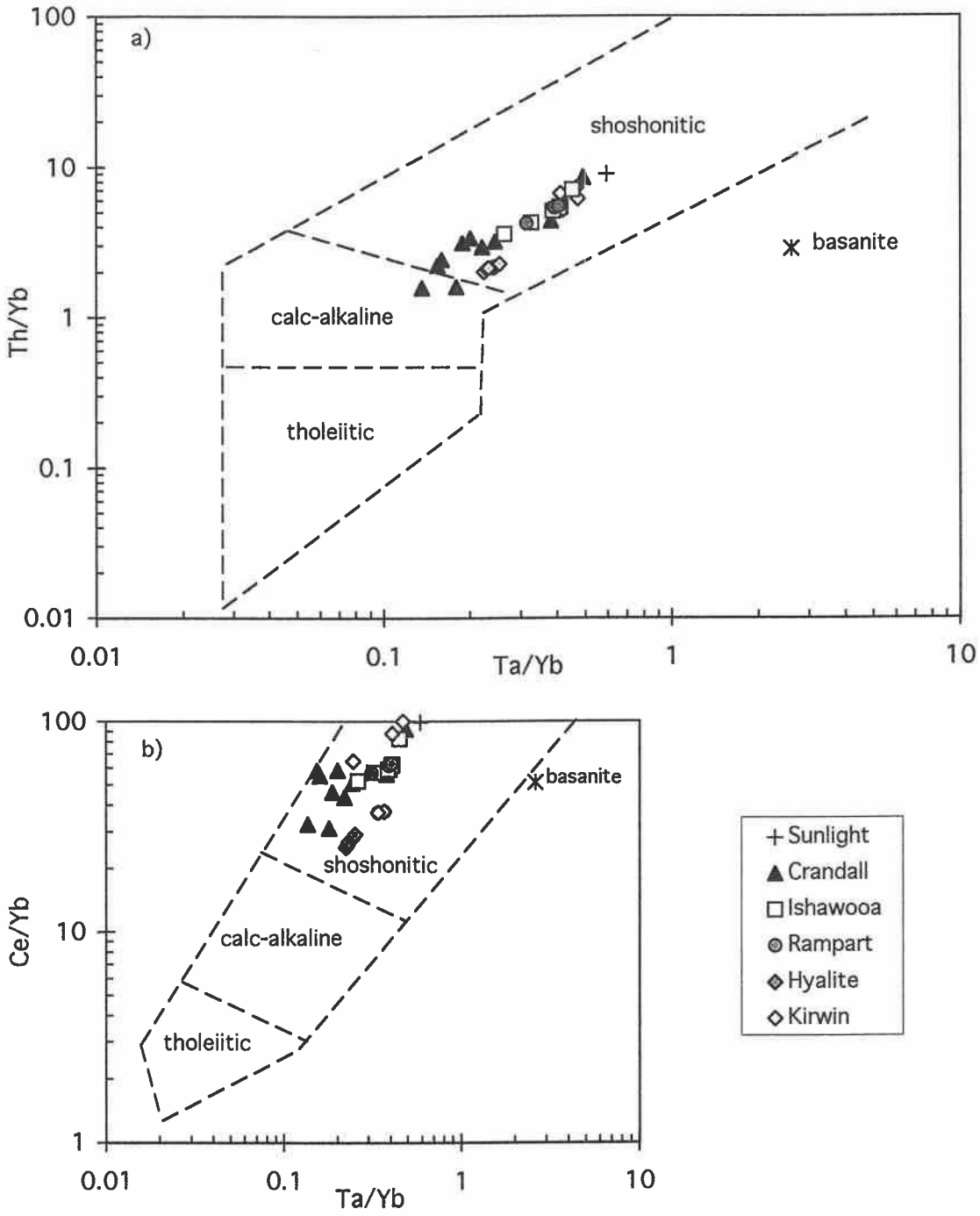

Figure 2.16. Trace element ratios of mafic samples from each of the volcanic centers (<54% SiO_2, >4% MgO) showing subdivisions for classification of volcanic rocks by Muller and Groves (1991): a) Th/Yb versus Ta/Yb, b) Ce/Yb versus Ta/Yb.

Samples Peripheral to Volcanic Centers

Samples from regions peripheral to the volcanic centers include compositions from both mafic and silicic ends of the compositional spectrum, as well as shoshonite. Basanite (BHM195), sampled from the northern Absaroka province is among the most mafic of samples analyzed in this study, with the lowest SiO_2 (Figure 2.3). Unlike other sampled flows, it is not depleted in TiO_2 or HFSE, and has high Ta (Table 2.1). Chondrite-normalized REE patterns for the basanite are LREE enriched and HREE depleted (Figure 2.17). Other mafic rocks include an olivine-normative absarokite (WR1494) with MgO (9.8 wt%) comparable to the basanite, and high Cr (488 ppm), which was sampled from the Kirwin area in the southern Absaroka volcanic province. This sample has Zr/Ta and K/Rb equivalent to other mafic olivine normative samples which were sampled from the Crandall volcanic center, and similar P_2O_5/Zr (Figures 2.10 and 2.11). Nepheline-normative monzogabbro (Smg496) sampled south of the Crandall volcanic center, in the vicinity of the Sunlight volcanic center, has high P_2O_5/Zr, high Rb, and low K/Rb, similar to other nepheline-normative samples (HPt296, ISH5095) from the Rampart and Ishawooa volcanic centers.

Intermediate composition samples include shoshonite from the Kirwin area, Elk Creek Basalt from northern Yellowstone, and a dike from the Golmeyer Creek volcanic center. The Golmeyer volcanics lie stratigraphically below flows of the Hyalite volcanic center, and are separated from them by an angular unconformity. The dike sample from Golmeyer (PR295) exhibits greater enrichment in LREE, Sr and Ba than overlying lavas of the Hyalite volcanic center, but is also lower in K_2O, Rb, Zr and TiO_2 (Table 2.1). Flows of Elk Creek basalt (YEC193) were sampled at the type locality of Smedes and Prostka (1972), and in an additional location mapped as Elk Creek Basalt (YT194) by Prostka and others (1975). The type locality of the

Elk Creek basalt is badly weathered, making analysis of fresh samples difficult. Analysis of an additional sample of Elk Creek basalt, from the second location in northeast Yellowstone, has similar petrographic features, major and trace element composition to the type locality, but is higher in alkaline earths (Table 2.1). Elk Creek basalt samples (YT194 and YEC193) are actually of moderately potassic shoshonitic composition, with MgO <4% and 70-100 ppm Cr (Table 2.1, Figure 2.3). Trace element concentrations for Elk Creek basalt have low Sr with La/Yb similar to shoshonites of the Hyalite Peak volcanic center.

Silicic rocks include the Slough Creek tuff (YSC495 and YSC595) from the northern Absaroka province, which is trachytic to rhyolitic in composition, and rhyolite intrusions from the extreme southern Absaroka volcanic province (WR1694 and WR1394). The more alkaline Slough Creek Tuff is more enriched in incompatible elements, with higher in Rb, Sr, Th, La, and 10 times the Zr of younger silicic intrusions from the southern Absaroka province (Figure 2.5).

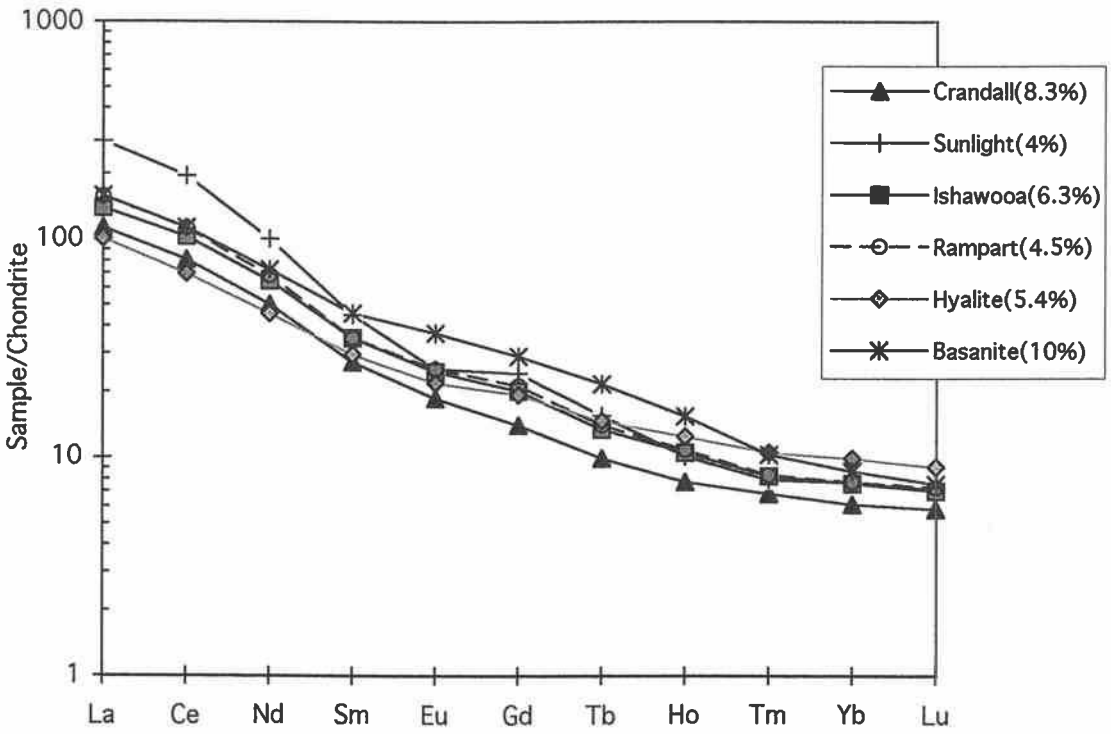

Figure 2.17. Chondrite normalized REE for mafic end-member samples from each of the volcanic centers and for sampled basanite. (Percent MgO for samples is shown in parenthesis.)

MINERAL COMPOSITIONS

Olivine

All samples with less than 52% SiO_2 contain olivine phenocrysts. In general glassy samples have phenocrysts which exhibit normal zonation, whereas holocrystalline samples have phenocrysts of homogenous composition. Olivine from basanite is zoned from Fo_{85} to Fo_{80} from core to rim. In contrast, absarokites and shoshonites of the Rampart and Ishawooa volcanic centers have Fo_{75} olivine with little zonation (Table 2.3). Olivine from Hyalite volcanic center shoshonite consists of small groundmass phenocrysts of $Fo_{65\text{-}68}$. Olivine from glomerocrysts in a mafic intrusion at the Crandall volcanic center is higher in MgO (Fo_{83}) than those from other volcanic centers.

Pyroxene

All mafic and intermediate rocks have clinopyroxene, the most conspicuous phase in the Absaroka volcanic province. Clinopyroxene ranges from diopside to augite. Orthopyroxene is less common, and occurs in trachyandesites of the Hyalite volcanic center, and in a widespread group of high MgO silicic (>60% SiO_2) rocks (See Appendix D). Zoning is common in rocks with glassy textures, especially in high-MgO silicic samples, where augite often forms rims on orthopyroxene phenocrysts.

Table 2.3. Composition of olivine phenocrysts from mafic flows from different volcanic centers, and a peripheral basanite flow of the Absaroka province.

Sample	Crandall		Ishawooa	Rampart		Hyalite		Basanite
core	HM2	HM19	HISH50	HPt1	HPt2	HGB13	HGB12	BHM1
SiO_2	38.33	37.25	37.03	36.73	36.47	37.01	37.54	38.47
MgO	42.70	37.06	38.28	37.95	37.76	36.63	34.14	43.91
Fe_2O_3	17.37	24.65	24.43	24.60	25.40	25.40	27.95	17.02
CaO	0.19	0.30	0.29	0.20	0.28	0.24	0.20	0.20
TiO_2	0.0	0.06	0.02	0.01	0.01	0.02	0.02	0.0
MnO	0.35	0.39	0.65	0.63	0.64	0.59	0.56	0.44
NiO	0.17	0.15	0.08	0.02	0.04	0.02	----	0.19
	99.21	99.85	100.78	100.14	100.60	99.91	100.39	100.23
Fo	83	75	76	75	75	67	68	84
rim								
SiO_2	38.03	36.66	36.98	36.72	36.88			38.34
MgO	39.18	34.40	36.50	34.93	37.21			41.12
Fe_2O_3	21.94	27.15	25.67	26.96	24.58			19.53
CaO	0.21	0.28	0.29	0.24	0.30			0.22
TiO_2	0.04	0.07	0.00	0.01	0.03			0.00
MnO	0.39	0.61	0.64	0.65	0.70			0.32
NiO	0.11	0.11	0.04	0.03	0.02			0.19
	99.90	99.28	100.14	99.55	99.72			99.74
Fo	78	72	74	72	75			81

Augite phenocrysts are remarkably uniform in sampled shoshonites from the Ishawooa and Rampart volcanic centers. The one exception is augite from the Rampart volcanic center mafic vitrophyre (HPt296), which has augite phenocrysts that are zoned from higher Al_2O_3 (5.4 to 4.2%) and TiO_2 (1.4 to 1.0%; Figure 2.18a). Augites from a high MgO, high Cr silicic intrusion at the Ishawooa volcanic center, also have unusual compositions, they are much higher in MgO and CrO, and zoned to lower Al_2O_3 and TiO_2 (Figure 2.18a, and 2.18b). Fine-grained silicic rocks, such as this one, sampled from both the Ishawooa and Rampart volcanic centers, and northeastern Yellowstone Park, are similar to banakite samples described by Nicholls and Carmichael (1969). Orthopyroxene phenocrysts examined in rocks from both studies commonly have incomplete rims of augite. Nicholls and Carmichael (1969) describe a banakite sample with similar mineralogy, which also contained orthopyroxene phenocrysts with augite exsolution lamellae.

Phenocrysts from samples of early and late eruptive products from the Crandall and Hyalite volcanic centers also show changes in mineral chemistry. Augite compositions from a fine-grained plagioclase-free sample of the Crandall volcanic center has higher Cr and Al_2O_3 than phenocrysts which crystallized in later intermediate composition plagioclase bearing intrusions of the Crandall volcanic center. The youngest mafic samples from the Crandall center have augite phenocrysts with distinctively higher TiO_2/Al_2O_3, and higher MgO.

Augite phenocrysts from sampled basanite are distinctly higher in Al_2O_3 and TiO_2, and lower in Fe_2O_3 and MgO (Figure 2.18a, 2.18b, 2.18c). Whereas augite from Hyalite volcanic center samples are higher in Fe_2O_3 and CrO.

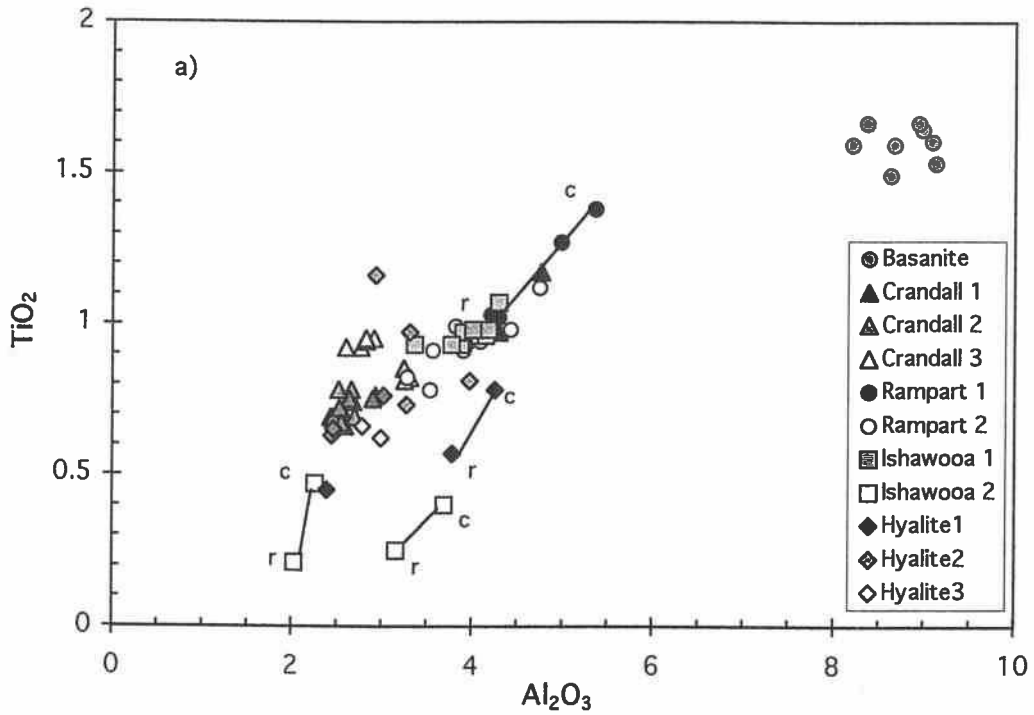

Figure 2.18 a) Al_2O_3 versus TiO_2 for augite phenocrysts from sampled rocks of mafic, intermediate and silicic compositions from different volcanic centers, and for sampled basanite. Numbers indicate the stratigraphic order in which flows and intrusions erupted at each volcanic center, and r and c indicate rim and core, respectively, of individual phenocrysts. (Rampart 1: mafic vitrophyre from Rampart volcanic center; Ishawooa 2: olivine and orthopyroxene-bearing silicic intrusion)

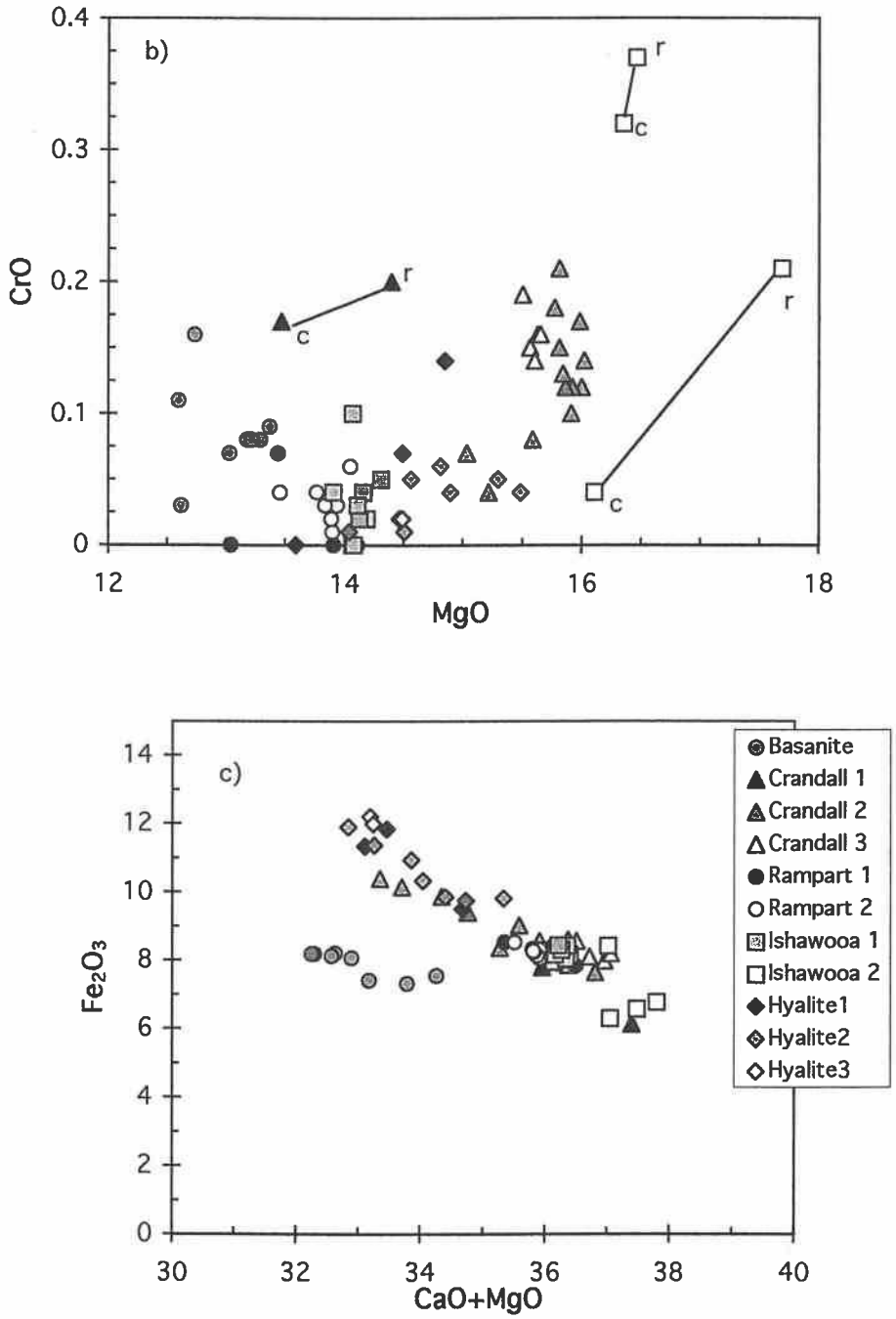

Figure 2.18 (Continued) b) CrO versus MgO for augite phenocrysts c) Fe_2O_3 versus CaO+MgO for augite phenocrysts. Numbers indicate the stratigraphic order in which flows and intrusions erupted at each volcanic center, and r and c indicate rim and core, respectively, of individual phenocrysts. (Rampart 1: mafic vitrophyre from Rampart volcanic center; Ishawooa 2: olivine and orthopyroxene-bearing silicic intrusion.)

When comparing orthopyroxene phenocrysts from shoshonites of the Hyalite volcanic center, to those from a high MgO silicic sample of the Ishawooa volcanic center, orthopyroxenes from the Ishawooa sample are zoned to higher MgO and CrO (Figure 2.19).

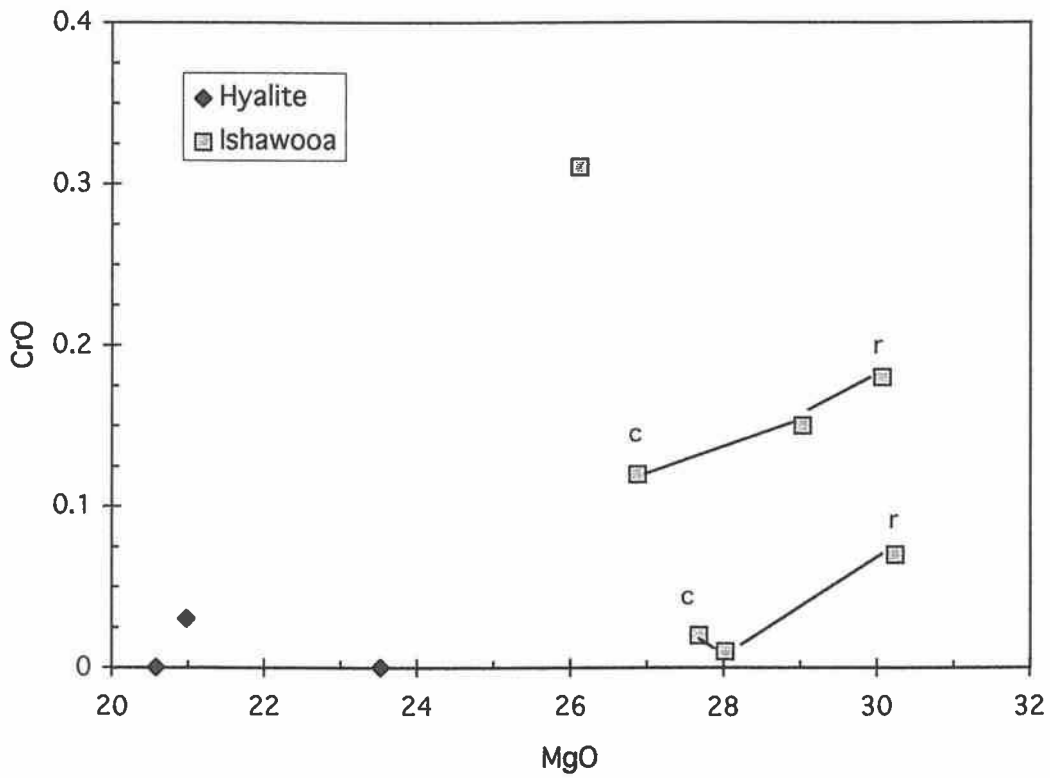

Figure 2.19. CrO versus MgO for orthopyroxene phenocrysts from shoshonite of the Hyalite volcanic center, and for a high MgO silicic sample of the Ishawooa volcanic center. The letters r and c indicate rim and core, respectively, of individual phenocrysts.

DISCUSSION

Each volcanic center in the Absaroka Volcanic province represents a magmatic series with distinctive mineralogy. In this discussion we address crystal fractionation, partial melting and magma mixing as viable mechanisms for producing the diversity of igneous compositions in the Absaroka volcanic province. Least squares calculations were run using a program by Bevington (1969) to test the role to fractionation played relative to other magmatic processes. Phenocryst compositions used in the calculations were determined by electron microprobe spot analyses (Tables 2.3 and 2.4). Excel spreadsheet programs were devised for three separate calculations: 1) calculation of trace element composition by Rayleigh fractionation, using a bulk distribution coefficient, and amount of fractionation derived from the least squares fractionation assemblage, 2) calculation of mixing between Hyalite volcanic center samples, and 3) calculation of assimilation and fractional crystallization, using equations of DePaolo (1981). In addition, a partial melting model similar to Bevington's PROGRAM 8-2 LEGFIT (Legendre polynomial fit), modified by Budahn and Schmitt (1985) to include a PROGRAM B-2 subroutine, was used to model partial melting and constrain the source mineralogy of mafic end-member samples (HM6A94 and HM294) from the Crandall volcanic center. This program allows for partial melting to occur in two cycles with fractionation of olivine and orthopyroxene, and also allows for the specification of mineralogy and mode of the source melt and residue.

Table 2.4. Pyroxene and Feldspar Compositions from selected samples of the Absaroka volcanic province.

Crandall Volcanic Center									*Basanite Flow*
wt%	Augite-HM694	Augite HM694	Augite-HM1995	Augite HM1195	Plagioclase HM1995	Plagioclase HM1195	Plagioclase HM694	Sanidine HM1995	Augite BHM195
SiO_2	49.26	51.84	50.52	49.92	54.451	52.57	55.10	64.43	48.31
Al_2O_3	6.78	2.76	2.91	3.24	27.62	29.55	28.11	20.07	9.13
Fe_2O_3*	7.48	8.06	8.6	10.39	0.42	0.66	0.65	0.37	8.13
MgO	17.33	16.09	15.63	16.07	0.06	0.09	0.10	0.01	13.22
CaO	15.94	20.76	20.74	18.32	10.53	12.33	10.49	1.42	19.35
Na_2O	1.16	0.20	0.34	0.57	4.26	4.10	4.80	4.85	1.23
K_2O	nd	nd	nd	nd	1.29	0.44	1.04	8.37	nd.
TiO_2	0.94	0.60	0.95	0.85	nd	nd	nd	nd	1.53
MnO	0.20	0.39	0.2	0.24	nd	nd	nd	nd	0.08
BaO	nd	nd	nd	nd	0.18	0.04	0.13	0.23	nd.
CrO	0.46	0.37	.0.16	0.17	nd	nd	nd	nd	0.08
NiO	nd	nd	nd	nd	nd	nd	nd	nd	nd.
total	99.55	101.07	100.05	99.68	100.31	99.78	100.09	99.77	101.06
Wo	34	42	43	39 An	53	61	51	07	Wo 45
En	54	46	45	45 An	39	47	43	44	En 42
Fs	12	12	12	16 Or	08	07	06	49	Fs 13

Ishawooa Volcanic Center				
wt%	Augite HISH5095	Augite HISH5095	Plagioclase groundmass	Sanidine groundmass
SiO_2	48.19	50.25	53.01	64.75
Al_2O_3	5.36	3.87	29.28	20.08
Fe_2O_3*	8.53	8.02	0.42	0.35
MgO	13.04	14.16	0.05	0.00
CaO	22.31	22.23	10.12	0.93
Na_2O	0.50	0.58	4.92	5.70
K_2O	nd	nd	1.16	7.88
TiO_2	1.38	0.93	nd	nd
MnO	0.22	0.22	nd	nd
BaO	nd	nd	0.20	0.28
SrO	nd	nd	0.84	0.38
CrO	0.45	0.20	nd	nd
NiO	nd	nd	nd	nd
total	99.98	100.50	100.44	99.97
Wo	48	48 An	50	05
En	39	41 An	43	50
Fs	13	11 Or	07	45

Hyalite Volcanic Center								
wt%	Augite HGB1395		Plagioclase HGB2195		Hypersthene HGB795		Plagioclase HGB795	
SiO_2	50.88		52.94		52.73		53.52	
Al_2O_3	3.78		29.63		0.84		28.68	
Fe_2O_3*	9.5		1.05		20.85		0.71	
MgO	14.85		0.14		23.52		0.08	
CaO	19.87		12.97		1.75		11.70	
Na_2O	0.50		3.68		0.03		4.48	
K_2O	nd		0.44		nd		0.56	
TiO_2	0.57		0.02		0.26		0.01	
MnO	0.39		0.01		0.47		0.00	
BaO	nd		nd		nd		nd	
SrO	nd		nd		nd		nd	
CrO	nd		nd		0.01		nd	
NiO	0.19		nd		nd		nd	
total	100.05		100.13		100.47		99.76	
Wo	42	An	68	Wo	04	An	58	
En	44	An	30	En	67	An	39	
Fs	14	Or	02	Fs	29	Or	03	

Crandall volcanic center

Fractionation calculations were done using high-MgO samples HM6A-94 HM2-94, and HM18-94 as potential starting compositions. Least squares fractionation calculations gave poor results using HM6A-94 as a mafic end-member for major element variation (with the sum of residuals >>1). Starting compositions HM2-94 and HM18-94 gave satisfactory results for major element variation by fractionation to composition HM15-94. The calculated best fit, (with the sum of the residuals = 0.38) requires 7% fractionation, with the removal of olivine (3%), augite (3%) and plagioclase (1%) from sample HM18-94 (Table 2.5). However, the difference in La concentration between the same samples cannot be accounted for by such a small percentage of fractionation, and requires fractionation in excess of 40% (Figure 2.20). Although the fractionation assemblage is consistent with major element variation and the mineralogy of these few samples, most of the major element variation from the Crandall volcanic center gave poor results. None of the calculated fractionation assemblages adequately describe the wide variation of trace elements in mafic samples, such as Th and La, with nearly constant SiO_2.

The large variation in trace element composition, and an inverse relationship between weight % MgO and LREE enrichment suggests that mafic compositions from the Crandall volcanic center may be related by different degrees of partial melting (Figures 2.7, 2.9, and 2.20). The partial melting program of Budahn and Schmitt (1985) was used to test the probability that mafic end-members HM6a94 and HM294 were produced by partial melting of a garnet and amphibole-bearing mantle source. The source mineralogy was chosen to include garnet and amphibole based on low HREE abundances, and relative depletion of Zr and Ta for Crandall samples. The relative percent of each phase in source, and the degree of partial melting, and relative amounts of olivine and pyroxene fractionation and residue in the source were then adjusted and calculated by the modeling program for the best fit to the data.

Table 2.5. Least Squares Calculations. (Cpx-clinopyroxene, Plag-plagioclase, Ol-Olivine, Ti-Mg - Ti-magnetite, Calc - calculated composition, % dif- percent difference between analyses and calculated composition)

For the Crandall volcanic center.

	Cpx	Plag	Ol	Ti-Mg	HM15	HM2	Calc	%dif	fit
SiO_2	51.84	52.51	38.33	0.00	53.20	53.1	53.34	0.5	0.008
TiO_2	0.60	0.00	0.02	14.00	0.97	0.79	0.75	-5.9	0.312
Al_2O_3	2.76	27.29	0.07	4.3	16.41	15.66	15.59	-0.4	0.006
Fe_2O_3*	9.50	0.64	17.37	80.00	8.90	8.17	8.38	12.5	0.258
MgO	16.09	0.07	42.7	0.20	4.65	7.15	7.08	-1.0	0.036
CaO	20.76	10.53	0.19	0.00	7.44	7.83	7.84	0.1	0.000
Na_2O	0.20	4.26	0.00	0.00	3.54	3.28	3.29	0.6	0.13
K_2O	0.00	1.29	0.00	0.00	1.80	2.13	1.64	-29.7	1.311
% of components						Sum of the residuals = 0.65			
Cpx	Plag	Ol	Ti-Mg	HM15					
4.1	3.6	5.4	-1.0	88.6					
±1.9	±8.5	±1.6	±0.9	±11.7					

	Cpx	Plag	Ol	Ti-Mg	HM15	HM18	Calc	%dif	fit
SiO_2	51.84	52.51	38.33	0.00	53.20	53.6	54.41	1.5	0.092
TiO_2	0.60	0.00	0.02	14.00	0.97	0.78	0.82	5.2	0.266
Al_2O_3	2.76	27.29	0.07	4.3	16.41	16.01	16.10	0.6	0.013
Fe_2O_3*	9.50	0.64	17.37	80.00	8.90	8.81	8.58	-2.6	0.264
MgO	16.09	0.07	42.7	0.20	4.65	6.20	6.23	0.6	0.013
CaO	20.76	10.53	0.19	0.00	7.44	7.91	7.86	-0.6	0.015
Na_2O	0.20	4.26	0.00	0.00	3.54	3.52	3.46	-1.9	0.132
K_2O	0.00	1.29	0.00	0.00	1.80	1.56	1.74	12.0	0.358
% of components						Sum of the residuals = 0.38			
Cpx	Plag	Ol	Ti-Mg	HM15					
2.8	0.9	3.0	-0.9	96.4					
±1.5	±6.5	±1.2	±0.7	±8.9					

	Cpx	Plag	Ol	Ti-Mg	HM20	HM6A	Calc	%dif	fit
SiO_2	51.84	52.51	38.33	0.00	56.1	53.8	54.8	1.80	0.134
TiO_2	0.60	0.00	0.02	14.00	0.97	0.80	0.94	16.9	2.857
Al_2O_3	2.76	27.29	0.07	4.3	16.50	14.22	14.65	3.0	0.364
Fe_2O_3*	9.50	0.64	17.37	80.00	6.46	8.96	8.21	-9.2	2.816
MgO	16.09	0.07	42.7	0.20	3.53	8.27	8.50	2.9	0.333
CaO	20.76	10.53	0.19	0.00	4.81	8.60	8.48	-1.4	0.076
Na_2O	0.20	4.26	0.00	0.00	3.85	3.11	2.99	-4.2	0.636
K_2O	0.00	1.29	0.00	0.00	4.81	1.66	3.05	84.0	0.000
% of components						Sum of the residuals = 3.61			
Cpx	Plag	Ol	Ti-Mg	HM15					
19.1	15.6	7.8	1.7	59.2					
±5.2	±15.5	±3.6	±1.5	±20.1					

Table 2.5. (Continued) Least Squares Calculations. (Cpx-clinopyroxene, Plag-plagioclase, Ol-Olivine, Ti-Mg - Ti-magnetite, Calc - calculated composition, % dif-percent difference between analyses and calculated composition)

Ishawooa volcanic center.

	Cpx	Ol	Ti-Mg	ISH46	ISH50	Calc	%dif	fit
SiO_2	49.86	37.01	0.01	53.0	50.20	52.5	4.6	0.607
TiO_2	1.07	0.02	10.00	0.81	0.95	1.03	9.0	0.228
Al_2O_3	4.29	0.00	4.30	19.10	16.99	16.86	-0.7	0.170
Fe_2O_3*	8.41	24.40	85.00	4.89	8.56	8.36	-2.4	0.102
MgO	13.91	38.28	0.20	2.19	5.41	5.44	0.5	0.055
CaO	22.45	0.24	0.00	4.89	6.65	6.54	-1.6	0.006
Na_2O	0.54	0.00	0.00	4.82	4.33	4.18	-3.7	1.338
K_2O	0.00	0.00	0.00	3.78	3.09	3.23	4.6	0.076

% of components				Sum of the residuals = 0.65
Cpx	Ol	Ti-Mg	HGB7	
10.5	5.5	2.3	85.4	
±1.4	±0.7	±0.4	±2.3	

	Cpx	Ol	Ti-Mg	ISH46	ISH9	Calc	%dif	fit
SiO_2	49.86	37.01	0.01	53.0	49.50	50.77	2.6	0.266
TiO_2	1.07	0.02	10.00	0.81	1.08	1.28	18.5	3.439
Al_2O_3	4.29	0.00	4.30	19.10	15.1`	15.12	0.1	0.001
Fe_2O_3*	8.41	24.40	85.00	4.89	11.2	10.57	-6.0	1.285
MgO	13.91	38.28	0.20	2.19	6.27	6.38	1.7	0.116
CaO	22.45	0.24	0.00	4.89	8.18	8.01	-2.2	0.18
Na_2O	0.54	0.00	0.00	4.82	3.93	3.66	-7.4	1.904
K_2O	0.00	0.00	0.00	3.78	1.95	2.79	43.0	4.625

% of components				Sum of the residuals = 2.95
Cpx	Ol	Ti-Mg	HGB7	
19.6	5.3	4.7	73.7	
±3.4	±1.8	±1.0	±4.5	

Hyalite volcanic center.

	Cpx	Plag	Ol	Ti-Mg	HGB7	HGB13	Calc	%dif	fit
SiO_2	50.88	52.18	37.54	0.30	58.1	52.9	54.96	3.9	0.607
TiO_2	0.57	0.02	0.02	11.00	0.92	1.04	0.99	-5.0	0.228
Al_2O_3	3.78	29.63	0.01	1.51	17.00	15.6	15.92	2.1	0.170
Fe_2O_3*	9.50	1.05	27.95	77.00	7.36	9.62	9.77	1.6	0.102
MgO	14.85	0.14	34.14	1.66	2.55	5.42	5.36	-1.2	0.055
CaO	19.87	15.00	0.20	0.17	5.44	7.93	7.90	-0.4	0.006
Na_2O	0.50	3.68	0.00	0.00	3.26	2.96	2.79	-6.1	1.338
K_2O	0.00	0.44	0.00	0.00	3.27	2.24	2.36	5.5	0.076

% of components					Sum of the residuals = 0.86
Cpx	Plag	Ol	Ti-Mg	HGB7	
11.6	11.6	5.2	2.5	70.7	
±3.0	±5.3	±1.7	±0.7	±6.6	

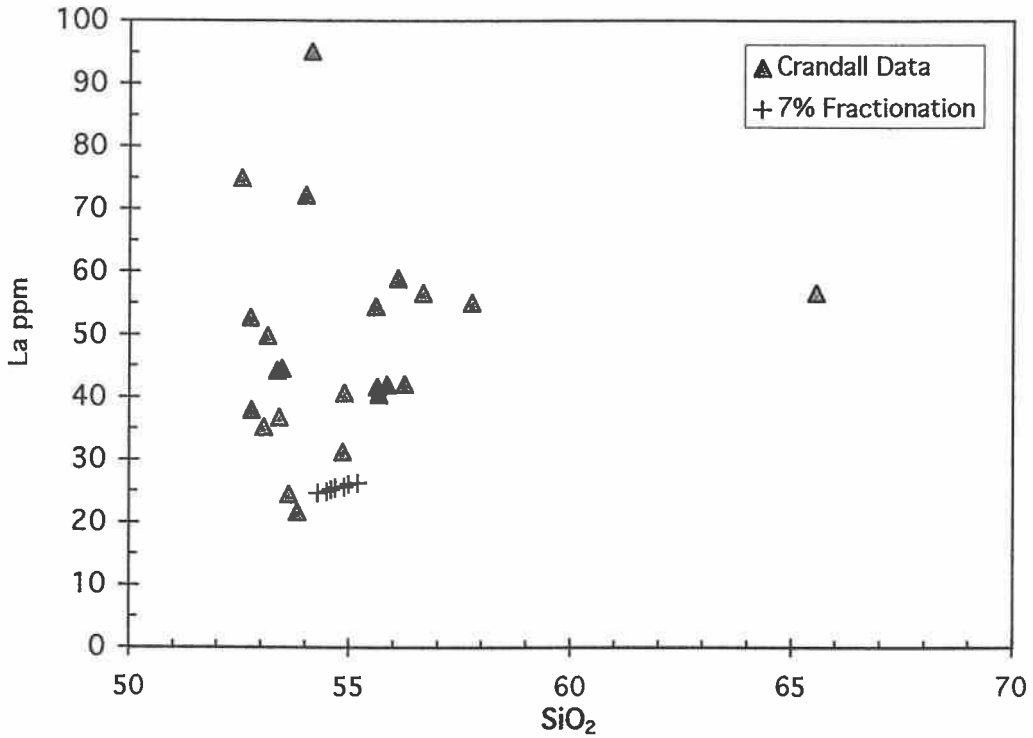

Figure 2.20. La versus SiO_2 for samples from the Crandall volcanic center showing variation allowed by calculated 7% fractionation of augite, olivine and plagioclase.

The results of the model show that samples HM294 and HM6A94 can be derived from partial melting of a garnet peridotite source containing amphibole. Although more than one solution to the data was possible, a good fit to the data set requires that garnet be present in the source (Table 2.6). Samples HM294 and HM6a94 can be derived from 2.5% and 5.5% partial melts, respectively, of a peridotite source-1, containing 48% olivine, 18% orthopyroxene, 23% clinopyroxene, 6% garnet and 5% amphibole (Figure 2.21, a and b). Alternatively, these samples may also be derived from a source containing a greater percentage of amphibole, shown as source-2 (up to 25%), and 2.5% garnet, with 10% clinopyroxene, 15% orthopyroxene, and 47% olivine (Figure 2.22, a and b). Garnet peridotite xenoliths found in Eocene alkaline igneous rocks and diatremes of the northern Cordillera, which is a region where crustal thickness exceeds 50 km, have kelphytic rims which commonly surround minerals (Hearn and McGee, 1984). The source-2 model, which contains a very large percentage of amphibole, may represent

preferential melting of these rims which contain amphibole and clinopyroxene. Alternatively, the amphibole-bearing source of Crandall samples may not be represented by these xenoliths, and could be However, the source-2 model also requires that the source contain a separate more pronounced enrichment of LREE, produced by other factors. Alternative LREE enrichment of the source, such as melt metasomatism and LREE enrichment of clinopyroxene are viable mechanisms of enrichment in this model (Nielson and Noller, 1987).

Table 2.6a. Mineralogy of Source, and Proportion of Melt Fraction and Residue, for Modeled Partial Melts.

	Olivine	Orthopx	Clinopx	Garnet	Amph	Ol-frac	Opx-frac
Source -1	48%	18%	23%	6%	5%	0	0
melting	15%	5%	30%	30%	20%	0	0
Prop in residue	49%	18%	23%	5%	5%	0	0
Fractionating Assemblage						80%	20%
Melt fraction =2.5% for HM294						15% Fractionation	
Melt fraction =5.5% for HM6A94						of Ol and Opx	
Source -2	45%	10%	18%	2.5%	24.5%	0	0
melting	15%	5%	25%	5%	50%	0	0
Prop in residue	46%	10%	18%	2%	24%	0	0
Fractionating Assemblage						80%	20%
Melt Fraction =2.5% for HM294						15% Fractionation	
Melt Fraction=7.5% for HM6A94						of Ol and Opx	

Table 2.6b. Weighted fit of Source Mineralogy to Trace Elements of Partial Melt. Melt-1 is a partial melt of the source composition, and Melt-2 includes 15% fractionation of olivine and orthopyroxene at the source.

Source with 48% Ol, 18% Opx, 23% Cpx, 6% Gnt, and 5% Amph									
		For 2.5% Melting				For 5.5% Melting			
	Source	Melt-1 2.5%	Solid	Melt-2 2.5%	HM294	Melt 1 5.5%	Solid	Melt 2 5.5%	HM6A 94
La	1.10	22.83	0.54	31.54	35.30	14.38	0.33	19.87	21.80
Ce	2.70	42.33	1.68	58.46	65.60	29.61	1.13	40.89	42.10
Nd	1.65	18.26	1.22	25.20	30.30	14.24	0.92	19.66	21.60
Sm	0.48	3.98	0.39	5.49	5.35	3.34	0.31	4.61	4.33
Eu	0.17	1.20	0.14	1.66	1.38	1.05	0.11	1.44	1.23
Gd	0.50	3.32	0.43	4.57	3.66	2.94	0.36	4.06	3.43
Tb	0.08	0.44	0.07	0.60	0.47	0.40	0.06	0.56	0.43
Y	3.00	15.15	2.69	20.87	18.40	14.26	2.34	19.64	18.40
Ho	0.11	0.5	0.10	0.69	0.56	0.48	0.09	0.67	0.52
Tm	0.05	0.17	0.05	0.23	0.22	0.17	0.04	0.24	0.23
Yb	0.32	0.97	0.30	1.33	1.29	1.00	0.28	1.37	1.36
Lu	0.05	0.13	0.05	0.18	0.19	0.14	0.04	0.19	0.20
Sc	11.7	12.55	11.68	15.65	20.50	12.84	11.63	16.01	27.60
Ni	2850	1412	2887	403.89	187.00	1422	2933	406.58	90.10
Cr	3250	1016	3307	331.79	425.00	1027	3379	335.50	345.00

Source with 45% Ol, 10% Opx, 18% Cpx, 2.5% Gnt, and 25 % Amph									
		For 2.5% Melting				For 5.5% Melting			
	Source	Melt-1 2.5%	Solid	Melt-2 2.5%	HM294	Melt 1 5.5%	Solid	Melt 2 5.5%	HM6A 94
La	1.10	22.83	0.54	31.54	35.30	14.38	0.33	19.87	21.80
Ce	2.70	42.33	1.68	58.46	65.60	29.61	1.13	40.89	42.10
Nd	1.65	18.26	1.22	25.20	30.30	14.24	0.92	19.66	21.60
Sm	0.48	3.98	0.39	5.49	5.35	3.34	0.31	4.61	4.33
Eu	0.17	1.20	0.14	1.66	1.38	1.05	0.11	1.44	1.23
Gd	0.50	3.32	0.43	4.57	3.66	2.94	0.36	4.06	3.43
Tb	0.08	0.44	0.07	0.60	0.47	0.40	0.06	0.56	0.43
Y	3.00	15.15	2.69	20.87	18.40	14.26	2.34	19.64	18.40
Ho	0.11	0.5	0.10	0.69	0.56	0.48	0.09	0.67	0.52
Tm	0.05	0.17	0.05	0.23	0.22	0.17	0.04	0.24	0.23
Yb	0.32	0.97	0.30	1.33	1.29	1.00	0.28	1.37	1.36
Lu	0.05	0.13	0.05	0.18	0.19	0.14	0.04	0.19	0.20
Sc	11.7	12.55	11.68	15.65	20.50	12.84	11.63	16.01	27.60
Ni	2850	1412	2887	403.89	187.00	1422	2933	406.58	90.10
Cr	3250	1016	3307	331.79	425.00	1027	3379	335.50	345.00

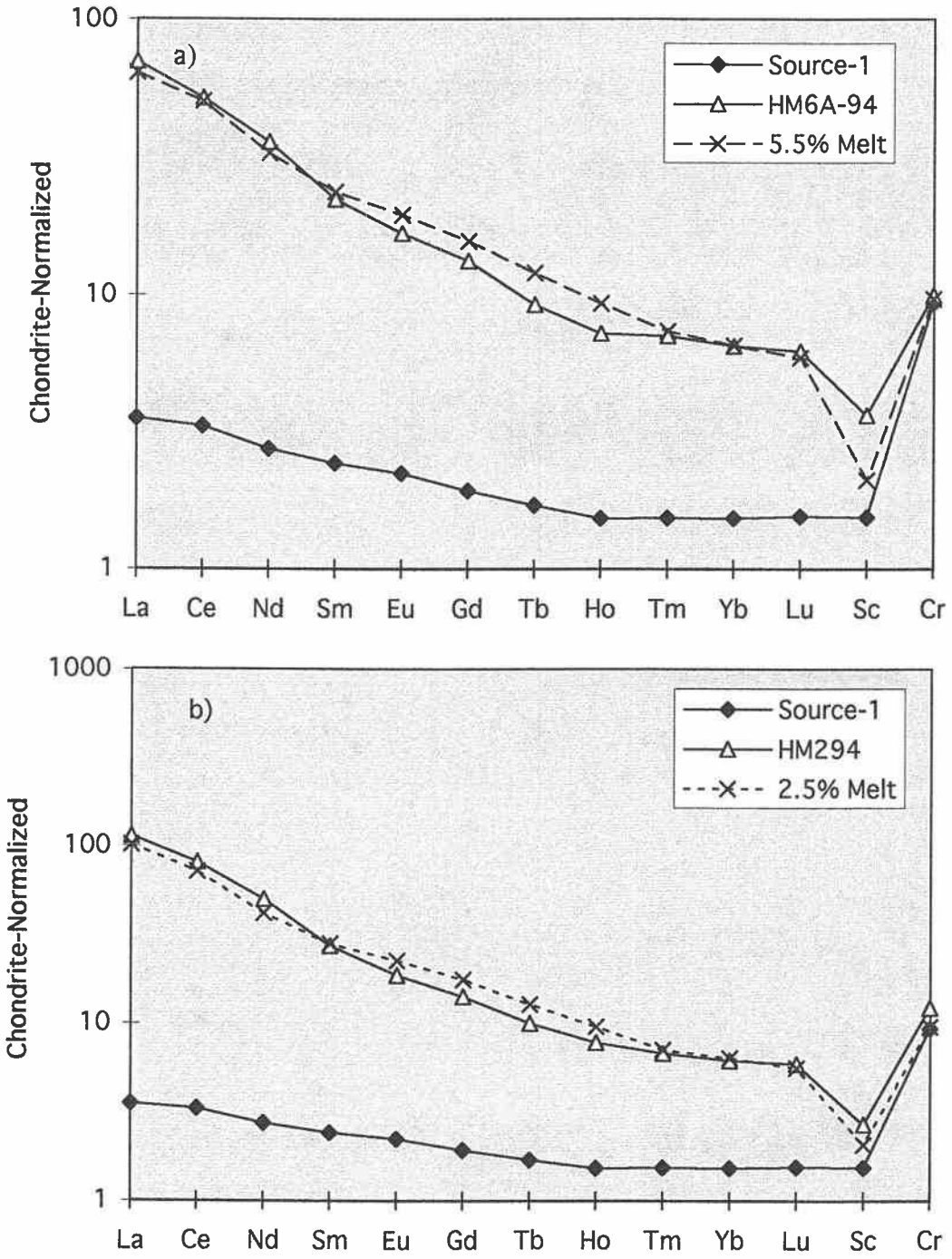

Figure 2.21. Chondrite-normalized plot of REE, Sc and Cr (x100), for Crandall volcanic center samples, and source-1 composition, and calculated partial melts. a) 5.5% melt is shown with composition of sample HM6A-94, and b) 2.5% melt is shown with composition of sample HM2-94.

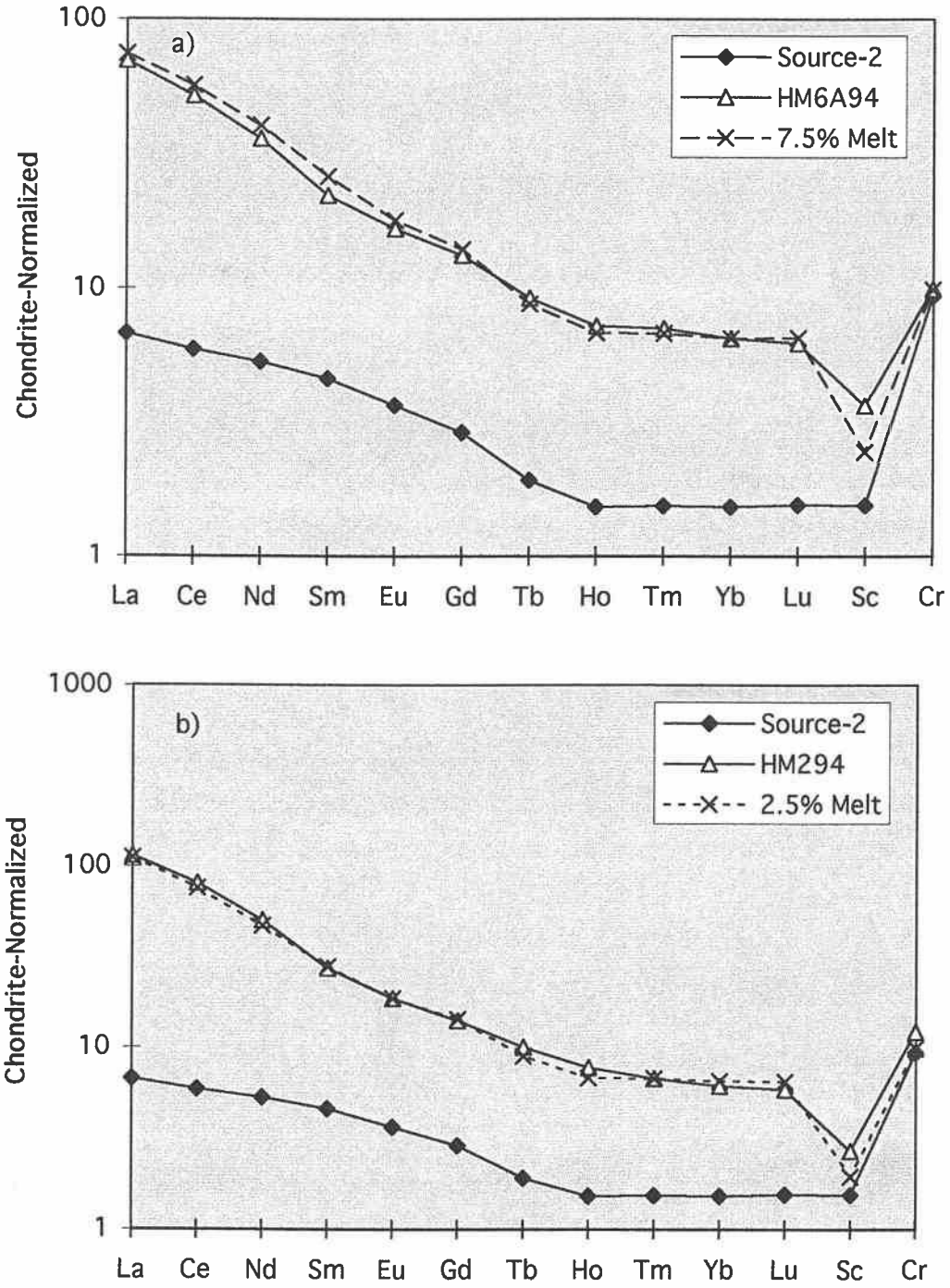

Figure 2.22. Chondrite-normalized plot of REE, Sc and Cr (x100), for Crandall volcanic center samples, and source-2 composition, and calculated partial melts. a) 7.5% melt is shown with composition of sample HM6A-94, and b) 2.5% melt is shown with composition of sample HM2-94.

A large percentage of amphibole, as well as clinopyroxene in a mantle source requires substantial enrichment by metasomatic processes. However, the ancient nature of subcontinental lithosphere in the region of the Absaroka volcanic province, which is part of the Archean Wyoming craton, allows adequate time for extensive metasomatism to occur, including well documented early Proterozoic enrichment (Peterman, 1981: Mueller et al., 1983; Dudas et al., 1987; Mueller et al., 1988). It is also likely that less refractory phases should dominate the melting assemblage.

Although more than one source composition provides a good fit to the data, the model suggests that mafic samples are related by partial melting from a garnet- and amphibole- bearing peridotite source. Estimates of the composition of continental lithospheric mantle by McDonough (1990, 1991), based on a compilation of spinel and garnet peridotite xenoliths, suggest that the median composition of lithospheric mantle enrichment in LREE is from 1.4 to 4 times chondritic values. Cratonic lithospheric mantle estimates of LREE are similar, but with lower relative HREE. These estimates are consistent with both modeled sources, but closer to the source-1 composition, containing a lower percentage of amphibole.

Ishawooa volcanic center

At the Ishawooa volcanic center, least squares calculations used to model fractionation are only feasible for low SiO_2 compositions of absarokite and shoshonite. The absarokite end-member (ISH995) at the Ishawooa volcanic center has 5% olivine replaced by calcite and gave poor results. Least squares calculations using sample ISH5095 as a parent, with fractionation of 5.5% olivine, 10.5% augite and 2.3% Ti-magnetite can produce shoshonite with the major element composition of ISH4695 (Table 2.5) A correction of the major element analysis of sample ISH995, by calculating a replacement of 5% $CaCO_3$ with olivine, produced a composition which falls along the calculated fractionation trend (Figure 2.3a).

Calculated Rayleigh fractionation, based on the least squares assemblage produced a good fit for observed enrichment in trace elements from absarokite to shoshonite (Figure 2.23b, Table 2.7).

Rocks from the Ishawooa volcanic center which are low in K_2O, high in Cr, MgO and have >60% SiO_2 cannot be derived from shoshonite through fractionation. The zonation of pyroxenes from one such sample, to phenocryst rims with higher MgO and CrO, and the presence of augite rims on orthopyroxene suggests that these rocks are derived from magma mixing. Intermediate compositions between these high-SiO_2 rocks and shoshonite, also do not fall along the fractionation trend. Likewise, plagioclase and hornblende bearing dacites do not have compositions which can be derived by simple fractionation from shoshonite. Fractionation models do not adequately describe the decrease in K_2O and incompatible elements for intermediate, or more silicic, hornblende-bearing dacite compositions. These are most likely derived from mixing or assimilation of a less enriched silicic source (Figure 2.23, a and b).

Table 2.7. Actual and calculated trace element concentrations for Ishawooa lavas based on Rayleigh fractionation of least squares phenocrysts assemblage.

Element	ISH5095	D-ol	D-cpx	D-mag	Bulk D	Calculated	ISH4795
Sr	1680	0.0140	0.060	0.000	0.0074	2235	2240
Ba	2390	0.0099	0.020	0.000	0.0027	3082	2970
La	48.5	0.0067	0.050	0.006	0.0059	60.5	53.4
Nd	40.8	0.0066	0.19	3.000	0.2204	47.8	41.2
Sm	7.01	0.0066	0.29	2.200	0.3304	8.1	6.7
Zr	137	0.1700	0.12	8.000	0.1978	160.5	158.0

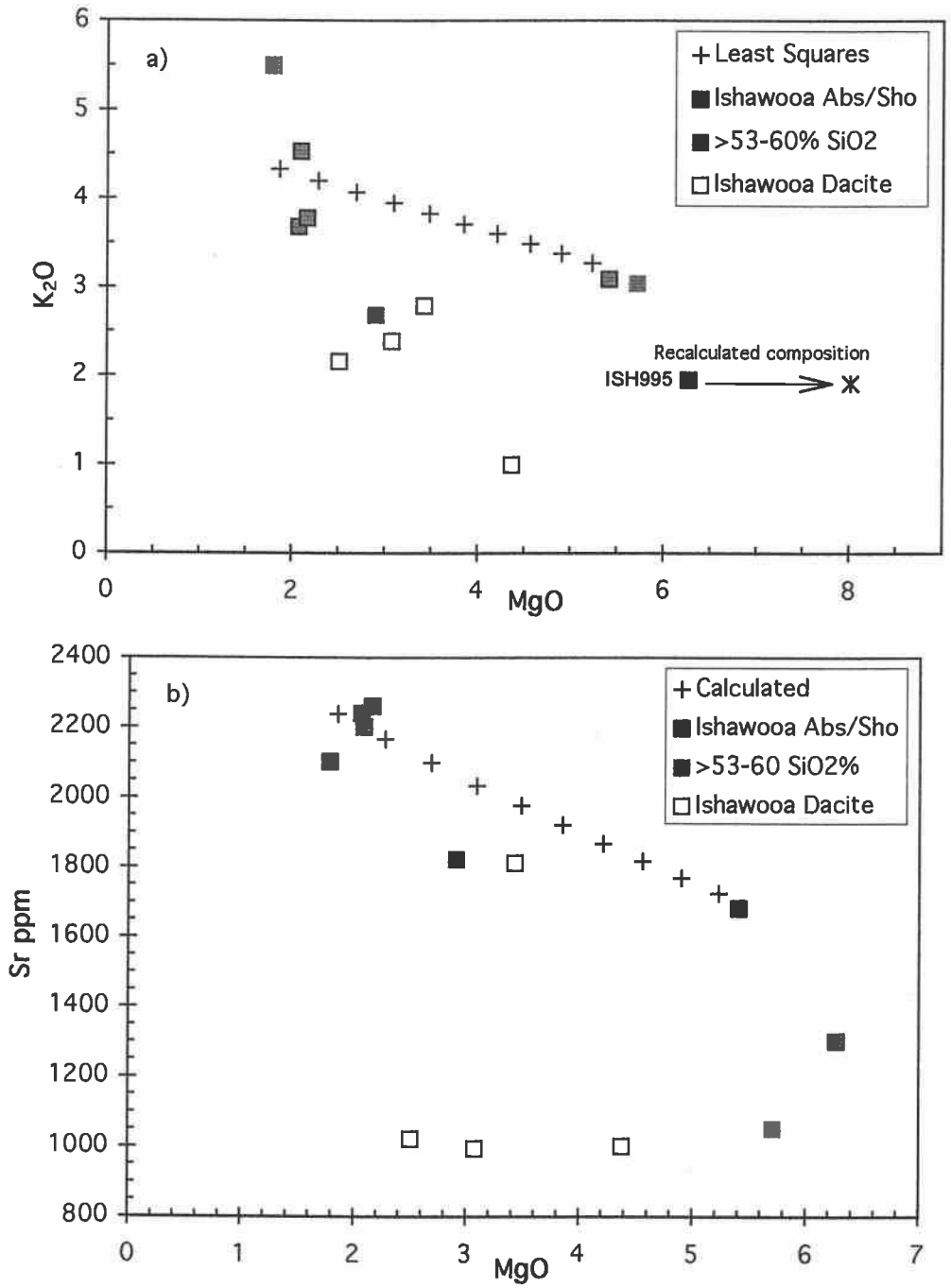

Figure 2.23. Compositions from the Ishawooa volcanic center shown with those derived from fractionation calculations. a) K_2O versus MgO with mafic end-member sample which does not fit least squares calculation shown in darker gray, and recalculated composition of same sample shown with an x. b) Sr versus MgO based on Rayleigh fractionation using least squares assemblage.

Hyalite volcanic center

Major element variation diagrams show that unlike other volcanic centers, compositions from the Hyalite volcanic center plot in simple linear trends which could be produced by fractionation processes or magma mixing (Figure 2.4). A least squares calculated fractionation assemblage consists of olivine (5%), plagioclase (12%), augite (12%), and Ti-magnetite (2.5%), with 0.86 for the sum of the residuals. Calculations also show that fractionation may have produced some of the observed variation in trace element concentrations. However, trace element variation by Rayleigh fractionation does not produce the variation of Ba and Sr for all samples (Figure 2.24a). Magma mixing can also produce linear trends similar to the variation produced by fractionation. A combination of crystal fractionation and binary mixing of Hyalite volcanic center melts with a source which has lower concentrations of incompatible elements, such as Sr, can produce the observed variation in both major and trace element composition (Figure 2.24b).

Comparison of Fractionation Paths

Potassic mafic rocks of the Ishawooa and Hyalite volcanic centers can be partly modeled by fractionation processes. Fractionation alone cannot account for the extreme incompatible enrichment of all mafic samples, such as those at the Crandall volcanic center, which are most likely derived by different degrees of partial melting. As magmas at individual volcanic centers become more differentiated, mixing with less enriched sources, which may be derived from crustal melts, become the dominant processes, as shown by the variation in composition of intermediate to silicic compositions from the Ishawooa and Hyalite volcanic center.

Different fractionation assemblages for the Hyalite and Ishawooa volcanic centers may have resulted from variation in the depth of fractionation and P_{H2O}. At

the Ishawooa volcanic center, where plagioclase crystallization is lacking, fractionation may have taken place at greater depths with higher P_{H2O} (Moore and Carmichael, 1998). Shoshonite can be modeled by least squares fractionation of olivine and clinopyroxene (with minor spinel) from absarokite, also indicating that plagioclase did not contribute to the genesis of early rock types at the Ishawooa volcanic center. The higher relative proportion of pyroxene fractionation necessary to produce sampled compositions at Ishawooa, further suggests that they crystallized at higher pressure (Mahood and Baker, 1986). In contrast, fractionation at the Hyalite volcanic center took place at lower P_{H2O}, a condition necessary for plagioclase stability (Moore and Carmichael, 1998). Crandall volcanic center samples exhibit a more complex mineralogy, with crystallization of clinopyroxene in early melts, signifying at greater depths (and higher PH_2O), followed by plagioclase, olivine, and pyroxene crystallization in later intrusions, which probably took place at shallower levels.

Trace element vs. SiO_2 variation diagrams highlight distinctive fields of trace element enrichment for volcanic centers from each group (Figure 2.5). These differences can be explained, in part, by the fractionation of different mineral assemblages. Highly potassic samples from the Ishawooa and Rampart volcanic centers exhibit greater enrichment in La, Rb, Ba, and Sr, which may be enhanced by fractionation of clinopyroxene, in which these elements are incompatible. Plagioclase fractionation at the Hyalite volcanic center produces lower Sr, which behaves more compatibly. The presence of plagioclase and shallow fractionation processes, may have also produced more moderate Ba and K enrichment trends, because D_{Ba} for plagioclase is greater than ten times D_{Ba} for clinopyroxene (Rollinson, 1993).

Intermediate to silicic rocks which, in general, have lower concentrations of K, P, LREE, Sr, Rb, Ba, Zr and Hf, do not result from clinopyroxene dominated fractionation. Mixing or assimilation with a silicic crustal source with less pronounced enrichment in incompatible elements is likely to have produced lower-K_2O, intermediate compositions at the Ishawooa volcanic center. These intermediate rocks would be classified as calc-alkaline andesites on the total alkalis versus silica diagram of Le Maitre et al., (1989) (Figure 2.3).

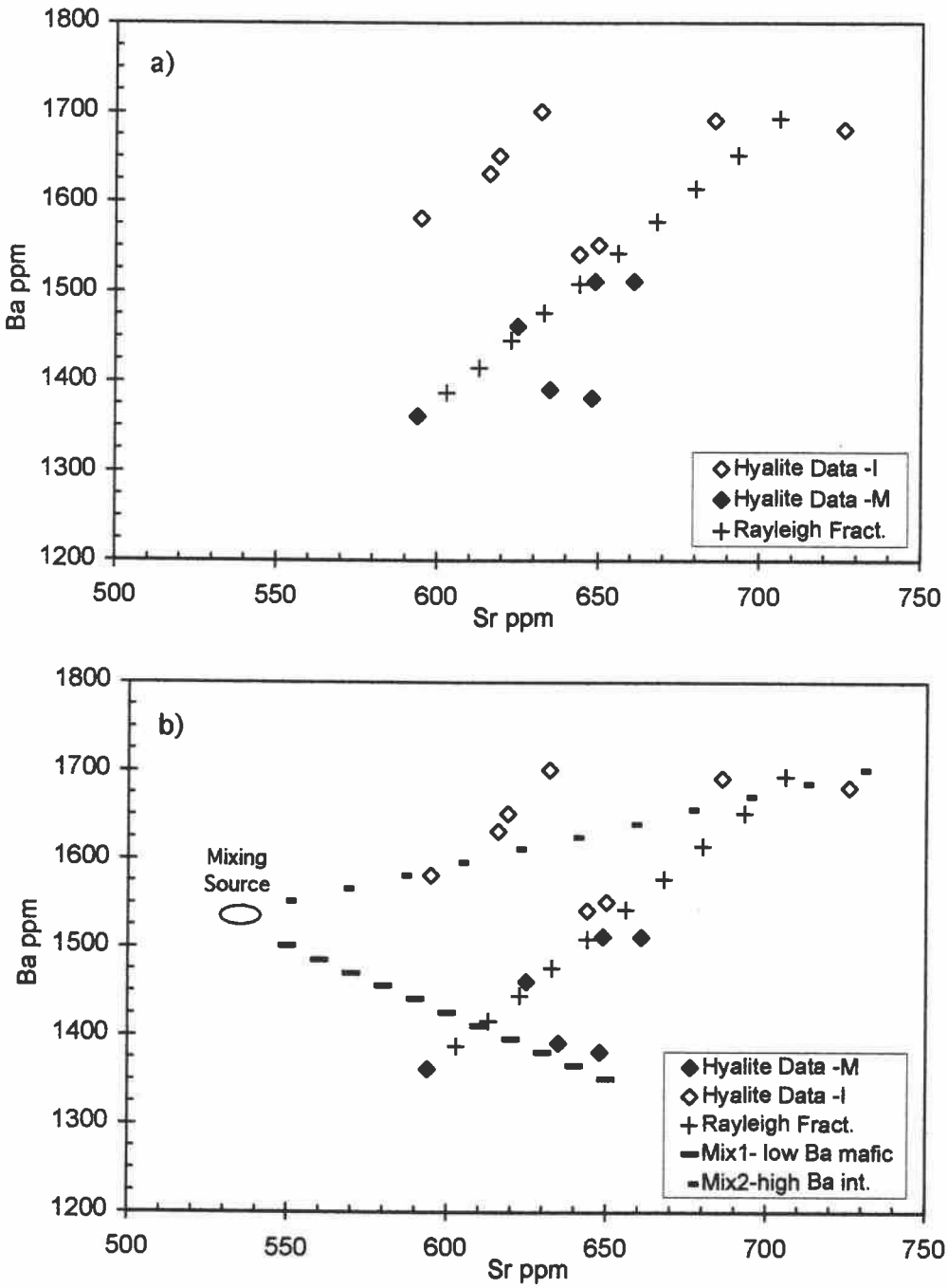

Figure 2.24. Ba versus Sr for the Hyalite volcanic center data. a) Hyalite volcanic center data is shown with variation calculated by Rayleigh fractionation; b) Hyalite volcanic center data are shown with variation calculated by Rayleigh fractionation and magma mixing curves derived from mixing both mafic Hyalite compositions, and more fractionated intermediate Hyalite compositions with a low Sr source.

Source Enrichment

Even though some differences in trace element enrichment can be explained by separate fractionation paths at each of the four volcanic centers, other trace element characteristics suggest that melt sources for volcanic centers from each group are distinct. There are fundamental differences in normative composition and trace element enrichment of the least-evolved rock types among the different volcanic centers. When comparing the most primitive samples from each of the volcanic centers, quartz-normative samples from the Hyalite volcanic center show a distinctively flatter REE pattern (Figure 2.16). This difference cannot be due to LREE enrichment induced by clinopyroxene fractionation, because compositions shown from the Ishawooa and Crandall volcanic centers, and sampled basanite, have similar or higher wt% MgO. In addition, olivine-normative mafic samples from the Crandall volcanic center which are higher in MgO and Cr than mafic samples from other volcanic centers have the lowest concentrations of HREE and HFSE.

Mafic nepheline-normative samples of Rampart, Ishawooa, and Sunlight have higher Sr, Rb, P_2O_5/Zr, Ta/Yb, Th/Yb and Ce/Yb and lower Rb/K (Figure 2.4, Figure 2.10, Figure 2.11, Figure 2.12a and 2.12b). Higher trace element ratios in these samples suggest that although incompatible element enrichment in these samples is enhanced by the fractionation of clinopyroxene, these samples are derived from a source which is fundamentally more enriched than olivine and quartz normative compositions.

Source Mineralogy

High Rb and low K/Rb (150-250) in mafic nepheline-normative samples with the greatest enrichment in incompatible elements suggest that these samples are derived from a phlogopite-bearing source (Beswick, 1976). Phlogopite-bearing

xenoliths are common in minettes of the Wyoming province, which erupted coeval with igneous activity of Absaroka volcanic province (Carter and Hearn, 1986; Hearn et al., 1991; Carlson and Irving, 1994). Ba enrichment and particularly elevated Ba/Sr is considered indicative of a source containing phlogopite (Irving and Frey, 1984; O'Brien et al, 1991). However, enrichment of Sr relative to Ba is strongly dependent on the stability of feldspars in the source region, which break down at conditions of elevated P_{H2O} (Thompson et al, 1998; Moore and Carmichael, 1998).

AFC calculations demonstrate that partial melting of a phlogopite-bearing source by an OIB-like melt, similar in composition to the basanite sample, will produce an enrichment in Sr and Ba under conditions of high water pressure, above the plagioclase stability field. Using the calculation for AFC from DePaolo (1981), bulk assimilation of 10% phlogopite with fractionating proportions of 5% olivine, 15% augite was modeled (See Appendix F). Concentrations of Rb, Sr, Ba, La, and Zr were calculated for 5% increments of fractionation and a rate ratio (r) of assimilation to crystallization of 0.1. Calculations included both OIB and basanite starting compositions. OIB starting concentrations are based on the modal composition of 897 samples of Ocean Island Basalt from Fitton et al. (1991). Trace element concentrations for phlogopite were taken from LaTourrette et al. (1995). The partition coefficients for augite and magnetite are from experimental data from Meen (1988 and 1990) for an anhydrous 10 kbar basaltic melt. The olivine partition coefficients are from Rollinson (1993) (Table 2.6).

Table 2.8. Compositions (in ppm) used in AFC modeling of phlogopite assimilation.

	OIB	Phlogopite	Distribution coefficients for Bulk D		
	Fitton et al, 1991	La Tourrette, 1995	Ol	Cpx	Ti-magnetite
Rb	29.4	3869	0.0098	0.32	0.00
Sr	718	194	0.014	0.08	0.00
Ba	511	5189	0.0099	0.02	0.00
La	45	7.7	0.0067	0.10	0.00
Zr	255	7.0	0.012	0.25	0.40

With assimilation of phlogopite, Ba and Sr in the melt increases dramatically, and is coupled with moderately increasing Zr and La. Using concentrations from the sampled basanite and a phlogopite assimilant with F = 80 (fraction remaining) produced trace element concentrations which are most similar to the nepheline normative sample from the Sunlight monzogabbro intrusion (Table 2.7). Although the assimilation model does not produce the exact compositions of nepheline normative rocks, it closely approximates Rb enrichment and relative abundances of Ba and Sr. If the fractionating assemblage excludes plagioclase, which did not crystallize from nepheline-normative AVP samples, Sr and Ba are both enriched with a gradual increase in Ba/Sr (Figure 2.24). These calculations also demonstrate that bulk assimilation of all elements in phlogopite should also produce enrichment in Zr, which is not observed. If phlogopite assimilation produced incompatible element enrichment in nepheline-normative samples, additional phases must control the concentration of Zr and other HFSE.

Table 2.9. Trace element concentrations for nepheline normative samples HMD4 and HPt2 shown together with calculated OIB+ phlogopite assimilant (OIB+PHL), and basanite with phlogopite assimilant (BAS+PHL) in ppm. (F=80, and r = 0.1 for both calculated compositions.)

Element (ppm)	# Smg496 Sunlight	# HPt296 Rampart	OIB+ Phlogopite	Basanite+ Phlogopite
Rb	140	144	140	141
Sr	1430	1580	886	1227
Ba	1270	2280	760	936
La	87.8	49	60	64
Zr	215	138	312	350
Ba/Sr	0.88	1.44	0.86	0.76

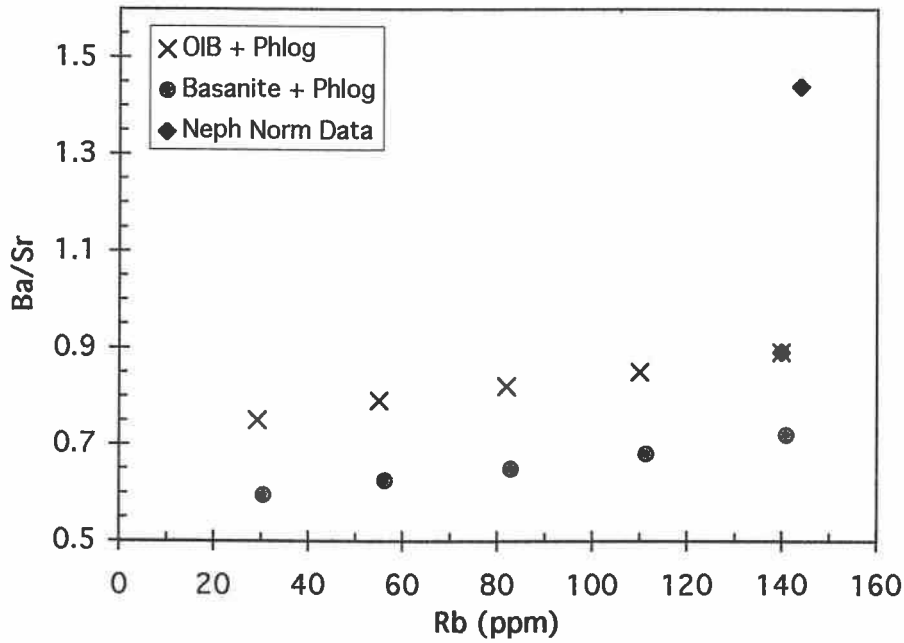

Figure 2.25. Ba/Sr versus Rb for AFC calculated compositions of sampled basanite assimilating phlogopite, and an average OIB composition assimilating phlogopite. Both calculations are shown in increments of 5 % assimilation and fractionation of olivine and clinopyroxene, with an "r" value of 0.1. Mafic nepheline normative compositions from the Rampart and Sunlight volcanic centers of Absaroka volcanic province are shown for comparison.

AFC models demonstrate that Sr enrichment similar to that of nepheline-normative shoshonite samples can be produced without crustal assimilation, but by phlogopite assimilation into an enriched mafic OIB-type melt under water saturated conditions and high pressure. These calculations also suggest that mafic end-member nepheline-normative samples, such as those from the Ishawooa, Sunlight and Rampart volcanic centers, can be produced from assimilation of a phlogopite-enriched source by a melt of similar composition to the basanite sample. Variation in mineralogy and the fractionation assemblages at each volcanic center suggest that fundamental differences in pressure and volatile content of the magmas existed, which is difficult to model in simple AFC calculations. If nepheline-normative melts fractionated above the plagioclase stability field under hydrous conditions, then the source region could contain phlogopite along with additional hydrous phases, such as amphibole. Depletion of HFSE (including Zr) can be explained by the addition of amphibole in the source (Green, 1994). Alternatively, other residual phases such as

Ti-magnetite which are more stable at high pressures and under H_2O and CO_2 saturated conditions may also contribute to depletion in TiO_2, Ta and Zr (Green and Pearson, 1987; Hay and Wendlandt, 1995).

In general, most of the Absaroka volcanic province samples are depleted in HFSE and TiO_2. Depletion in HFSE may be partly controlled by fractionation of Ti-magnetite and spinel which is a part of the fractionating assemblage at the Ishawooa and Hyalite volcanic centers, and also by the presence of iron-titanium oxides in the source region, such as ilmenite, which is a common phase in mantle xenoliths from the region (Pearce and Norry, 1979; Carter and Hearn, 1986). Mafic samples from the Crandall volcanic center have higher Zr/Ta, lower HREE and HFSE. These relative abundances of trace elements are also consistent with amphibole in the source region (Green, 1994). Mafic Crandall samples which are olivine normative have relatively constant K/Rb = 450, whereas nepheline-normative samples have K/Rb= 160-200 (Figure 2.10). Higher K/Rb of the Crandall samples is also more consistent with an amphibole-bearing source. K/Rb less than 200, in nepheline-normative samples is typical of micaceous kimberlites, mica lamprophyres, and other ultrapotassic rocks which are assumed to have phlogopite in the source (Beswick, 1976). The steeper REE pattern of samples from Crandall, Ishawooa, Rampart and the sampled basanite also suggests that they are derived from a source in which garnet is stable (Rollinson, 1993). These observations are consistent with AFC calculations which suggest that phlogopite is present in the source, and partial melting calculations of the Crandall volcanic center, with garnet in the source mineralogy. The occurrence of garnet peridotite xenoliths sampled from other regional Eocene potassic rocks and diatremes, and high estimates of crustal thickness also suggest that a regional mantle source contains garnet (Carter and Hearn, 1986).

Samples which are quartz normative from the Hyalite volcanic center tend to have slightly higher TiO_2, Zr, and Yb (Figure 2.5). They also have K/Rb which are intermediate, falling between samples with olivine and nepheline in the norm, and those with olivine and hypersthene in the norm. Hyalite samples have Na_2O/K_2O slightly higher than one (Table 2.1). Therefore, no clear link to source enrichment of a potassic phase is evident in these samples. Flatter REE patterns, lower Sr, and fractionation trends which can be modeled by fractionation of plagioclase implies that

the source for the Hyalite volcanic center samples was less hydrous, and less enriched, and probably evolved at shallower levels.

Early eruptions in the Absaroka volcanic province consist of shoshonitic flows from the Crandall volcanic center. These samples exhibit enrichment which is not straightforward, but can be characterized by LREE and HFSE depletion as well as K/Rb which suggests amphibole source enrichment. Mafic eruptive products with higher Rb/K from the Ishawooa and Rampart volcanic centers erupt after magmatism at the Crandall volcanic center had ceased, and are similar in age to the nepheline-normative Sunlight intrusion. When comparing mafic compositions, these rock types exhibit the greatest enrichment in LREE and have pronounced Sr enrichment, suggesting conditions of elevated PH_2O in the melt source. Eruptions from the Sunlight, Rampart, and Ishawooa volcanic centers occur after Crandall, and exhibit more pronounced enrichment in K, Rb, Ba and Sr, with K/Rb which suggests the presence of phlogopite in the source. This relationship may be suggestive of the relative stability of amphibole and phlogopite, which are important contributing phases in an enriched source region. Phlogopite melts at higher temperatures than amphibole, and amphibole becomes less stable under water saturated conditions (Hay and Wendlandt, 1995). The relative stability of phlogopite to amphibole, rather than the depth of melting, may have contributed to changing trace element concentrations in early melts, through progressive breakdown and enrichment by hydrous phases.

The source mineralogy for Hyalite center samples is unique among those chosen for this study, although Elk Creek basalt exhibits similar enrichment behavior. Rb and K are equally incompatible for samples from the Hyalite Volcanic center as well as Elk Creek basalt, suggesting that hydrous phases such as amphibole and phlogopite are not predominating phases in the source region for these quartz normative rock types. Flatter HREE suggests the source of Hyalite volcanic center rocks is shallower (garnet free). Plagioclase crystallization suggests a melt in equilibrium with shallower and drier conditions. These differences in Hyalite volcanic center rocks suggest that the source of melting may have become shallower during later eruptive activity.

Very distinct mineralogical, textural, and chemical characteristics of Hyalite volcanic rocks compared to Crandall center volcanic rocks suggest these two volcanic centers, previously considered to be related to a northwestern volcanic belt have different origins. Samples from the Hyalite volcanic center were derived from later eruptions in the history of the Absaroka province. These later melts may have interacted with a separate source region, or a region which was depleted by earlier Eocene AVP magmatism.

CONCLUSIONS

Volcanic centers of the Absaroka volcanic province exhibit broad similarities in major element chemistry. However, each of the volcanic centers exhibits distinct compositional and petrologic characteristics produced as a result of the unique conditions under which each individual body of magma evolved. Potassic lavas at the Ishawooa and Rampart volcanic centers are nepheline normative and have the petrographic attributes of type absarokites, whereas quartz-normative trachybasalts from the Hyalite volcanic center do not. In addition, olivine- and hypersthene-normative lavas from the Crandall volcanic center have mineralogic and textural features which are not common to flows from any of the other three volcanic centers.

Between suite variation in trace element abundances for volcanic centers from Absaroka volcanic province are distinctive, even though all mafic lavas are shoshonitic, and fall into the Ta/Yb versus Ce/Yb and Th/Yb shoshonitic fields of Muller and Groves (1991). Differences between suites represent fundamentally distinct melt compositions which reflect differences in mantle sources and source mineralogy. Nepheline-normative Rb-enriched parental melts from the Ishawooa and Rampart volcanic centers includes both an OIB and phlogopite-bearing mixture of mantle sources. This contrasts strongly with mafic lavas from the Crandall volcanic center that can be closely approximated as partial melts of an amphibole-bearing garnet peridotite. Hyalite volcanic center lavas are more homogenous, and are less

enriched in LREE, Rb, Sr, and K. Because the ages of these volcanic centers are different, between suite variations may be related to a temporal change in melt source composition and the depth of melt generation.

Although each volcanic center evolves along a distinct path, similarities in the processes involved in magma differentiation exist. Mafic lava flows erupt early at each volcanic center, followed by more diverse and differentiated lavas. Mafic lavas erupt both early and late at Crandall, yet the more diverse and silicic to intermediate rock types are predominantly younger at this volcanic center, as well as the others. Within suite variations in mafic lavas from the Hyalite and Ishawooa volcanic centers are mainly accounted for by crystal fractionation. Distinct fractionation paths for each suite are most likely controlled by differences in depth and volatile content of separate magma batches. Although fractionation is the dominant process in mafic lavas, younger intermediate and more silicic rock types are less potassic and show petrographic evidence and variation in composition that suggest these are the products of mixing and assimilation.

REFERENCES CITED-2

Baedecker, P.A., and McKown, D.M. (1987) Intstrumental neutron activation analysis of geochemical samples: *In* Methods for Geochemical Analyses, P.A. Baedecker,(ed.) US Geological Survey Bulletin 1770, Chapter H, p.H1-H14.

Beswick, A.E. (1976) K an Rb relations in basalts and other mantle derived materials. Is phlogopite the key? : Geochimica et Cosmochimica Acta, vol. 40, p.1167-1183.

Bevington, P.R. (1969) Data Reduction and Error Analysis in the Physical Sciences, McGraw-Hill, 462 p.

Budahn J.R., and Schmitt, R.A. (1985) Petrogenetic modeling of Hawaiian tholeiitic basalts: a geochemical approach: Geochimica et Cosmochimica Acta, vol. 49, p. 67-87.

Carlson, R.W., and Irving, A.J. (1994) Depletion and enrichment history of subcontinental lithopheric mantle: An Os, Sr, Nd, and Pb isotopic study of ultramafic xenoliths from the northwestern Wyoming Craton: Earth and Planetary Science Letters, vol. 126, p. 457-472.

Chadwick, R.A. (1970) Belts of eruptive centers in the Absaroka-Gallatin volcanic province, Wyoming-Montana: Geological Society of America Bulletin, vol. 81, p.267-273.

Decker, P.L. (1990) Style and mechanics of liquefaction-related deformation, lower Absaroka Volcanic Supergroup (Eocene), Wyoming: Geological Society of America Special Paper 240, 71p.

DePaolo, D.J. (1981) Trace element and isotopic effects of combined wallrock assimilation and fractional crystallization: Earth and Planetary Science Letters, vol. 53, p.189-202.

Dudas, F.O. (1991) Geochemistry of igneous rocks from the Crazy Mountains, Montana, and tectonic models for the Montana alkalic province: Journal of Geophysical Research, vol. 96, p.13261-13278.

Dudas, F.O., Carlson, R.W., and Eggler, D.H. (1987) Regional middle Proterozoic enrichment of the subcontinental mantle source of igneous rocks from central Montana: Geology, vol. 15, p. 22-25.

Fitton, J.G., James, D., Kempton, P.D., Omerod, D.S., and Leeman, W.P. (1988) The role of lithospheric mantle in the generation of late cenezoic basic magmas in the western United States: Journal of Petrology, Special Lithosphere Issue, p.331-349.

Foose, R.M., Wise, D.U., and Garbarini, G.S. (1961) Structural Geology of the Beartooth Mountains, Montana and Wyoming: G.S.A. Bulletin, vol. 72, p. 1143- 1172.

Gest D.E., and McBirney, A.R. (1979) Genetic relations of shoshonitic and absarokitic magmas, Absaroka Mountains, Wyoming: Journal of Geology and Geothermal Research, vol. 6, p. 85-104.

Green, T.H. (1994) Experimental studies of trace-element partitioning applicable to igneous petrogenesis-Sedona 16 years later: Chemical Geology, p.1-36.

Green, T.H., and Pearson, N.J. (1987) An experimental study of Nb and Ta partitioning between Ti-rich minerals and silicate liquids at high pressure and temperature: Geochimica et Cosmochimica Acta, vol. 51, p.55-62.

Hague, A. (1899) Absaroka folio: U.S. Geological Survey Geol. Atlas of the United States, Folio no. 52

Hague, A., Iddings, J.P., and Weed, W.H. (1899) Geology of Yellowstone National Park: Pt II, Descriptive geology, petrography, and paleontology: U.S. Geological Survey Monograph 32, 439 p.

Hay, D.E., and Wendlandt, R.F. (1995) The origin of Kenya rift plateau-type flood phonolites: Results of high-temperature/high-pressure experiments in the systems phonolite-H_2O and phonolite-H_2O-CO_2: Journal of Geophysical Research, vol. 100, p. 400-411

Hickenlooper J.W., and Gutman, J.T. (1982) Geology of the Slough Creek Tuff, northern Absaroka volcanic field, Park County, Montana: Wyoming Geological Association 33rd Annual Field Conference Guidebook, p. 55-63.

Hearn B.C. Jr., and McGee, E.S. (1984) Garnet peridotites from Williams kimberlites, north-central Montana, USA: *in* Kimberlites and Related Rocks II, Kornprobst, J. (ed.) Elsevier, New York, p. 255-283.

Hearn B.C. Jr:, Collerson, K.D., Upton, B.G.D., and MacDonald, R.A. (1991) Ancient and enriched upper mantle beneath north-central Montana: evidence from xenoliths: Montana Bureau of Mines Special Publication 100, p.133-135.

Iddings, J.P. (1895) Absarokite-shoshonite-banakite series: Journal of Geology, vol.3, p.935-959.

Iddings, J.P. (1899) The igneous rocks of Electric Peak and Sepulchre Mountain, U.S. Geological Survey Monograph 32, pt. 2, p. 89-148.

Irving A. J., and Frey, F.A. (1984) Trace element abundances in megacrysts and their host mafic volcanics: constraints on partition coefficients and megacryst genesis: Geochimica et Cosmochimica Acta, vol. 48, p. 1201-1221.

LaTourrette, T., Hervig, R.L., and Holloway, J.R. (1995) Trace element partitioning between amphibole, phlogopite, and basanite melt: Earth and Planetary Science Letters, vol. 135, p.13-30.

Le Maitre, R.W., Bateman, P., Dudek, A., Keller, J. Lameyre Le Bas, M.J., Sabine, P.A., Schmid, R., Sorensen, H., Streckeisen, A., Woolley, A.R., and Zanettin, B. (1989) A classification of igneous rocks and glossary of terms, Balckwell, Oxford, 193 p.

Lipman, P.W., and Glazner, A.F. (1991) Introduction to middle Tertiary Cordilleran volcanism: Magma sources and relations to regional tectonics: Journal of Geophysical Research, vol. 96, p.13,193-13,199.

Love, J.D. (1939) Geology along the southern margin of the Absaroka Range, Wyoming: G.S.A. Spec. Paper 20, 134 p.

Mahood, G.A., and Baker, D.R. (1986) Experimental constraints on depths of fractionation of mildly alkalic basalts and associated felsic rocks: Pantelleria, Strait of Sicily: Contributions to Mineralogy and Petrology, vol. 93, p.251-264.

Malone, David H. (1995) Very large debris-avalanche deposit within the Eocene volcanic succession of the northeatsrn Absaroka Range, Wyoming: Geology, vol. 23, no. 7, p. 661-664.

McDonough, W.F. (1990) Constraints on the composition of the continental lithospheric mantle: Earth and Panetary Science Letters, vol. 101, p. 1-18.

McDonough, W.F. (1991) Chemical and isotopic systematics of continental lithospheric mantle: In Proseedings of the Fifth International Kimberlite Conference, vol. 1, Kimberlites and Related Rocks and Mantle Xenoliths, H.O.A. Meyer, and O.H. Leonardos, (eds.) p.478-485.

Meen, J.K. (1985) The origin and evolution of a continental volcano- Independence, Montana, Ph.D. dissertation, Penn State University, University Park, PA.

Meen, J.K. (1987) Formation of shoshonites from calcalkaline basalt magmas: geochemical and experimental constraints from the type locality: Contributions to Mineralogy and Petrology, vol. 97, p. 333-351.

Meen, J.K., and Eggler, D.H. (1987) Petrology and geochemistry of the Cretaceous Independence volcanic suite, Absaroka Mountains, Montana: clues to the composition of the Archean sub-Montanan mantle, G.S.A. Bulletin, vol. 98, p. 238-247.

Meen, J.K. (1990) Elevation of potassium content of basalt magma by fractional crystallization: the effect of pressure: Contributions to Mineralogy and Petrology, vol. 104, p. 309-331.

Moore, G., and Carmichael, I.S.E. (1998) The hydrous phase equilibria (to 3 kbar) of an andesite and basaltic andesite from western Mexico: constraints on water content and conditions of phenocryst growth: Contibutions to Mineralgy and Petrology, vol. 130, p.304-319.

Mueller, P.A., Wooden, J.L. Schulz, K., and Bowes, D.R. (1983) Incompatible-element-rich andesitic amphibolites from the Archean of Montana and Wyoming: Evidence for mantle metasomatism: Geology, vol. 11, p.203-206.

Mueller, P.A., Wooden, J.L. (1988) Evidence for Archean subduction and crustal recycling, Wyoming Province: Geology, vol. 16, p.871-874.

Muller, D. and Groves, D.I. (1997) Potassic Igneous Rocks and Associated Gold-Copper Mineralization: Springer-Verlag Berlin Heidelberg, 210 p.

Nelson , W.H., and Pierce, W.G. (1968) Wapiti Formation and Trout Peak Trachyandesite, northwestern Wyoming, U.S.G.S. Bulletin 1254-H, 11p.

Nicholls J., and Carmichael, I.S.E. (1969) Commentary on the absarokite-shoshonite-banakite series of Wyoming, U.S.A. Schweiz. Mineralogische und Petrographische Mitteilungen, vol. 49, p.47-64.

Nielson, J.E., and Noller, J.S. (1987) Processes of mantle metasomatism; Constraints from observations of composite peridotite xenoliths: Geological Society of America Special Paper 215, p.61-76.

O'Brien, H.E., Irving, A.J., McCallum, I.S. (1991) Eocene potassic magmatism in the Highwood mountains, Montana: petrology, geochemistry, and tectonic implications: Journal of Geophysical Research, vol. 96, p.13,237-13,260.

Parsons, W.H. (1939) Volcanic centers of the Sunlight area, Park County Wyoming: Journal of Geology, vol. 47, p. 1-26.

Pearce, J.A., and Norry, M.J. (1979) Petrogenetic implications of Ti, Zr, Y, and Nb variations in volcanic rocks; Contributions to Mineralogy and Petrology, vol. 69, p. 33-47.

Peterman, Z.E., Doe, B.R., and Protska, H.J. (1970) Lead and strontium isotopes in rocks of the Absaroka volcanic field, Wyoming: Contributions to Mineralogy and Petrology, vol. 27, p.121-130.

Prostka, H.J. Ruppel, E.T., and Christiansen, R.L. (1975) Geologic Map of the Abiathar Peak quadrangle, Yellowstone National Park, Wyoming and Montana: Map GQ-1244.

Reid, R.R. (1957) Bedrock geology of the north end of the Tobacco Root Mountains, Madison County, Montana: Montana Bureau of Mines and Geology Memoir 36, 24 p.

Rollinson, H. (1993) Using Geochemical Data: Evaluation, Presentation, Interpretation; Longman Scientific and Technical, John Wiley and Sons, New York, p. 108.

Rubel, D.N. (1964) Geology of the Independence area, Sweet Grass and Park Counties, Montana: PhD. dissertation, University of Michigan, Ann Arbor, 208 p.

Shultz, C.H. (1962) Petrology of Mt Washburn, Yellowstone National Park, Wyoming: Ph. D. dissertation Ohio State University, Columbus, 267 p.

Smedes H.W., and Protska, H.J. (1972) Stratigraphic framework of the Absaroka Volcanic Supergroup in the Yellowsone Park region: U.S. Geological Survey Professional Paper 729-C, 33 p.

Sundell, K.A. (1993) A geologic overview of the Absaroka volcanic province: *In* A.W. Snoke, J.R. Steidman, and S.M. Roberts, (eds.) Geological Survey of Wyoming Memoir No. 5, p. 480-506.

Taggart, J.E.Jr, Lindsay J.R.,Scott, B.A., Vivit, D.V., Bartel, A.J., and Stewart, K.C. (1987) Analysis of Geologic Materials by Wavelength-Dispersive X-Ray Flourescence Spectrometry: *In* Methods for Geochemical Analyses, P.A. Baedecker, (ed.), US Geological Survey Bulletin 1770, Chapter H, p.H1-H14.

Thompson, P., Parsons, I., Graham, C.M., and Jackson, B. (1998) The breakdown of potassium feldspar at high water pressures: Contributions to Mineralogy and Petrology, vol.130, p.176-186.

Wilson, J. Tuzo (1936) The geology of the Mill Creek-Stillwater area, Montana: Ph.D. thesis, Princeton Univ., Princeton, NJ.

CHAPTER 3

The Petrogenesis of Mafic Potassic Magmas, Absaroka Volcanic Province, Wyoming Montana

Margaret M. Hiza, Anita L. Grunder, Daniel M.Unruh

To be submitted to the *Journal of Geophysical Research*
American Geophysical Union, Washington, D.C.
47 pages

INTRODUCTION

Absarokites are high-K mafic rocks with olivine and clinopyroxene phenocrysts in a groundmass of sanidine and plagioclase. They have been described from a variey of tectonic settings, from the Cascadia subduction zone (Conrey, 1997), from back-arc environments of Indonesia (Edwards et al., 1991), from post-subduction back-arc rift-zones, Fiji (Rogers and Setterfield, 1994), and from Cordilleran Miocene - Recent rifts in Colorado (Leat et al, 1988). Yet little is known about the origin and tectonic setting of "type absarokites" from the Wyoming Province, first described by J.P. Iddings in 1895. These potassic rocks of the Absaroka volcanic province erupted between 53 and 43 Ma, as part of a diverse and widespread group of Eocene volcanic rocks. Middle Eocene Absaroka province volcanism, in Montana and Wyoming, which produced absarokite lavas, also includes basanite, shoshonite, banakite and phonolite, as well as calc-alkaline high-K andesite, dacite and rhyolite. Absaroka volcanic rocks were emplaced atop the Archean Wyoming Province craton with coeval minette, mafic phonolite, and theralite of the Highwood Mountains, Crazy Mountains and Bearpaw Mountains, and carbonatite and kimberlite of the Missouri Breaks diatremes (O'Brien et al, 1995; MacDonald et. al, 1992; Dudas, 1991; Scambos, 1991; Hearn and McGee, 1984; Figure 3.1). Smokey Butte lamproite is younger (27 Ma, K/Ar), and represents magma derived from the ancient Wyoming Province lithospheric mantle (Fraser et. al, 1986). Middle Eocene alkaline rocks which occur in the Wyoming Province are part of a broad belt of enigmatic volcanic fields which erupted contemporaneously from western Washington and Oregon to the Black Hills of South Dakota (Marvin et. al, 1980; Eggler et. al, 1988; Karner, 1989; Dudas, 1991; Harlan et. al., 1991; Mitchell and Bergman, 1991; Harlan et al, 1996; Morris and Hooper, 1997; Chapter 1).

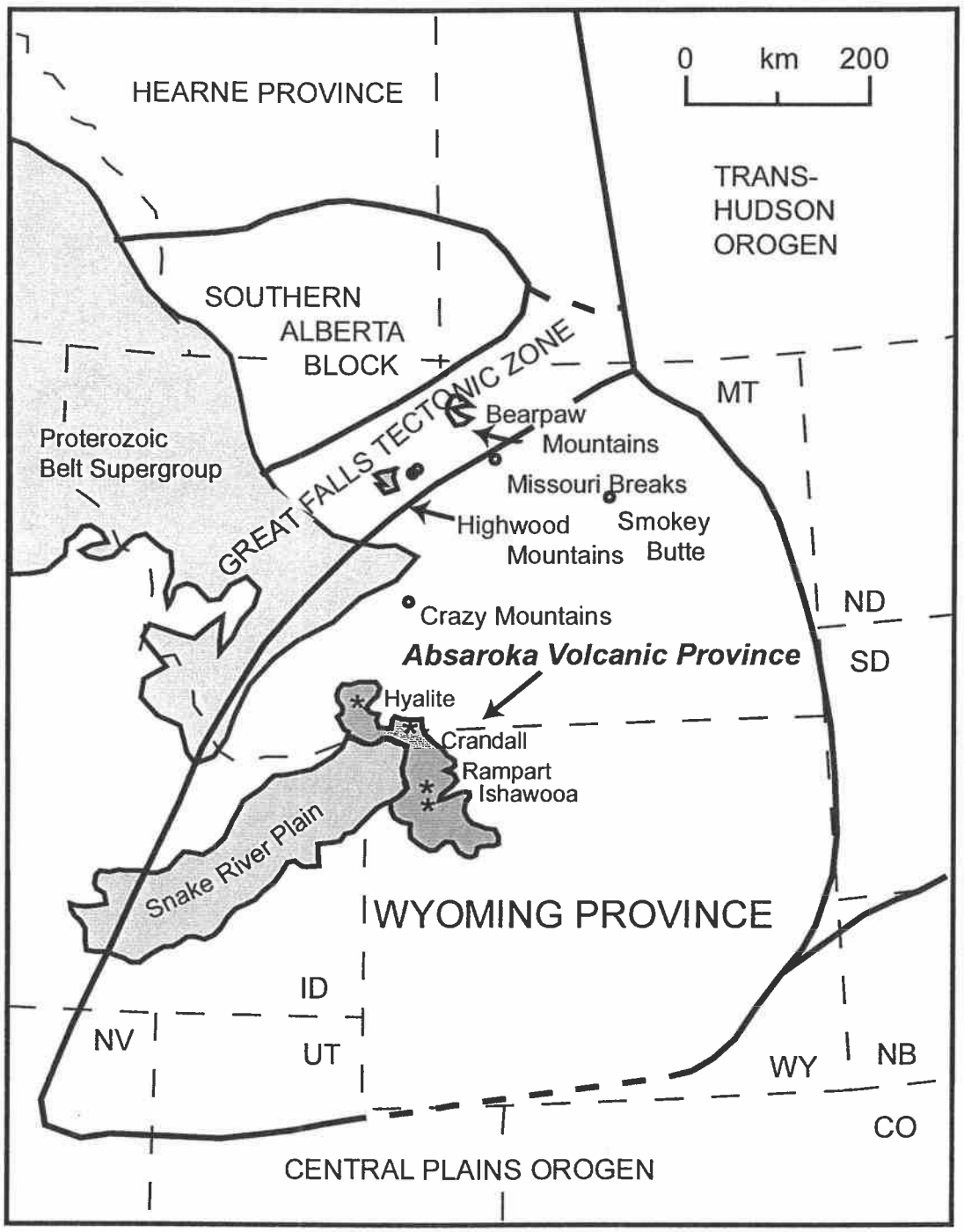

Figure 3.1. Schematic map showing the Absaroka volcanic province and sampled volcanic centers. Locations of some Eocene and Oligocene alkaline igneous rocks in Montana and Wyoming, USA, in relation to Archean cratonic provinces and Proterozoic orogenic belts are modified after Dutch and Nielsen (1990), Hoffman, (1990) and O'Brien et. al., (1995). Stars indicate volcanic centers sampled in this study.

Eocene Cordilleran volcanism has been largely interpreted to be related to subduction, based on the petrologic association of alkaline rocks with calc-alkaline rocks (Chadwick, 1970; Lipman, 1980; Dickinson, 1972; O'Brien, et. al. 1991). However, the origin of this magmatic episode remains a puzzle. Subduction-related processes fail to provide the heat source necessary for widespread volcanic activity which occurred simultaneously from near the plate margin to as far inland as 1500 km from the plate boundary (Dudas, 1991). A wide range of sources have been inferred for this middle Eocene volcanism: Old continental crust of variable composition, asthenospheric mantle, and a metasomatized or enriched source which may be ancient lithospheric mantle or subducted oceanic crust (Dudas et al, 1987; Meen and Eggler 1987 ; Eggler et al., 1988; Dudas, 1991; Norman and Mertzman, 1991; O'Brien et al, 1991; Scambos, 1991; MacDonald et al., 1992; O'Brien et al, 1995).

In this paper we report chemical compositions, Nd, Sr, and Pb isotope data from four volcanic centers in the Absaroka volcanic province, which provide constraints on the nature of magmatic sources. The volcanic rocks exhibit strong LREE enrichment, enrichment in alkaline earths, and depletion in HFSE, which are typical characteristics of subduction-related magmas (Pearce, 1983) However, important variations in chemical and isotopic compositions suggest that melting was derived primarily from the lithospheric mantle and asthenosphere with additional upper and lower crustal components, and requires no genetic link to subduction.

GEOLOGIC SETTING

The Absaroka volcanic province is the largest of the middle Eocene volcanic fields of western North America, and consists of two belts of well-preserved volcanic centers coincident with northeast-southwest trending Precambrian lineaments (Chadwick, 1970). Recent gravity surveys combined with seismic reflection data corroborate a close spatial association between northwest-trending fracture zones in Precambrian crystalline basement and the locus of middle Eocene igneous complexes in the southern Wyoming Province (Kleinkopf, 1991).

Volcanic Centers

Individual volcanic centers within the Absaroka volcanic province are characterized by thick sequences of lava flows with a mafic platform at the base, cut by radial dike swarms, and cored with intermediate to silicic intrusions. Crudely conformable upper flow sequences exhibit primary dips $\geq 10^{\circ}$ away from the center. Samples from individual volcanic centers range in composition from absarokite to dacite. This study includes mapping and detailed sampling of four volcanic centers in order to encompass spatial and compositonal variations across the Absaroka volcanic province: the Hyalite and Crandall volcanic centers from the northeastern belt, and the Ishawooa and Rampart volcanic centers from the southwestern belt (Figure 3.1). Associated ash-flow tuffs and volcaniclastic sequences have not been assigned to specific volcanic centers. Additional samples of basanite and rhyolite ash-flow tuff peripheral to the volcanic centers are included to complete the characterization of the compositional spectrum.

$^{40}Ar/^{39}Ar$ data from volcanic centers and ash-flow tuffs exhibit a general north to south age progression (Chapter 1, Figure 1.2). However, in detail, age relationships exhibit greater complexity: The Crandall volcanic center (>50.0 to 49.1 Ma) is the oldest volcanic center included in this study, Ishawooa and Rampart are similar in age (≥48 to 46.5 Ma), and the youngest eruptions from these volcanic centers overlap with generally later eruptive activity at the Hyalite volcanic center (≤47 Ma). The youngest volcanic rocks sampled include a basanite from the northern part of the province, and rhyolite from Dunrud Peak in the south.

Samples

Samples from each volcanic center were collected with a view toward spanning the age and compositional range. Samples from early flows of the Crandall volcanic center are fine-grained rocks containing augite and sparse forsteritic olivine. Samples from cross-cutting dikes and intrusions are porphyritic, with plagioclase, olivine and clinopyroxene phenocrysts. Also included in the suite of samples from Crandall is a trachyte tuff with phenocrysts of hornblende, biotite, and plagioclase.

Samples from early flows of the Ishawooa volcanic center include type absarokites with olivine and augite in a groundmass of sanidine, plagioclase and spinel. Apatite is a common accesssory phase, and is usually enclosed within olivine phenocrysts. Associated shoshonites are petrographically similar with less olivine and pyroxene. Cross-cutting dacites have plagioclase, quartz, biotite and amphibole.

Samples from the base of the sampled section at the Rampart volcanic center include a plagioclase-bearing mafic vitrophyre, and a shoshonite flow similar to those at the Ishawooa volcanic center. Silicic flows have distinct petrographic features with rare olivine, orthopyroxene (some with incomplete rims of augite) and clinopyroxene. The top of the sampled section is a crystal-rich tuff, with phenocrysts of hornblende, plagioclase and quartz.

Mafic samples from the base of the Hyalite volcanic center are fine-grained, with a microlitic to trachytic groundmass with phenocrysts (<1mm - 4 mm) of clinopyroxene, olivine, plagioclase, and magnetite. Samples from more silicic lavas are more porphyritic, containing phenocrysts of plagioclase, clinopyroxene and hypersthene.

MAJOR AND TRACE ELEMENT COMPOSITIONS

Major Elements

The Absaroka volcanic province suite overall is composed mainly of rocks having alkalic mafic to intermediate compositions, namely shoshonites and banakites (Figure 3.2a) but includes a broad spectrum from basanite to rhyolite. The suite as a whole, and individual volcanic centers within it, however, define trends that range from calc-alkaline to shoshonitic (Figure 3.2b). Although most rocks are variably differentiated, a few compositions may be mafic parental magmas. Because mafic compositions are rare, most rocks sampled have MgO <9%, with Cr 50-200 ppm and Ni 30-100 ppm. However, high MgO samples do occur, and may be more common in areas peripheral to volcanic centers. Rocks with comparably high Mg numbers (>70), Cr >300 ppm and Ni > 75 ppm have been sampled from the Crandall volcanic center (Figures 3.3a and 3.3b). Highly potassic samples from Ishawooa and Rampart volcanic centers are lower in MgO due primarily to fractionation of olivine and clinopyroxene (Chapter 2). Moderately potassic samples from the Hyalite volcanic center also have low Mg numbers, although least squares calculations suggest that plagioclase fractionation predominates at this volcanic center (ibid). Samples which are considered mafic end-members of volcanic centers have >5% MgO, <54% SiO2, and >75 ppm Cr. The Crandall volcanic center has the largest number of samples which fall into this category. Basanite is not a characteristic rock type of volcanic centers, and is an isolated lava flow from the

northern Absaroka volcanic province. Representative samples which are considered silicic have >60% SiO_2, even though some of these samples are moderately high in MgO (≥4%), Cr (≥200 ppm) and Ni (≥100 ppm). High MgO, high Cr samples which are also high in SiO_2 have petrographic features which suggest they are derived from a mixture of sources (Chapter 2).

Trace Elements

Mafic alkaline rocks from the Absaroka volcanic province contain high abundances of Ba, Rb, K, Sr, Th and LREE which are comparable to abundances typical of ultrapotassic rocks found elsewhere (Beswick, 1969; Leat et. al., 1988; Muller and Groves, 1997). Abundances of Zr, Hf, Ti and Ta vary, and are highest in sampled basanite (Figure 3.4). Most samples have low Ta, but do have chondrite normalized Ta similar to K. Zr, Ta and HREE are lowest for samples from the Crandall volcanic center. Mafic end-member samples from this volcanic center can be modeled as partial melts derived from a garnet- and amphibole-bearing peridotite source (Chapter 2). The Crandall center samples also have distinctly higher Ba/Rb and K/Rb (Figure 3.5). Nepheline normative samples, from the Ishawooa and Rampart volcanic centers have lower K/Rb and Ba/Rb due to higher concentrations of Rb in these rocks (K/Rb ≤ 250). These samples also tend to have higher Rb/Sr than olivine normative rocks, such as those from the Crandall volcanic center and the sampled basanite flow (Figure 3.6) Hyalite volcanic center samples, which are quartz normative, also tend to have higher Rb/Sr because these samples lack enrichment in Sr (Figure 3.4).

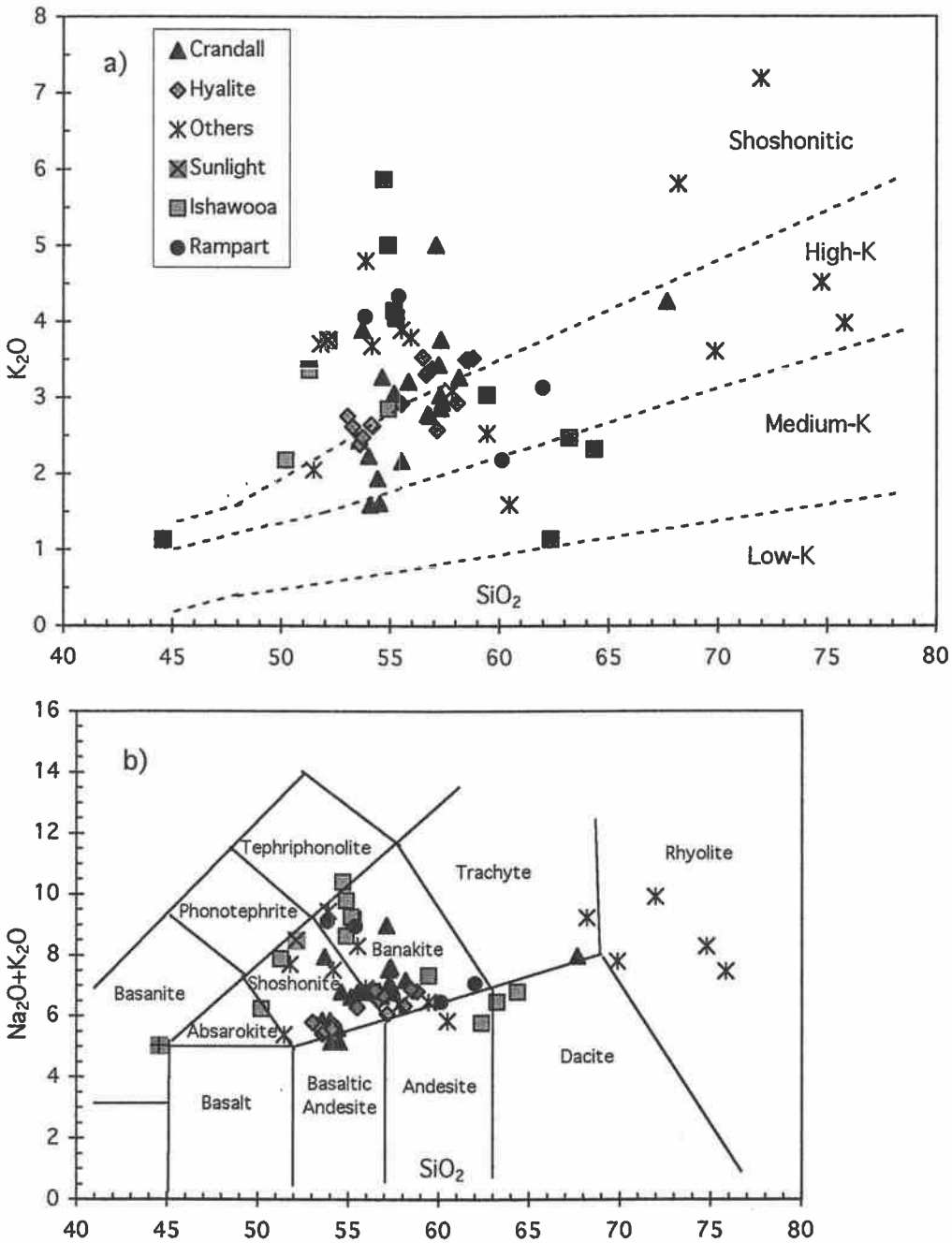

Figure 3.2. Chemical classification and nomenclature of volcanic rocks showing distribution of sampled rock types from the Absaroka volcanic province, a) by the subdivision of subalkalic rocks using the K_2O vs. SiO_2 diagram, b) using the total alkalis vs. SiO_2 diagram (subdivisions from Le Maitre et. al., 1989). Samples recalculated to 100% on an H2O- and CO2- free basis.

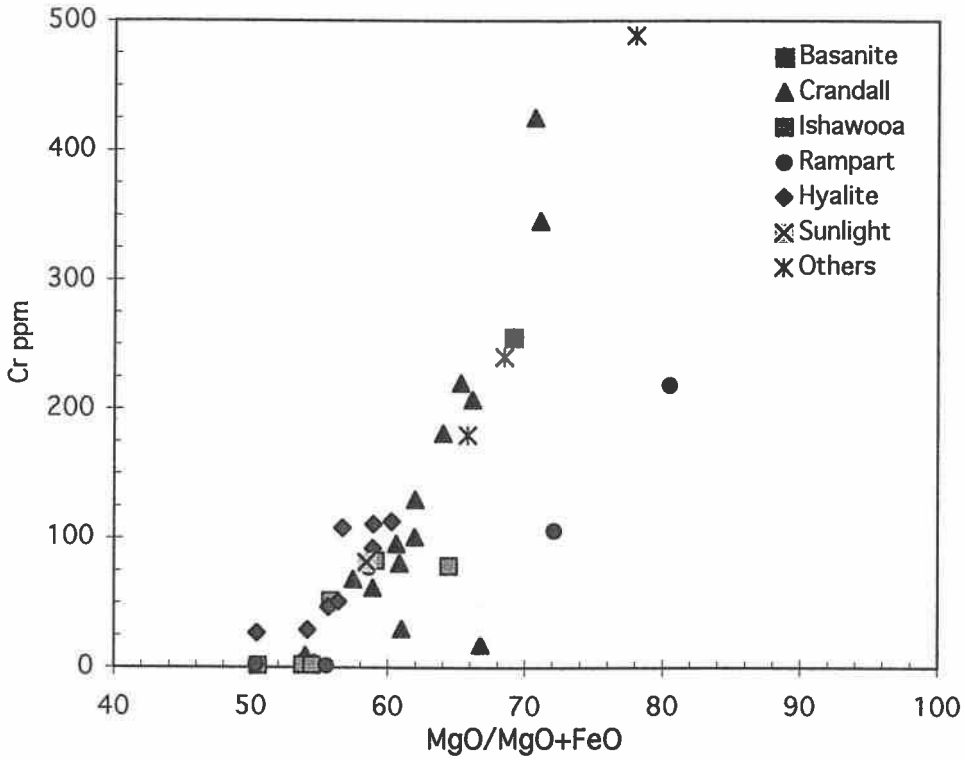

Figure 3.3a. Cr vs. Mg# ($Mg^{2+}/(Mg^{2+}+Fe^{2+})$) for samples <55%$SiO_2$ from the Absaroka volcanic province. (Mg# calculated by methods of Irvine and Baragar, 1971.)

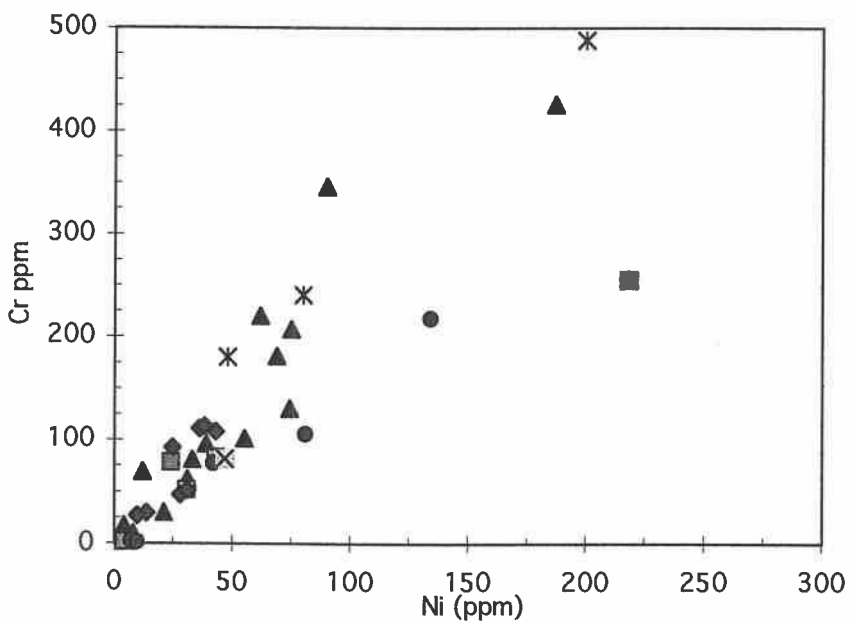

Figure 3.3b. Cr vs. Ni for samples <55%SiO_2 from the Absaroka volcanic province.

Hyalite volcanic center samples are distinctly less enriched in K, Sr , and Rb, and have lower La/Sm and Ce/Yb. Although mafic samples from the Hyalite volcanic center are less enriched in U, they have higher Th/U (Figure 3.5). High Th/U and low U are compositional charcteristics of lower crust (Kay and Kay, 1986). Similarly, Th/La can be used to distinguish upper crust, lower crust, and mantle reservoirs. Th/La of mafic samples from the Absaroka volcanic province are ≤ 0.14 and within the range of primitive mantle to EM1 OIB sources (Saunders et al, 1988). Rhyolites (silicic rocks peripheral to volcanic centers) have either higher Th/La and low Th/U, or low Th/La and high Th/U and plot beyond the field of mafic and intermediate samples. In contrast, silicic rocks (>60% SiO_2) sampled within volcanic centers tend to have either slightly higher Th/La or Th/U, but exhibit overlap with intermediate and mafic samples, particularly from the Hyalite volcanic center. When examining enrichment patterns of individual volcanic centers, systematic differences between mafic and silicic to intermediate samples are more easily discerned. Samples from the Crandall volcanic center exhibit a trend toward higher Th/La and slightly higher Th/U from mafic to silicic compositions, although some intermediate compositions show significant overlap with mafic rocks. Samples from the Ishawooa volcanic center exhibit a semi-linear trend toward higher Th/U and slightly higher Th/La from mafic to silicic compositions. Intermediate compositions from the Hyalite volcanic center are higher in Th/La than mafic samples. However, samples from the Rampart volcanic center have no systematic variation in Th/La or Th/U.

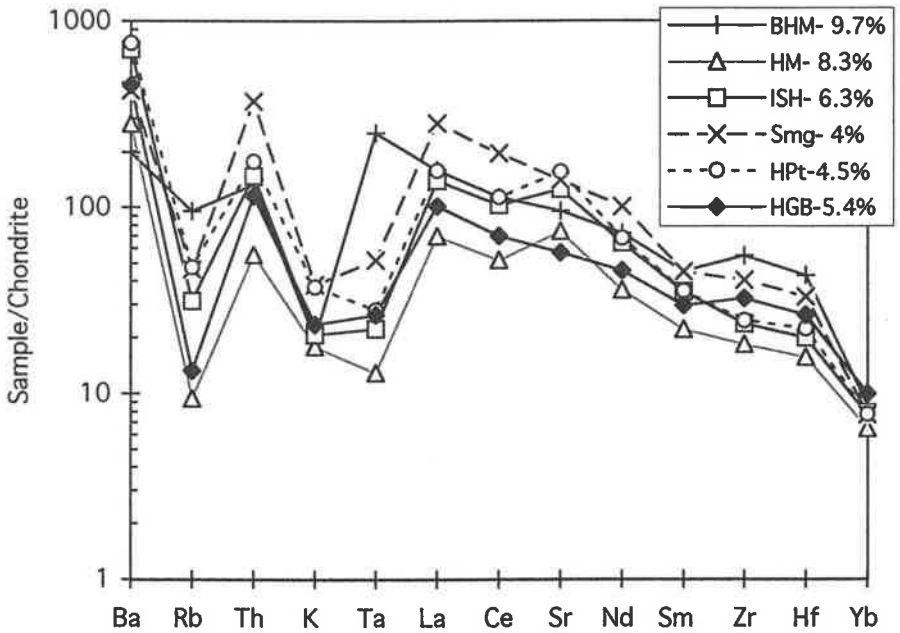

Figure 3.4. Chondrite normalized trace elements for mafic samples (<54% SiO_2) showing wt% MgO for each. Samples are from the Crandall (HM), Ishawooa (ISH), Rampart (HPt), and Hyalite (HGB) volcanic centers, monzogabbro from the vicinity of the Sunlight volcanic center (Smg), and a peripheral basanite flow (BHM).

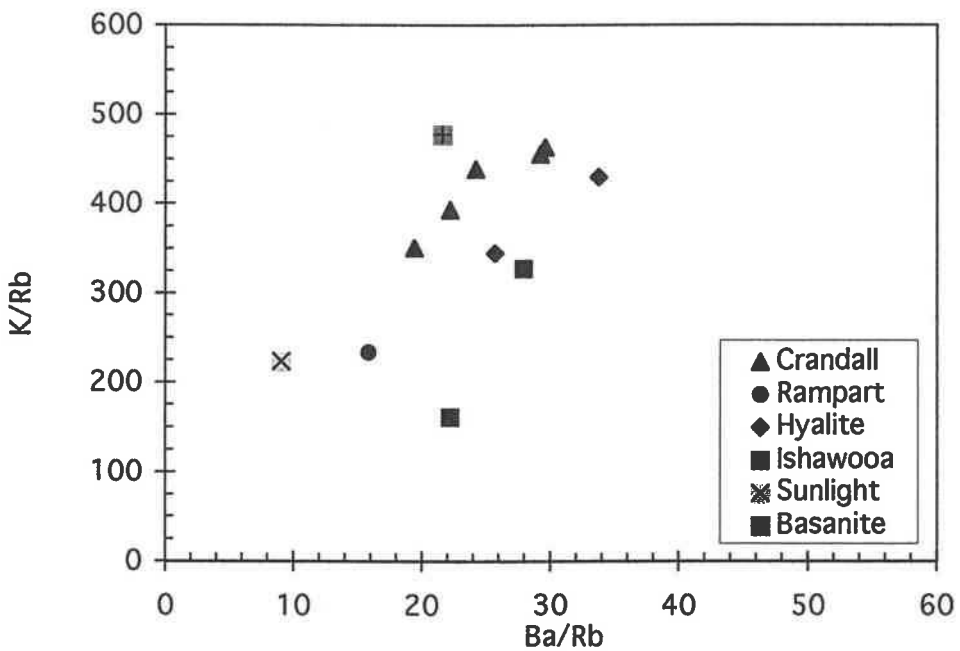

Figure 3.5. K/Rb versus Ba/Rb for samples from the Crandall, Ishawooa, Rampart and Hyalite volcanic centers, monzogabbro from the vicinity of the Sunlight volcanic center, and a peripheral basanite flow.

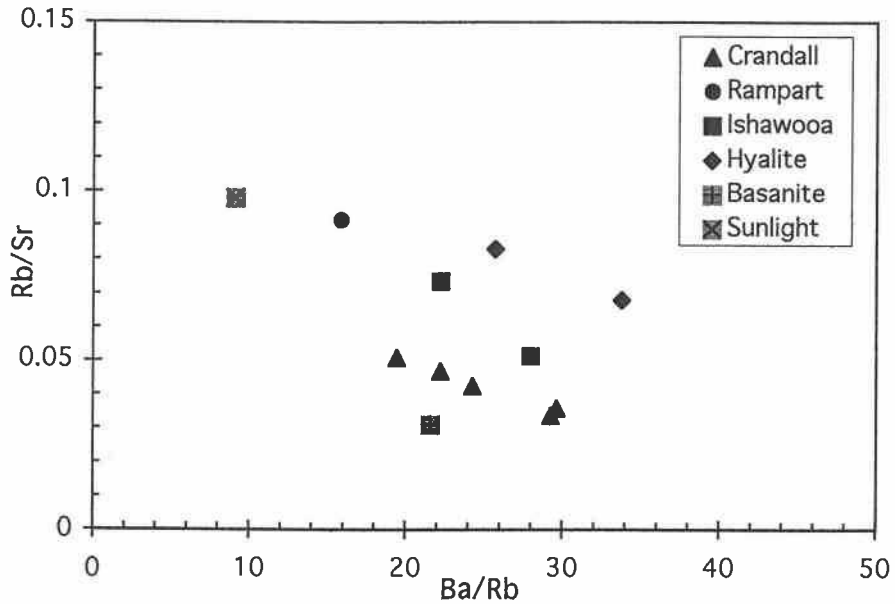

Figure 3.6. Rb/Sr versus Ba/Rb for samples from the Crandall, Ishawooa, Rampart and Hyalite volcanic centers, monzogabbro from the vicinity of the Sunlight volcanic center, and a peripheral basanite flow.

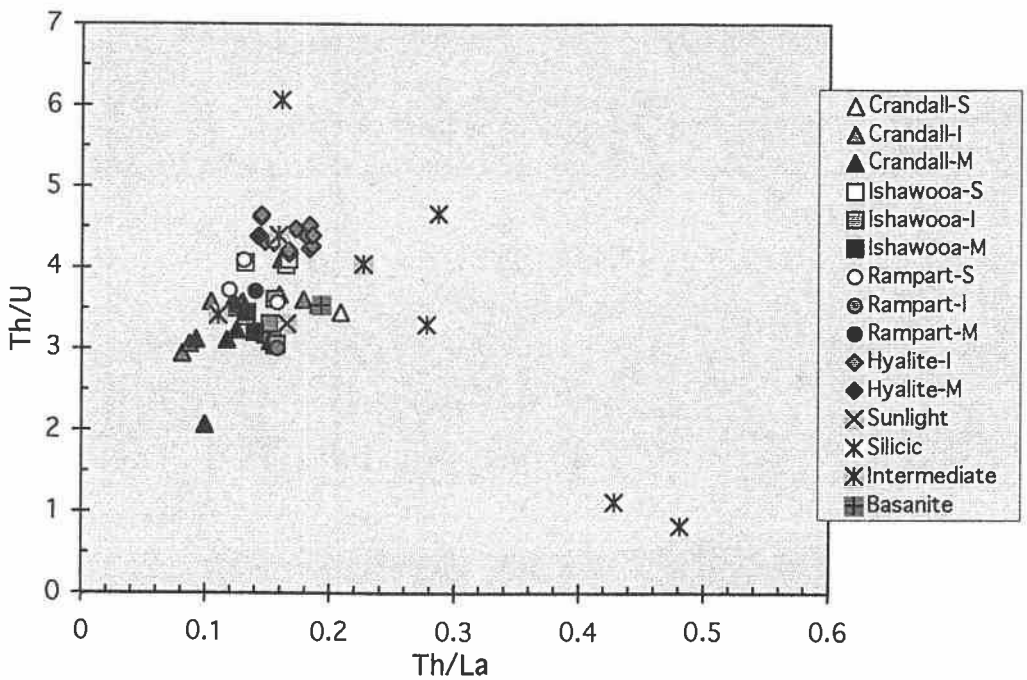

Figure 3.7. Th/U vs Th/La for samples from the Crandall, Ishawooa, Rampart and Hyalite volcanic centers. (S:>60% SiO_2, M:>4%MgO and <54% SiO_2, I: intermediate compositions) Additional outlying samples include silicic rocks which are predominantly rhyolite

ISOTOPIC COMPOSITIONS OF ABSAROKA SAMPLES

Nd and Sr Isotopes

Mafic rocks from the Crandall, Ishawooa and Rampart volcanic centers have a low narrow range of $^{87}Sr/^{86}Sr$, from 0.70426 to 0.70454, and low but variable $^{143}Nd/^{144}Nd$, from 0.51152 to 0.51193 (Table 3.1). The basanite sample, with higher $^{143}Nd/^{144}Nd$, plots above other mafic samples and closer to the mantle array (Figures 3.8a). The representative mafic sample from the Hyalite volcanic center has $^{87}Sr/^{86}Sr$ =0.70709. All of the Hyalite volcanic center samples, together with outlying intermediate rocks have higher $^{87}Sr/^{86}Sr$, whereas mafic samples from other volcanic centers form a vertical array.

A comparison of $^{143}Nd/^{144}Nd$ and $^{87}Sr/^{86}Sr$, for Absaroka volcanic province rocks to other samples of the Wyoming province is shown in Figure 3.8b. Rocks interpreted as coeval primitive, mantle-derived Wyoming province melts and melt sources, are Haystack Butte monticellite peridotite (O'Brien, 1995), Missouri Breaks kimberlite and alnoite (Scambos, 1991), mica-dunite xenoliths from the Highwood Mountains (Carlson and Irving, 1994), and Smokey Butte lamproites (Fraser et al, 1986). In comparison, mafic compositions from the Crandall volcanic center have lower and more extreme isotopic compositions than other igneous rocks of the Wyoming Province, including Smokey Butte lamproites which are derived from an ancient lithospheric mantle source (Fraser et al, 1986). The basanite sample is similar in isotopic composition to coeval kimberlite, alnoite, and carbonatite of the Missouri Breaks diatremes (Scambos, 1991).

Table 3.1. Compositions of Selected Igneous Rocks, Absaroka Volcanic Province, Wyoming and Montana

	Crandall Volcanic Center (HM)								*Slough Creek Tuff*		*peripheral samples*		
wt%	**HMf 895** flow	**HMf 1894** flow	**HMaf 1795** AF tuff	**HMd 1195** dike	**HMi 6A94** r. dike	**HMi 694** r. dike	**HM 194** intr.	**Smg 496** intr.	**YSC v495** AF Tuff	**YSC 595** AF Tuff	**WR 1694** Intr.	**BHM 195** flow	**BHM 295** intr.
SiO_2	52.8	53.6	65.6	55.6	53.8	57.8	54.9	51.1	68.02	70.7	74.0	43.78	68.52
Al_2O_3	15.9	16.0	15.6	16.4	14.2	16.7	16.7	17.9	15.7	13.63	15.4	13.51	14.1
Fe_2O_3*	9.28	8.81	3.09	6.59	8.96	6.72	8.29	8.07	3.8	2.71	0.69	12.91	3.36
MgO	5.69	6.20	1.29	3.93	8.27	3.84	4.61	3.96	0.26	0.07	0.24	9.62	0.7
CaO	7.61	7.91	2.82	5.12	8.60	5.50	6.22	6.27	1.94	0.79	1.21	9.44	2.69
Na_2O	3.33	3.52	3.55	3.63	3.11	3.85	4.54	4.61	4.51	2.69	3.41	3.81	4.12
K_2O	2.2	1.56	4.09	3.55	1.66	3.17	2.08	3.57	2.72	7.05	3.87	1.03	3.52
TiO_2	0.86	0.78	0.36	0.94	0.80	0.78	0.75	0.99	0.21	0.39	0.07	2.91	0.63
P_2O_5	0.36	0.33	0.21	0.50	0.33	0.45	0.41	1.12	0.15	0.18	0.08	0.78	0.38
MnO	0.13	0.14	0.07	0.12	0.15	0.11	0.14	0.11	0.03	0.01	0.08	0.18	0.04
LOI	1.48	0.44	2.40	2.93	-0.04	0.20	0.54	1.25	1.50	0.82	2.0	1.65	2.00
Total	99.65	99.34	99.00	99.28	99.89	99.07	99.18	99.00	99.18	99.0	99.6	99.60	99.56
						Parts Per Million							
Ni	55	62	4	68	90	31	31	47	8	9	6	218	5
Cr	101	220	17	119	345	66	99	81	5	9	0.2	255	26
Sr	1140	947	770	967	805	1200	1010	1430	193	155	306	996	940
Rb	48	31	99	85	29	75	41	140	230	175	94	31	69
Ba	1160	918	1860	1620	844	1780	1170	1270	2260	1970	1630	594	2330
U	1.3	1.1	3.4	2.7	1.1	3.0	0.9	4.4	3.0	1.6	4.9	1.6	2.1
Th	4.6	2.3	11.8	8.3	2.2	10.5	2.7	14.5	15.4	14.0	5.44	5.19	12.8
La	38	25	57	55	22	55	31	88	55.5	48.9	12.7	49.3	79.9
Nd	31.8	23.5	32.7	44.5	21.6	41.8	29	60.9	41.2	37.9	10.3	43.6	42.5
Sm	5.9	4.7	4.6	7.3	4.3	6.8	5.3	8.8	7.39	6.93	1.90	8.85	5.17
Yb	1.48	1.44	0.986	1.52	1.36	1.47	1.47	1.55	2.83	2.52	0.85	1.81	0.52
Lu	0.22	0.21	0.15	0.22	0.20	0.21	0.20	0.23	0.40	0.36	0.118	0.24	0.08
Zr	119	90.7	152	184	95.9	164	133	215	377	349	30	286	180
Hf	2.6	2.4	4.4	4.2	2.2	3.9	2.9	4.5	8.94	7.77	2.29	5.93	5.04
Ta	0.28	0.20	0.72	0.73	0.24	0.56	0.21	0.95	1.19	1.12	2.27	4.73	0.85
Sc	23	24	5	13	28	15	13	11	14	12	2	22	4

Table 3.1. (Continued) Compositions of Selected Igneous Rocks, Absaroka Volcanic Province, Wyoming and Montana

	HMf 895	HMf 1894	HMaf 1795	HMd 1195	HMi 6A94	HMi 694	HM 194	Smg 496	YSCv 495	YSC 595	WR 1694	BHM1 95	BHM 295
$^{87}Sr/^{86}Sr_M$	0.704496	0.704322	0.704636	0.704537	0.704378	0.704502	0.704406	0.704582	0.713495	0.715662	0.706673	0.703404	0.705016
±	0.000021	0.000021	0.000022	0.000021	0.000020	0.000021	0.000021	0.000021	0.000037	0.000034	0.000021	0.000015	0.000014
$^{87}Sr/^{86}Sr_i$	0.704415	0.704258	0.704477	0.704366	0.704311	0.704380	704327	0.704582	0.70842	0.71347	0.706069	0.703344	0.704621
$^{143}Nd/^{144}Nd_M$	0.511686	0.511557	0.511798	0.511703	0.511662	0.511696	0.511419	0.511805	0.511687	0.511692	0.511692	0.512822	0.511487
±	0.000016	0.000027	0.000024	0.000033	0.000015	0.000014	0.000015	0.000054	0.000014	0.000014	0.000012	0.000014	0.000015
$^{143}Nd/^{144}Nd_i$	0.511651	0.511519	0.511772	0.511672	0.511624	0.511665	0.511385	0.511778	0.511653	0.511657	0.511657	0.512784	0.511464
$^{206}Pb/^{204}Pb$	16.638	16.566	16.318	16.507	16.553	16.505	16.680	16.871	17.724	17.629	16.711	18.135	15.704
±	0.014	0.014	0.010	0.012	0.010	0.012	0.012	0.010	0.011	0.011	0.010	0.015	0.010
$^{207}Pb/^{204}Pb$	15.326	15.307	15.287	15.297	15.307	15.310	15.319	15.360	15.636	15.586	15.425	15.480	15.225
±	0.017	0.017	0.014	0.014	0.014	0.014	0.014	0.014	0.014	0.014	0.014	0.015	0.014
$^{208}Pb/^{204}Pb$	36.826	36.734	36.530	36.661	36.693	37.679	36.793	37.128	37.814	37.149	37.566	37.932	36.493
±	0.050	0.050	0.044	0.044	0.044	0.044	0.044	0.045	0.046	0.046	0.045	0.048	0.044
T_{DM}	2.00	2.46	1.46	1.77	2.26	1.76	2.35	1.48	1.94	1.98	1.99	0.39	1.68

All analyses were prepared from sample powders at the US Geological Survey, Denver Federal Center (See Chapter 2). Major element data by XRF; Trace element data by INAA; (For Nd, Sr, and Pb experimental procedures see below). Initial values are calculated with an assumed average age of 49 Ma.
Fe_2O_3*: All Fe calculated as ferric.

HM- Samples from the Crandall volcanic center; Smg-Sunlight monzogabbro; WR- Kirwin area, BHM- Beartooth Wilderness, YSC-Slough Creek Tuff
ISH- Ishawooa volcanic center, HPt- Rampart volcanic center, PR-Golmeyer Creek volcanics; HGB- Hyalite volcanic center
f-flow, AF tuff- ash-flow tuff, r. dike - ring dike, intr. - intrusion, v-vitrophyre

Table 3.1. (Continued) Compositions of Selected Igneous Rocks, Absaroka Volcanic Province, Wyoming and Montana

	Ishawooa Volcanic Center (ISH)						*Rampart Volcanic Center (HPt)*				*Hyalite Volcanic Center (HGB)*			
wt%	**ISH 5095** flow	**ISH 4995** flow	**ISH 995** flow	**ISH 795** dike	**ISH 2995** dike	**ISH 3795** Intr.	**HPt v196** v.flow	**HPt 296** flow	**HPt 496** flow	**HPt 696** AF tuff	**PRd 295** dike	**HGB 1395** flow	**HGB7 95** flow	**HGB 1995** flow
SiO_2	50.2	53.1	49.5	55.2	61.4	61.4	51.9	50.2	61.04	59.1	55.78	52.9	58.1	56.4
Al_2O_3	16.99	19.5	15.1	15.2	16.0	16.3	20.17	16.81	15.18	16.84	14.8	15.6	17.0	15.9
Fe_2O_3*	8.56	5.76	11.2	6.7	4.79	4.12	5.57	8.61	4.37	5.04	5.96	9.62	7.36	8.08
MgO	5.41	1.79	6.27	5.71	4.39	3.08	1.69	4.43	4.67	3.91	3.72	5.42	2.55	4.09
CaO	6.65	4.90	8.18	6.55	5.26	4.97	5.57	6.80	4.66	6.04	6.07	7.93	5.44	6.20
Na_2O	4.33	4.32	3.93	3.32	4.58	3.88	4.73	3.77	3.79	4.22	3.62	2.96	3.26	3.28
K_2O	3.09	5.49	1.95	3.04	1.00	2.38	3.67	3.48	2.97	2.03	2.26	2.24	3.27	3.04
TiO_2	0.95	0.79	1.08	0.90	0.51	0.50	0.77	0.91	0.62	0.57	0.63	1.04	0.92	0.99
P_2O_5	0.95	0.60	0.77	0.49	0.21	0.27	0.59	0.74	0.31	0.33	0.30	0.40	0.46	0.44
MnO	0.15	0.12	0.19	0.10	0.10	0.06	0.12	0.15	0.06	0.08	0.06	0.15	0.11	0.14
LOI	2.67	2.42	1.18	2.08	1.61	2.46	3.16	3.09	1.25	1.64	5.82	1.75	1.17	0.82
Total	100	98.79	99.35	99.3	99.85	99.42	98.50	99.0	98.90	99.8	99.00	100.0	99.70	99.38
							Parts Per Million							
Ni	33	4	43	111	99	47	7	42	134	159	94	38	10	51
Cr	87	1	83	22	190	75	2	77	218	298	185	113	27	173
Sr	1680	2100	1300	1050	998	993	594.0	1518	1250	970.0	1060	594	650	616
Rb	85.5	123	95	93	87	48	147	144	45	46	42	40	85	84
Ba	2390	2960	2110	1750	1290	1930	3010	2280	1850	1600	1830	1360	1550	1630
U	2.1	2.7	1.7	4.3	1.2	2.3	2.6	1.9	2.4	1.6	1.7	1.0	1.9	1.9
Th	6.76	8.27	5.76	17.7	3.94	9.39	7.84	6.86	6.47	3.79	7.65	4.47	7.72	7.93
La	48.5	53.2	43.3	76.4	29.8	56.5	49.8	49	49.7	34.5	48.4	31.5	42.8	42.8
Nd	40.8	41.7	38.8	58.4	21.9	36.6	37.5	41.2	36.7	27.3	33.7	27.5	34.9	36.4
Sm	7.01	6.55	6.91	8.35	3.21	4.90	6.2	6.93	4.77	4.12	5.37	5.8	6.89	7.00
Yb	1.58	1.52	1.6	1.33	0.755	.875	1.46	1.62	0.60	0.967	1.21	2.08	2.57	2.59
Lu	0.23	0.21	0.23	0.18	0.10	0.13	0.21	0.23	0.09	0.15	0.17	0.29	0.36	0.37
Zr	156	146	123	232	92	144	164	138	173	106	134	168	208	224
Hf	3.07	3.38	2.75	6.27	2.49	4.0	3.20	3.06	5.13	2.94	3.43	3.62	5.08	5.35
Ta	.52	0.62	0.42	0.88	0.25	0.59	0.57	0.51	0.38	0.24	0.55	0.50	0.75	0.82
Sc	18	7	27	17	11	9	7	18	9.7	13	13	24	12	17

Table 3.1. (Continued) Compositions of Selected Igneous Rocks, Absaroka Volcanic Province, Wyoming and Montana

	ISH 5095	ISH 4995	ISH 995	ISH 795	ISH 2995	ISH 3795	HPt 196	HPt 296	HPt 496	HPt 696	PRd 295	HGB 1395	HGB 795	HGB 1995
$^{87}Sr/^{86}Sr_M$	0.704638	0.704615	0.704651	0.705326	0.704654	0.705682	0.704706	0.704614	0.704712	0.704842	0.706224	0.707226	0.707793	0.707820
±	0.000016	0.000021	0.000019	0.000021	0.000019	0.000020	0.000029	0.000024	0.000021	0.0021	0.000021	0.000021	000020	0.000020
$^{87}Sr/^{86}Sr_i$	0.704793	0.704501	0.704509	0.70532	0.704486	0.705589	0.704591	704442	0.704642	0.704793	0.706148	0.707094	0.707563	0.707558
$^{143}Nd/^{144}Nd_M$	0.511958	0.512037	0.511844	0.511665	0.511527	0.511535	0.512029	0.511971	0.511519	0.511574	0.511713	0.511652	0.511652	0.511623
±	0.000012	0.000015	0.000013	0.000015	0.000014	0.000015	0.000015	0.000015	0.000019	0.000014	0.000015	0.000014	0.000015	0.000013
$^{143}Nd/^{144}Nd_i$	0.511925	0.512007	0.511810	0.511638	0.511499	0.511510	0.511998	0.511939	0.511494	0.511548	0.511683	0.511612	0.511613	0.511587
$^{206}Pb/^{204}Pb$	17.047	17.248	16.841	16.756	15.926	16.508	17.247	17.033	15.962	16.124	15.940	16.905	16.779	16.824
±	0.010	0.013	0.016	0.012	0.010	0.012	0.011	0.010	0.010	0.010	0.012	0.013	0.012	0.012
$^{207}Pb/^{204}Pb$	15.375	15.399	15.359	15.403	15.301	15.417	15.395	15.378	15.299	15.334	15.251	15.359	15.391	15.384
±	0.014	0.014	0.017	0.014	0.014	0.014	0.014	0.014	0.014	0.014	0.014	0.014	0.014	0.014
$^{208}Pb/^{204}Pb$	37.149	37.329	37.048	37.387	36.531	37.359	37.320	37.161	36.553	36.807	36.849	37.754	37.596	37.576
±	0.045	0.045	0.050	0.045	0.045	0.045	0.045	0.045	0.044	0.045	0.045	0.046	0.045	0.045
T_{DM}	1.49	1.28	1.71	1.64	1.83	1.72	0.96	1.06	1.44	1.71	1.71	2.45	2.34	2.21

Experimental procedures for Nd, Sr and Pb isotopes were similar to those employed by Tatsumoto et al. (1987) with minor modifications. Samples weighing approximately 100 mg were dissolved in a solution of HF-HNO_3 in PFA-teflon screw-cap vials at approximately 80°C for 48 hours. Lead was separated using anion exchange in 1.2N HBr medium. Strontium and the REE were then separated using cation exchange in 2.5 N Hcl medium. Neodymium was isolated from the other REE using cation exchange in 2-methyllactic acid with pH adjusted to 4.50 (Lugmair et al., 1975). Analytical blanks were 0.1-0.2 ng for Pb, 0.5-1.5 ng for Sr, and 0.075 ng for Nd. Samples for Pb isotopic analyses were loaded onto Re filaments using the conventional phosphoric acid-silica gel technique. Pb isotopic data were acquired on a VG instruments, Sector 54, 7-collector mass spectrometer run instatic mode. Pb data were corrected for 0.12 ± 0.03%/AMU mass fractionation during mass spectrometry based on replicate analyses of NIST standard SRM-981 (Todt et al., 1993) Sr and Nd data were acquired on a VG Instruments single-collector mass spectrometer. Fractions for Sr isotopic analyses were loaded onto oxidized Ta filaments using phosphoric acid. Five analyses of NIST standard SRM-987 gave a mean 87Sr/86Sr value of 0.710261 ± 8(95% C.I.). Neodymium fractions were run in a triple-filament configuration with Ta side filaments and a Re center filament. Thirteen analyses of the La Jolla Nd standard run during the course of this study gave a mean 143Nd/144Nd value of 0.511855 ± 4.

Hyalite volcanic center samples, with higher $^{87}Sr/^{86}Sr$, plot below the field of mafic rocks derived from continental subduction (Tatsumi and Eggins, 1995). In comparison, early and middle Archean crustal granitoids and amphibolites exposed in the Beartooth and Gallatin Ranges of the Wyoming Province have $^{87}Sr/^{86}Sr$ in the range of 0.706 to 0.783 but much lower $^{143}Nd/^{144}Nd$ than any samples from the Absaroka volcanic province (from 0.5098 to 0.5106), and fall outside the compositional range shown in Figure 3.8b (Wooden and Mueller, 1988). Lower crustal and cumulate xenoliths sampled by Eocene Highwood, and Bearpaw volcanic rocks of the Wyoming province have higher $^{143}Nd/^{144}Nd$, from 0.5122 to 0.5116, and inconsistent $^{87}Sr/^{86}Sr$ which is for the most part higher than 0.706 (Joswiak, 1992; Collerson et al, 1989). These compositions overlap with samples of Wyoming Province such as Smokey Butte Lamproites, derived from lithospheric mantle (Fraser et al, 1986). Snake River Plain lower crustal granulite xenoliths have lower $^{143}Nd/^{144}Nd$ than mafic samples from the Absaroka province, extremely variable $^{87}Sr/^{86}Sr$ and overlap in composition with some of the intermediate to silicic samples from this study (Leeman et. al., 1985).

In a plot of Th/U versus $^{87}Sr/^{86}Sr$, intermediate compositions with higher $^{87}Sr/^{86}Sr$ (0.705 to 0.7076), and all samples from the Hyalite volcanic center have higher Th/U than mafic rocks from other volcanic centers which fall in a tight cluster (Figure 3.9). These samples show significant similarities in isotopic composition to some silicic rock types. Silicic rocks fall into a larger field of scattered, separate groups that vary in Th/U and $^{87}Sr/^{86}Sr$, and $^{143}Nd/^{144}Nd$. Silicic rocks with the highest $^{87}Sr/^{86}Sr$ tend to have low but variable Th/U, and higher $^{143}Nd/^{144}Nd$ than other silicic rocks. Silicic samples with Th/U similar to, or higher than mafic samples, tend to have lower $^{87}Sr/^{86}Sr$ and $^{143}Nd/^{144}Nd$ (Figure 3.8a, Figure 3.9).

For samples from the Absaroka volcanic province as a whole, there is a crude positive correlation between SiO_2 and $^{87}Sr/^{86}Sr$, but intermediate composition rocks have a wide range in $^{87}Sr/^{86}Sr$ (0.7044 to 0.7075) (Figure 3.10). $^{87}Sr/^{86}Sr$ remains constant with differentiation at the Crandall volcanic center, slightly increases with differentiation at the Ishawooa and Rampart volcanic centers, and is variable and elevated (0.7068 to 0.7076) within the narrow compositional range of Hyalite volcanic center.

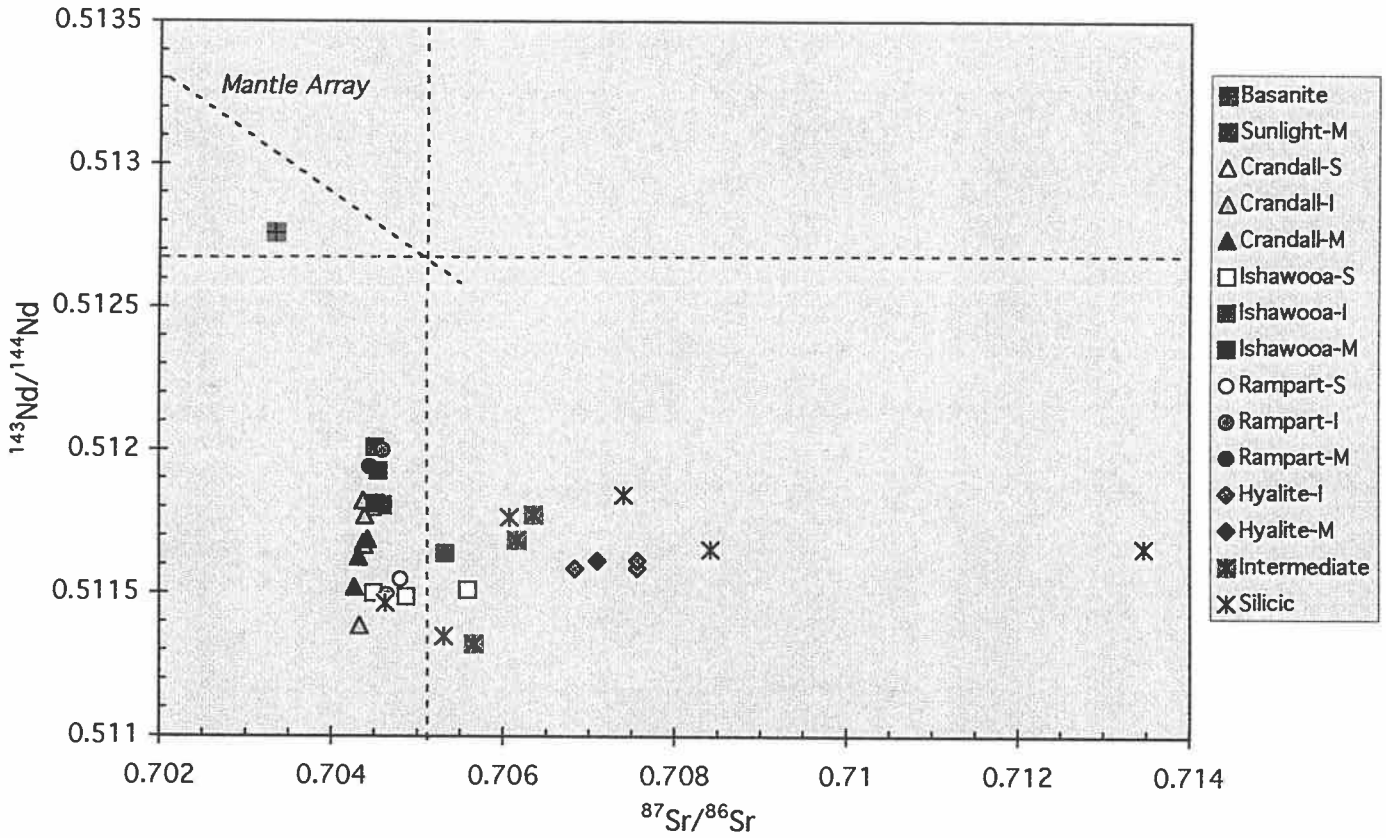

Figure 3.8a. $^{87}Sr/^{86}Sr$ vs. $^{144}Nd/^{143}Nd$ for samples from the Crandall, Ishawooa, Rampart, and Hyalite volcanic centers of the Absaroka volcanic province. (Different compositions from the volcanic centers are represented by -M-mafic, -I-intermediate, S- silicic. Other samples from the Absaroka province are shoshonite (Intermediate) and rhyolite (Silicic) which have not been assigned to specific volcanic centers.

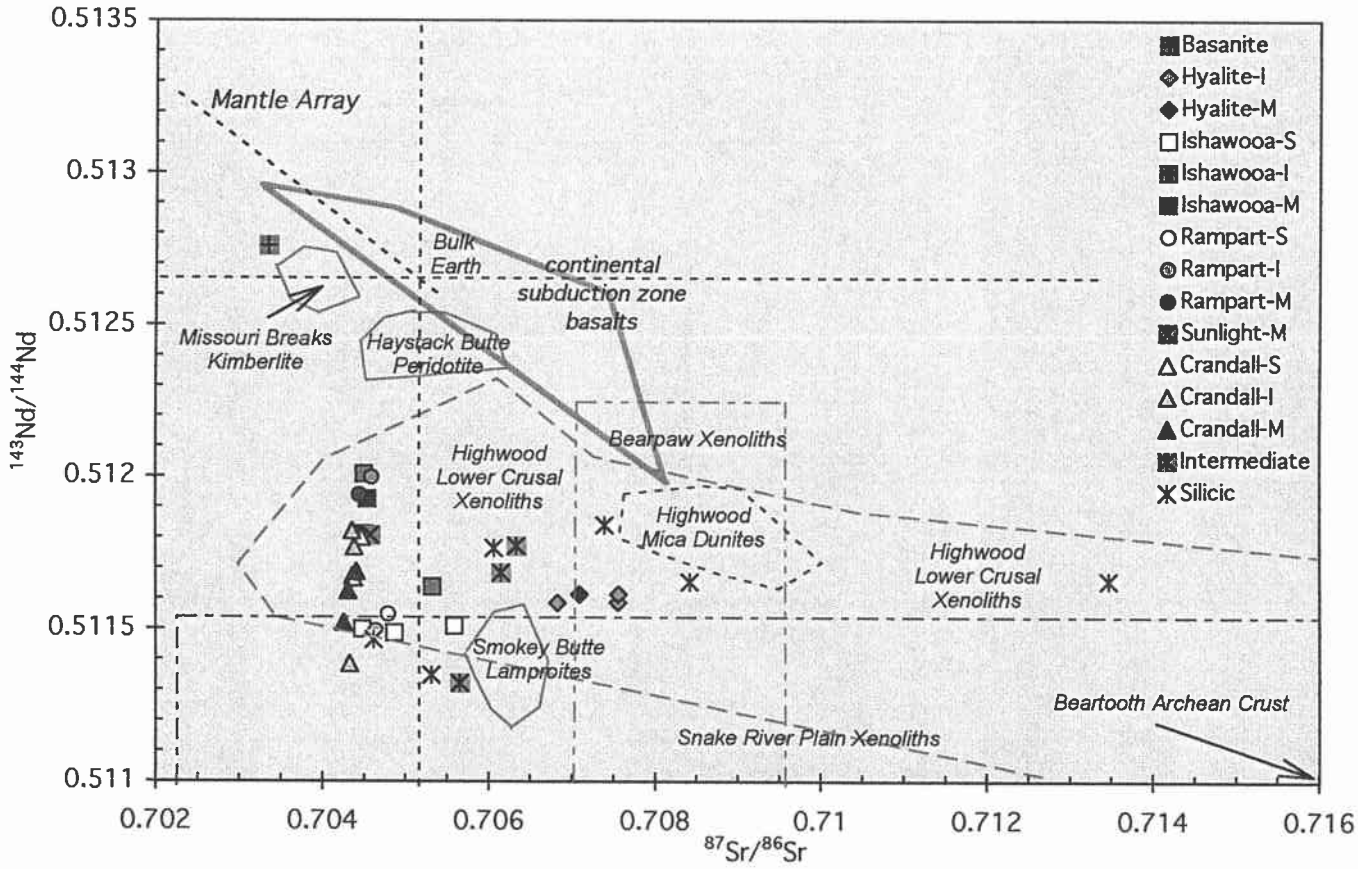

Figure 3.8b. $^{87}Sr/^{86}Sr$ vs. $^{144}Nd/^{143}Nd$ for samples from the Crandall, Ishawooa, Rampart, and Hyalite volcanic centers of the Absaroka volcanic province, and composional fields for selected mafic alkalic and crustal rocks of the Wyoming Province. (Different compositions from the volcanic centers are represented by -M-mafic, -I-intermediate, S- silicic. Other samples from the Absaroka province are shoshonite (Intermediate) and rhyolite (Silicic) which have not been assigned to specific volcanic centers. Other Wyoming Province rocks are from MB-Missouri Breaks, HB-Haystack Butte, SB-Smokey Butte, HW-LCrust- Highwood lower crust, and Mica dunite xenoliths also sampled from the Highwood Mountains. References for Wyoming Province samples are discussed in text.)

A plot of $^{87}Sr/^{86}Sr$ versus 1/Sr will exhibit a simple linear trend if samples are derived from simple binary mixing. The data show a similar trend to $^{87}Sr/^{86}Sr$ versus SiO_2 as both show a crude positve correlation exhibited primarily by intermediate and silicic rocks (Figure 3.10). This broad positive trend includes samples from the Hyalite volcanic center. Mafic compositions, with the exception of the Hyalite sample, do not exhibit this trend. Instead, they plot in a small field and show slightly decreasing 1/Sr with increasing$^{87}Sr/^{86}Sr$.

A plot of $^{87}Sr/^{86}Sr$ versus Rb shows that mafic samples that are Sr enriched, with low$^{87}Sr/^{86}Sr$, are variably enriched in Rb (Figure 3.12). Nepheline normative samples are enriched in Rb, and have low and constant $^{87}Sr/^{86}Sr$. Intermediate and silicic samples with higher $^{87}Sr/^{86}Sr$ do not show a clear trend, but tend to show more or less constant Rb.

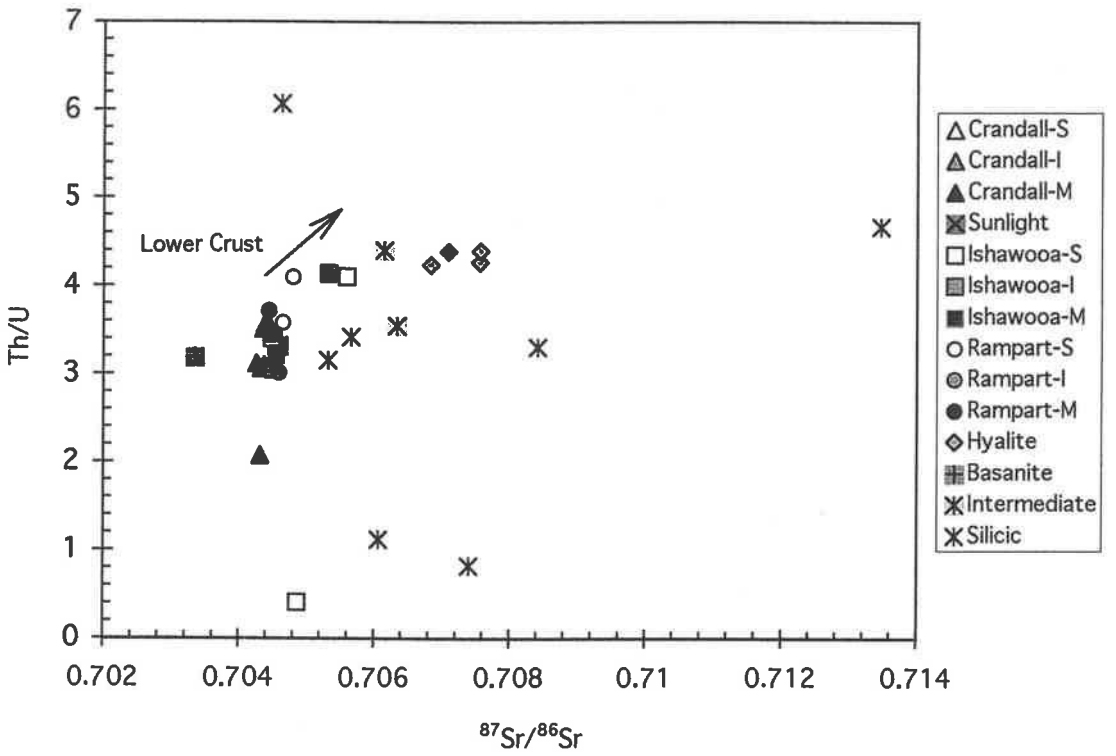

Figure 3.9. Th/U versus $^{87}Sr/^{86}Sr$ for samples from the Absaroka province.

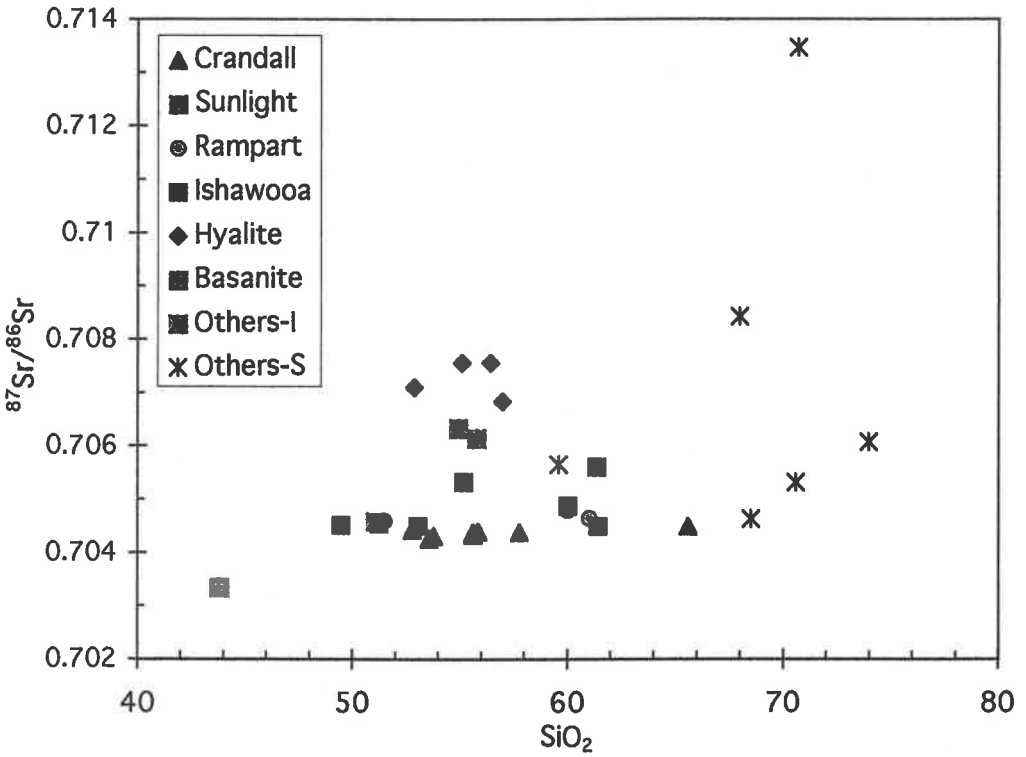

Figure 3.10. $^{87}Sr/^{86}Sr$ vs. SiO_2 for samples from the Absaroka Volcanic Province.

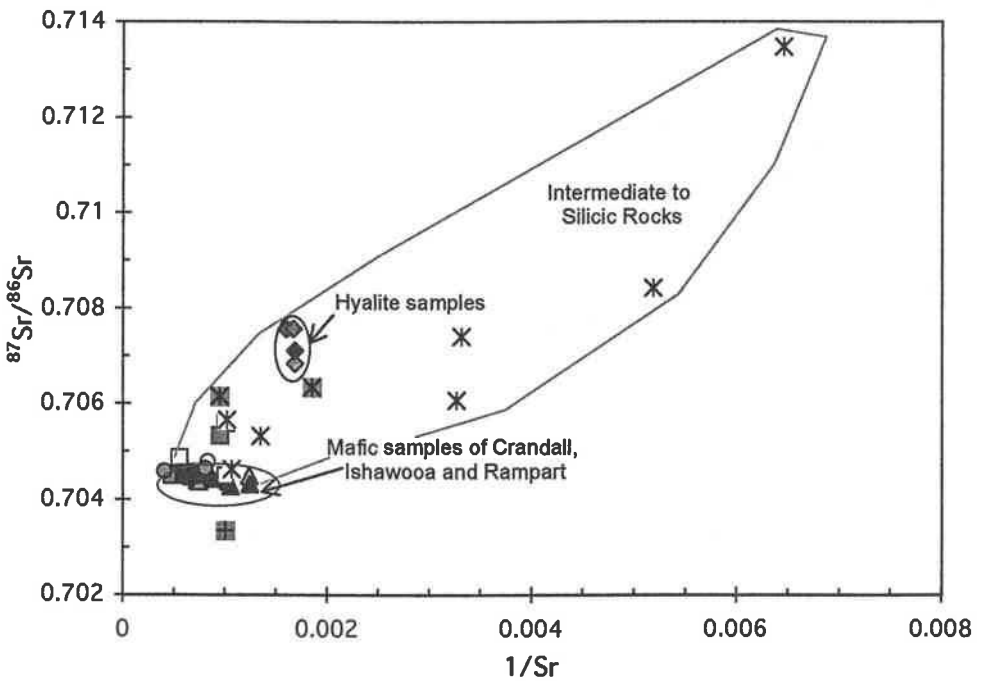

Figure 3.11 $^{87}Sr/^{86}Sr$ versus 1/Sr for samples from the Absaroka Volcanic Province.

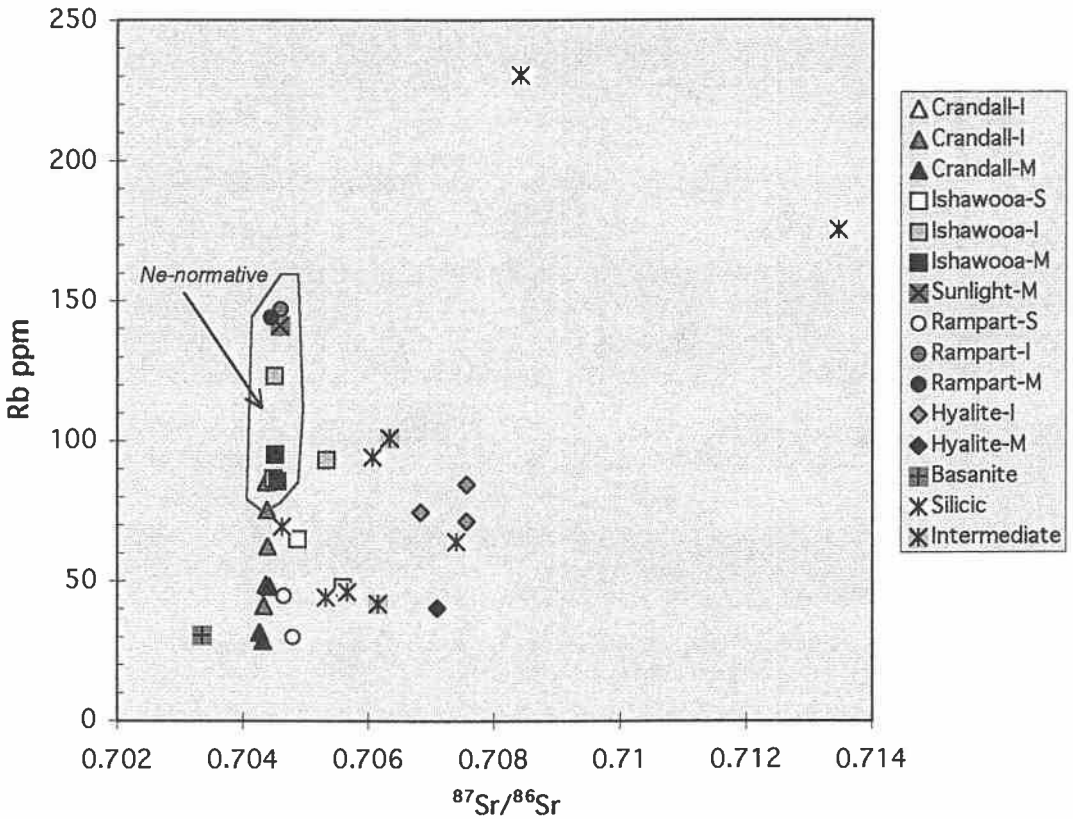

Figure 3.12. Rb versus $^{87}Sr/^{86}Sr$ for samples from the Absaroka Volcanic Province.

The variation of $^{143}Nd/^{144}Nd$ relative to 1/Nd also differs between mafic and silicic compositions (Figure 3.13a). Although the data set as a whole exhibits significant overlap of rocks which vary in differerentiation, mafic samples have a vertical trend, whereas silicic rocks show a crude horizontal trend. Similarly, in a plot of $^{143}Nd/^{144}Nd$ versus Sm/Nd, mafic samples exhibit a semi-linear trend which is somewhat perpendicular to the positive trend exhibited by more evolved compositions (Figure 3.13b). The basanite, with higher Sm, plots above the mafic trend with higher $^{143}Nd/^{144}Nd$.

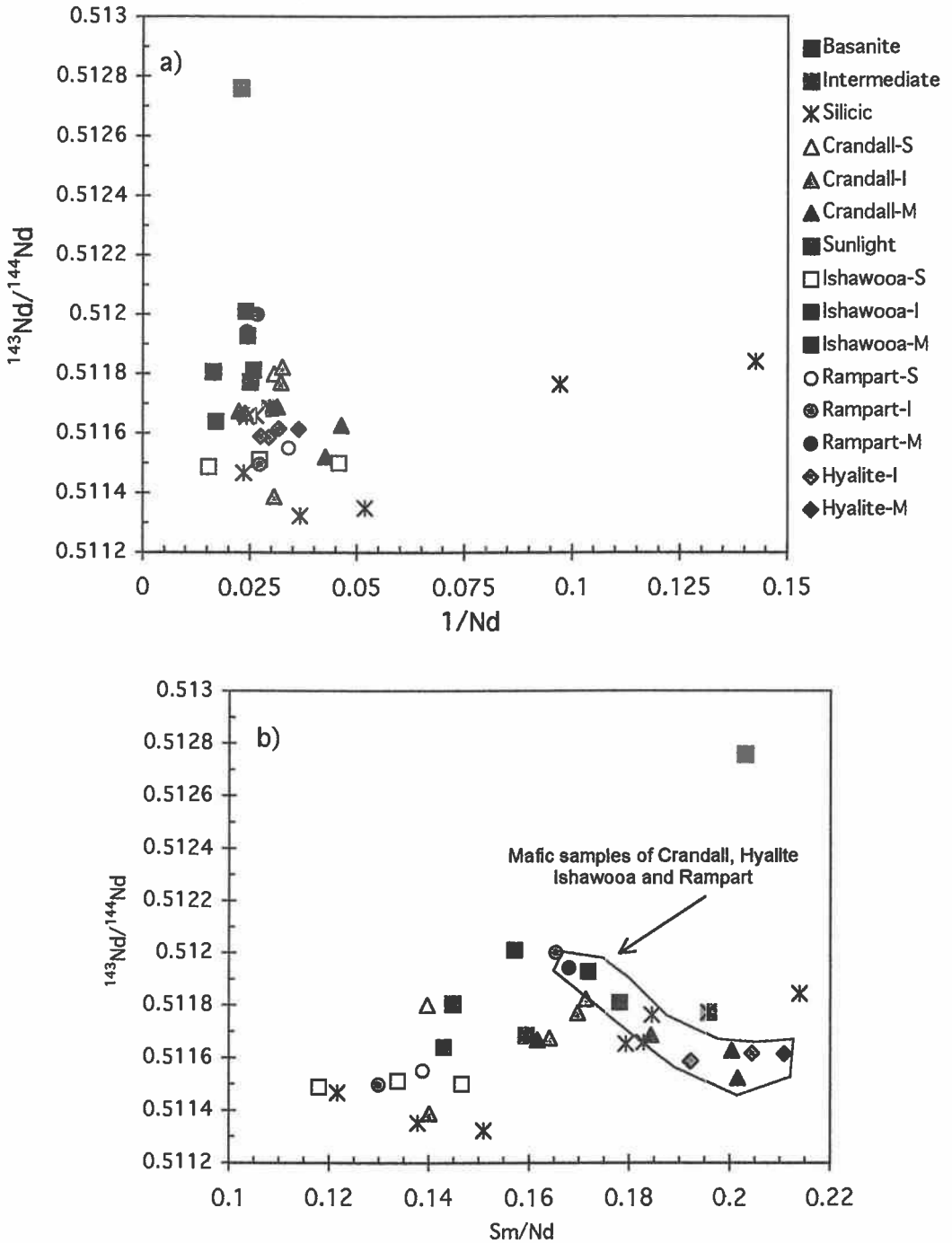

Figure 3.13 a. $^{143}Nd/^{144}Nd$ versus 1/Nd for samples of the Absaroka volcanic province. b) $^{143}Nd/^{144}Nd$ versus Sm/Nd for samples of the Absaroka volcanic province.

Pb Isotopes

Plots of $^{207}Pb/^{204}Pb$ versus $^{206}Pb/^{204}Pb$, and $^{208}Pb/^{204}Pb$ versus $^{206}Pb/^{204}Pb$ show a well-defined, linear array of mafic samples parallel to the northern hemisphere reference line with the basanite to the right of the 4.55 Ga geochron, in the OIB field, and mafic Ishawooa and Rampart volcanic center samples, together with Crandall volcanic center samples plotting to the left of the geochron (Figure 3.14a and 3.14b). The Crandall end member (HM6A94) is characterized by epsilon Nd $\leq$ -24, $^{87}Sr/^{86}Sr \approx 0.7043$, and $^{206}Pb/^{204}Pb \approx 16.55$. Based on an Mg#>70, with 345 ppm Cr, it is the among the most mafic samples from the Crandall volcanic center. The array defined by the Absaroka Province mafic rocks can be extended in either direction to include Pb isotopic compositions from Missouri Breaks kimberlite, and Smokey Butte lamproite.

Compared to the other volcanic centers, Hyalite lavas have distinct Pb isotopic compositions, as well as higher $^{87}Sr/^{86}Sr$ (0.7068-0.7075). Silicic to intermediate samples show the greatest variation in isotopic composition and overlap with the field defined by the Hyalite volcanic center (Figures 3.8 a and b, and 3.14 a and b). Intermediate to silicic compositions, in general, have higher $^{208}Pb/^{204}Pb$ and $^{207}Pb/^{204}Pb$. In the plot of $^{207}Pb/^{204}Pb$ versus $^{206}Pb/^{204}Pb$, silicic to intermediate lavas, and lavas from the Hyalite volcanic center plot away from the northern hemisphere reference line near the Stacey-Kramer terrestrial Pb curve (Figure 3.14a).

$^{208}Pb/^{204}Pb$ versus $^{206}Pb/^{204}Pb$, and $^{208}Pb/^{204}Pb$ versus $^{206}Pb/^{204}Pb$ fields for Wyoming Province crust are defined by isotopic data from feldspars of Mesozoic and Tertiary plutons from the Wyoming Province. These plutons are interpreted as melts derived from both Archean mafic lower crust, and upper crust which may contain a Proterozoic end-member (Gunn, 1991). This crust is closest in composition to rhyodacite ash-flow tuff from the Beartooths in the northern Absaroka volcanic province, as well as the Hyalite volcanic center, which have both $^{208}Pb/^{204}Pb$ and

$^{207}Pb/^{204}Pb$ which overlap with this field. The field for Archean crust of eastern Beartooth Mountains is shown on the $^{207}Pb/^{204}Pb$ versus $^{206}Pb/^{204}Pb$ (Wooden and Mueller, 1988; Gunn, 1991). $^{208}Pb/^{204}Pb$ for Archean Beartooth crust is higher, and lies beyond the field shown in the diagram (Wooden and Mueller, 1988). Rhyolites from the southern Absaroka volcanic province and silicic rocks of the Ishawooa and Rampart volcanic centers, which have lower $^{208}Pb/^{204}Pb$, $^{207}Pb/^{204}Pb$ and $^{208}Pb/^{204}Pb$, have Pb isotopic compositions which fall between the field for data from Beartooth crustal rocks, and mafic compositions. These silicic rocks all have higher $^{87}Sr/^{86}Sr$ but vary widely in $^{143}Nd/^{144}Nd$, $^{87}Sr/^{86}Sr$. Rhyodacites from the northern Absaroka volcanic province have the highest $^{87}Sr/^{86}Sr$, although these Sr isotopic compositions are not as high as Archean Beartooth crust (Wooden and Mueller, 1988).

Examination of isotopic data relative to sample ages shows that mafic lavas from the Crandall, Ishawooa, and Rampart volcanic centers, which are all $\geq$ 48 Ma, plot in a separate field of lower $^{87}Sr/^{86}Sr$ and higher $^{143}Nd/^{144}Nd$ (Figures 3.15a and 3.15b) . Post 48-Ma lavas are primarily silicic to intermediate in composition, although basanite is included in the group of younger rocks. Post-48 Ma rocks, except for the basanite, trend toward higher $^{87}Sr/^{86}Sr$ and show a trend that extends from lower $^{143}Nd/^{144}Nd$ to higher $^{143}Nd/^{144}Nd$. These isotopic trends are mirrored by trace element compositions. Mafic and intermediate composition rocks that erupted before 48 Ma have Th/U from 2.0 to 3.5. Post 48 Ma rocks of intermediate composition, and intermediate and mafic samples from the Hyalite volcanic center, have Th/U $\geq$ 4.0 (Figure 3.16). Silicic lavas which erupt late have variable Th/U.

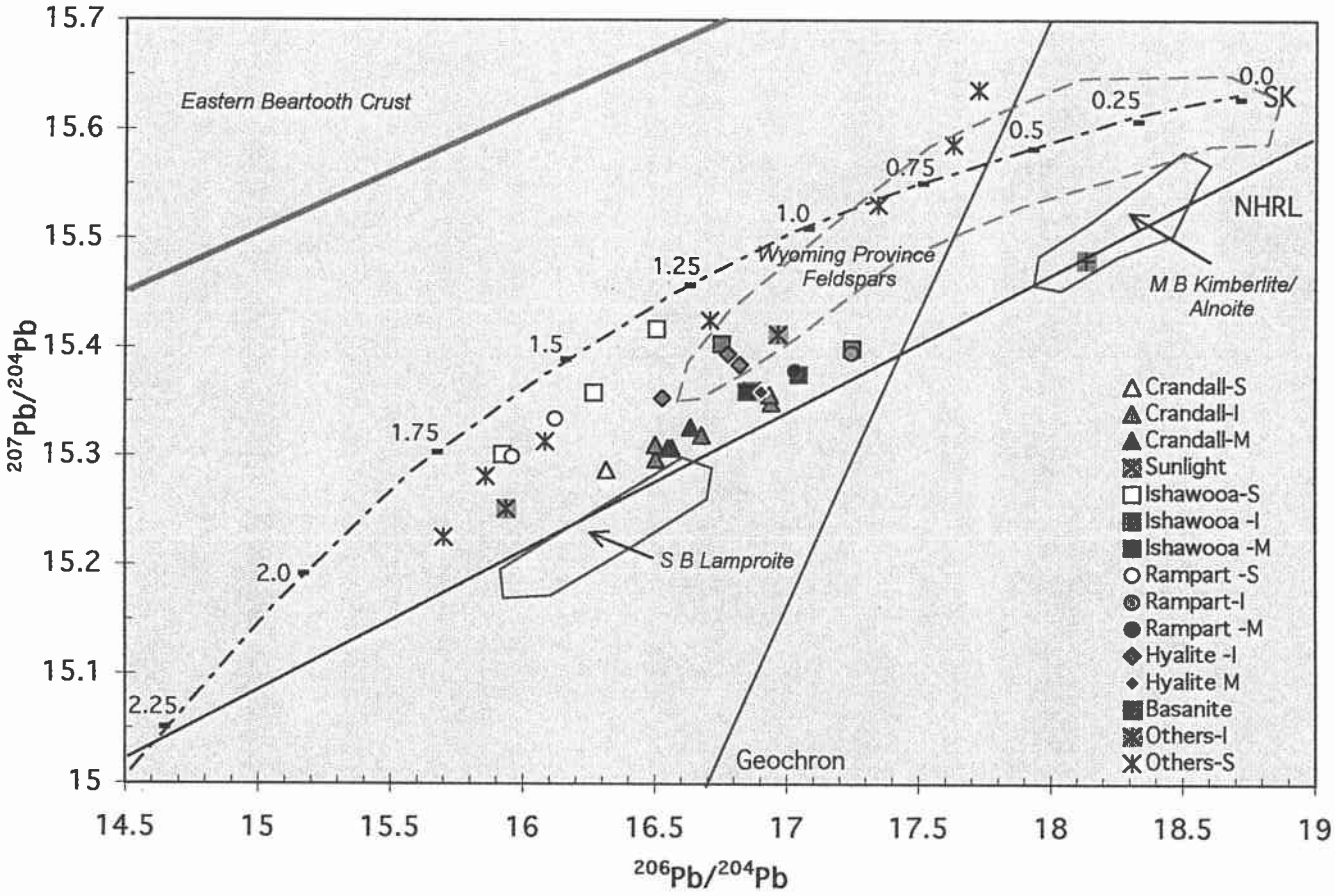

Figure 3.14a. $^{207}Pb/^{204}Pb$ versus $^{206}Pb/^{204}Pb$, of samples from the Crandall, Ishawooa, Rampart , and Hyalite volcanic centers, and shoshonite and rhyolite (-IS) of the Absaroka volcanic province. Fields for other rocks from the Wyoming Province plotted for comparison are MB-Missouri Breaks kimberlite and alnoite, SB- Smokey Butte lamproite, Archean Beartooth crust, and feldspars from crust-derived plutons of the Wyoming Province. (References in Text.) Shown for reference are the Stacey-Kramers (1975) two-stage terrestrial lead isotope curve, the geochron (Tatsumoto et al., 1973) and the Northern Hemisphere Reference Line (Hart, 1984).

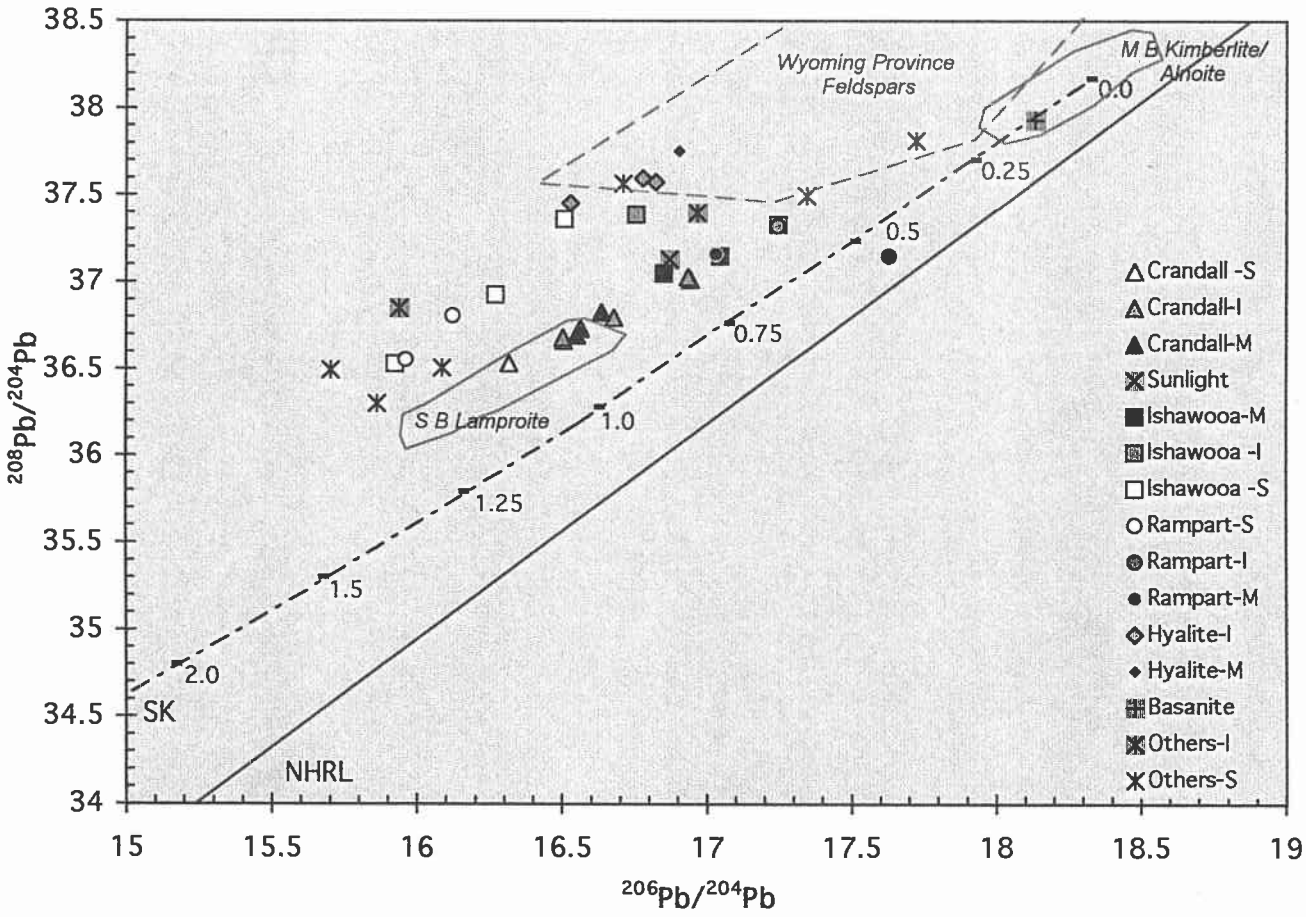

Figure 3.14b. $^{208}Pb/^{204}Pb$ versus $^{206}Pb/^{204}Pb$, of samples from the Crandall, Ishawooa, Rampart , and Hyalite volcanic centers, and shoshonite and rhyolite (-IS)of the Absaroka volcanic province. Fields for other rocks from the Wyoming Province plotted for comparison are MB-Missouri Breaks kimberlite and alnoite, SB- Smokey Butte lamproite, and feldspars from crust-derived plutons (references in text). Shown for reference are the Stacey-Kramers (1975) two-stage terrestrial lead isotope curve, and the Northern Hemisphere Reference Line (Hart, 1984).

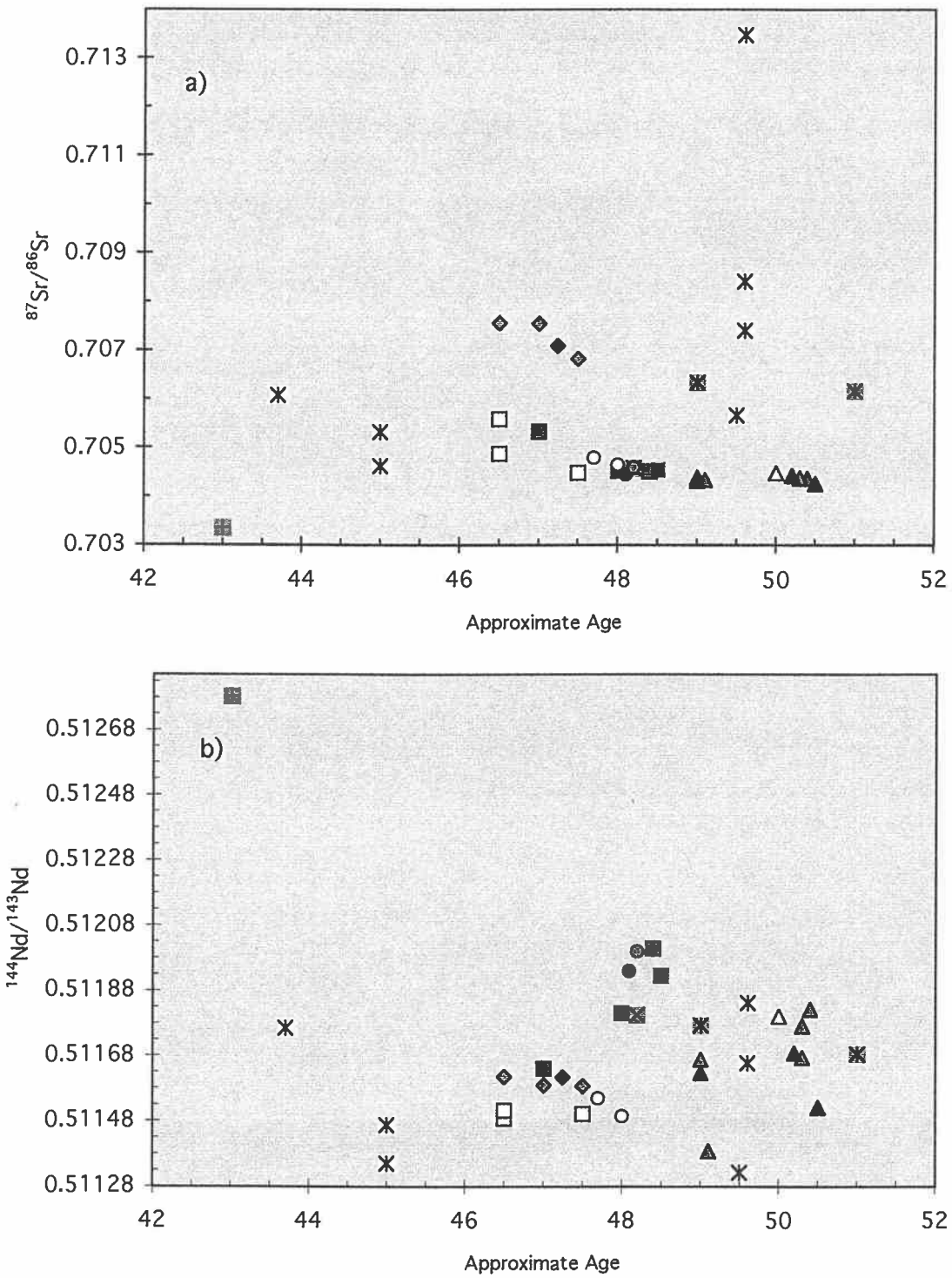

Figure 3.15. a) $^{87}Sr/^{86}Sr$ versus age, and b) $^{143}Nd/^{144}Nd$ versus age for rocks from the Absaroka volcanic province.

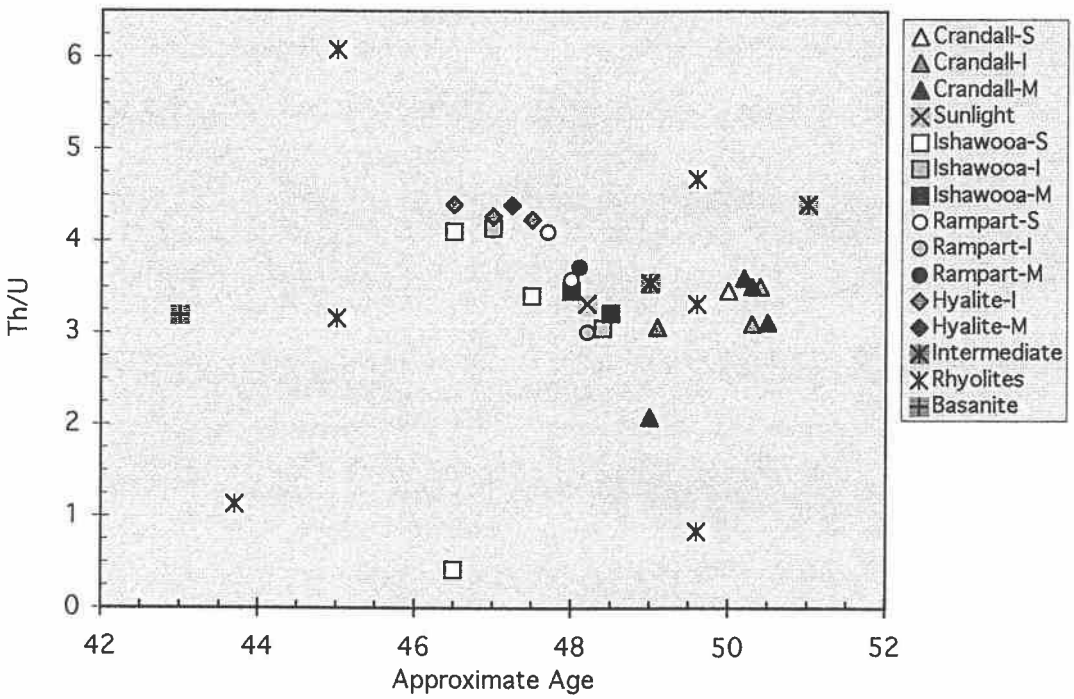

Figure 3.16. Th/U versus age for rocks from the Absaroka volcanic province.

DISCUSSION

The isotopic data presented here requires derivation of parental magmas from different sources. It is possible that isotopic characteristics of the samples reflect contributions from either the asthenospheric mantle (represented by the basanite, BHM1-95), or the lithospheric mantle (represented by the lowest $^{87}Sr/^{86}Sr$ and low $^{143}Nd/^{144}Nd$ samples of the Crandall trend, HM6A-94); lower crust (silicic and intermediate rocks with variable $^{87}Sr/^{86}Sr$ and low $^{207}Pb/^{204}Pb$), and upper continental crust (with higher $^{87}Sr/^{86}Sr$ and $^{207}Pb/^{204}Pb$, represented by rhyolites).

Alternatively, the differences in Nd, Sr, and Pb isotopic compositions of volcanic centers may be due to melting and assimilation, by an OIB magma, of variable lower crustal components. For example, Hyalite samples, together with intermediate Ishawooa and Rampart samples and rhyolite, exhibit elevated $^{208}Pb/^{204}Pb$ and do not lie on a trend with intermediate Crandall samples, which would suggest that they represent isotopically separate crustal sources (Figure 3.14a). Low $^{143}Nd/^{144}Nd$ and low $^{87}Sr/^{86}Sr$ of intermediate Crandall samples may represent one localized crustal source, while higher $^{143}Nd/^{144}Nd$ and $^{87}Sr/^{86}Sr$ samples represent another. On the $^{207}Pb/^{204}Pb$ diagram (Figure 3.14a) the data define two apparent trends that intersect at a presumed lower-crust isotopic composition. The $^{207}Pb/^{204}Pb$ isotopic composition of a crustal end-member rhyolite, together with intermediate Ishawooa and Rampart center samples, and the separate Crandall trend on the Pb isotopic diagram both intersect the Stacey-Kramers curve at 2.1 ± 0.4 Ga and suggest that this crust is early Proterozoic to Archean in average age. Either interpretation of the isotopic data, derivation of lower crustal melts from an OIB source, or melting which also includes a lithospheric mantle component suggests that enrichment is derived from ancient Wyoming province sources. The isotopic data do not suggest that the LILE and LREE enriched signature Absaroka volcanic province magmatism was produced from a young (> 30 Ma) oceanic slab, such as the Farallon Plate, and do not require enrichment from a recent event, such as contemporaneous subduction.

Mafic Lavas of the Crandall, Ishawooa, Rampart, and Sunlight Volcanic Centers

The low $^{143}Nd/^{144}Nd$ and low $^{87}Sr/^{86}Sr$ isotopic compositions, and the linear trend towards low $^{208}Pb/^{204}Pb$ and low $^{207}Pb/^{204}Pb$ in mafic rocks may represent contributions from an ancient lithospheric mantle source for the following reasons:

1) It was demonstrated through AFC modeling that mafic nepheline-normative samples from Rampart, Ishawooa and Sunlight volcanic centers can be produced from assimilation of a phlogopite-bearing source by a melt with a composition similar to the sampled basanite (See chapter 2). This suggests that

samples in the middle of the trend line, although somewhat differentiated, are derived from contributions of both asthenospheric and lithospheric mantle sources.

2) The most mafic samples from the Crandall volcanic center, with Mg numbers higher than the sampled basanite, high Cr (220-425 ppm) and high Ni (60-190 ppm) are most likely mantle-derived. Two samples from this volcanic center (HM6A-94 and HM2-94) can be modeled as partial melts of an amphibole-enriched garnet-bearing peridotite (Chapter 2). One of these samples (HM6A-94) is included in the isotopic data set, and has low $^{143}Nd/^{144}Nd$ (0.51162) and low $^{87}Sr/^{86}Sr$ (0.7043) together with low $^{208}Pb/^{204}Pb$ (36.7) and low $^{207}Pb/^{204}Pb$ (15.3). Other mafic samples from Crandall also have similar isotopic compositions (HM1894, HM895). High-Mg rocks with consistently low and extreme isotopic composition suggests derivation from an ancient enriched mantle source (Fraser et. al., 1986; Fitton et. al, 1988).

3) Trend lines of mafic Absaroka province samples for both $^{207}Pb/^{204}Pb$ versus $^{206}Pb/^{204}Pb$, and $^{208}Pb/^{204}Pb$ versus $^{206}Pb/^{204}Pb$, coincide with a trend for Smokey Butte lamproites from subcontinental lithospheric mantle, and Missouri Breaks kimberlite, derived from Wyoming Province mantle sources (Scambos, 1991; Fraser et al., 1986).

4) Both lower and upper crustal rocks from the Wyoming Province have similar isotopic compositions to this proposed lithospheric mantle source, which is both ancient and enriched. However, extreme variability is exhibited in sampled isotopic compositions from crustal sources, resulting from isolation of heterogeneous crustal material over long periods of geologic time (Leeman et. al., 1985; See Figure 3.8b). This should produce enormous scatter in isotopic data of melts derived from separate pockets of assimilated crust. The linearity of the trend line defined by Crandall, Ishawooa, and Rampart volcanic center samples for $^{207}Pb/^{204}Pb$ versus $^{206}Pb/^{204}Pb$, and $^{208}Pb/^{204}Pb$ versus $^{206}Pb/^{204}Pb$, as well as $^{143}Nd/^{144}Nd$ versus $^{87}Sr/^{86}Sr$, suggests that the source of mafic melts has been subjected to similar enrichment events. This source is more homogeneous than that which would be expected of a lower crustal source, because the linear trend observed in mafic samples is unlikely to occur if they are from separate, distinct, ancient lower crustal sources, in which isotopic variability is extreme.

Lavas from the Hyalite Volcanic Center, and Other Intermediate Compositions

All samples from the Hyalite volcanic center have higher $^{87}Sr/^{86}Sr$ and $^{208}Pb/^{204}Pb$ isotopic compositions which are distinct from other volcanic centers. Sr and Pb isotopic compositions are both consistent with derivation from a lower crustal source. As mentioned above, this evidence alone is not definitive, because lower crustal and lithospheric mantle isotopic compositions overlap and both are characteristically variable (Menzies and Halladay, 1988; Kay and Kay, 1986, Menzies et al, 1983). Other factors, such as trace element composition, must also be considered in order to determine to what extent crust and mantle sources contributed to Absaroka volcanic province magmas, including that of the Hyalite volcanic center.

Overall, mafic and intermediate Hyalite lavas exhibit lower concentrations of incompatible elements (most notably Th, Sr, and Rb), and have low Ce/Yb, high Th/U and Th/La which are considered characteristic of trace element abundances in lower continental crust (Collerson and Fryer, 1978; Taylor and McClennan, 1979; Kay and Kay, 1985). These characteristics are distinctive of the Hyalite volcanic center compared to mafic lavas of other volcanic centers in this study. However, samples from the Independence volcanic center of the northern Absaroka province, studied by Meen and Eggler, (1987) show trace element enrichment similar to mafic Hyalite lavas (Ce/Yb=25, Th/U=3.0-4.5). Samples from the Independence study are isotopically similar to intermediate to silicic compositions of this study, and have higher $^{87}Sr/^{86}Sr$ compared to mafic samples from the Crandall, Rampart, and Ishawooa volcanic centers (Meen and Eggler, 1987).

Based on modern velocity profiles of the lower crust, the Wyoming Archean craton is thought to consist predominantly of mafic granulite and amphibolite (Henstock et al, 1998), such as some of the xenoliths sampled by Eocene magmas from the Highwood Mountains (Joswiak, 1992). Mafic Archean Lewisan granulites, which have compositions similar to lower crustal xenoliths from both Scotland and the Wyoming province may be considered representative of ancient lower crust (Halliday et al., 1993; Joswiak, 1992: Collerson et al., 1988) Trace element

concentrations of mafic end-member samples from each of the volcanic centers, normalized to average mafic Lewisan granulites of Taylor and McLennan (1984) are shown in Figure 3.16. Hyalite volcanic centers show greater similarity to mafic granulites than do other mafic samples from the Absaroka volcanic province, suggesting they have a larger component of lower crust.

Th/U and Th/La are distinctive among enriched and depleted mantle, upper and lower crustal reservoirs: Lower crust has characteristically low Th and U, but high Th/U, and lower Th/La than upper crust (Collerson and Fryer, 1978; Weaver and Tarney, 1981; Weaver, 1981; Kay and Kay, 1985; Leeman et al., 1985; Saunders et al., 1988). Hyalite volcanic center samples have higher Th/U and $^{87}Sr/^{86}Sr$, which is similar to dacites from the Ishawooa and Rampart volcanic centers, and other intermediate and silicic samples. Dacites, as well as Hyalite volcanic center samples, are less enriched in incompatible elements than mafic samples from other volcanic centers which suggests that they are produced by assimilation of a less enriched source. These samples also show overlap in isotopic composition with intermediate to silicic rocks from other areas of the Absaroka volcanic province (Figure 3.8a, and 3.14a).

Hyalite volcanic center samples fall on an isotopic mixing line between Highwood lower crustal granulite samples of Joswiak (1992) and Absaroka province basanite. However, AFC modeling, using sampled xenoliths from the Highwoods, and a starting composition of the sampled basanite requires 80% assimilation of depleted lower crust to produce trace element concentrations similar to Hyalite samples, and results in higher La/Yb. Derivation of Hyalite volcanic center samples from such a large fraction of lower crustal melt is unrealistic. High Th/La in partial melting calculations for lower crust suggests that if the melt parental to Hyalite volcanic centers compositions is thus derived, that the melt source is less enriched than the basanite, and more tholeiitic in character. Large amounts of melting are required when modeling the melting lower crust primarily in order to dilute the enriched character of the melt source, but also because of the more refractory nature of the lower crust. If magmatic fluids are involved, melts may be more easily derived. The anhydrous nature of depleted and refractory mafic granulite suggests that a significant proportion of mantle melt and/or mantle-derived fluids are necessary

to produce the conditions required for lower crustal melting to occur. The introduction of fluids is problematic, because they are associated with enrichment in incompatible elements, but when combined with other, more depleted melt components, may be the source of moderate enrichment in Hyalite volcanic center samples.

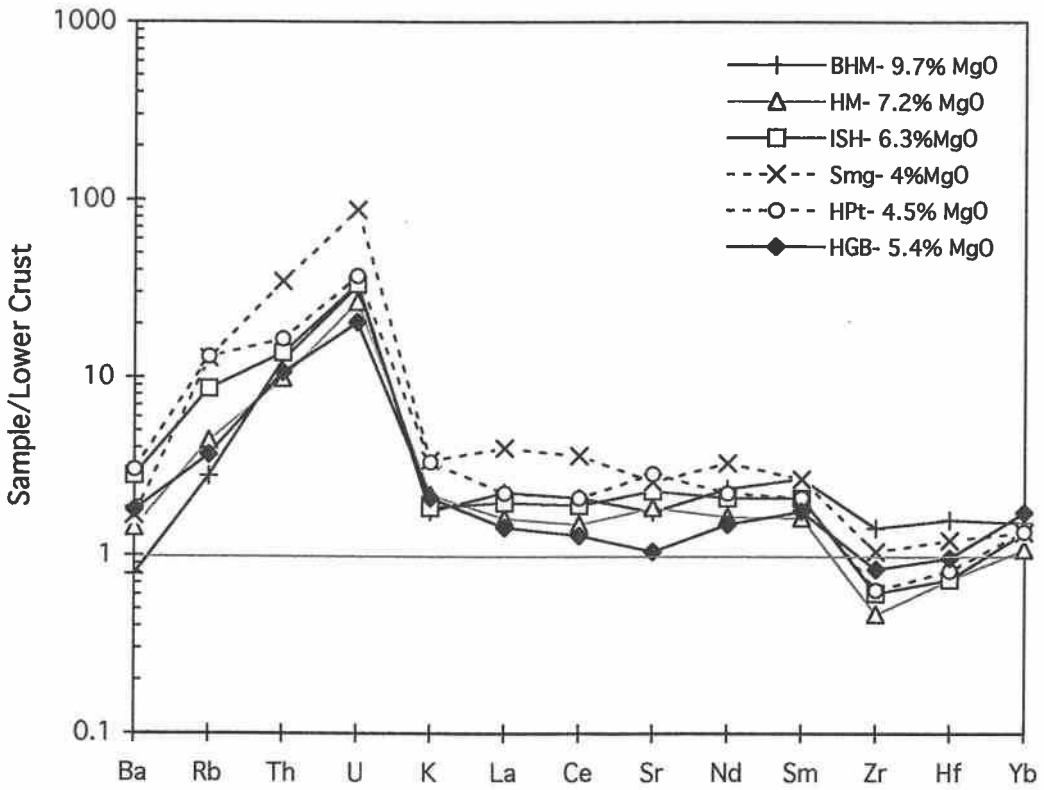

Figure 3.16 Mafic end-member samples from volcanic centers normalized to estimated mafic granulite lower crust of Weaver and Tarney (1984). Samples from volcanic centers, with weight % MgO, are symbolized by the following: HM- Crandall volcanic center; ISH- Ishawooa volcanic center; HPt-Rampart volcanic center; Smg - Sunlight volcanic center, and HGB-Hyalite volcanic center; basanite (BHM) is also shown

Although geophysical data suggests that a mafic lower crust exists within the region at present, lower crustal xenoliths in Pliocene lavas sampled by Leeman et. al. (1985) were >65% SiO_2, a large portion of melt derived from lower crust of this composition would result in a silicic melt. Granulites from the Eocene Highwood Mountains are more mafic in composition, from 50 to 70% SiO_2, but would still produce partial melts more silicic, with lower MgO than samples from the Hyalite volcanic center. Petrologic work by Weaver and Tarney (1984) and Taylor and McClennan (1981, 1986) also debate the mafic nature of Archean lower crust, and suggest that it is more likely to be andesitic in composition, although great heterogeneity exists (Dewey, 1985). Mafic Hyalite samples are from 4.5 to 5.5% MgO, and have uniform Cr (100 ppm) and Ni (35-45 ppm) that suggests that they are not entirely crustal melts. Therefore, these samples are not interpreted as resulting from simple mixing of two isotopic end members, but may be derived from lower crust assimilation by a tholeiitic OIB-type source, and simply includes a fluid-rich lithospheric mantle component.

Hyalite samples are more enriched than lower crust, and partial melting calculations do not show clear evidence they are derived from lower crustal melting by potential primary sources such as the basanite. However, the following evidence strongly suggests that they have interacted with, and assimilated lower crust:

1) Hyalite volcanic center samples show evidence of plagioclase fractionation which takes place at shallower levels under less hydrous conditions (Chapter 2). Therefore, it is more likely that parental Hyalite volcanic center magma resided at crustal levels.

2) Hyalite volcanic center samples have higher Th/U, and relatively low U which is characteristic of lower crust, and would produce higher $^{208}Pb/^{204}Pb$ in samples derived from an ancient lower crustal source. (Moorbath and Taylor, 1986).

3) Most importantly, Hyalite volcanic center samples have $^{208}Pb/^{204}Pb$ and $^{207}Pb/^{204}Pb$ isotopic compositions which are most similar, and overlap with silicic plutons of the Wyoming Province, derived from melting of lower and upper crust (Gunn, 1991). They also show a greater variability in isotopic composition over a narrower compositional range than other volcanic centers, with variation in $\%SiO_2 \approx$ 4%, but $^{87}Sr/^{86}Sr$ from 0.7068 to 0.7076, and $^{208}Pb/^{204}Pb$ from 37.45 to 37.75.

Variation in $^{87}Sr/^{86}Sr$ is not systematic, the sample from Hyalite which has the lowest MgO (3.0%) and highest SiO_2 (57%) also has the lowest $^{87}Sr/^{86}Sr$ (0.7068). This relationship implies interaction of Hyalite volcanic center melts with isotopically heterogenous lower crust.

Enrichment and Metasomatism of Mafic Lavas

The trace element composition of low K/Rb, high Rb, nepheline-normative rocks from Ishawooa, Rampart, and Sunlight can be modeled using AFC calculations as basanite with 20% assimilation of phlogopite, which suggests that they are derived from a mixture of asthenospheric and lithospheric mantle sources (Chapter 2). This interpretation is consistent with sampled peridotite xenoliths from the Wyoming Province which contain phlogopite (Carlson and Irving, 1994). In addition, the isotopic composition of these rocks, can be calculated using the two component mixing equation of DePaolo and Wasserburg (1979a) and requires 25% of the Crandall (lithospheric) end-member be mixed with 75% of the basanite to produce the $^{144}Nd/^{143}Nd$ isotopic composition of Rb enriched samples.

Low and nearly constant $^{87}Sr/^{86}Sr$ in mafic samples results from low $^{87}Sr/^{86}Sr$ in both asthenosperic and lithospheric mantle sources. Both the basanite end-member and the Crandall end-member have low $^{87}Sr/^{86}Sr$ values. Mixing or assimilation of an enriched component with an asthenospheric source does not require that primary Sr enrichment and low $^{87}Sr/^{86}Sr$ be derived from the lithospheric mantle source. Deep level fractionation of fluid-rich mantle-derived melts excludes plagioclase, which is not stable, and produces Sr enrichment in the asthenosphere-derived melt because of its incompatible behavior. Fractionation at depth in the absence of plagioclase crystallization enhances this enrichment (Chapter 2). Because Sr enrichment is pronounced under these conditions, the asthenospheric melt may potentially impart the resulting Sr-enriched melt with a low asthenosphere-derived $^{87}Sr/^{86}Sr$ isotopic signature. Alternatively, Sr enrichment also occurs during metasomatism, although it is a less mobile element during volatile exsolution than Rb

or Cs (Tatsumi and Eggins, 1995). Sr enrichment, and lower $^{87}Sr/^{86}Sr$ of absarokites and shoshonites of the Absaroka province in comparison to Smokey Butte Lamproite could also be derived from heterogeneity in enrichment of the lithospheric mantle source (Menzies et. al., 1983). In a plot of Rb versus $^{87}Sr/^{86}Sr$, Rb enrichment does not coincide with changes in $^{87}Sr/^{86}Sr$, which remains nearly constant for mafic samples (Figure 3.12). This implies that Rb is derived from a source which is independant of crustal assimilants, and decoupled from the source of Sr enrichment in mafic rocks. This relationship is consistent with Rb inherited from a lithospheric mantle source, but separate from the source of Sr enrichment. Such pronounced Sr enrichment, which is most pronounced in samples from the Ishawooa and Rampart volcanic centers may be enhanced primarily by early, deep fractionation processes rather than lithospheric mantle enrichment (Chapter 2).

The low $^{87}Sr/^{86}Sr$ and low $^{143}Nd/^{144}Nd$ of samples from the Crandall volcanic center are lower and more extreme than Smokey Butte lamproites, and may primarily reflect variation in the type of metasomatic enrichment. Enrichment by phlogopite in the source will increase Rb and produce samples with higher $^{87}Sr/^{86}Sr$ over a long period of geologic time, whereas metasomatic enrichment of LREE in pyroxene will produce lower $^{87}Sr/^{86}Sr$ and low $^{143}Nd/^{144}Nd$ (Schmidt et al., 1999). Samples from the Ishawooa and Rampart volcanic center also have lower $^{87}Sr/^{86}Sr$, although they can be modeled as melts which have assimilated phlogopite. In such a model, the low $^{87}Sr/^{86}Sr$ in these samples primarily reflects the low $^{87}Sr/^{86}Sr$ isotopic values which fall on a mixing line with the composition of the asthenospheric source (represented by the sampled basanite).

Rhyolites have variable Th/U, $^{87}Sr/^{86}Sr$, $^{207}Pb/^{204}Pb$, and $^{208}Pb/^{204}Pb$. Distinctive Pb isotopic compositions for rhyolites of the northern and the southern Absaroka volcanic province, show that rhyolite and rhyodacite ash-flow tuffs are closest to the isotopic composition of Mesozoic and Tertiary plutons of the Wyoming Province which have been interpreted as crustal melts (Gunn, 1991). These silicic tuffs are likely to be derived from crustal melting. Variation in isotopic composition of silicic and intermediate rocks of the Ishawooa and Rampart volcanic centers, which are intermediate between data for crustal rocks and mafic samples suggest they are derived from crustal assimilation by a mafic melt.

Mineralogic Trace Element and Isotopic Variations with Time

The Absaroka volcanic province has been cited as an example of geochemical and petrologic zonation of a maturing subduction related arc (Chadwick, 1970; Lipman et al., 1972; Dickinson, 1979; and Chadwick, 1985). However, early eruptions within the volcanic field are characteristically more potassic and highly enriched in incompatible elements, and are followed by less enriched magmatism. Alkaline rocks have long been thought to be spatially associated with a back-arc region in many cases (Tatsumi and Eggins, 1995). Potassic magmas are not spatially associated with one another, occur throughout the volcanic province, and therefore are not spatially associated with the position of a purported descending slab. In addition, isotopic compositions of Absaroka province samples suggests that the extreme trace element enrichment characteristic of these rocks has been imparted by an ancient source, which we have interpreted as lithospheric mantle. Because the enrichment of these samples is old, it is not likely to be derived from contemporaneous subduction. This is especially true in the Eocene Cordillera, where subduction models require that the descending Farallon slab is $\leq$ 30 Ma (Stock and Molnar, 1988).

Given the wealth of modern age data on middle-Eocene volcanic fields, it has become apparent that magmatism within the Absaroka volcanic province is synchronous with melting across a broad region of the Cordillera (Holder et al., 1990; Dudas, 1991; Harlan et al., 1991; O'Brien et al., 1995; M'Gonigle and Dalrymple, 1996; Morris and Hooper, 1997). Subduction-related models cannot account for broad regions of melting, which extend far inland from the plate margin, and no modern or ancient counterpart within a continental subduction setting exists.

The Absaroka volcanic province exhibits geochemical and mineralogic characteristics which suggest that magmatism evolved in response to lithospheric extension, rather than subduction. The oldest rocks sampled in the province show evidence of clinopyroxene and olivine fractionation, and are free of plagioclase except for groundmass phases, which suggests that early fractionation occurred at

deeper levels, under conditions of high P_{H2O} (Hay et al., 1995; Mahhod and Baker, 1986; Tatsumi, 1982). Rocks which are younger, or later eruptive products from long-lived volcanic centers crystallize plagioclase, and exhibit geochemical trends which suggest that fractionation of plagioclase occurred. This requires that fractionation at these volcanic centers took place at shallower crustal levels, under less hydrous conditions (Moore and Carmichael, 1998). The progression of early fractionation at deeper levels, followed by later fractionation at shallower levels is characteristic of extension-related magmatism. At early stages of extension, the lithosphere is relatively cold, which promotes crystallization at deeper levels in the rising magma. Models suggest that as magmatism proceeds in extensional settings, that ponding of melts at mid-crustal levels occurs (Gans and Bohrsen, 1998). This provides a mechanism for more extensive assimilation and fractionation at shallower levels during later stages of magmatism (Figure 3.17).

Plots of changing Nd and Sr isotopic composition and estimated age of samples are shown in Figures 15a and 15b. Samples from 48 to 52 Ma are bimodal, they are mafic (<54% SiO_2) and have low $^{87}Sr/^{86}Sr$ (0.7042-0.7045) and low $^{143}Nd/^{144}Nd$ (<0.5120), or they are silicic to intermediate with high $^{87}Sr/^{86}Sr$, and lower $^{143}Nd/^{144}Nd$ than mafic rocks (<0.5115). This suggests that early magmatism was primarily derived from lithospheric mantle and upper crust. After 48 Ma, magmatism is characterized by melting from less enriched, more silicic sources. Silicic rocks with low and variable $^{87}Sr/^{86}Sr$, and low $^{143}Nd/^{144}Nd$, and isotopically similar intermediate to mafic Hyalite volcanic center rocks are the characteristic products of this later stage of magmatism. These rocks are less enriched in incompatible elements and have higher Th/U which suggests that they have assimilated lower crust. Basanite with an enriched OIB isotopic composition is among the last products to erupt from tha Absaroka volcanic province.

Isotopic, geochemical and mineralogic variability in Absaroka samples are consistent with magmatism evolving from early enriched mafic melts to later depleted silicic melts. Based on interpretations of sampled isotopic compositions, melting is initially derived from the base of the lithosphere, but includes silicic upper crustal melting, then progresses to melting of lower crust, and ends with a small volume of

asthenosphere-derived melt. This sequence of melting shows striking similarity to models of extension-related magmatism by McKenzie (1989) and McKenzie and Bickle (1988) which suggest that early extension-related melts are derived from metasomatized sources, and that only late in the sequence of magmatism, under conditions of continued lithospheric extension do small volumes of asthenosphere-derived melt erupt.

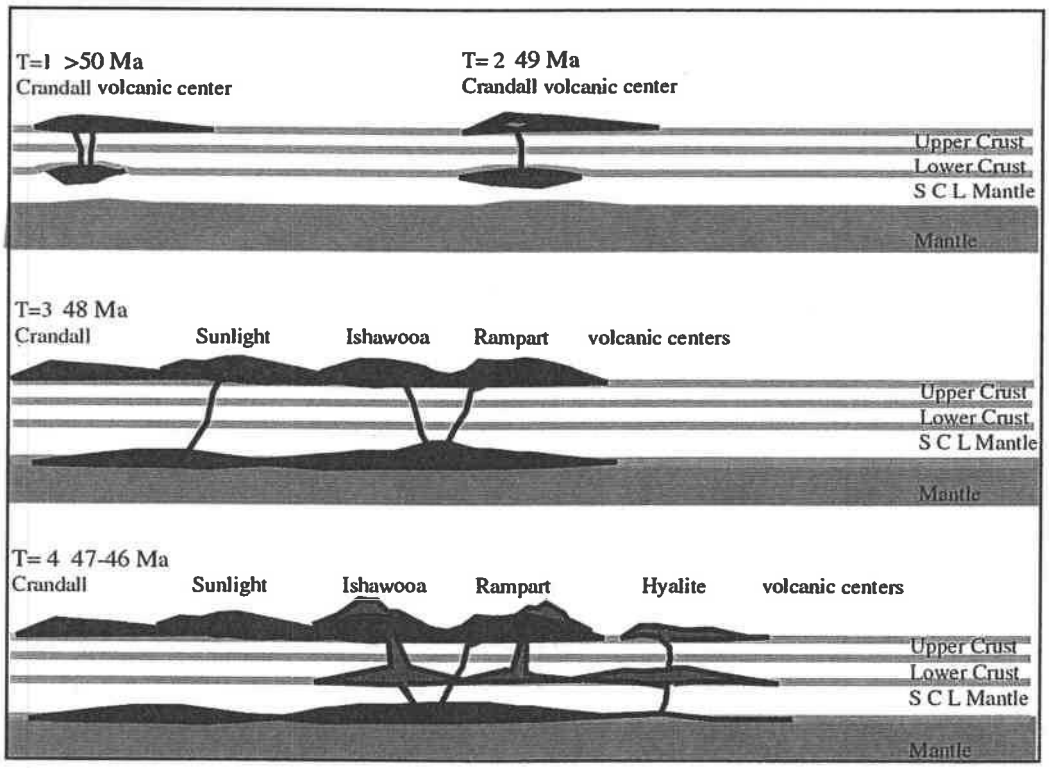

Figure 3.17. Schematic diagram showing changing depth of melt sources with time.

CONCLUSIONS

1) Mafic absarokite and shoshonite of the Absaroka volcanic province are characterized by low $^{143}Nd/^{144}Nd$ and low $^{87}Sr/^{86}Sr$, in the lower left hand quadrant of the Nd-Sr isotope diagram, and have more extreme values than other alkaline rocks of the Wyoming Province.

2) Low $^{206}Pb/^{204}Pb$, $^{206}Pb/^{204}Pb$, and $^{206}Pb/^{204}Pb$ ratios for mafic samples from three separate volcanic centers lie between Smokey Butte lamproites of lithospheric mantle composition, and kimberlites of the Missouri Breaks, suggesting that they are derived by binary mixing of lithospheric mantle and asthenospheric sources.

3) Nepheline-normative, high Rb samples have trace element compositions which have been modeled as a mixture of asthenospheric and lithospheric mantle components. These calculations are consistent with two-component mixing calculations of using Nd isotopic compositions of lithospheric mantle and asthenospheric mantle end-members.

4) Extreme trace element enrichment (most notably Sr) due to deep fractionation in the absence of plagioclase, combined with metasomatism of parental sources, produces mafic melts that are isotopically insensitive to contamination by crust.

5) Less enriched quartz-normative mafic samples from the Hyalite volcanic center are isotopically distinct, and have low Sr, Ce/Yb and Th/U, have relatively higher $^{208}Pb/^{204}Pb$, and higher, variable $^{87}Sr/^{86}Sr$ within a narrow range of compositions, which suggests that they contain a lower crust component. However, AFC models demonstrate that simple two component mixing of asthenospheric basanite and lower crust requires an unrealistically large degree of assimilation to

produce compositions which are similar to Hyalite samples, and are higher in La/Yb. Therefore, these samples are more likely derived by melting of lower crust by a melt source which is more tholeiitic in character. The addition of a fluid- and LREE-enriched lithospheric component, may have enhanced lower crustal melting.

6) Low Nd, Sr, and Pb isotopic compositions of Absaroka samples suggests that enrichment of the melt source is ancient, and not derived from a contemporaneous subduction event, or from a young oceanic slab such as the Farallon Plate.

7) Middle Eocene volcanic rocks of the Absaroka volcanic province erupted from 53 to 43 Ma. Early magmatism $\leq$ 48 Ma is dominated by mafic alkaline absarokite and shoshonite which are interpreted here as having a lithospheric mantle component, and also includes rhyolites produced by crustal melting. Post 48 Ma eruptions are less enriched in incompatible elements and are dominantly silicic. Higher Th/U in late eruptive products suggest that these rocks are partly derived from melting of lower crust.

REFERENCES CITED-3

Berger, B.R., and Snee. L.W. (1992) Thermochronological constraints on mylonite and detachment fault development, Kettle Highlands, northeastern Washington and southern British Columbia; Geological Society of America Abstracts with Programs, vol. 24, no.7, p.65.

Beswick, A.E. (1976) K and Rb relations in basalts and other mantle derived materials, Is phlogopite the key?; Geochimica et Cosmochimica Acta, vol. 40, p. 1167-1183.

Carlson, R.W., and Irving, A.J. (1994) Depletion and enrichment history of subcontinental lithospheric mantle: An Os, Sr, Nd and Pb isotopic study of ultramafic xenoliths from the northwestern Wyoming Craton, Earth and Planetary Science Letters, vol. 126, p.457-472.

Chadwick, R.A. (1970) Belts of eruptive centers in the Absaroka-Gallatin volcanic province, Wyoming-Montana: Geological Society of America Bulletin, vol. 81, p.267-273.

Collerson, K.D., and Fryer, B.J. (1978) The role of fluids in the formation and development of Early Continental Crust; Contributions to mineralogy and Petrology, vol. 67, p.151-167.

Collerson, K.D., Hearn, B.C., Macdonald , R.A., Upton, B.G.J., and Park, J.G. (1988) Granulite xenoliths from the Bearpaw Mountains, Montana: Constraints on the character and evolution of the lower continental crust; NATO Advanced Research Workshop on Petrology and geochemistry of Granulites, Clermont-Ferrand, France, Sept. 5-9, 1988, Terra Cognita, vol.8, p. 270.

Conrey, R.M., Sherrod, D.R., Hooper, P.R., and Swanson, D.A. (1997) Diverse primitive magmas in the Cascade Arc, northern Oregon and southern Washington: The Canadian Mineralogist, v. 35, p.367-396.

DePaolo D.J., and Wasserburg, G.J. (1979a) Petrogenetic mixing models and Nd-Sr isotopic patterns; Geochimica et Cosmochimica Acta, vol.43, p. 615-627.

Dewey, J.F. (1986) Diversity in the lower continental crust; *In* Dawson, J.B., Carswell, D.A., Hall, J. and Wedepohl, K.H. (eds.) The Nature of the Lower Continental Crust, Geological Society Special Publication No. 24, Blackwell Scientific Publications, Oxford, London, Edinburgh, Boston, Palo Alto, Melbourne, p.71-78.

Edwards, C., Menzies, M. and Thirwall, M. (1991) Evidence from Muriah, Indonesia for the Interplay of Supra-Subduction Zone and Intraplate Processes in the Genesis of Potassic Alkaline Magmas: Journal of Petrology, vol. 32, p.555-592.

Eggler D.H., Meen, J.K., Welt, F., Dudas, F.O., K.P. Furlong, K.P., McCallum, M.E., Carlson, R.W. (1988) Tectonomagmatism of the Wyoming Province: in Cenozoic Volcanism in the southern Rocky Mountains Revisited: A Tribute to Rudy C. Epis-Part-3, Drexler, J.W., and Larson, E.E., eds., Colorado School of Mines Quarterly, vol. 83, no.2, p.25-40.

Dudas, F.O. (1991) Geochemistry of igneous rocks from the Crazy Mountains, Montana, and tectonic models for the Montana alkalic province: Journal of Geophysical Research, vol. 96, p.13,261-13,278.

Fraser, K.J., Hawkesworth, C.J., Erlank, A.J., Mitchell, R.H., and Scott-Smith, B.H. (1985) Sr, Nd, and Pb isotope and minor element chemistry of lamproites and kimberlites; Earth and Planetary Science Letters, vol. 76, p.57-70.

Frost, C.D., Chamberlain, K.R., and Frost, B.R. (1998) Archean evolution of the Wyoming Province: Evidence from the Bighorn Mountains; Geological Society of America Abstracts with Programs, vol. 30, no.7. p. A-395.

Frost, B.R., Chamberlain, K.R., Swapp, S.M., and Frost, C.D. (1998) The age of granulite metamorphism in the Wind River Range, Wyoming: The granulite uncertainty principle compounded; Geological Society of America Abstracts with Programs, vol. 30, no.7. p. A-154.

Gans, P.B., and Bohrson, W.A. (1998) Supression of volcanism during rapid extension in the Basin and Range province, United States: Science, vol. 279, p. 66-68.

Gunn, S.H. (1991) Isotopic constraints on the crustal evolution of southwestern Montana: Ph.D. dissertation University of California, Santa Cruz, 146 p.

Halladay, A.N., Dickin, A.P., Hunter, R.N., Davies, G.R., Dempster, T.J., Hamilton, P.J., and Upton, B.G.J. (1993) Formation and composition of the lower continental crust: Evidence from xenolith suites: Journal of Geophysical Research, vol. 98, no. B1, p.581-607.

Harlan, S.S., Mehnert, H.H., Snee, L.W., and Meen, J.K. (1991) Preliminary isotopic and age determinations from selected Late Cretaceous and Tertiary rocks in Montana: in Guidebook of the Central Montana Alkalic Province, Montana Bureau of Mines Special Publication 100, p. 136-137.

Harlan, S.S., Snee, L.W., and Geissman, J. W. (1996) $^{40}Ar/^{39}Ar$ geochronology and paleomagnetism of Independence Volcano, Absaroka Volcanic Supergroup, Beartooth Mountains, Montana: Canadian Journal of Earth Sciences, vol. 33, p. 1648-1654.

Hay, D.E., and Wendlandt, R.F. (1995) The origin of Kenya rift plateau-type flood phonolites: Results of high-temperature/high-pressure experiments in the systems phonolite-H_2O and phonolite-H_2O-CO_2: Journal of Geophysical Research, vol. 100, p. 400-411

Hearn B.C. Jr., and McGee, E.S. (1984) Garnet peridotites from Williams kimberlites, north-central Montana, USA: in Kimberlites and Related Rocks II, Kornprobst, J. ed., Elsevier, New York, p. 255-283.

Holder, R.W., Holder, G.A.M., and Carlson, D.H. (1990) Middle Eocene dike swarms and their relation to contemporaneous plutonism, volcanism, core complex mylonitization, and graben subsidence, Okanagan Highlands, Washington; Geology, vol. 18, p.1082-1085.

Iddings, J.P., (1895) Absarokite-shoshonite-banakite series: Journal of Geology, vol.3, p.935-959.

James, H.L., and Hedge, C.E. (1980) Age of the basement rocks of southwest Montana; Geological Society of America Bulletin, vol. 91, p. 11-15.

Joswiak, D. (1992) Composition and evolution of the Lower Crust, Central Montana: Evidence from granulite xenoliths; M.S. Thesis University of Washington, 156 p.

Karner, F.R. (1989) Devils Tower-Black Hills Alkalic Igneous Rocks and General Geology: *in* American Geophysical Union Guidebook T131, F.R. Karner, (ed.), vol. 1, p. 1-2.

Kay, R.W., and Kay, S.M. (1986) Petrology and geochemistry of the lower continental crust: *In* Dawson, J.B., Carswell, D.A., Hall, J. and Wedepohl, K.H. (eds.) The Nature of the Lower Continental Crust, Geological Society Special Publication No. 24, Blackwell Scientific Publications, Oxford, London, Edinburgh, Boston, Palo Alto, Melbourne, p. 147-159

Kleinkopf, M.D. (1991) Regional geophysical investigations of the Central Montana Alkalic Province: Montana Bureau of Mines Special Publication 100, p. 131-132.

Leat, P.T., Thompson, R.N., Morrison, M.A., Hendry, G.L., and Dickin, A.P. (1988) Compositionally-diverse Miocene-Recent rift-related magmatism in northwest Colorado: Partial melting and mixing of mafic magmas from 3 different asthenospheric and lithospheric mantle sources: Journal of Petrology, Special Lithosphere Issue, p. 351-377.

Leeman, W.P., Menzies, M.A., Matty, D.J., and Embree, G.F. (1985) Strontium, neodymium and lead isotopic compositions of deep crustal xenoliths from the Snake River Plain: evidence for Archean basement: Earth and Planetary Science Letters, vol. 75, p. 354-368.

Lipman, P.W., Protska, H.J., and Christiansen, R.L. (1972) Evolving subduction zones in the western United States; Science, vol. 174, p. 821-825

Lugmair, G.W., Scheinin, N.B., and Marti, K. (1975) Sm/Nd age and history of Apollo 17 basalt 75075: Evidence for early differentiation of the lunar exterior: Proceedings of the 6th Lunar Science Conference, p. 1419-1429.

MacDonald R., Upton, B.G.J., Collerson, K.D., Hearn, B.C., Jr., and James, D. (1992) Potassic mafic lavas of the Bearpaw Mountains, Montana: Mineralogy, chemistry, and origin: Journal of Petrology, vol. 33, pt. 2, p. 305-346.

Mahood, G.A., and Baker, D.R. (1986) Experimental constraints on depths of fractionation of mildly alkalic basalts and associated felsic rocks: Pantelleria, Strait of Sicily: Contributions to Mineralogy and Petrology, vol. 93, p. 251-264.

Meen, J.K. (1987) Sr, Nd, and Pb isotopic compositions of Archean basement rocks, Boulder River region, Beartooth Mountains, Montana; Isochron/West, no. 50, p. 13-24.

Meen, J.K., and Eggler, D.H. (1987) Petrology and geochemistry of the Cretaceous Independence volcanic suite, Absaroka Mountains, Montana: Clues to the composition of the Archean sub-Montanan mantle; Geological Society of America Bulletin, vol. 98, p. 238-247.

Menzies, M.A., and Halladay, A. (1988) Lithospheric mantle domains beneath the Archean and Proterozoic crust of Scotland; Journal of Petrology, Special Lithosphere Issue, p. 275-302.

Menzies, M.A., Leeman, W.P., and Hawkesworth, C.J. (1983) Isotope geochemistry of Cenozoic volcanic rocks reveals mantle heterogeneity below western USA; Nature, vol. 303, p. 205-209.

M'Gonigle, J.W.M., and Dalrymple, G.B. (1996) $^{40}Ar/^{39}Ar$ ages of some Challis Volcanic Group rocks and initiation of Tertiary sedimentary basins in southwestern Montana; U.S. Geological Survey Bulletin 2132, 17 p.

Mitchell, R.H., Platt, R.G., and Downey, M. (1987) Petrology of lamproites from Smokey Butte, Montana: Journal of Petrology, vol. 28, no. 6, p.645-677.

Mogk, D.W., Mueller, P.A., and Wooden, J.L. (1988) Archean tectonics of the north Snowy Block, Beartooth Mountains, Montana: Journal of Geology, vol. 96, p.125-141.

Moore, G., and Carmichael, I.S.E. (1998) The hydrous phase equilibria (to 3 kbar) of an andesite and basaltic andesite from western Mexico: constraints on water content and conditions of phenocryst growth: Contributions to Mineralogy and Petrology, vol. 130, p.304-319.

Moorbath, S. and Taylor, P.N. (1986) Geochronology and related isotope geochemistry of high grade metamorphic rocks from the lower continental crust: *In* Dawson, J.B., Carswell, D.A., Hall, J. and Wedepohl, K.H. (eds.) The Nature of the Lower Continental Crust, Geological Society Special Publication No. 24, Blackwell Scientific Publications, Oxford, London, Edinburgh, Boston, Palo Alto, Melbourne, p. 211-220

Montgomery, C.W., and Lytwyn, J.H. (1984) Rb-Sr systematics and ages of principal lithologies in the South Snowy Block, Beartooth Mountains: Journal of Geology, vol. 92, p. 103-112.

Morris, G.A. and Hooper, P.R. (1997) Petrogenesis of the Colville Igneous Complex, northeast Washington: Implications for Eocene tectonics in the northern U.S. Cordillera; Geology, vol. 25, p.831-834.

Mueller, P.A., Wooden, J.L. and Nutman, A.P. (1992) 3.96 Ga zircons from Archean quartzite, Beartooth Mountains, Montana: Geology, vol. 20, p.327-330

Muller, D. and Groves, D.I. (1997) Potassic Igneous Rocks and Associated Gold-Copper Mineralization: Springer-Verlag Berlin Heidelberg, 210 p.

O'Brien, H.E., Irving, A.J., McCallum, I.S. and Thirwall, M.F. (1995) Strontium, neodymium, and lead isotopic evidence for the interaction of post-subduction asthenospheric potassic magmas of the Highwood Mountains, Montana, USA, with ancient Wyoming craton lithospheric mantle; Geochimica et Cosmochimica Acta, vol. 29, no. 21, p.4539-4562.

O'Brien, H.E., Irving, A.J., McCallum, I.S., (1991) Eocene potassic magmatism in the Highwood mountains, Montana: petrology, geochemistry, and tectonic implications: Journal of Geophysical Research, vol. 96, p. 13237-13260.

Pearce, J.A. (1983) Role of sub-continental lithosphere in magma genesis at active continental margins: *In* Hawkesworth, C.J., and Norry, M. J. (eds.) Continental Basalts and Mantle xenoliths, Shiva, Nantwich, p.230-249.

Pearce, J.A., and Norry, M.J. (1979) Petrogenetic implications of Ti, Zr, Y, and Nb variations in volcanic rocks; Contributions to Mineralogy and Petrology, vol. 69, p. 33-47.

Rogers, N.W., and Setterfield, T.N. (1994) Potassium and incompatible -element enrichment in shoshonitic lavas from the Tavua volcano, Fiji: Chemical Geology, vol. 118, p.43-62.

Saunders, A. D., Norry, M.J., and Tarney, J. (1988) Origin of MORB and chemically depleted mantle reservoirs: trace element constraints; Journal of Petrology, Special Lithosphere issue, p. 415-445.

Scambos, T.A. (1991) Isotopic and Trace element Characteristics of the Central Montana Alkalic Province Kimberlite-Alnoite Suite; Montana Bureau of Mines Special Publication 100, p. 93-109.

Stock, J., and Molnar, P. (1988) Uncertainties and implications of the Late Cretaceous and Tertiary positions of North America relative to the Farallon, Kula, and Pacific Plates: Tectonics, vol. 7, p. 1339-1384.

Tatsumi, Y., and Eggins, S. (1995) Subduction Zone Magmatism; Blackwell Science, Frontiers in Earth Sciences, (p. 74-77, 142-143) 211p.

Tatsumoto, M., Hegner, E., and Unruh, D.M. (1987) Origin of west Maui volcanic rocks inferred from Pb, Sr, and Nd isotopes and a multicomponent model for oceanic basalt: *In* Volcanism in Hawaii, R.W. Decker, and P.H. Stauffer, (eds.) U.S. Geological Survey Professional Paper 1350, p. 723-744.

Taylor S.R., and McClennan, S.M.(1979) Discussion on "Chemistry, thermal gradients and evolution of the lower continental crust" by Tarney and B.F. Windley; Journal of the geological Society of London, vol. 136, p.497-500.

Todt, W.., Cliff, R.A., Hanser, A., and Hofmann, A.W. (1993) Re-calibration of lead standards using a $^{202}Pb + {}^{205}Pb$ double spike: 7th Meeting of the European Union of Geosciences Abstract Volume, p. 396.

Weaver, B.L. (1991) The origin of ocean island basalt end-member compositions: trace element and isotopic constraints; Earth and Planetary Science Letters, vol. 104, p.3810-3970.

Weaver, B.L., and Tarney, J. (1984) Empirical approach to estimating the composition of the continental crust; Nature, vol. 310, p. 575-570.

Weaver, B.L., and Tarney, J. (1980) Continental crust composition and nature of the lower crust: constraints from mantle Nd-Sr isotope correlation; Nature, vol. 286, p.342-346.

Wooden, J.L., and Mueller, P.A. (1988) Pb, Sr, and Nd isotopic compositions of a suite of Late Archean, igneous rocks, eastern Beartooth Mountains: implications for crust-mantle evolution, Earth and Planetary Science Letters, vol. 87, p. 59-72.

CHAPTER 4

Synextensional Magmatism of White Mountain Monzogabbro and its Relationship to Regional Volcanism in the Eocene Absaroka Volcanic Province: Implications for the Heart Mountain Detachment

Hiza, M. M., Grunder, A. L., and Snee, L. W.

To be submitted to *Geology*, Geological Society of America, Boulder, CO
23 Pages

INTRODUCTION

The Heart Mountain detachment fault in the Absaroka Volcanic province of northwestern Wyoming has remained an enigmatic structural feature despite many studies since 1941 (e.g., Pierce, 1941; Hauge, 1982, 1993; Pierce and Nelson, 1969; Pierce and others, 1991; Tokarski and others, 1994; Templeton, 1995; Beutner and Craven, 1996). It is an enormous, low-angle (< 2°) bedding-plane parallel fault, extending tens of kilometers, that lies principally within Ordovician Bighorn Dolomite (Figure 4.1). The upper plate consists of blocks of Mississipian, Devonian, and Ordovician carbonate strata, and Eocene lava flows and volcaniclastic strata of the Absaroka Volcanic Supergroup. These units are juxtaposed against footwall carbonate strata of Bighorn Dolomite which overlies the Cambrian Snowy Range Formation, and crystalline Precambrian granitic rocks (Figure 4.2).

No single model yet explains all of the attributes of the Heart Mountain detachment. There is wide agreement that upper plate extension and movement took place along the fault horizon simultaneous with volcanism in the Absaroka Province, which occurred from 53 to 43 Ma (Pierce, 1963, 1982; Hauge, 1993; Chapter 1). Disagreement remains as to whether displacement occurred catastrophically, and to what extent Eocene volcanic strata were displaced by faulting, or deposited after faulting occurred (Pierce 1982, Hague, 1990). Pierce and others (1973) divided the upper plate into 50 or more discrete blocks which were displaced catastrophically from the Abiathar break-away, locally producing an exposed fault surface. Volcaniclastic debris and lava flows were then rapidly deposited between detached fault blocks. In contrast, Hauge (1982) suggested that the bedding plane detachment moved as a continuously extending mass, involving the faulting and displacement of both Paleozoic carbonate strata and Eocene volcanic strata. In the model proposed by Hauge, faulting was synchronous with a longer period of Eocene volcanism than envisioned by Pierce.

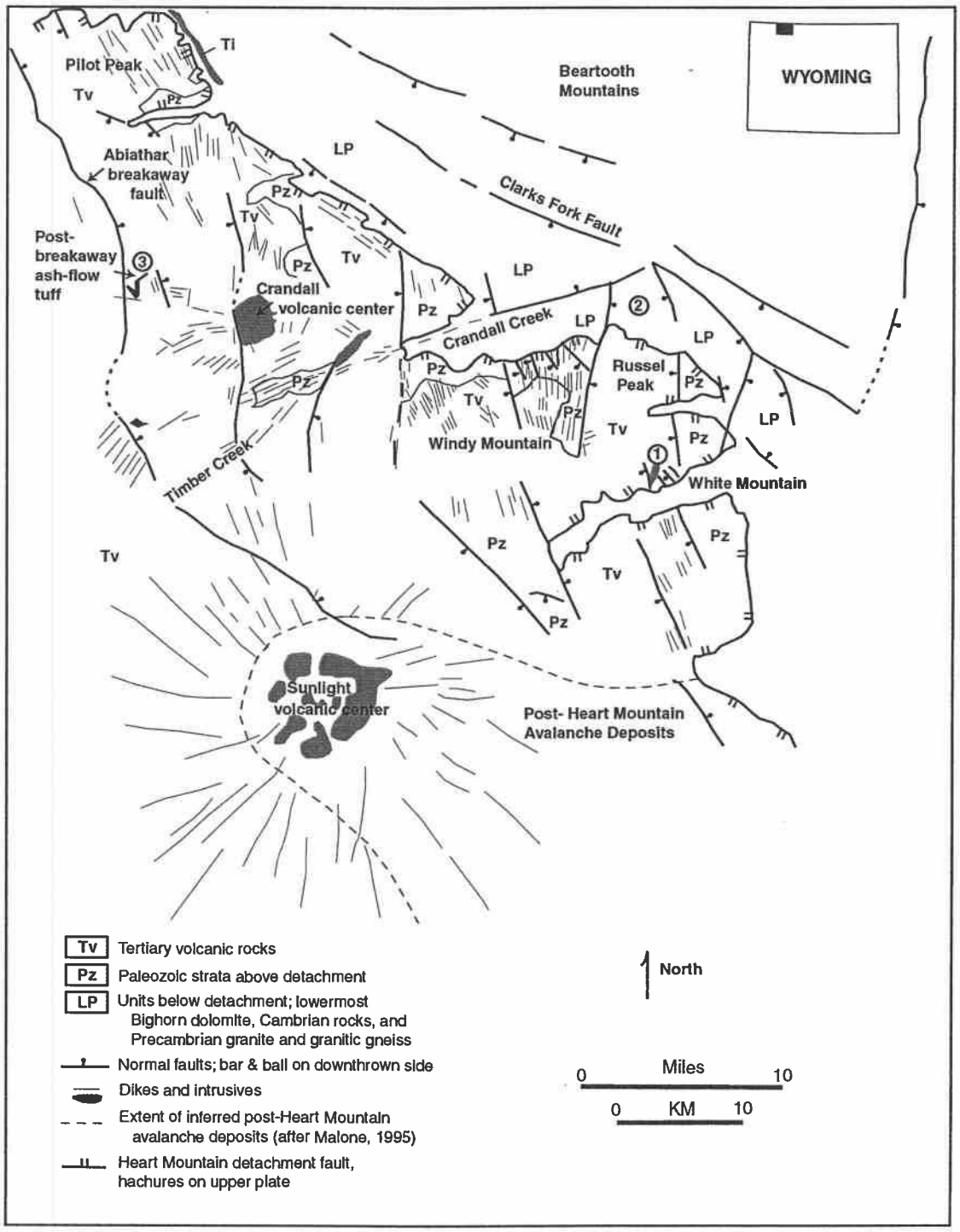

Figure 4.1. Generalized geologic map of the northeastern Absaroka Range. Features shown include the northern Heart Mountain fault area,Crandall volcanic center, and Sunlight volcanic center (modified from Pierce, 1997). Numbers refer to localities discussed in text: 1) White Mountain sample locality, 2) Area of exposed faults below the detachment horizon, 3) Post-faulting ash-flow tuff sample locality.

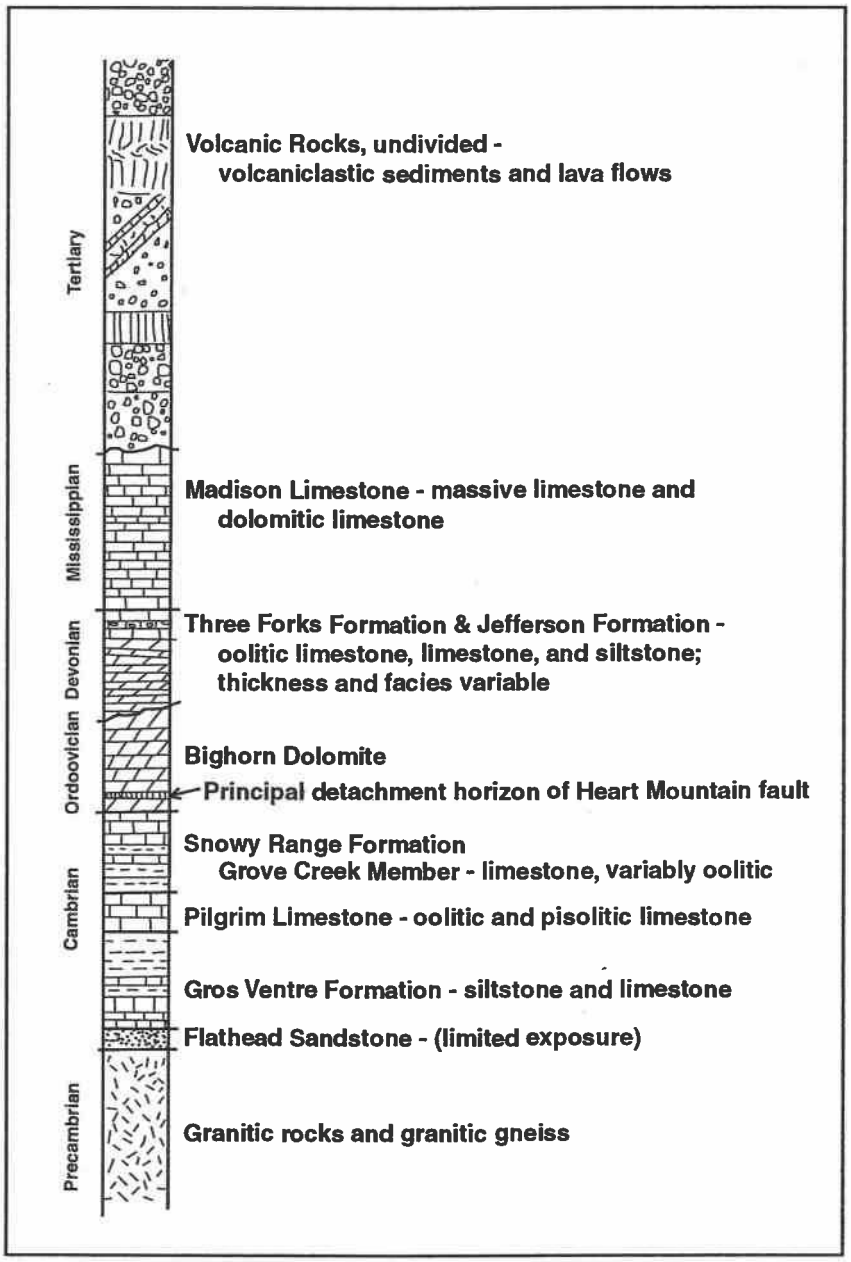

Figure 4.2. Stratigraphic column showing formations exposed in map area of Figure 4.1, and general location of detachment horizon (modified from Hauge, 1993).

Other important features in the region of the Heart Mountain detachment recently recognized by Malone (1995) include a debris avalanche deposit, which overlies large portions of the upper plate of the detachment in the southern half of Heart Mountain fault area (Figure 4.1). This deposit, the Deer Creek debris avalanche, is interpreted as subsequent to movement along the Heart Mountain fault (ibid). Additionally, Templeton et. al. (1995) show that fluids migrated along the detachment; Low $\partial^{18}O$ and low$\partial^{13}C$ values within calcite veins associated with the detachment horizon suggest that meteoric water migrated along the fault plane which is parallel to bedding, and may have influenced the style of fault deformation. Other recent work by Pierce et al. (1991), Tokarski et al. (1994), and Beutner and Craven (1996) has argued for catastrophic emplacement of the Heart Mountain detachment based on textural and petrographic features of breccia from the detachment horizon. Their model includes truncation of igneous intrusions by detachment faulting, followed by deposition of ash-fall tuff, originating from the Crandall volcanic center (Figure 4.1). Beutner and Craven (1996), interpret these features to be related to the same igneous event.

Here, we present additional field and age data, and integrate them with previous studies to focus on timing, transport and offset along the Heart Mountain detachment surface. In particular, we evaluate the history of intrusion and dike emplacement, in the northeastern Absaroka volcanic province, especially in the vicinity of White Mountain and the Crandall volcanic center (Figure 4.1). $^{40}Ar/^{39}Ar$ age data from an ash-flow tuff, deposited after detachment faulting, and a monzogabbro intrusion which is interpreted herein as emplaced during faulting preclude the possibility of a catastrophic detachment event originating at the break-away fault. Field relationships of dikes and faults, and petrographic data from the monzogabbro intrusion and samples from the detachment horizon, indicate that motion associated with Heart Mountain faulting is linked to regional extensional faulting which occurred gradually and concurrently with volcanism.

FIELD RELATIONSHIPS AT WHITE MOUNTAIN

Fault and Intrusion Relationships

White Mountain, a block of faulted and deformed Ordovician Bighorn Dolomite, and overlying Mississipian Madison Limestone in the upper plate of the Heart Mountain detachment, is one of a few localities where the detachment fault surface is well exposed (Figure 4.1, location 1). The detachment is parallel to bedding in the Bighorn Dolomite (Figure 4.2). The carbonate strata are invaded by multiple intrusions, including a prominent biotite pyroxene monzogabbro dike approximately 6 meters wide that cross-cuts branching dikes that are primarily monzonitic and shoshonitic. Parts of the older dikes have sharp intrusive contacts with limestone while other sections exhibit cataclastic deformation, shearing, rotation, and boudinage (Figure 4.3). Dike rotation is accomplished by horizontal shearing and domino-style movement along local listric faults. The degree of cataclasis increases with rotation and with distance from the main body of monzogabbro. The monzogabbro itself exhibits minor deformation, in narrow microcrystalline shear zones parallel to strike and adjacent listric faults, and horizontal offset in fractured and microfaulted phenocrysts (Figure 4.4). Late thin vertical dikes, are undeformed and similar in composition to early deformed dikes, which they cross-cut. An elongate funnel-shaped monzonite intrusion, 120 meters across and 300 meters long, crops out on the west side of White Mountain. The long axis of this intrusion trends parallel to the late undeformed dikes.

Breccia exposed along the Heart Mountain detachment surface is dark gray with a 20 to 30 cm red oxidized zone at the upper contact. The fault breccia exhibits a cataclastic texture in which preferred orientation of clasts is subtle (Figure 4.5a). It includes clasts of sparry calcite, pisolitic carbonate, rounded friable siltsone fragments, ooid- and fossil- bearing carbonate rock fragments, angular volcanic rock

fragments, and delicately shaped droplets (0.5 to < 0.5 mm in diameter) of well preserved palagonitic mafic volcanic glass with phenocrysts of olivine, pyroxene, plagioclase and sanidine (Figures 4.5b, and 4.5c). Minerals also occur as individual euhedral and broken phenocrysts rimmed with brown glass. Quenched glassy textures within the Heart Mountain detachment horizon are similar to those observed in peperites (Cas and Wright, 1987). Droplets of volcanic glass, commonly surround or partially engulf comminuted sparry calcite grains.

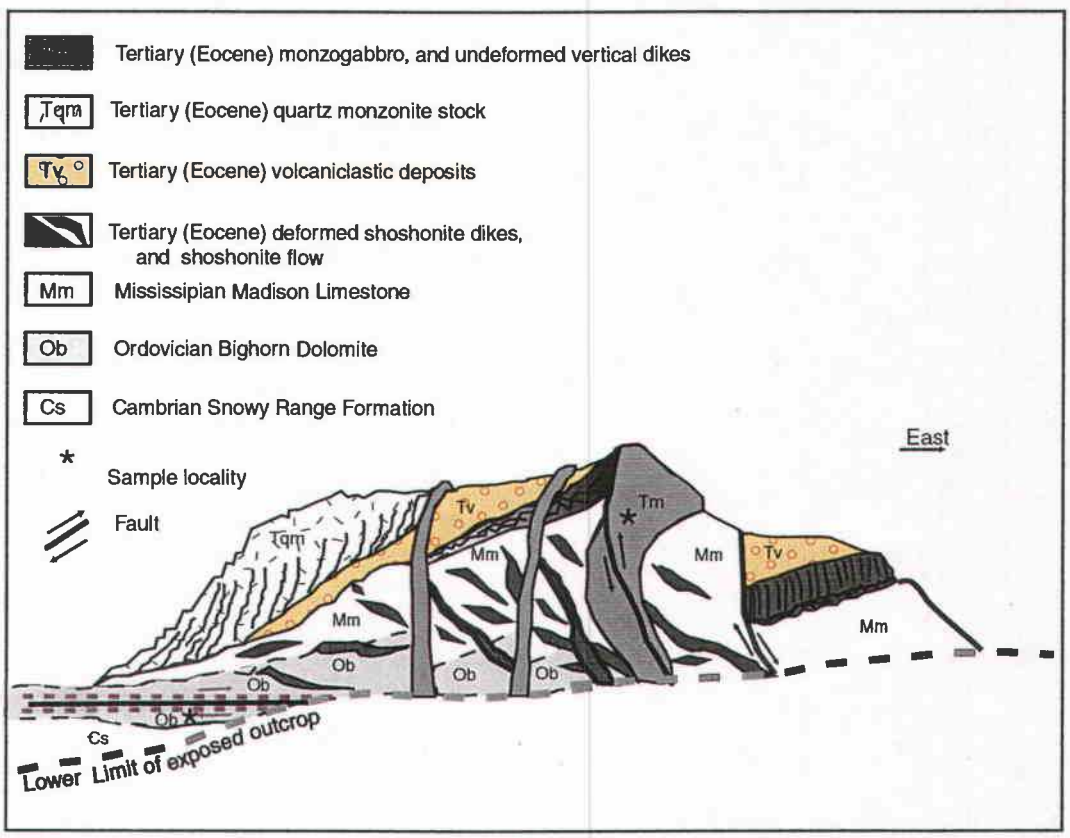

Figure 4.3. Idealized sketch of White Mountain, showing rotated and deformed early shoshonite dikes, sheared monzogabbro, late cross-cutting vertical dikes, and exposure of the detachment horizon and cataclastic breccia. White Mountain is also shown at location 1, Figure 4.1a. The length of the sketched exposure is approximately 2 km.

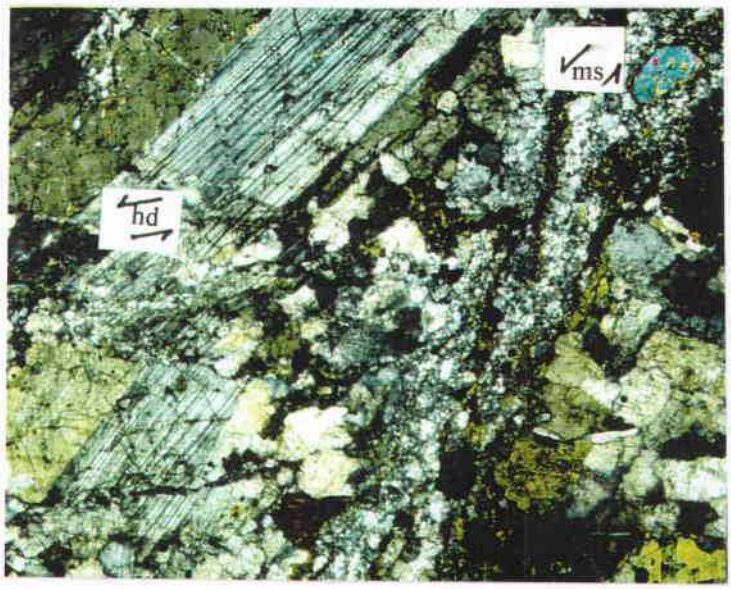

Figure 4.4. Photomicrograph of White Mountain monzogabbro. Arrows indicate microcrystalline shear (ms) parallel to listric faulting and dike orientation, and horizontal displacement (hd) along phenocryst microfractures, normal to dike orientation and shearing. (Crossed polarized light; Field of view = 5mm.)

Evidence for Thermal Effects

Strata within the upper plate of the detachment are not discolored or bleached near intrusive contacts. Metamorphic minerals were not found in the carbonate strata. Examination of thin sections from Bighorn Dolomite samples immediately above the detachment horizon provides no evidence of thermal modification. The Bighorn Dolomite and Madison Limestone are light colored in the upper plate at White Mountain, where these units have been fragmented into a jumbled mass. We interpret the color change to be related to low-temperature brecciation. The footwall of the detachment is too poorly exposed to make a direct assessment of the extent of metamorphism and intrusion below the detachment horizon.

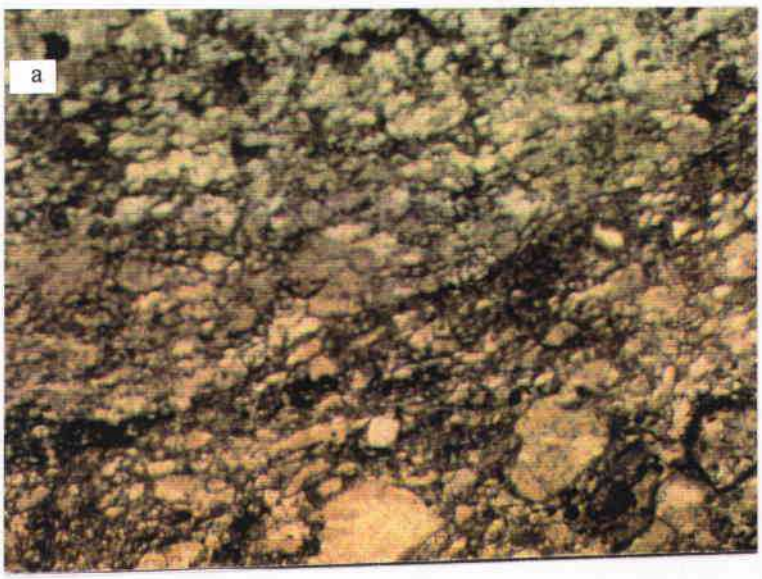

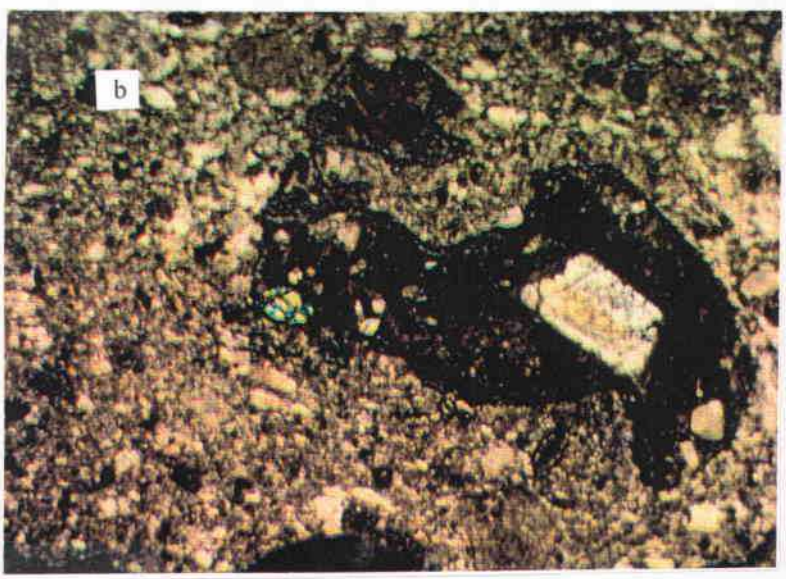

Figure 4.5. Photomicrographs showing breccia within the detachment horizon. The following textural features are shown: a) Cataclastic texture of detachment fault breccia b) Palagonitic glass with phenocrysts of olivine, pyroxene, and plagioclase, partially engulfing sparry calcite grain; (Crossed polarized light; Width of field = 5 mm)

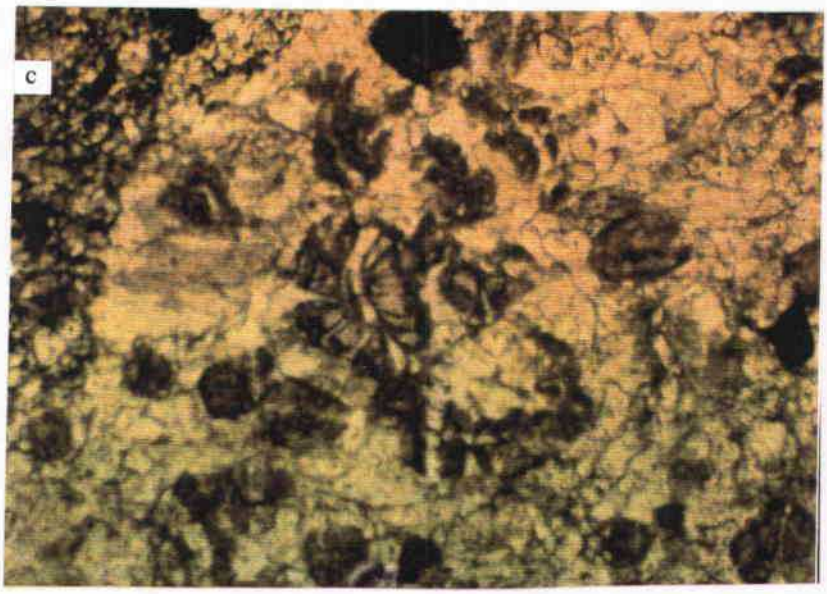

Figure 4.5. (Continued) Photomicrograph showing breccia within the detachment horizon. The textural feature shown is c) Carbonate rock fragment containing fossil fragments also from the detachment horizon; (Crossed polarized light; Width of field = 5 mm)

Interpretation of Field and Petrologic Features

Glass fragments with delicate, quenched outlines, and well preserved unfragmented phenocrysts are features which cannot survive significant cataclasis. The pristine condition of the volcanic glass suggests that significant recrystallization of volcanic components has not occurred. Pods and droplets of palagonitic volcanic glass within cataclastic fault breccia of the Heart Mountain detachment must have been entrained within the fault horizon after most of the fault motion and cataclasis of other lithologies occurred. The peperite texture suggests that the quenching occurred in the fault zone. We suggest that the source of the quenched magma was the monzogabbro, because it exhibits offset and horizontal shear consistent with emplacement during late stage faulting. Overall, field and lithologic associations suggest late syndeformational emplacement of the White Mountain monzogabbro.

Adjacent rotated and deformed dikes were intruded by the main body of monzogabbro during faulting(Figure 4.6). Early intruded dikes exhibit the greatest degree of cataclasis, and may have preceded fault movement. Successive dikes are less deformed because they were involved in less movement and rotation of fault blocks in the detached upper plate. Pockets of magma from the main intrusive body were entrained during later fault motion, and became distributed as small pods of glass within the fault breccia (Figure 4.5b).

The presence of quenched palagonitic glass with the texture of peperites and sparry calcite within the detachment horizon suggests that magma intruded into strata containing water. In addition, calcite veins and carbonate clastic dikes with fragments of Eocene volcanic rocks are commonly associated with, and intrude strata above and below the detachment horizon (Pierce, 1979: Templeton, 1995). These features suggest that heating and expansion of carbonate-saturated fluids migrated through fractures associated with the detachment. Heat from intruding magma into wet rock can produce pressure increases greater than 10 MPa, and causes migration of water away from the heat source (Delaney, 1982). Pressure increases associated with dike emplacement are greater in shallow environments (< 1km depth), and could act to mechanically weaken and fracture the upper plate, enhancing dike propagation and fault movement.

Rock fragments from samples within the detachment horizon that have diverse lithologies could have originated from above or below the detachment. These lithologies would not be present if the detachment occurred solely within the Bighorn dolomite as an isolated planar fault. Foreign rock fragments include fossiliferous and oolitic carbonate fragments which may have originated from the Snowy Range Formation, a stratigraphic unit immediately below the Bighorn Dolomite which contains ooids. Other rock fragments within the detachment horizon include angular igneous lithologies which may be derived from cataclastically deformed dikes, and siltsone fragments, which may be derived from the underlying Gros Ventre Formation. The inclusion of other lithologies within the detachment horizon suggests that faulting may involve units above and below the Bighorn dolomite, or that associated listric faults cross-cut the detachment horizon before lateral motion along the detachment had ceased.

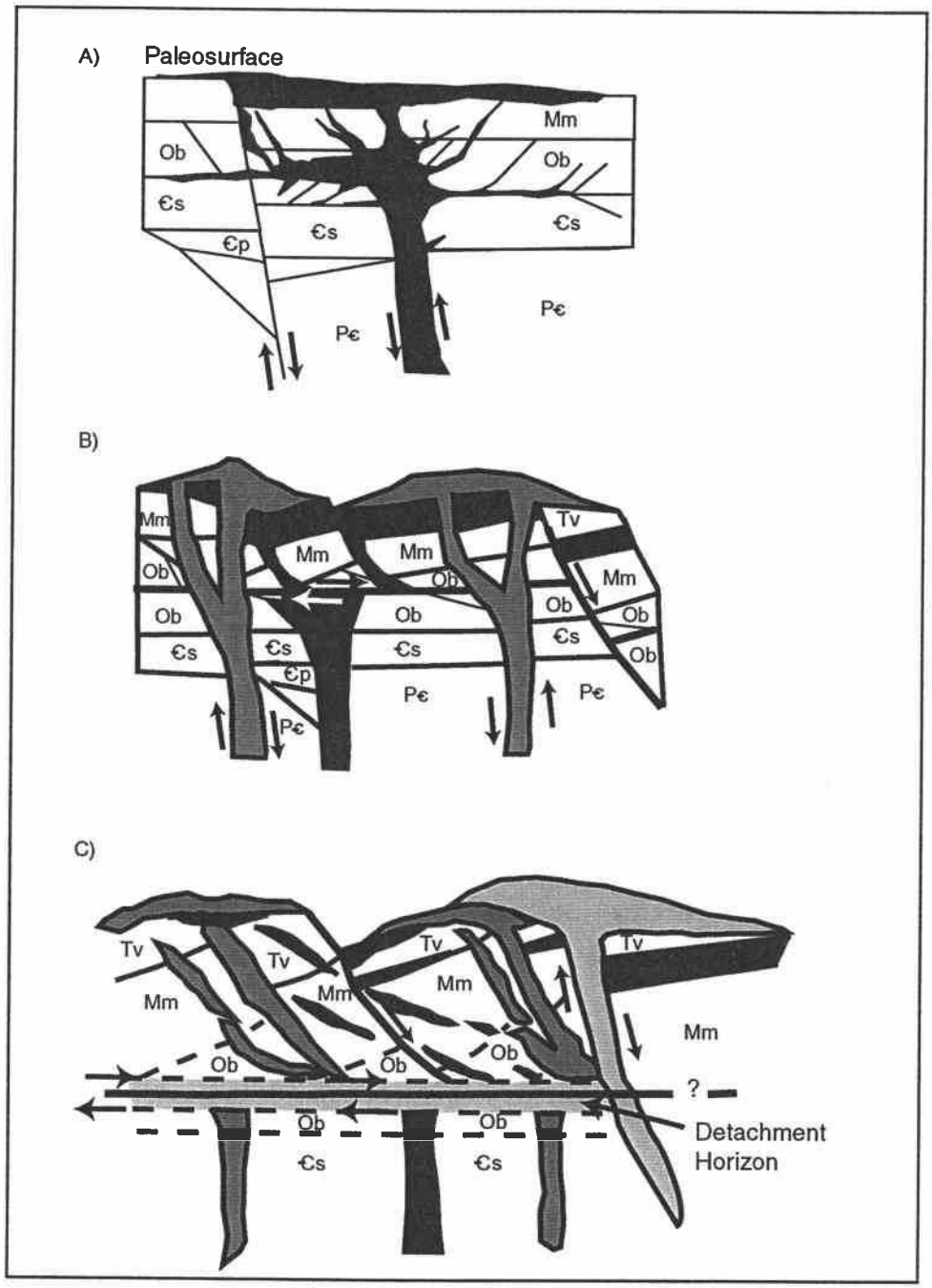

Figure 4.6. Proposed sequence of intrusion and deformation at White Mountain based on interpretation of field and lithologic relationships. a) Dike emplacement along fault. (Fractures enhanced by expansion of meteoric water.) b) Lateral displacement of detachment in fractured Bighorn Dolomite, continued dike emplacement and normal faulting. c) Continued faulting, rotation and boudinage of earlier dikes.

REGIONAL DIKE AND FAULT RELATIONSHIPS

Observations

Dikes and faults within the area of the Heart Mountain detachment mimic the regional pattern. Radial arrays of dikes are typical of volcanic edifices in the Absaroka Volcanic Province in general, but are largely absent north of the Sunlight volcanic center. Three prominent sets of dike and fault orientations occur (Figure 4.7). Two sets, N 45° E and N 30° W to N 40° W, exhibit cross-cutting relationships, and overlap one another temporally. The northeast-striking set of dikes includes the White Mountain monzogabbro, and are best exposed near Timber Creek and White Mountain (Figure 4.1). Field reconnaissance shows that they are more common than published maps suggest. They are most numerous parallel to and in a direct line with a prominent normal fault near Crandall Creek. The northeast strike of these dikes is normal to the transport direction of the Heart Mountain detachment inferred by Hauge (1993). The second northwest-striking set of dikes crops out between White Mountain and the north fork of Crandall Creek, and is parallel to the Clarks Fork normal fault, and other normal faults in the region. A few dikes of this set strike parallel to nearby normal faults (Figure 4.1). Both sets of dikes and faults cross cut each other, and exhibit rotation and displacement by faulting. A third set of vertical dikes strikes north (N 10°W to N 10° E) and cross cuts all others. These are especially numerous in the vicinity of Windy Mountain, northwest of White Mountain. These dikes are parallel to prominent normal faults which are best exposed west and northwest of Windy Mountain. North-south normal faults in Cambrian and Precambrian strata below the detachment fault, particularly in the Russel Peak and Windy Mountain vicinity have been interpreted as not related to deformation above the detachment horizon (Pierce and Nelson, 1971) although they exhibit the same strike and sense of offset as that between volcanic and Paleozoic units in the upper plate (Locality 2, Figure 4.1).

Faults and dikes exposed above and below the detachment horizon exhibit the same orientation (Figure 4.7). The remarkable coincidence of these features illustrates that deformation seen exposed above the detachment horizon is related to the same stress regime as footwall deformation. The style of intrusion and deformation changes upward: dikes and faults in the upper plate are more numerous. More than 100 dikes on Windy Mountain are parallel to normal faults, and many more occur northward in the Crandall Creek area. Increased fragmentation and dike propagation in the upper plate may be at least partly due to lithologic differences between hanging wall and footwall rocks. The footwall is structurally dominated by Precambrian granite, while the hanging wall contains weaker thinly bedded Paleozoic carbonate strata and poorly consolidated, interlayered volcaniclastic debris and lava flows.

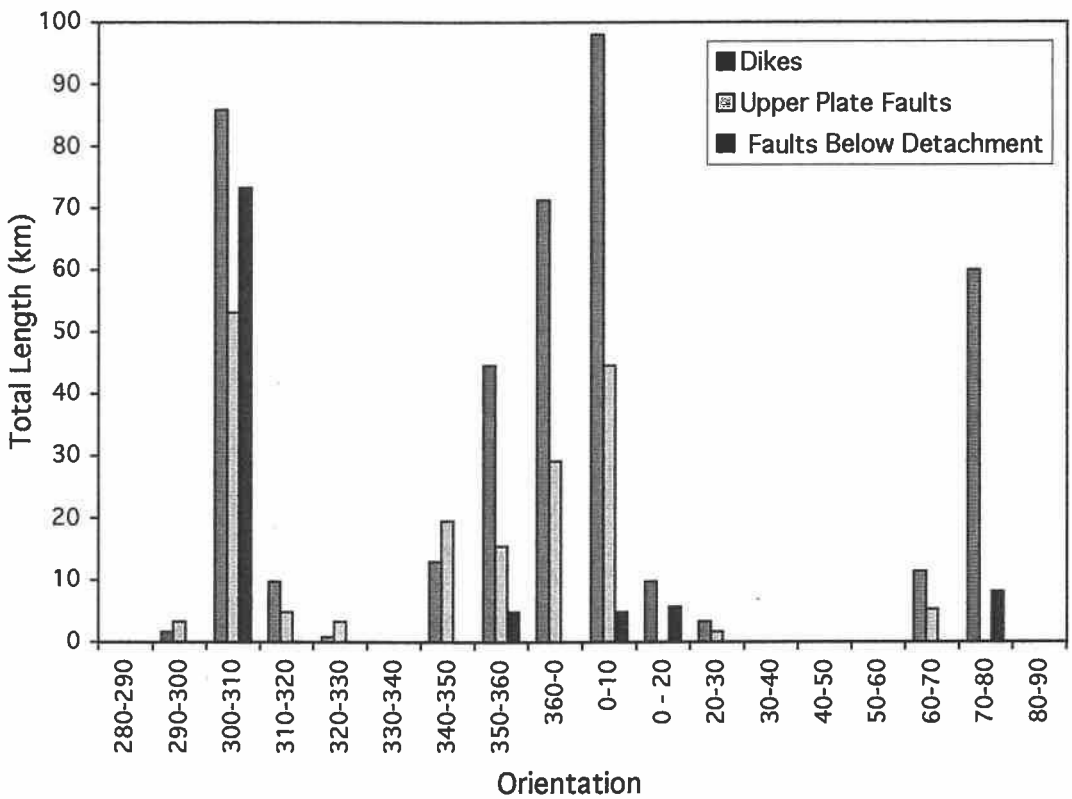

Figure 4.7. Orientation of faults and dikes of the northeastern Absaroka volcanic Province, above and below the Heart Mountain detachment.

Interpretation of Dike and Fault Relationships

Dikes and other intrusive features in the area surrounding White Mountain exhibit orientations parallel to structural features, which suggest that emplacement of magma was influenced largely by the same regional stress field that governed faulting. Multiple generations of dikes, each with the same orientation as nearby faults, both above and below the Heart Mountain detachment horizon, is strong evidence that deformation in the upper and lower plate are linked. In addition, uplift and exposure of Paleozoic fault blocks occurred preferentially in regions where the total volume of intrusions are highest, such as White Mountain, Windy Mountain, Pilot Peak, and the Crandall volcanic center, which implies that magma emplacement from below produced complex horst-like structures.

The clear spatial relationship of dikes parallel to normal faults, documents that extension occurred coeval with volcanism. Faults exhibit cross-cutting relationships which suggest that motion occurred during more than one interval. During the Eocene, the competent Precambrian Beartooth block, to the northeast of the Heart Mountain fault zone was strusturally high (Foose, 1961; and Simons et. al., 1979). This is consistent with the northward decrease in deformation observed in this study. Field data suggest that north-south trending dikes are less numerous to the north in comparison to those south of the Crandall Creek. In addition, sinistral offset along the prominent NE-SW fault along Crandall and Timber Creeks is coincident with the southern edge of the Beartooth block (Figure 4.8).

The lack of rotation of young dikes exposed in the upper plate suggests that significant post-dike lateral transport above the detachment surface is unlikely. In addition, undeformed vertical dikes and normal faults which formed earlier than deformation associated with the Heart Mountain detachment, recognized by Pierce (1963, 1973) as Reef Creek faulting, are unlikely to be preserved subsequent to significant horizontal displacement of the upper plate.

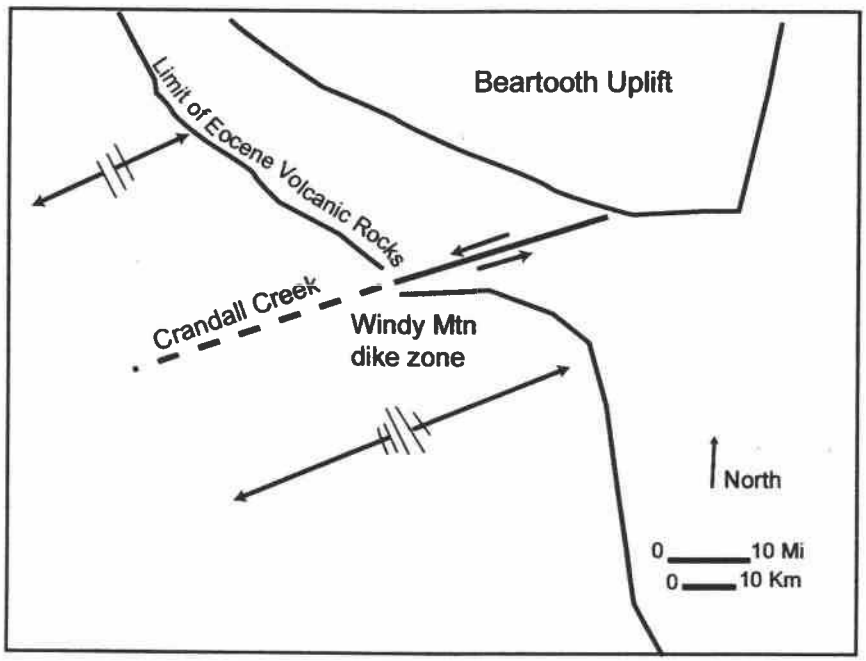

Figure 4.8. Schematic diagram showing differential extension and rotation, and orientation of faults and dikes adjacent to the southern edge of the Beartooth plateau.

AGE RELATIONSHIPS

Observations

Age data from two localities are used to constrain the timing of deformation at the detachment at White Mountain, and its relationship to other structural and igneous features (Table 4.1; Figure 4.9). The first sample is from an ash-flow tuff, mapped as part of the Langford Formation, located above the break-away of the detachment (Pierce et al., 1973, Figure 4.1, locality 3). It is a flat-lying unit at the top of the stratigraphic sequence exposed west of the Crandall volcanic center, and is interbedded with trachyandesite flows which post-date the Abiathar break-away

(Pierce, 1987, 1989; Nelson and others, 1980; Tokarski and others, 1994). $^{40}Ar/^{39}Ar$ analysis of a biotite from this tuff yields a plateau age of 50.01±0.14 Ma. These data set an upper limit to the age of faulting associated with the break-away, which must have occurred prior to deposition of undeformed overlying units. The second set of age data is from the White Mountain Monzogabbro which shows evidence of emplacement and deformation during faulting. This intrusion has an $^{40}Ar/^{39}Ar$ age of 48.21±0.05 Ma (from biotite). Therefore, break-away faulting predates the age of dikes deformed by detachment faulting at White Mountain.

Interpretation

The age difference between post-break-away deposits and intrusions in the hanging wall of the detachment precludes the possibility of detachment and motion of the Heart Mountain fault as a single catastrophic event. Including errors in $^{40}Ar/^{39}Ar$ ages (2 sigma) between break-away faulting and the last period of deformation at White Mountain, the period of time between break-away of the detachment and late stage faulting is at least 1.3 to 1.8 million years. Previous workers have interpreted the monzogabbro intrusion, dikes, and listric faults in the upper plate as features truncated by detachment faulting (Nelson and Pierce, 1971; Nelson, 1986; Hauge, 1985, 1990; Beutner and Craven, 1996). This interpretation implies that intrusion of monzogabbro predates detachment motion at this locality, that faulting at White Mountain is younger than 48.2 Ma. These models require that the difference between break-away faulting and detachment fault motion is greater than the age difference between both volcanic units. Alternatively, we interpret intrusion and deformation of the monzogabbro as features related to and linked with detachment motion, because of horizontal shearing within the dike, and the relationship of dike and fault orientation to detachment features. If intrusion of White Mountain monzogabbro intruded after most of the fault movement was completed, as we have suggested, then the the last period of detachment faulting occurred 48.5 Ma, and the time span associated with detachment faulting is $\geq$ 1.5 Ma.

Table 4.1. Age data from samples of the northern Absaroka volcanic province.

Sample No.	Rock Type	Mineral Type	Age (Ma) and error	Character of age spectrum
HHMD17B-95	trachyte ash-flow tuff	Biotite	50.01±0.14	Plateau date; 64.8% $^{39}Ar_K$
HMD4-96	monzogabbro intrusion	Biotite	48.21±0.08	Plateau date; 80.6% $^{39}Ar_K$

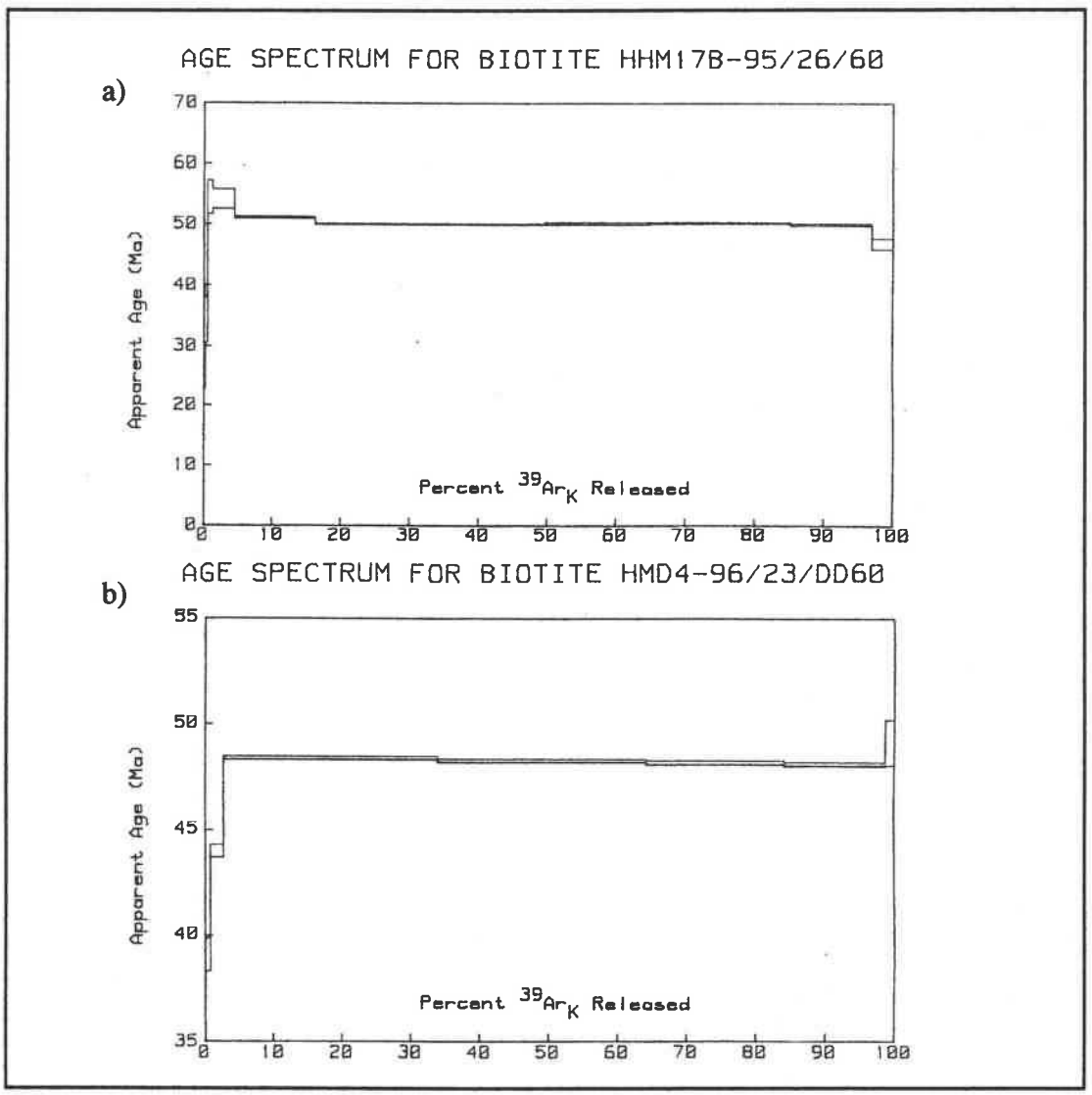

Figure 4.9. $^{40}Ar/^{39}Ar$ age spectra for samples from the northeastern Absaroka volcanic province: a) Biotite from ash-flow tuff which post-dates and overlies the Abiathar break-away fault, b) Biotite from the White Mountain monzogabbro intrusion, interpreted as synchronous with late stage detachment motion.

DISCUSSION

Features at White Mountain suggest that dike emplacement, faulting, and deformation occurred over a protracted period of time, early in the history of the Absaroka Volcanic Province. Previous studies by Hauge (1982, 1990, 1993) indicating that the Heart Mountain detachment moved as a gradually extending mass, are consistent with much of the data presented here. On the north side of White Mountain, intrusion of numerous dikes represented extension estimated to be more than 50% (Hauge, 1982). Because the lower plate is not well exposed, there is no clear evidence that many intrusive bodies and faults do not extend into strata below the detachment. The presence of fossil- and ooid-bearing fragments within the fault breccia, as well as volcanic glass, which are not present in the Bighorn Dolomite, implies that movement related to detachment faulting was not isolated to a bedding horizon within that formation, but involved other units, such as the Snowy Range Formation or Pilgrim Limestone. The trend of dikes and extensional features in the upper plate strongly correlate with those exposed in the lower plate, suggesting that many faults and dikes cut the detachment (Figure 4.1 and 4.7). Rapid and catastophic lateral movement of the upper plate should have produced chaotic rotation of vertical dikes if they are allochthonous truncated features of the detached hanging wall.

The presence of volcanic glass and rock fragments in cataclastic breccia within the detachment horizon has also been noted at other localities where the Heart Mountain fault is overlain by volcanic strata (Tokarski and others, 1994; and Pierce and others, 1991). These earlier studies suggest that the volcanic glass is a tuff deposit, based on a model whereby faulting occurred before deposition of overlying volcanic strata. However, pods of volcanic glass surround carbonate fragments within the breccia suggesting that a magma intermingled with and surrounded the carbonate fragments. Moreover, igneous rock fragments and volcanic glass at White Mountain are found within a portion of the detachment horizon where carbonate strata of the hanging wall overlies carbonate strata of the footwall and no exposure to

surficial volcanic rocks occurs. The glass is therefore interpreted as being derived from magma that fed dikes rather than from the deposition of a tuff subsequent to faulting. Based on the unfragmented nature of the pods of volcanic glass, related dikes must have occurred late in the sequence of events.

Pre-existing Laramide reverse faults may have acted as conduits for magma rising to the surface. The bedding horizon within the Bighorn Dolomite that forms the principal detachment surface is a permeable horizon which probably contained a significant amount of meteoric water, this is consistent with the presence of palagonitic volcanic glass, low $\partial^{18}O$ and low$\partial^{13}C$ values of Templeton and others (1995), and the presence of carbonate dikes associated with the detachment horizon (Pierce, 1979). Heat from intruding magma probably interacted with meteoric water, which would release mechanical energy during dike emplacement and may have acted to enhance brittle deformation, fracturing the carbonate strata and producing a weak horizon along which faulting could occur. Lateral movement and listric-style faulting in the upper plate was most likely enhanced by magma injection. These faults and fractures provided conduits for continued intrusion of magma. Where intrusions are most numerous, magma tended to inflate the Paleozoic section, producing uplifts.

The strong correlation between the orientations of normal faults and dikes with regional structural trends suggests that dike emplacement took place during crustal extension. Both listric and normal faults have been widely recognized and mapped across the Absaroka Volcanic Province, although they have not always been acknowledged as products of regional extension (Wilson, 1936; Lammers, 1939; Dunrud, 1962; Fisher, 1966, 1972; Chadwick, 1969; Reid and others, 1975; Montagne and Chadwick, 1982; Sundell, 1982, 1990; Barnes, 1985; Smedes and others, 1989). Although most of the normal faulting west of the break-away zone has been related to Miocene and younger Basin and Range faulting, the end of Laramide compression between $40^{0}30'$N and 49^{0} N occurred between 54 and 51 Ma (Constensius, 1996). Regional extension has been documented as occurring as early as 49 Ma to 50 Ma (Janecke, 1992; Hodges and Applegate, 1993; Janecke and Snee, 1993; Janecke, 1994; Costensius, 1996; M'Gonigle and Dalrymple, 1996). Although additional field and analytical data is required to be conclusive, the data presented here suggests that Eocene extension may have begun prior to 50 Ma.

CONCLUSIONS

1) Faulting and rotation is more severe in dikes at White Mountain which were emplaced relatively early. These are cross-cut by dikes and intrusions which are less deformed. This suggests that faulting and dike emplacement at White Mountain are linked, and took place as a gradual, rather than catastrophic, process.

2) Coincident orientation of faults and dikes above and below the Heart Mountain detachment horizon suggest that they are related to the same extensional stress.

3) $^{40}Ar/^{39}Ar$ ages constrain the age of the faulting at the Abiathar break-away to >50.01± 0.14 Ma, and that of intrusion associated with detachment faulting at White Mountain to ≤48.21 ±0.08 Ma, which precludes the possibility of correlating deformation and detachment faulting at White Mountain to a catastrophic break-away event.

4) Petrographic textures associated with fault breccia from the detachment horizon at White Mountain include delicate fragments of quenched volcanic glass, siltstone, volcanic rock fragments, and carbonate fragments containing fossil fragments and ooids, which cannot be derived from Bighorn Dolomite, the principal unit of the detachment horizon. Quenched droplets of volcanic glass could not survive significant lateral displacement and cataclasis. Therefore, intrusion associated with the volcanic glass must have occurred late in the sequence of deformation. These petrographic textures are consistent with observations made by Tokarski and others, 1996; and Pierce and others, 1991 at other sample localties along the Heart Mountain detachment.

REFERENCES CITED-4

Barnes, B. (1985) Stratigraphy of Eocene volcaniclastic rocks, Dick Creek Lakes Quadrangle, Wyoming, University of Wyoming M.S. Thesis, p. 103, 118-127.

Beutner E.C., and Craven, A. E. (1996) Volcanic fluidization and the Heart Mountain detachment, Wyoming; Geology, v. 24, no. 7, p. 595-598.

Cas, R.A.F., and Wright, J.V. (1987) Volcanic Successions, Modern and Ancient; Chapman and Hall, London, Glasgow, New York, Tokyo, Melbourne, Madras; p. 43.

Constensius, K.N. (1996) Late Paleogene extensional collapse of the Cordilleran foreland fold and thrust belt: GSA Bulletin, v. 108; no. 1, p. 20-39.

Dunrud, R. (1962) Volcanic rocks of the Jack Creek area, southeastern Absaroka Range, Park County, Wyoming: M.S. Thesis, University of Wyoming, p. 64.

Fisher, F.S. (1966) Tertiary Intrusive Rocks and Mineralizationin the Stinkingwater Mining Region, Park County, Wyoming; University of Wyoming Ph.D. Thesis, p. 88-89.

Fisher, F.S. (1972) Tertiary Mineralization and Hydrothermal Alteration in the Stinkingwater Mining Region, Park County, Wyoming; Geological Survey Bulletin 1332-C, p. C9.

Hauge, T.A. (1993) The Heart Mountain detachment, northwestern Wyoming: 100 years of controversy: *in* A.W. Snoke, J.R. Steidmann, and S.M. Roberts, eds., Geology of Wyoming: Geological Survey of Wyoming Memoir No. 5, p.530-571.

Hauge, T.A. (1990) Kinematic model of a continuous Heart Mountain allochthon: Geological Society of America Bulletin, v. 102, p. 1174-1188.

Hauge, T.A. (1985) Gravity-spreading origin of the Heart Mountain allochthon, northwestern Wyoming: Geological Society of America Bulletin, v. 96, p. 1440-1456.

Hauge, T.A. (1982) The Heart Mountain detachment fault, norhwest Wyoming: Involvement of Absaroka volcanic rock; Wyoming Geological Association Guidebook, Thirty-Third Annual Field Conference, p. 175-179.

Hodges, K.V. and Applegate, J.D. (1993) Age of Tertiary extension in the Bitterroot metamorphic core complex, Montana and Idaho: Geology, v. 21, p. 161-164.

Janecke, S.U. (1992) Kinematics and timing of three superposed extensional systems, east central Idaho: evidence for an Eocene tectonic transition: Tectonics, v. 11, p. 1121-1138.

Janecke, S.U., and Snee, L.W. (1993) Timing and Episodicity of Middle Eocene Volcanism and Onset of Conglomerate Deposition, Idaho; Journal of Geology, vol. 101, p. 603-621.

Janecke, S.U. (1994) Sedimentation and paleogeography of an Eocene to Oligocene rift zone, Idaho and Montana: Geological Society of America Bulletin, v. 106, p. 1083-1095.

Malone, David H. (1995) Very large debris-avalanche deposit within the Eocene volcanic succession of the northeatsrn Absaroka Range, Wyoming: Geology, v. 23, no. 7, p. 661-664.

M'Gonigle, J.W., and Dalrymple, G.B. (1996) $^{40}Ar/^{39}Ar$ Ages of Some Challis Volcanic Group Rocks and the Initiation of Tertiary Sedimentary Basins in Southwestern Montana; U.S, Geological Survey Bulletin 2132, 17 p.

Montagne, J., and Chadwick, R.A. (1982) Cenezoic history of the Yellowstone Valley between Yellowstone Park and Livingston, Montana; Wyoming Geological Association Guidebook, Thirty-Third Annual Field Conference, p.31-51.

Nelson, W.H. (1986) White Mountain, northwestern Wyoming, a pseudo-volcanic neck; Montana Geological Society YBRA Field Conference Guidebook, p.165-168.

Nelson, W.H., Prostka, H.J. and Williams, F.E. (1980) Geology and Mineral Resources of the North Absaroka Wilderness and Vicinity, Park County, Wyoming; Geological Survey Bulletin 1447, 101 p.

Pierce, W.G. (1980) The Heart Mountain break-away fault, northwestern Wyoming; Geological Society of America Bulletin, Part 1, v. 91, p. 272-281.

Pierce, W.G. (1979) Clastic Dikes of Heart Mountain Fault Breccia, Northwestern Wyoming, and Their Significance: U.S. Geological Survey Professional Paper 1133, 25p.

Pierce, W.G. (1973) Relation of volcanic rocks to the Heart Mountain Fault; Wyoming Geological Association Guidebook, Thirty-Third Annual Field Conference, p. 181-212.

Pierce, W.G. (1973) Principal Features of the Heart Mountain Fault and the Mechanism Problem: *in* K.A. De Jong, and R. Scholten, eds.: Gravity and Tectonics, p. 457-471.

Pierce, W.G. (1968) Tectonic denudation as exemplified by the Heart Mountain fault, Wyoming; in Orogenic belts: 23rd International Geologic Congress, Prague, Czechoslovakia Report, Section 3, Proceedings, p. 191-197.

Pierce, W.G. (1957) Heart Mountain and South Fork detachment thrusts of Wyoming; American Association of Petroleum Geologists Bulletin, v. 41, no. 4, p. 591-626.

Pierce, W.G. (1941) Heart Mountain and South Fork Thrusts, Wyoming: American Association of Petroleum Geolgists Bulletin, v. 25, p. 2021-2045.

Pierce, W.G., Nelson, W.H., Tokarski, A.T., Piekarska (1991) Heart Mountain, Wyoming, detachment lineations: Are they in microbreccia or volcanic tuff?; Geological Society of America Bulletin, v. 103, p. 1133-1145.

Pierce, W.G., and Nelson, W.H. (1971) Geologic Map of the Beartooth Butte quadrangle, Park County, Wyoming; U.S. Geological Survey Geologic Quadrangle Map GQ-935.

Smedes, H. W., M'Gonigle, J.W., and Prostka, H.J. (1989) Geology of the Two Ocean Pass quadrangle, Yellowstone National Park, Wyoming; U.S. Geological Survey Quadrangle Map GQ-1667.

Sundell, K.A. (1990) Sedimentation and Tectonics of the Absaroka Basin of northwestern Wyoming; Wyoming Geological Society Guidebook, Forty-First Annual Field Conference, p.105-122.

Templeton, A.S., Sweeney, J.S., Jr., Manske, H. Tilghman, J.F., Calhoun, S.C., Violich, A., and Chamberlain, C.P. (1995) Fluids at the Heart Mountain fault revisited: Geology, v. 23, no. 10, p. 929-932.

Tokarski, A.K., Pierce, W.G., Piekarska, E., Nelson, W.H. (1994) A sedimentary origin for "microbreccia" associated with the Heart Mountain detachment fault; Contributions to Geology, University of Wyoming, v. 30, no. 2, p. 157-162.

SUMMARY AND CONCLUSIONS

The Crandall, Hyalite, Rampart and Ishawooa volcanic centers of the Absaroka volcanic province are built upon broad platforms of fissure-fed absarokite, shoshonite, and trachyandesite flows. Absarokites are fine grained and sparsely porphyritic, with phenocrysts of olivine and clinopyroxene, and have apatite as an accessory phase in a groundmass of sanidine and plagioclase. Shoshonites are similar, but have little or no olivine, and include augite which may have a substantial aegerine component. Trachyandesites contain plagioclase and augite ± olivine and orthopyroxene. These flows are cross cut by clustered dikes and intrusions which define the volcanic centers themselves.

The Rampart and Ishawooa volcanic centers exhibit the characteristics of stratovolcanoes, with interbedded flows and volcaniclastic strata that exhibit primary dips away from central intrusions. Dikes of variable composition are oriented radially to these intrusions, which are dominantly dacite and banakite. The Crandall and Hyalite volcanic centers have a broader morphology, resembling shield volcanoes. Dikes associated with these volcanic centers tend to be more mafic than at Ishawooa and Rampart, and exhibit strong preferred orientations with regional structural fabrics.

Overall, age relationships based on $^{40}Ar/^{39}Ar$ data from individual volcanic centers and province-wide correlations define a north to south age in progression from 53 to 43.5 Ma. The ages of both intrusions and associated ash-flow tuffs of volcanic centers exhibit a significant overlap in age, with widespread magmatism from 50 to 48 Ma.

The Crandall volcanic center is the oldest of those studied in detail. Early mafic alkaline lava flows are older than 50.0 Ma, constrained by the age of an interbedded ash-flow tuff at the top of the stratigraphic sequence. Intrusions within

the volcanic center are slightly younger; one has an age of 49.1 Ma. The Rampart, Ishawooa and Hyalite volcanic centers erupted after igneous activity at the Crandall volcanic center had ceased. The age of the Rampart volcanic center, from $\leq$ 47.7 Ma to $\geq$ 46.6 Ma, is constrained by the age of ash-flow tuff interbedded with lava flows, a cross-cutting banakite intrusion, and paleomagnetic data (Pruss, 1975). Magmatism at the Ishawooa volcanic center is older than 46.8 Ma, constrained by the age of a banakite dike that cross-cuts highly alkaline absarokite flows, which themselves are at least 48 Ma, based on field relationships and paleomagnetic data (Shive and Pruss, 1970). Flows of the Hyalite volcanic center are younger than 48 Ma, based on an estimate of their stratigraphic position relative to a well-developed unconformity. Eruptive activity in the vicinity of the Kirwin volcanic center of the southwestern volcanic belt continued for 3 million years after most mafic alkaline magmatism had ended, producing dacitic and rhyolitic magmas until 43.7 Ma.

The duration of eruptive activity of the Absaroka volcanic province is less than 10 million years (from 53 to 43.5 Ma) and covered more than 25,000 km^2. During this period more than 23,000 km^3 of material was produced, but more than 60% of the total volume erupted between 50 and 48 Ma. The estimated average overall eruption rate of 2.5 x 10^{-3} km^3/yr is essentially the same as the present Yellowstone-Snake River Plain system (c.f., Crisp, 1984). The average estimated magma output rate is an order of magnitude greater compared to magmatic activity of the Central Andes since the Miocene. The differences in duration, volume, and intensity of magmatic activity between the Absaroka volcanic province and the classical arc-type magmatism of the Central Andes demands reassessment of the arc model for Absaroka volcanism.

In addition to the differences in magma output rate of the Absaroka volcanic province to that of a typical subduction-related arc, this study finds no evidence of arc-like spatial zonation. Differences in ages and major element chemistry previously used to define separate belts of volcanic centers do not exist. There is no spatial segregation of alkaline rock types. Mafic (<53% SiO_2, >4% MgO) compositions are more alkaline than typical of arcs and characterize the early eruptive products at all of the volcanic centers. Eruptive products diversify and include more silicic compositions as magmatism continues. Sampled rock types encompass a province-

wide compositional spectrum from basanite to rhyolite; however, individual volcanic centers exhibit a more limited range, from absarokite to dacite. Mafic rocks are compositionally diverse, but those from each of the volcanic centers are distinct in composition and mineralogy.

Mafic compositions are those least affected by crustal processes and therefore the most useful for identifying mantle contributions. Mafic rocks from each of the volcanic centers, and a basanite flow exhibit light rare earth element enrichment, and have low heavy rare earth element concentrations. Mafic end-member compositions from the Ishawooa and Rampart volcanic centers, which are nepheline-normative, are the most light rare earth element enriched, while quartz-normative samples from the Hyalite volcanic center have the flattest rare earth element pattern. Mafic compositions from the Crandall volcanic center are olivine- and hypersthene-normative and have distinctly lower heavy rare earth element concentrations. Mafic lavas from each group have distinct patterns of trace element composition (Chapter 2). The basanite is distinctly richer in Ta, Zr and Ti, and has trace element abundances similar to an enriched ocean island basalt. Mafic compositions of the Crandall volcanic center have trace element characteristics which suggest that they have amphibole and garnet in the source region, because they have low concentrations of high field strength elements, low heavy rare earth element concentrations, and high Ba/Rb and K/Rb. Mafic end member compositions from the Crandall volcanic center can be approximated by modeling different degrees of partial melting of a garnet peridotite containing amphibole. Nepheline normative samples from both Ishawooa and Rampart may be considered a single group, because they are similar in composition. These rocks are distinctly enriched in Rb, and have low K/Rb, high Rb/Sr, Ta/Yb and Ce/Yb. These trace element characteristics, combined with AFC calculations, suggest that they are derived from partial melting of a source containing phlogopite by a magma similar in composition to the sampled basanite. Trace element characteristics of the Hyalite volcanic center, such as low Ce/Yb and less pronounced light rare earth element enrichment suggest they are derived from a higher degree of partial melting. Mafic Hyalite compositions also have distinctly higher Th/U, with lower U, which suggests they have a depleted mafic lower crustal component.

Mafic absarokite and shoshonite of the Absaroka volcanic province are characterized by low $^{87}Sr/^{86}Sr$ and low $^{143}Nd/^{144}Nd$, which plot in the lower left hand quadrant of the Nd-Sr isotope diagram, and have more extreme values than other alkaline rocks of the Archean Wyoming Province. The most mafic sample from the Crandall volcanic center, (with 8.3% MgO and 425 ppm Cr) has the lowest $^{143}Nd/^{144}Nd$ (0.51162) and the lowest $^{87}Sr/^{86}Sr$ (0.70431) of samples from volcanic centers. $^{206}Pb/^{204}Pb$, $^{207}Pb/^{204}Pb$, and $^{208}Pb/^{204}Pb$, for mafic samples from the Crandall, Ishawooa, and Rampart volcanic centers lie on a trend line between Smokey Butte lamproites of lithospheric mantle composition, and kimberlites of the Missouri Breaks, suggesting they are derived from binary mixing of lithospheric mantle and asthenospheric sources. The low Nd and Sr and Pb isotopic compositions indicate that mafic compositions from volcanic centers have distinct, ancient, enriched sources. For the Crandall, Ishawooa and Rampart volcanic centers, these are interpreted as distinct contributions from enriched subcontinental lithospheric mantle (Chapter 3). Because the source enrichment is old, isotopic compositions do not suggest that source enrichment is derived from subduction of a young ($\leq$30 Ma) Farallon oceanic plate, as described in popular tectonic models.

Less enriched lavas of Hyalite volcanic center have isotopic compositions distinct from other volcanic centers, and similar to intermediate and silicic samples from the Absaroka volcanic province, with higher $^{87}Sr/^{86}Sr$ (0.70709) and low $^{143}Nd/^{144}Nd$ (0.51161). Higher $^{207}Pb/^{204}Pb$ and $^{208}Pb/^{204}Pb$ of Hyalite volcanic center samples, as well as silicic ash-flow tuff, overlap with the field defined by Mesozoic and Tertiary plutons of the Wyoming Province which have been interpreted as melts derived from upper and lower crust (Gunn, 1991). The isotopic composition of the Hyalite volcanic center source, as well as its less enriched character, suggest it contains a substantial crustal component. Because Hyalite samples are less enriched than those from other volcanic centers, they may also be isotopically more sensitive to crustal assimilation.

A basanite flow has the highest $^{143}Nd/^{144}Nd$ (0.51278) and the lowest $^{87}Sr/^{86}Sr$ (0.70334) and is only slightly lower in $^{143}Nd/^{144}Nd$ than compositions of the Mantle Array. $^{206}Pb/^{204}Pb$, $^{207}Pb/^{204}Pb$, and $^{208}Pb/^{204}Pb$ of the basanite coincides with the field for ocean island basalts, as well as the field of kimberlites of the same

age and the same region from the Missouri Breaks, and indicate that it is of asthenospheric isotopic composition. Mafic nepheline-normative rocks of Ishawooa and Rampart lie in a field between the Crandall volcanic center samples and the basanite, with low $^{87}Sr/^{86}Sr$ (0.70444 - 0.70454) and intermediate $^{143}Nd/^{144}Nd$ (0.51180 - 0.51201). The isotopic composition of mafic lavas from Ishawooa and Rampart can be calculated as two component mixtures using Nd isotopic compositions of lithospheric mantle and asthenospheric mantle end members.

Trace element and isotopic compositions of mafic rocks indicate that they are derived from three sources. The basanite has characteristics of an enriched ocean island basalt source, whereas, mafic end-members from Crandall, Ishawooa and Rampart are derived from subcontinental lithospheric mantle. Hyalite volcanic centers are derived, in part, from depleted, old, deep crust. The contributions from these source components change with time. Magmatism before 47 Ma produces the majority of mafic alkaline rocks that have characteristics which indicate a subcontinental lithospheric mantle source. From 47 Ma to 43.5 Ma, when eruptive activity ends, most of the volcanism is silicic to intermediate in composition, but includes mafic Hyalite samples with a source contribution from the lower crust. Basanite, with an enriched asthenospheric composition also erupts at the end of Absaroka volcanic province volcanism.

The overall trend in isotopes suggests that magma is derived from progressively shallower sources, followed by a deep mantle source, which is consistent with models of lithosphere extension-related magmatism of McKenzie and Bickle (1988) and Harry and Leeman (1995). These models suggest that volatile-rich components are preferentially incorporated into the earliest melts. These are represented by samples derived from sources containing hydrous phases, such as the mafic end-members of the Crandall, Rampart, and Ishawooa volcanic centers. As extension proceeds the degree of partial melting increases, producing less enriched melts which reside at progressively shallower levels as the base of the lithosphere is heated, and thinning of the lithosphere continues. This later period of melting is represented by samples from the Hyalite volcanic center, as well as intermediate and silicic rocks from other parts of the Absaroka volcanic province, which reside and mix with continental crust. As extension proceeds and the lithosphere becomes

thinner, samples from deeper mantle sources, such as the basanite, may invade the surface (McKenzie and Bickle, 1988). Unless volatile constituents are replenished, the mantle will be come depleted in hydrous phases, and revert to dry melting conditions (Harry and Leeman, 1995). When this occurs, magmatism ceases.

The coincidence of dikes and extensional faults in the region of the Crandall volcanic center document concurrent magmatism and extension in the Absaroka volcanic province. An intrusion south of the Crandall center, in the vicinity of the Sunlight volcanic center, contains microcrystalline fault-parallel shear planes which suggest that it was emplaced during faulting related to the Heart Mountain detachment (Chapter 4). An $^{40}Ar/^{39}Ar$ age of 48.2 Ma for this intrusion, and field relationships, indicates that extensional faulting occurred during peak igneous activity. A second $^{40}Ar/^{39}Ar$ age from a 50.0 Ma ash-flow tuff which overlies and post-dates the Heart Mountain detachment fault indicates that 1) Heart Mountain detachment faulting, and associated shallow extension of the upper plate of the detachment occurred as a continuous process during volcanism, rather than as a catastrophic event, and 2) this extension began prior to 50 Ma, which is consistent with the earliest ages of documented extension in the northern Cordillera of Montana and Idaho. Normal faults which are exposed above the Heart Mountain detachment have strikes coincident with those exposed below the detachment and suggests that they are related to the same regional extension. The data further suggest that faults with coincident orientation above and below the detachment cross cut this structural feature. Middle Eocene extension in adjacent areas of the Cordillera, coeval with Challis volcanism in Idaho, begins at about 49-48 Ma (Janecke, 1992; Janecke et al, 1997). Similarly, documented extension of the Bitterroot metamorphic complex occurred from 48 to 46 Ma (Hodges and Applegate, 1993) However, extensional reactivation of thrust faults occurred as early as 50 Ma, concurrent with basin formation in western Montana in the region north of the Absaroka volcanic province (Constensius, 1996). These ages are similar to the timing of early extensional faulting during igneous activity in the Absaroka volcanic province.

Although magmatism in the Absaroka volcanic province begins prior to 50 Ma, models which describe and document extension related magmatism in the Basin and Range show that the inception of volcanism typically predates the peak of

extension (Gans and Bohrson, 1998). Gans and Bohrson (1998) document that during rapid extension magmatism is suppressed, and produces ponding of melts at lower to middle crustal levels. The similar style of extension and volcanism suggests that middle Eocene, as well as later Basin and Range extension are the products of active rifting. Extension and calc-alkaline volcanism in the northern Basin and Range of Nevada begins during the Eocene, as igneous activity in the Absaroka volcanic province and north of the Snake River Plain ends (Brooks et al, 1995; McGrew and Snee, 1994). The southward shift of volcanism may be related to well documented 42 Ma plate reorganization, although extension and volcanism prior to this event from British Columbia to Idaho and Montana also exhibits a general southward migration. The southward age progression in volcanism of the Absaroka volcanic province is consistent with this overall trend.

The age relationships and compositions of rocks from the Absaroka volcanic province indicate that no separate calc-alkaline and alkaline belts exist. Potassic alkaline volcanism occurred early at each of the volcanic centers. Magmatism at individual volcanic centers then evolves to include differentiated rocks with crustal assimilation. Isotopic and trace element compositions of mafic end-members indicate that melting was initially derived from subcontinental lithospheric mantle, with a larger contribution of ancient depleted lower crust with time. The basanite represents a separate enriched asthenopheric mantle source, as a late eruptive product. Magmatism at this and other middle Eocene volcanic fields occurred during a brief period, and over a broad region. The age and composition of rock types, which erupt far inland from the plate margin, do not have the characteristics of subduction-related magmatism. Instead, the eruption of potassic rocks which occurred early and for a brief period, suggests that magmatism in the Absaroka volcanic province is related to crustal extension.

BIBLIOGRAPHY

Armstrong, R.L. (1974) Geochronometry of the Eocene volcanic-plutonic episode in Idaho: Northwest Geology, vol. 3, p.1-15.

Armstrong, R.L. (1988) Mesozoic and Cenozoic magmatic evolution of the Canadian Cordillera: *in* Processes in Continental Lithospheric Deformation, S.P. Clark, B.C.Burchfiel, and J. Suppe, (eds.) GSA Special Paper 218, p. 55-91.

Armstrong, R.L., and Ward, P. (1991) Evolving geographic patterns of Cenozoic magmatism in the North American Cordillera: The temporal and spatial association of magmatism and metamorphic core complexes: Journal of Geophysical Research, vol. 96, p.13201-13224.

Baedecker, P.A., and McKown, D.M. (1987) Intstrumental neutron activation analysis of geochemical samples: *In* Methods for Geochemical Analyses, Baedecker, P.A., (ed.) US Geological Survey Bulletin 1770, Chapter H, p.H1-H14.

Baker (1987) Central Montana Alkalic Province: Critcal Review of Laramide Plate Tectonics Models that Extract Alkalic Magmas from Abnormally Thick Precambrian Lithospheric Mantle:

Barnes, B.K. (1985) Stratigraphy of Eocene volcaniclastic rocks, Dick Creek Lakes quadrangle, Wyoming: Iowa State University M.S. Thesis, Ames, 221p.

Berger, B.R., and Snee. L.W. (1992) Thermochronological constraints on mylonite and detachment fault development, Kettle Highlands, northeastern Washington and southern British Columbia; Geological Society of America Abstracts with Programs, vol. 24, no.7, p.65.

Beswick, A.E. (1976) K an Rb relations in basalts and other mantle derived materials. Is phlogopite the key? : Geochimica et Cosmochimica Acta, vol. 40, p.1167-1183.

Bevington, P.R. (1969) Data Reduction and Error Analysis in the Physical Sciences, McGraw-Hill, 462 p.

Bown, T.M. (1982) Geology, paleontology, and correlation of Eocene volcaniclastic rocks, southeast Absaroka Range, Hot Springs County, Wyoming: US Geological Survey Professional Paper 1201-A, 75 p.

Budahn J.R., and Schmitt, R.A. (1985) Petrogenetic modeling of Hawaiian tholeiitic basalts: a geochemical approach: Geochimica et Cosmochimica Acta, vol. 49, p. 67-87.

Carlson, R.W., and Irving, A.J. (1994) Depletion and enrichment history of subcontinental lithospheric mantle: An Os, Sr, Nd and Pb isotopic study of ultramafic xenoliths from the northwestern Wyoming Craton, Earth and Planetary Science Letters, vol. 126, p. 457-472.

Carlson, D.H., Fleck, R., Moye, F.J., and Fox, K.F. (1991) Geology, geochemistry, and isotopic character of the Colville Igneous Complex, northeastern Washington: Journal of Geophysical Research, vol. 96, p. 13313-13333.

Cas, R.A.F., and Wright, J.V. (1987) Volcanic Successions, Modern and Ancient; Chapman and Hall, London, Glasgow, New York, Tokyo, Melbourne, Madras; (p. 43), 528 p.

Chadwick, R.A. (1968) Structural and chemical relationships in the Eocene Absaroka-Gallatin volcanic province, Wyoming-Montana: (abs.) Geological Society of America Annual Meeting Abstracts with Programs, p. A50--A51.

Chadwick, R.A. (1969) The northern Gallatin Range, Montana: northwestern part of the Absaroka-Gallatin volcanic field: University of Wyoming Contributions to Geology, vol. 8, no. 2, pt. 2, p.150-166.

Chadwick, R.A. (1970) Belts of eruptive centers in the Absaroka-Gallatin volcanic province, Wyoming-Montana: Geological Society of America Bulletin, vol. 81, p. 267-273.

Chadwick, R.A. (1981) Chronology and Structural Setting of Volcanism in Southwestern and Central Montana: Southwest Montana Guidebook, Montana Geological Society Field Conference and Symposium, p. 301-310.

Chadwick, R.A. (1985) Overview of Cenezoic volcanism in the west-central United States, in Kaplan, S.S., and Flores, R.M., eds.: Economic Paleontologists and Mineralogists, Rocky Mountain Paleogeography, Symposium 3, p. 359-381.

Christiansen, R.L. (1989) Volcanism associated with post-Laramide tectonic extension in the western U.S., Abs in IAVCEI meeting on Continental Magmatism, Santa Fe, New Mexico: New Mexico Bureau of Mines and Mineral Resources Bulletin 131, p. 51.

Collerson, K.D., and Fryer, B.J. (1978) The role of fluids in the formation and developement of Early Continental Crust; Contributions to mineralogy and Petrology, vol. 67, p. 151-167.

Collerson, K.D., Hearn, B.C., Macdonald , R.A., Upton, B.G.J., and Park, J.G. (1988) Granulite xenoliths from the Bearpaw Mountains, Montana: Constraints on the character and evolution of the lower continental crust; NATO Advanced Research Workshop on Petrology and geochemistry of Granulites, Clermont-Ferrand, France, Sept. 5-9, 1988, Terra Cognita, vol. 8, p. 270.

Conrey, R.M., Sherrod, D.R., Hooper, P.R., and Swanson, D.A. (1997) Diverse primitive magmas in the Cascade Arc, northern Oregon and southern Washington: The Canadian Mineralogist, vol. 35, p. 367-396.

Constensius, K.N. (1996) Late Paleogene extensional collapse of the Cordilleran foreland fold and thrust belt: GSA Bulletin, vol. 108; no. 1, p. 20-39.

Crisp, J.A. (1984) Rates of magma emplacement and volcanic output: Journal of Volcanology and Geothermal Research, vol. 20, p. 177-211.

Cross, T.A., and Pilger, R.H., Jr. (1982) Controls on subduction geometry, location of magmatic arcs, and tectonics of arc and back-arc regions: Geological Society of America Bulletin, vol. 93, p. 545-562.

Dalrymple, G.B., and Lanphere, M.A. (1969) Potassium-Argon dating, W.H. Freeman, San Fransisco, California, 251 p.

Davis J., and Hawkesworth, C.J. (1993) The petrogenesis of 30-20 Ma basic and intermediate volcanics from the Mogollon Datil volcanic field, New Mexico, USA: Conrtibutions to Mineralogy and Petrology, vol. 115, p. 165-183.

Decker, P.L. (1990) Style and mechanics of liquefaction-related deformation, lower Absaroka Volcanic Supergroup (Eocene), Wyoming: Geological Society of America Special Paper 240, 71p.

DePaolo D.J., and Wasserburg, G.J. (1979a) Petrogenetic mixing models and Nd-Sr isotopic patterns; Geochimica et Cosmochimica Acta, vol.43, p. 615-627.

DePaolo, D.J. (1981) Trace element and isotopic effects of combined wallrock assimilation and fractional crystallization: Earth and Planetary Science Letters, vol. 53, p. 189-202.

Dewey, J.F. (1986) Diversity in the lower continental crust: *In* Dawson, J.B., Carswell, D.A., Hall, J. and Wedepohl, K.H. (eds.) The Nature of the Lower Continental Crust, Geological Society Special Publication No. 24, Blackwell Scientific Publications, Oxford, London, Edinburgh, Boston, Palo Alto, Melbourne, p.71-78.

Dickinson, W.R., (1979) Cenozoic plate tectonic setting of the Cordilleran region in the United States, in J.M. Armentrout, M.R. Cole, and Terbest (eds.) Cenezoic paleogeography of the western United States, Society of Economic Paleontology and Mineralogy, Pacific Section, p. 1-13.

Dudas, F.O. (1991) Geochemistry of igneous rocks from the Crazy Mountains, Montana, and tectonic models for the Montana alkalic province: Journal of Geophysical Research, vol. 96, p. 13261-13278.

Dudas, F.O., Carlson, R.W., and Eggler, D.H. (1987) Regional middle Proterozoic enrichment of the subcontinental mantle source of igneous rocks from central Montana: Geology, vol. 15, p. 22-25.

Dunrud. C.R. (1962) Volcanic rocks of the Jack Creek area, southeastern Absaroka Range, Park County, Wyoming: M.S. Thesis University of Wyoming, Laramie, 92 p.

Edwards, C., Menzies, M. and Thirwall, M. (1991) Evidence from Muriah, Indonesia for the Interplay of Supra-Subduction Zone and Intraplate Processes in the Genesis of Potassic Alkaline Magmas: Journal of Petrology, vol.32, p. 555-592.

Eggler D.H., Meen, J.K., Welt, F., Dudas, F.O., K.P. Furlong, K.P., McCallum, M.E., Carlson, R.W. (1988) Tectonomagmatism of the Wyoming Province: in Cenozoic Volcanism in the southern Rocky Mountains Revisited: A Tribute to Rudy C. Epis-Part-3, J.W. Drexler, and E.E. Larson, (eds.) Colorado School of Mines Quarterly, vol. 83, no.2, p. 25-40.

Engebetson, D.C., Cox, A., and Gordon, R.G. (1985) Relative motions between oceanic and continental plates of the Pacific Basin: Geological Soceity of America Special Paper 206, 59p.

Fisher, F.S. (1966) Tertiary Intrusive Rocks and Mineralizationin the Stinkingwater Mining Region, Park County, Wyoming; Ph.D. dissertation, University of Wyoming, Laramie, (p. 88-89), 140 p.

Fisher, F.S. (1972) Tertiary Mineralization and Hydrothermal Alteration in the Stinkingwater Mining Region, Park County, Wyoming; Geological Survey Bulletin 1332-C, (p. C9), 33 p.

Fitton, J.G., James, D., Kempton, P.D., Omerod, D.S., and Leeman, W.P. (1988) The role of lithospheric mantle in the generation of late Cenozoic basic magmas in the western United States: Journal of Petrology, Special Lithosphere Issue, p. 331-349.

Fleck, R.J., Sutter, J.F., and Elliot, D.H., (1977) Interpretation of discordant $^{40}Ar/^{39}Ar$ age spectra of Mesozoic tholeiites from Antarctica: Geochimica et CosmoChimica Acta, vol. 41, p.15-32.

Foose, R.M., Wise, D.U., and Garbarini, G.S. (1961) Structural Geology of the Beartooth Mountains, Montana and Wyoming: Geological Society of America Bulletin, vol. 72, p. 1143- 1172.

Fraser, K.J., Hawkesworth, C.J., Erlank, A.J., Mitchell, R.H., and Scott-Smith, B.H. (1985) Sr, Nd, and Pb isotope and minor element chemistry of lamproites and kimberlites: Earth and Planetary Science Letters, vol. 76, p. 57-70.

French, A.N., and Vander Voo, R. (1978) A Summary Report of a Paleomagnetic Study of Lower Eocene Volcanics: Yellowstone National Park Library Report, 12 p.

Frost, C.D., Chamberlain, K.R., and Frost, B.R. (1998) Archean evolution of the Wyoming Province: Evidence from the Bighorn Mountains; Geological Society of America Absatracts with Programs, vol. 30, no.7. p. A-395.

Frost, B.R., Chamberlain, K.R., Swapp, S.M., and Frost, C.D. (1998) The age of granulite metamorphism in the Wind River Range, Wyoming: The granulite uncertainty principle compounded; Geological Society of America Absatracts with Programs, vol. 30, no.7. p. A-154.

Furlong, K.P., Chapman, D.S., and Alfeld, P.W. (1982) Thermal modeling of the geometry of subduction and implications for the tectonics of the overriding plate: Journal of Geophysical Research, vol. 87, p. 1786-1802.

Gans, P.B., Mahood, G.A., and Schermer, E. (1989) Synextensional magmatism in the Basin and Range province: A case study from the eastern Basin and Range: Geological Society of America Special Paper 233, 53 p.

Gans, P.B., and Bohrson, W.A. (1998) Supression of volcanism during rapid extension in the Basin and Range province, United States: Science, vol. 279, p. 66-68.

Gest D.E., and McBirney, A.R. (1979) Genetic relations of shoshonitic and absarokitic magmas, Absaroka Mountains, Wyoming: Journal of Geology and Geothermal Research, vol. 6, p. 85-104.

Green, T.H. (1994) Experimental studies of trace-element partitioning applicable to igneous petrogenesis-Sedona 16 years later: Chemical Geology, p.1-36.

Green, T.H., and Pearson, N.J. (1987) An experimental study of Nb and Ta partitioning between Ti-rich minerals and silicate liquids at high pressure and temperature: Geochimica et Cosmochimica Acta, vol. 51, p. 55-62.

Gunn, S.H. (1991) Isotopic constraints on the crustal evolution of southwestern Montana: Ph.D. dissertation University of California, Santa Cruz, 146 p.

Hague, A. (1899) Absaroka folio: U.S. Geological Survey Geol. Atlas of the United States, Folio no. 52.

Hague, A., Iddings, J.P., and Weed, W.H. (1899) Geology of Yellowstone National Park: Pt II, Descriptive geology, petrography, and paleontology: U.S. Geological Survey Monograph 32, 439 p.

Halladay, A.N., Dickin, A.P., Hunter, R.N., Davies, G.R., Dempster, T.J., Hamilton, P.J., and Upton, B.G.J. (1993) Formation and composition of the lower continental crust: Evidence from xenolith suites: Journal of Geophysical Research, vol. 98, no. B1, p. 581-607.

Hamilton, W.B., (1969) The volcanic central Andes: A modern model for the Cretaceous batholiths and tectonics of western North America, in Proceedings of the Andesite Conference, Bulletin of the Oregon Department of Geology and Mineralogic Industry, vol. 65, p. 175-184.

Harlan, S.S., Mehnert, H.H.,Snee, L.W., and Meen, J.K. (1991) Preliminary isotopic and age determinations from selected Late Cretaceous and Tertiary rocks in Montana: *in* Guidebook of the Central Montana Alkalic Province, Montana Bureau of Mines Special Publication 100, p. 136-137.

Harlan, S.S., Snee, L.W., and Geissman, J. W. (1996) $^{40}Ar/^{39}Ar$ geochronology and paleomagnetism of Independence Volcano, Absaroka Volcanic Supergroup, Beartooth Mountains, Montana: Canadian Journal of Earth Sciences, vol. 33, p. 1648-1654.

Hauge, T.A. (1993) The Heart Mountain detachment, northwestern Wyoming: 100 years of controversy; *in* A.W. Snoke, J.R. Steidmann, and S.M. Roberts, (eds): Geology of Wyoming: Geological Survey of Wyoming Memoir No. 5, p. 530-571.

Hauge, T.A. (1990) Kinematic model of a continuous Heart Mountain allochthon: Geological Society of America Bulletin, vol. 102, p. 1174-1188.

Hauge, T.A. (1985) Gravity-spreading origin of the Heart Mountain allochthon, northwestern Wyoming: Geological Society of America Bulletin, vol. 96, p. 1440-1456.

Hauge, T.A. (1982) The Heart Mountain detachment fault, norhwest Wyoming: Involvement of Absaroka volcanic rock; Wyoming Geological Association Guidebook, Thirty-Third Annual Field Conference, p. 175-179.

Hay, D.E., and Wendlandt, R.F. (1995) The origin of Kenya rift plateau-type flood phonolites: Results of high-temperature/high-pressure experiments in the systems phonolite-H_2O and phonolite-H_2O-CO_2: Journal of Geophysical Research, vol. 100, p. 400-411

Hickenlooper J.W., and Gutman, J.T. (1982) Geology of the Slough Creek Tuff, northern Absaroka volcanic field, Park County, Montana: Wyoming Geological Association 33rd Annual Field Conference Guidebook, p. 55-63.

Hearn B.C. Jr., and McGee, E.S. (1984) Garnet peridotites from Williams kimberlites, north-central Montana, USA: *in* Kimberlites and Related Rocks II, Kornprobst, J. (ed.) Elsevier, New York, p. 255-283.

Hearn B.C. Jr., Collerson, K.D., Upton, B.G.D., and MacDonald, R.A. (1991) Ancient and enriched upper mantle beneath north-central Montana: evidence from xenoliths: Montana Bureau of Mines Special Publication 100, p.133-135.

Holder, R.W., and Holder, G.M. (1988) The Colville batholith: Tertiary plutonism in northeast Washington associated with graben and core-complex (gneiss dome) formation: Geological Society of America Bulletin, vol. 100, p. 1971-1980.

Holder, G.M. , Holder, R.W., and Carlson, D.H. (1990) Middle Eocene dike swarms and their relation to contemporaneous plutonism, volcanism, core-complex mylonitization, and graben subsidence, Okanagan Highlands, Washington : Geology, vol. 18, p.1082-1085.

Hooper, P.R., Bailey, D.G., and McCarley-Holder, G.A. (1995) Tertiary calc-alkaline magmatism associated with lithospheric extension in the Pacific Northwest: Journal of Geophysical Research, vol. 100, p. 10303-10319.

Iddings, J.P. (1895) Absarokite-shoshonite-banakite series: Journal of Geology, vol.3, p. 935-959.

Iddings, J.P. (1899) The igneous rocks of Electric Peak and Sepulchre Mountain, U.S. Geological Survey Monograph 32, pt. 2, p. 89-148.

Irving A. J., and Frey, F.A. (1984) Trace element abundances in megacrysts and their host mafic volcanics: constraints on partition coefficients and megacryst genesis: Geochimica et Cosmochimica Acta, vol. 48, p. 1201-1221.

Ispolatov, V.O., Dudas, F.O., Snee, L.W., and Harlan, S.S. (1996) Precise dating of the Lowland Creek volcanics, west-central Montana: Geological Society of America Abstracts with Programs, vol. 28, p. A484.

James, H.L., and Hedge, C.E. (1980) Age of the basement rocks of southwest Montana: Geological Society of America Bulletin, vol. 91, p. 11-15.

Janecke, S.U., and Snee, L.W. (1993) Timing and episodicity of middle Eocene volcanism and onset of conglomerate deposition, Idaho, The Journal of Geology, vol. 101, p. 603-621.

Joswiak, D. (1992) Composition and evolution of the lower crust, Central Montana: Evidence from granulite xenoliths: M.S.Thesis, University of Washington, Seattle, 156 p.

Karner, F.R., (1989) Devils Tower-Black Hills Alkalic Igneous Rocks and General Geology: *in* American Geophysical Union Guidebook T131, F.R. Karner, (ed.), vol. 1, p. 1-2.

Kay, R.W., and Kay, S.M. (1986) Petrology and geochemistry of the lower continental crust: *In* J.B. Dawson, D.A. Carswell, J. Hall, and K.H. Wedepohl, (eds.) The Nature of the Lower Continental Crust, Geological Society Special Publication No. 24, Blackwell Scientific Publications, Oxford, London, Edinburgh, Boston, Palo Alto, Melbourne, p. 147-159

Kleinkopf, M.D. (1991) Regional Geophysical Investigations of the Central Montana Alkalic Province; Montana Bureau of Mines Special Publication 100, p. 131-132.

LaTourrette, T., Hervig, R.L., and Holloway, J.R., (1995) Trace element partitioning between amphibole, phlogopite, and basanite melt: Earth and Planetary Science Letters, vol. 135, p. 13-30.

Leat, P.T., Thompson, R.N., Morrison, M.A., Hendry, G.L., and Dickin, A.P. (1988) Compositionally-Diverse Miocene-Recent Rift-Related Magmatism in Northwest Colorado: Partial Melting and Mixing of Mafic Magmas from 3 Different Asthenospheric and Lithospheric Mantle Sources; Journal of Petrology, Special Lithosphere Issue, p. 351-377.

Lee, T.Q., and Shive, P.N. (1983) Paleomagnetic study of the volcanic and volcaniclastic rocks from the southestern Absaroka, Wyoming: Bulletin of the Institute of Earth Sciences, Academia Sinica, vol.3, p.155-172.

Leeman, W.P., Menzies, M.A., Matty, D.J., and Embree, G.F. (1985) Strontium, neodymium and lead isotopic compositions of deep crustal xenoliths from the Snake River Plain: evidence for Archean basement; Earth and Planetary Science Letters, vol. 75, p.354-368.

Le Maitre, R.W., Bateman, P., Dudek, A., Keller, J. Lameyre Le Bas, M.J., Sabine, P.A., Schmid, R., Sorensen, H., Streckeisen, A., Woolley, A.R., and Zanettin, B. (1989) A classification of igneous rocks and glossary of terms, Blackwell, Oxford, 193 p.

Lipman, P.W., Protska, H.J., and Christiansen, R.L. (1972) Evolving subduction zones in the western United States; Science, vol. 174, p. 821-825.

Lipman, P.W. (1980) Cenozoic volcanism in the western United States: Implications for continental tectonics: *in* Contnental Tectonics, Studies in Geophysics., U.S. National Academy of Sciences, p. 161-174.

Lipman, P.W., and Glazner, A.F. (1991) Introduction to middle Tertiary Cordilleran volcanism: Magma sources and relations to regional tectonics: Journal of Geophysical Research, vol. 96, p. 13193-13199.

Love, J.D. (1939) Geology along the southern margin of the Absaroka Range, Wyoming: Geological Society of America Special Paper 20, 134 p.

Love, J.D. (1964) Uraniferous phosphatic lake beds of Eocene age in intermontane basins of Wyoming and Utah: U.S. Geological Survey Professional Paper 474-E, p. E4-E40.

Love, L.L., Kudo, A.M., and Love, D.W. (1976) Dacites of Bunsen Peak, the Birch Hills, and the Washakie Needles, and their relationship to the Absaroka volcanic field, Wyoming and Montana: Geological Society of America Bulletin, vol. 87, p. 1455-1462.

MacDonald R., Upton, B.G.J., Collerson, K.D., Hearn, B.C., Jr., and James, D. (1992) Potassic mafic lavas of the Bearpaw Mountains, Montana: Mineralogy, Chemistry, and Origin; Journal of Petrology, vol. 33, pt.2, p. 305-346.

Mahood, G.A., and Baker, D.R. (1986) Experimental constraints on depths of fractionation of mildly alkalic basalts and associated felsic rocks: Pantelleria, Strait of Sicily: Contributions to Mineralogy and Petrology, vol. 93, p. 251-264.

Malone, David H. (1995) Very large debris-avalanche deposit within the Eocene volcanic succession of the northeatsrn Absaroka Range, Wyoming: Geology, vol. 23, no. 7, p. 661-664.

Marvin, R.F., Hearn, B.C.Jr., Mehnert, H.H., Naeser, C.W., Zartman, R.E. and Linsey, D.A. (1980) Late Cretaceous-Paleocene-Eocene igneous activity in north central Montana: Isochron West, vol. 29, p. 5-25.

McGrew, A.J., and Snee, L.W. (1994) 40Ar/39Ar thermochronologic constraints on the tectonothermal evolution of the northern East Humboldt Range metamorphic core complex, Nevada: Tectonophysiscs, vol. 238, p. 425-450.

McMannis, W.J., and Chadwick, R.A., (1964) Geology of the Garnet Mountain quadrangle, Gallatin County Montana: Montana Bureau of Mines and Geology Bulletin 43, 47 p.

Meen, J.K. (1987) Sr, Nd, and Pb isotopic compositions of Archean Basement rocks, Boulder River region, Beartooth Mountains, Montana; Isochron/West, no. 50, p. 13-24.

Meen, J.K., (1987) Formation of shoshonites from calcalkaline basalt magmas: geochemical and experimental constraints from the type locality: Contributions to Mineralogy and Petrology, vol. 97, p. 333-351.

Meen, J.K., (1990) Elevation of potassium content of basalt magma by fractional crystallization: the effect of pressure: Contributions to Mineralogy and Petrology, vol. 104, p. 309-331.

Meen, J.K., and Eggler, D.H. (1987) Petrology and geochemistry of the Cretaceous Independence volcanic suite, Absaroka Mountains, Montana: Clues to the composition of the Archean sub-Montanan mantle; Geological Society of America Bulletin, vol. 98, p. 238-247.

Menzies, M.A., and Halladay, A. (1988) Lithospheric mantle domains beneath the Archean and Proterozoic crust of Scotland; Journal of Petrology, Special Lithosphere Issue, p. 275-302.

Menzies, M.A., Leeman, W.P., and Hawkesworth, C.J. (1983) Isotope geochemistry of Cenozoic volcanic rocks reveals mantle heterogeneity below western USA: Nature, vol. 303, p. 205-209.

Merrill, G.P. (1895) Notes on some Eruptive Rocks from the Gallatin, Jefferson, and Madison Counties Montana, Proc, U.S. National Museum, Washington, vol. 17, p. 637-673

M'Gonigle, J.W.M., and Dalrymple, G.B. (1996) $^{40}Ar/^{39}Ar$ ages of some Challis Volcanic Group rocks and initiation of Tertiary sedimentary basins in southwestern Montana; U.S. Geological Survey Bulletin 2132, 17 p.

Mitchell R.H. and Bergman, S.C. (1991) Petrology of Lamproites, Plenum, 447 p.

Mitchell, R.H., Platt, R.G., and Downey, M. (1987) Petrology of Lamproites from Smokey Butte, Montana; Journal of Petrology, vol. 28, no. 6, p.645-677.

Mogk, D.W., Mueller, P.A., and Wooden, J.L. (1988) Archean tectonics of the north Snowy Block, Beartooth Mountains, Montana; Journal of Geology, vol. 96, p. 125-141.

Montagne, J., and Chadwick, R.A. (1982) Cenozoic history of the Yellowstone Valley between Yellowstone Park and Livingston, Montana: Wyoming Geological Association Guidebook, Thirty-Third Annual Field Conference, p. 31-51.

Montgomery, C.W., and Lytwyn, J.H. (1984) Rb-Sr systematics and ages of principal lithologies in the South Snowy Block, Beartooth Mountains; Journal of Geology, vol. 92, p. 103-112.

Moorbath, S. and Taylor, P.N. (1986) Geochronology and related isotope geochemistry of high grade metamorphic rocks from the lower continental crust; *In* J.B. Dawson, D.A. Carswell, J. Hall, and K.H. Wedepohl, (eds.) The Nature of the Lower Continental Crust, Geological Society Special Publication No. 24, Blackwell Scientific Publications, Oxford, London, Edinburgh, Boston, Palo Alto, Melbourne, p. 211-220

Moore, G., and Carmichael, I.S.E. (1998) The hydrous phase equilibria (to 3 kbar) of an andesite and basaltic andesite from western Mexico: constraints on water content and conditions of phenocryst growth: Contibutions to Mineralgy and Petrology, vol. 130, p. 304-319.

Morris, G.A. and Hooper, P.R. (1997) Petrogenesis of the Colville Igneous Complex, northeast Washington: Implications for Eocene tectonics in the northern U.S. Cordillera; Geology, vol. 25, p. 831-834.

Mueller, P.A., Wooden, J.L. Schulz, K., and Bowes, D.R. (1983) Incompatible-element-rich andesitic amphibolites from the Archean of Montana and Wyoming: Evidence for mantle metasomatism: Geology, vol. 11, p. 203-206.

Mueller, P.A., Wooden, J.L. (1988) Evidence for Archean subduction and crustal recycling, Wyoming Province: Geology, vol. 16, p. 871-874.

Mueller, P.A., Wooden, J.L. and Nutman, A.P. (1992) 3.96 Ga zircons from Archean quartzite, Beartooth Mountains, Montana: Geology, vol. 20, p.327-330.

Muller, D. and Groves, D.I. (1997) Potassic Igneous Rocks and Associated Gold-Copper Mineralization: Springer-Verlag Berlin Heidelberg, 210 p.

Nelson, W.H. (1986) White Mountain, northwestern Wyoming, a pseudo-volcanic neck; Montana Geological Society YBRA Field Conference Guidebook, p. 165-168.

Nelson , W.H., and Pierce, W.G. (1968) Wapiti Formation and Trout Peak Trachyandesite, northwestern Wyoming, U.S. Geological Survey Bulletin 1254-H, 11p.

Nelson, W.H., Prostka, H.J. and Williams, F.E. (1980) Geology and Mineral Resources of the North Absaroka Wilderness and Vicinity, Park County, Wyoming; U.S. Geological Survey Bulletin 1447, 101 p.

Nicholls J., and Carmichael, I.S.E. (1969) Commentary on the absarokite-shoshonite-banakite series of Wyoming, U.S.A. Schweiz. Mineralogische und Petrographische Mitteilungen, vol. 49, p.47-64.

Nielson, J.E., and Noller, J.S. (1987) Processes of mantle metasomatism; Constraints from observations of composite peridotite xenoliths: Geological Society of America Special Paper 215, p.61-76.

Norman, M.D., and Mertzman, S.A. (1991) Petrogenesis of Challis Volcanics from central and southwestern Idaho: trace element and Pb isotopic evidence: Journal of Geophysical Research, vol. 96, p. 13279-13294.

O'Brien, H.E., Irving, A.J., McCallum, I.S., (1991) Eocene potassic magmatism in the Highwood mountains, Montana: petrology, geochemistry, and tectonic implications: Journal of Geophysical Research, vol. 96, p. 13237-13260.

O'Brien, H.E., Irving, A.J., McCallum, I.S. and Thirwall, M.F. (1995) Strontium, neodymium, and lead isotopic evidence for the interaction of post-subduction asthenospheric potassic magmas of the Highwood Mountains, Montana, USA, with ancient Wyoming craton lithospheric mantle; Geochimica et Cosmochimica Acta, vol.29, no. 21, p. 4539-4562.

Parsons, W.H. (1939) Volcanic centers of the Sunlight area, Park County Wyoming: Journal of Geology, vol. 47, p. 1-26.

Pearce, J.A. (1983) Role of sub-continental lithosphere in magma genesis at active continental margins: *In* Hawkesworth, C.J., and Norry, M. J. (eds.) Continental Basalts and Mantle xenoliths, Shiva, Nantwich, p. 230-249.

Pearce, J.A., and Norry, M.J. (1979) Petrogenetic implications of Ti, Zr, Y, and Nb variations in volcanic rocks; Contributions to Mineralogy and Petrology, vol. 69, p. 33-47.

Peterman, Z.E., Doe, B.R., and Protska, H.J. (1970) Lead and strontium isotopes in rocks of the Absaroka volcanic field, Wyoming: Contributions to Mineralogy and Petrology, vol. 27, p. 121-130.

Pierce, W.G. (1941) Heart Mountain and South Fork Thrusts, Wyoming: American Association of Petroleum Geolgists Bulletin, vol. 25, p. 2021-2045.

Pierce, W.G. (1957) Heart Mountain and South Fork detachment thrusts of Wyoming; American Association of Petroleum Geologists Bulletin, vol. 41, no. 4, p. 591-626.

Pierce, W.G. (1973) Relation of volcanic rocks to the Heart Mountain Fault: Wyoming Geological Association Guidebook, Thirty-Third Annual Field Conference, p. 181-212.

Pierce, W.G. (1973) Principal Features of the Heart Mountain Fault and the Mechanism Problem, in K.A. De Jong, and R. Scholten, (eds.): Gravity and Tectonics, p. 457-471.

Pierce, W.G. (1978) Geologic Map of the Cody 1°x2° Quadrangle, Wyoming:US Geological Survey Miscellaneous Field Studies Map MF-963.

Pierce, W.G. (1979) Clastic dikes of Heart Mountain fault breccia, northwestern Wyoming, and their significance: U.S. Geological Survey Professional Paper 1133, 25p.

Pierce, W.G. (1980) The Heart Mountain break-away fault, northwestern Wyoming; Geological Society of America Bulletin, Part 1, vol. 91, p. 272-281.

Pierce, W.G., and Nelson, W.H. (1971) Geologic Map of the Beartooth Butte quadrangle, Park County, Wyoming; U.S. Geological Survey Geologic Quadrangle Map GQ-935.

Pierce, W.G., Nelson, W.H., Tokarski, A.T., Piekarska (1991) Heart Mountain, Wyoming, detachment lineations: Are they in microbreccia or volcanic tuff?; Geological Society of America Bulletin, vol. 103, p. 1133-1145.

Prostka, H.J. Ruppel, E.T., and Christiansen, R.L. (1975) Geologic map of the Abiathar Peak quadrangle, Yellowstone National Park, Wyoming and Montana: Map GQ-1244.

Reid, R.R. (1957) Bedrock geology of the north end of the Tobacco Root Mountains, Madison County, Montana: Montana Bureau of Mines and Geology Memoir 36, 24 p.

Rohrer, W.L. and Obradovich, J.D. (1969) Age and stratigraphic relations of the Tepee Trail and Wiggins Formations, northwestern Wyoming: US Geological Survey Professional Paper 650-B, p.B57-B62.

Rogers, N.W., and Setterfield, T.N. (1994) Potassium and incompatible -element enrichment in shoshonitic lavas from the Tavua volcano, Fiji: Chemical Geology, vol. 118, p.43-62.

Rollinson, H. (1993) Using Geochemical Data: Evaluation, Presentation, Interpretation: Longman Scientific and Technical, John Wiley and Sons, New York, p. 108.

Rouse, J.T. (1940) Structural and volcanic problems in the southern Absaroka Mountains, Wyoming, Geological Society of America Bulletin, vol. 51, p.1413-1428.

Royden, L. (1988) Flexure of the continental lithosphere in Italy, constraints imposed by gravity and deflection data: Journal of Geophysical Research, vol. 93, p. 7747-7766.

Royden, L. (1993) Tectonic expression of slab-pull at continental convergent boundaries: Tectonics, vol. 12, p. 303-325.

Rubel, D.N. (1971) Independence volcano, a major Eocene eruptive center, northern Absaroka volcanic province: Geological Society of America Bulletin, vol. 82, p. 2473-2494.

Samson S.D., and Alexander, E.C. Jr. (1987) Calibration of interlaboratory ^{40}Ar-^{39}Ar dating standard, Mmhb-1: Chemical Geology, vol. 66, p. 27-34.

Saunders, A. D., Norry, M.J., and Tarney, J. (1988) Origin of MORB and chemically depleted mantle reservoirs: trace element constraints; Journal of Petrology, Special Lithosphere Issue, p. 415-445.

Scambos, T.A. (1991) Isotopic and trace element characteristics of the Central Montana Alkalic Province kimberlite-alnoite suite; Montana Bureau of Mines Special Publication 100, p. 93-109.

Simons, F.S., Armbrustmacher, T.J., Zilka, N.T., Federspiel, F.E., and Ridenour, J. (1979) Mineral resources of the Beartooth primitive area and vicinity, Carbon, Park, and Sweetgrass Counties, Montana: US Geological Survey Bulletin 1391-F, 125 p.

Shive, P.N., and Pruss, E.F. (1977) A paleomagnetic study of basalt flows from the Absaroka Mountains, Wyoming: Journal of Geophysical Research, vol. 82, p.3039-3048.

Shultz, C.H. (1962) Petrology of Mt. Washburn, Yellowstone National Park, Wyoming: Ph.D. dissertation Ohio State Universiy, Columbus, 267 p.

Smedes H.W., and Protska, H.J. (1972) Stratigraphic framework of the Absaroka Volcanic Supergroup in the Yellowsone Park region: U.S. Geological Survey Professional Paper 729-C, 33 p.

Smedes, H. W., M'Gonigle, J.W., and Prostka, H.J. (1989) Geology of the Two Ocean Pass quadrangle, Yellowstone National Park, Wyoming; U.S. Geological Survey Quadrangle Map GQ-1667.

Smith, E.I., Feuerbach, D.L., Nauman, T.R., and Mills, J.G. (1990) Mid-Miocene volcanic and plutonic rocks in the Lake Mead area of Nevada and Arizona, Geological Society of America Memoir 174, p. 169-194.

Snee, L.W. (1982) Emplacement and cooling of the Pioneer batholith: Ph.D. dissertation Ohio State University, Columbus, 320 p.

Snoke. A.W. (1993) Geologic history of Wyoming within the tectonic framework of the North America Cordillera: *In* A.W. Snoke, J.R. Steidman, and S.M. Roberts, (eds.) Geology of Wyoming: Geological Survey of Wyoming Memoir No. 5, p. 2-56.

Stock, J., and Molnar, P. (1988) Uncertainties and implications of the Late Cretaceous and Tertiary positions of North America relative to the Farallon, Kula and Pacific plates: Tectonics, vol. 7, p. 1339-1384.

Sundell, K.A. (1980) Geology of the North Fork of Owl Creek, Hot Springs County, Wyoming: M.S. Thesis University of Wyoming, Laramie, 158 p.

Sundell, K.A. (1990) Sedimentation and tectonics of the Absaroka basin of northwestern Wyoming; Wyoming Geological Society Guidebook, Forty-First Annual Field Conference, p. 105-122.

Sundell, K.A. (1993) A geologic overview of the Absaroka volcanic province: *In* A.W. Snoke, J.R. Steidman, and S.M. Roberts (eds.) Geological Survey of Wyoming Memoir No. 5, p. 480-506.

Sundell, K.A., and Eaton, J.G. (1982) Stratigraphic relations within the southeastern Absaroka volcanic sequence, northwestern Wyoming: Wyoming Geological Association Guidebook, Thirty-Third Annual Field Conference, p. 65-70.

Sundell, K.A., Shive, P.N., and Eaton, J.G. (1984) Measured sections, magnetic polarity, and biostratigraphy of the Eocene Wiggins, Tepee Trail, and Aycross Formations within the southeastern Absaroka Range, Wyoming: Wyoming Geological Association Earth Science Bulletin, vol. 17, p. 1-48.

Taggart, J.E.Jr, Lindsay J.R.,Scott, B.A., Vivit, D.V., Bartel, A.J., and Stewart, K.C. (1987) Analysis of Geologic Materials by Wavelength-Dispersive X-Ray Flourescence Spectrometry: *In* Methods for Geochemical Analyses, P.A. Baedecker (ed.) U.S. Geological Survey Bulletin 1770, Chapter H, p.H1-H14.

Tatsumi, Y., and Eggins, S. (1995) Subduction Zone Magmatism; Blackwell Science, Frontiers in Earth Sciences, (p. 74-77, 142-143) 211p.

Tatsumoto, M., Hegner, E., and Unruh, D.M. (1987) Origin of west Maui volcanic rocks inferred from Pb, Sr, and Nd isotopes and a multicomponent model for oceanic basalt: *In* Volcanism in Hawaii, R.W. Decker, and P.H. Stauffer, (eds.) U.S. Geological Survey Professional Paper 1350, p. 723-744.

Taylor S,R., and McClennan, S.M.(1979) Disscussion on "Chemistry, thermal gradients and evolution of the lower continental crust" by Tarney and B.F. Windley; Journal of the geological Society of London, vol. 136, p. 497-500.

Templeton, A.S., Sweeney, J.S., Jr., Manske, H. Tilghman, J.F., Calhoun, S.C., Violich, A., and Chamberlain, C.P. (1995) Fluids at the Heart Mountain fault revisited: Geology, vol. 23, p. 929-932.

Thompson, P., Parsons, I., Graham, C.M., and Jackson, B. (1998) The breakdown of potassium feldspar at high water pressures: Contributions to Mineralogy and Petrology, vol. 130, p. 176-186.

Todt, W.., Cliff, R.A., Hanser, A., and Hofmann, A.W. (1993) Re-calibration of lead standards using a $^{202}Pb + {}^{205}Pb$ double spike: 7th Meeting of the European Union of Geosciences Abstract Volume, p. 396.

Tokarski, A.K., Pierce, W.G., Piekarska, E., Nelson, W.H. (1994) A sedimentary origin for "microbreccia" associated with the Heart Mountain detachment fault: Contributions to Geology, University of Wyoming, vol. 30, no. 2, p. 157-162.

U.S. Geological Survey (1975) Geologic Map of Yellowstone National Park: Miscellaneous Investigation Series Map I-711.

Weaver, B.L. (1991) The origin of ocean island basalt end-member compositions: trace element and isotopic constraints: Earth and Planetary Science Letters, vol. 104, p. 3810-3970.

Weaver, B.L., and Tarney, J. (1984) Empirical approach to estimating the composition of the continental crust: Nature, vol. 310, p. 575-570.

Weaver, B.L., and Tarney, J. (1980) Continental crust composition and nature of the lower crust: constraints from mantle Nd-Sr isotope correlation: Nature, vol. 286, p. 342-346.

Wedow, H.Jr., Gaskill, D.L., Bannister, P.D., Pattee, E.C. (1975) Absaroka primitive area, Montana: U.S. Geological Survey Bulletin 1391-B, 115 p.

Wilson, J. Tuzo (1936) The geology of the Mill Creek-Stillwater area, Montana: Ph.D. dissertation Princeton University, Princeton, NJ, 167 p.

Wilson, W.H. (1963) Correlation of volcanic rock units in the southern Absaroka Mountains, northwest Wyoming: University of Wyoming Contributions to Geology, vol. 2, p. 13-20.

Wooden, J.L., and Mueller, P.A. (1988) Pb, Sr, and Nd isotopic compositions of a suite of Late Archean, igneous rocks, eastern Beartooth Mountains: implications for crust-mantle evolution, Earth and Planetary Science Letters, vol. 87, p. 59-72.

APPENDICES

Appendix A. $^{40}Ar/^{39}Ar$ analytical data for samples from the Absaroka volcanic province, northwest Wyoming and southwest Montana.

Temperature °C	$^{40}Ar_R$	$^{39}Ar_K$	$^{40}Ar/^{39}Ar$	$^{39}Ar/^{37}Ar$	$\%^{40}Ar_R$	$\%^{39}Ar$	Apparent Age (Ma ±1 sigma)	
Sample YRL1-93; Biotite: Measured $^{40}Ar^{36}Ar_a$=296.5; J=0.007028±0.1% (1-sigma)								
750	0.06352	0.03201	1.985	11.65	11.6	0.4	24.99	±0.92
900	0.09103	0.03345	2.721	6.41	28.2	0.5	34.17	±0.70
1000	0.23774	0.5235	4.541	4.94	26.4	0.7	56.68	±0.21
1100	0.70885	0.15525	4.566	19.92	70.8	2.1	56.98	±0.20
1200	2.70203	0.60510	4.465	61.67	85.4	8.3	55.75	±0.11
1300	7.44708	1.72700	4.312	49.54	90.1	23.6	53.86	±0.08
1350	7.68974	1.78408	4.310	14.80	91.5	24.3	53.84	±0.08
1400	6.96911	1.60465	4.343	13.39	92.2	21.9	54.24	±0.08
1450	4.81791	1.10620	4.355	43.15	93.1	15.1	54.39	±0.08
1550	0.9989	0.23167	3.316	9.99	87.3	3.2	53.91	±0.22
Total Gas			4.327				54.05	±0.10
Sample YGDC1-96; Hornblende: Measured $^{40}Ar^{36}Ar_a$=298.9; J=0.007028±0.1% (1-sigma)								
700	0.13448	0.02595	5.182	1.08	13.6	1.2	58.50	±0.80
850	0.24544	0.5262	4.664	1.65	32.2	2.5	52.75	±0.33
950	0.12817	0.02617	4.897	1.17	67.2	1.3	55.34	±2.13
1025	0.9129	0.01832	4.983	0.55	50.0	0.9	56.29	±0.36
1075	0.32589	0.06860	4.750	0.16	69.7	3.3	53.70	±0.44
1100	0.45292	0.09501	4.767	0.15	76.8	4.6	53.89	±0.21
1125	0.57571	0.12143	4.741	0.14	82.0	5.8	53.60	±0.12
1150	1.309950	0.27583	4.748	0.14	85.1	13.2	53.67	±0.13
1175	1.52901	0.31918	4.791	0.14	85.4	15.3	54.15	±0.09
1225	2.99680	0.62508	4.794	0.15	87.4	30.0	54.19	±0.08
1275	1.59821	0.31700	5.042	0.13	81.1	15.2	56.95	±0.09
1350	0.72616	0.13982	5.193	0.13	79.3	6.7	58.63	±0.09
Total Gas			4.851				54.82	±0.10
Sample PR2-93; Biotite: Measured $^{40}Ar^{36}Ar_a$=298.9; J=0.006223±0.1% (1-sigma)								
600	0.0425	0.00625	6.435	1.54	13.7	0.2	70.83	±5.64
700	0.02826	0.00562	5.027	0.46	31.9	0.1	55.57	±3.05
800	0.11378	0.1998	5.694	0.41	15.0	0.5	62.81	±4.87
900	1.29739	0.26372	4.920	37.12	89.4	6.9	54.40	±0.08
1000	2.10802	0.43747	4.819	91.93	95.0	11.4	53.30	±0.08
1100	4.09121	0.87044	4.700	25.20	95.9	22.6	52.01	±0.08
1150	4.76291	1.01540	4.691	9.56	97.7	26.4	51.90	±0.08
1200	4.34516	0.91613	4.743	15.62	97.3	23.8	52.48	±0.08
1250	1.11753	0.23437	4.768	12.32	94.0	6.1	52.75	±0.12
1300	0.37912	0.07720	4.911	5.71	86.9	2.0	54.31	±0.44
Total Gas			4.753				52.59	±0.12
Sample YSC5-95; Sanidine: Measured $^{40}Ar^{36}Ar_a$=296.5; J=0.00679±0.1% (1-sigma)								
550	0.4565	0.01244	3.671	5.25	29.6	0.1	44.42	±2.37
650	0.15008	0.03845	3.903		65.2	0.3	47.19	±0.79
750	0.33880	0.20560	4.080	41.74	59.7	1.7	49.29	±0.10
850	2.28135	0.55776	4.090	43.52	95.1	4.6	49.42	±0.08
950	4.09793	1.00187	4.090	53.35	96.8	8.3	49.42	±0.08
1000	4.75963	1.16347	4.091	55.38	97.0	9.6	49.43	±0.08
1050	5.09071	1.24039	4.104	55.17	98.2	10.2	49.58	±0.08
1100	5.61157	1.36800	4.102	48.34	98.3	11.3	49.56	±0.08
1150	6.01845	1.46806	4.100	54.33	98.4	12.1	49.53	±0.08
1200	6.67801	1.62358	4.113	50.38	98.5	13.4	49.69	±0.08
1250	6.86528	1.66901	4.113	56.34	98.4	13.8	49.69	±0.08
1350	7.36834	1.78630	4.125	60.62	97.9	14.7	49.83	±0.08
Total Gas			4.104				49.59	±0.08

Appendix A. (Continued) $^{40}Ar/^{39}Ar$ analytical data for samples from the Absaroka volcanic province, northwest Wyoming and southwest Montana.

Temperature °C	$^{40}Ar_R$	$^{39}Ar_K$	$^{40}Ar/^{39}Ar$	$^{39}Ar/^{37}Ar$	$\%^{40}Ar_R$	$\%^{39}Ar$	Apparent Age (Ma ±1 sigma)	
Sample YSC3-95; Biotite: Measured $^{40}Ar^{36}Ar_a$=296.5; J=0.006841±0.1% (1-sigma)								
800	0.46581	0.11494	4.053	27.26	19.6	1.4	49.33	±0.08
900	0.36947	0.06548	5.642	18.51	34.9	0.8	68.32	±0.33
1000	0.59134	0.09673	6.114	30.20	32.9	1.2	73.91	±0.60
1100	1.53687	0.32673	4.663	140.30	62.1	4.1	56.65	±0.09
1200	2.88354	0.68346	4.219	81.33	89.2	8.6	51.33	±0.08
1250	3.40521	0.81580	4.174	114.42	92.1	10.3	50.79	±0.08
1300	3.91789	0.94196	4.159	122.87	92.3	11.8	50.61	±0.08
1350	2.53769	0.61295	4.140	88.97	92.0	7.7	50.38	±0.15
1400	6.42789	1.55217	4.141	245.62	92.2	19.5	50.40	±0.08
1450	5.95945	1.44065	4.137	89.51	92.3	18.1	50.34	±0.08
1550	5.38944	1.29951	4.147	48.48	92.1	16.3	50.47	±0.08
Total Gas			4.210				51.22	±0.09
Sample YFP7-93; Biotite: Measured $^{40}Ar^{36}Ar_a$=298.9; J=0.007028±0.1% (1-sigma)								
700	0.11452	0.6992	1.638	11.88	22.8	1.6	18.00	±0.19
800	0.29453	0.7603	3.874	12.69	30.4	1.8	42.30	±0.35
850	0.45902	0.9931	4.622	68.47	78.4	2.3	50.35	±0.12
900	0.92776	0.20150	4.604	132.92	88.1	4.8	50.16	±0.08
950	0.89772	0.19440	4.618	152.67	92.0	4.6	50.31	±0.15
1000	1.38590	0.30162	4.595	208.59	94.2	7.1	50.06	±0.11
1050	2.63609	0.57438	4.589	192.69	95.4	13.5	50.00	±0.08
1100	3.61009	0.78698	4.587	168.47	96.3	18.6	49.98	±0.08
1150	2.35661	0.51384	4.586	105.37	95.4	12.1	49.97	±0.10
1200	2.72218	0.59750	4.556	60.21	96.5	14.1	49.64	±0.08
1250	2.11632	0.46696	4.532	25.74	96.2	11.0	49.39	±0.08
1300	1.62388	0.35955	4.516	15.51	95.7	8.5	49.22	±0.08
Total Gas			4.513				49.18	±0.10
Sample P348; Sanidine: Measured $^{40}Ar^{36}Ar_a$=299.3; J=0.005028±0.1% (1-sigma)								
600	0.00064	0.00292	0.219	217.17	0.2	0.0	1.99	±9.41
700	0.73224	0.13445	5.446	8.78	56.4	1.9	48.73	±0.08
800	1.40487	0.25971	5.409	----*	96.7	3.6	48.41	±0.12
850	1.12949	0.20760	5.441	8.76	97.7	2.9	48.69	±0.15
900	3.27423	0.60051	5.452	----	98.6	8.4	48.79	±0.08
950	3.96829	0.72773	5.453	30.71	98.9	10.1	48.80	±0.10
1000	4.51778	0.82931	5.448	56.13	99.2	11.6	48.75	±0.08
1100	9.56637	1.75570	5.449	24.21	99.3	24.5	48.76	±0.08
1150	6.76070	1.23916	5.456	----	99.4	17.3	48.82	±0.08
1200	6.59949	1.20205	5.490	54.97	99.3	16.8	49.12	±0.08
1250	0.90553	0.16505	5.487	----	95.7	2.3	49.09	±0.26
1400	0.27828	0.05112	5.443	8.94	88.0	0.7	48.71	±0.83
Total Gas			5.455				48.81	±0.17
*37Ar too decayed to measure								
Sample P306; Biotite: Measured $^{40}Ar^{36}Ar_a$=299.7; J=0.005075±0.1% (1-sigma)								
600	0.29135	0.06163	4.727	----	40.7	1.3	42.77	±0.10
700	0.69579	0.13630	5.105	----	49.9	2.9	46.14	±0.17
750	1.10767	0.20593	5.379	----	87.8	4.5	48.58	±0.07
800	3.74675	0.69103	5.422	----	95.8	15.0	48.97	±0.08
850	3.03302	0.56047	5.412	----	96.5	12.1	48.88	±0.08
900	2.02294	0.37399	5.409	----	95.4	8.1	48.85	±0.08
950	2.19494	0.40513	5.418	----	93.2	8.8	48.93	±0.08
1000	2.97461	0.55035	5.405	----	95.2	11.9	48.82	±0.08
1150	4.06737	0.74740	5.442	----	96.8	16.2	49.15	±0.11
1100	4.37315	0.80285	5.447	----	97.1	17.4	49.19	±0.37
1300	0.47260	0.08711	5.425	----	86.1	1.9	49.00	±0.08
Total Gas			5.404				48.81	±0.13

Appendix A. (Continued) $^{40}Ar/^{39}Ar$ analytical data for samples from the Absaroka volcanic province, northwest Wyoming and southwest Montana.

Temperature °C	$^{40}Ar_R$	$^{39}Ar_K$	$^{40}Ar/^{39}Ar$	$^{39}Ar/^{37}Ar$	$\%^{40}Ar_R$	$\%^{39}Ar$	Apparent Age (Ma ±1 sigma)	
Sample 3497; Feldspar: Measured $^{40}Ar^{36}Ar_a$=296.5; J=0.007131±0.1% (1-sigma)								
650	0.44103	0.12498	3.529	2.00	38.0	1.5	44.83	±0.12
750	0.76839	0.20127	3.818	4.22	86.8	2.4	48.46	±0.13
850	1.73362	0.45735	3.791	3.35	94.2	5.4	48.12	±0.08
950	3.06042	0.81401	3.760	2.25	98.2	9.6	47.73	±0.07
1000	2.45488	0.65199	3.765	3.20	99.1	7.7	47.80	±0.07
1050	3.06550	0.81241	3.773	3.84	99.5	9.6	47.90	±0.07
1100	2.79094	0.74219	3.760	4.53	99.1	8.7	47.74	±0.07
1150	3.58228	0.95088	3.767	5.68	99.1	11.2	47.82	±0.08
1200	3.12445	0.82566	3.784	7.00	99.3	9.7	48.04	±0.07
1250	3.73773	0.98577	3.792	7.93	98.8	11.6	48.13	±0.07
1350	7.35903	1.92377	3.825	9.92	99.1	22.7	48.55	±0.07
Total Gas			3.783				48.02	±0.08
Sample 68-0-51; Hornblende: Measured $^{40}Ar^{36}Ar_a$=296.5; J=0.005235±0.1% (1-sigma)								
800	0.07040	0.02248	3.132	1.90	6.6	1.4	29.34	±3.41
900	0.02706	0.00461	5.866	0.43	26.9	0.3	54.57	±8.06
950	0.25681	0.04997	5.139	0.21	70.7	3.2	47.89	±0.23
1000	1.56639	0.30743	5.095	0.19	93.4	19.4	47.49	±0.18
1050	3.79686	0.74028	5.129	0.18	95.0	46.7	47.80	±0.14
1100	1.63961	0.32039	5.118	0.14	94.0	20.2	47.69	±0.07
1150	0.44359	0.08622	5.145	0.17	90.3	5.4	47.94	±0.07
1200	0.09436	0.01911	4.937	0.15	79.0	1.2	46.03	±0.83
1250	0.07564	0.01238	6.111	0.16	82.5	0.8	56.81	±0.44
1350	0.12456	0.02238	5.565	0.17	90.2	1.4	51.81	±0.88
Total Gas							47.59	±0.24
Sample HHM17B-95; Biotite: Measured $^{40}Ar^{36}Ar_a$=298.9; J=0.006142±0.1% (1-sigma)								
600	0.01159	0.00406	2.854	8.34	4.3	0.3	31.35	±8.72
700	0.01395	0.00447	3.117	7.97	16.9	0.3	34.21	±3.64
800	0.05118	0.01025	4.993	7.55	9.5	0.8	54.49	±2.82
900	0.21564	0.04344	4.964	20.19	63.1	3.2	54.18	±1.62
1000	0.74617	0.15965	4.674	82.39	78.7	11.7	51.06	±0.15
1100	2.07725	0.45457	4.570	164.78	93.6	33.4	49.94	±0.08
1150	0.94856	0.20701	4.582	88.75	92.0	15.2	50.07	±0.21
1200	1.26524	0.27553	4.592	57.27	92.2	20.2	50.18	±0.11
1250	0.73206	0.16042	4.563	26.46	91.0	11.8	49.87	±0.16
1300	0.17717	0.04146	4.273	5.68	69.8	3.0	46.74	±0.84
Total Gas			4.584				50.09	±0.26
Sample HMD4-96; Hornblende: Measured $^{40}Ar^{36}Ar_a$=298.9; J=0.006128±0.1% (1-sigma)								
600	0.00189	0.00696	0.272	3.07	0.6	0.2	3.00	±1.13
700	0.08674	0.02427	3.575	5.68	19.3	0.7	39.09	±0.76
800	0.27087	0.06727	4.026	15.76	13.9	1.9	43.97	±0.30
1000	4.90478	1.10497	4.439	125.07	91.6	31.2	48.52	±0.07
1100	4.73206	1.06912	4.426	141.95	94.1	30.1	48.28	±0.07
1150	3.13562	0.70981	4.418	88.64	91.8	20.0	48.19	±0.09
1200	2.28599	0.51833	4.410	23.70	90.7	14.6	48.11	±0.09
1250	0.20931	0.04647	4.504	1.51	75.0	1.3	49.12	±1.06
Total Gas			4.406				48.06	±0.13

Appendix A. (Continued) $^{40}Ar/^{39}Ar$ analytical data for samples from the Absaroka volcanic province, northwest Wyoming and southwest Montana.

Temperature °C	$^{40}Ar_R$	$^{39}Ar_K$	$^{40}Ar/^{39}Ar$	$^{39}Ar/^{37}Ar$	$\%^{40}Ar_R$	$\%^{39}Ar$	Apparent Age (Ma ±1 sigma)	
Sample HM1-94; Hornblende: Measured $^{40}Ar^{36}Ar_a$=298.9; J=0.006265±0.1% (1-sigma)								
700	0.02344	0.00348	6.735	0.46	5.2	0.2	74.56	±7.22
850	0.04581	0.00611	7.500	0.36	4.8	0.3	82.83	±11.95
1000	0.04828	0.00791	6.102	0.34	23.2	0.4	67.68	±4.82
1050	0.01906	0.00345	5.529	0.19	12.4	0.2	61.43	±3.61
1100	0.37013	0.08201	4.513	0.14	55.1	3.8	50.30	±0.14
1150	1.30297	0.29688	4.389	0.14	71.1	13.9	48.93	±0.10
1175	1.47774	0.33490	4.413	0.13	83.9	15.6	49.19	±0.09
1200	1.73609	0.39394	4.407	0.13	89.2	18.4	49.13	±0.08
1225	2.70908	0.61444	4.409	0.13	92.5	28.7	49.15	±0.08
1275	1.52958	0.34430	4.443	0.13	86.0	16.1	49.52	±0.13
1350	0.17438	0.03851	4.528	0.13	68.6	1.8	50.46	±1.32
1400	0.07314	0.01549	4.723	0.13	47.7	0.7	52.61	±2.81
Total Gas			4.441				49.50	±0.17
Sample 71-0-4; Biotite: Measured $^{40}Ar^{36}Ar_a$=298.9; J=0.006380±0.1% (1-sigma)								
600	0.03741	0.02047	1.827	11.26	5.2	0.5	20.91	±0.36
700	0.06423	0.02513	2.556	18.67	21.4	0.6	29.18	±1.08
800	0.42074	0.10680	3.940	45.06	32.3	2.4	44.78	±0.15
900	1.60742	0.39042	4.117	83.57	81.6	8.8	46.77	±0.18
1000	2.15131	0.52159	4.125	86.90	91.7	11.8	46.86	±0.11
1050	1.99721	0.48399	4.127	75.13	91.7	10.9	46.88	±0.18
1100	3.15264	0.76472	4.123	62.97	93.2	17.3	46.84	±0.07
1150	3.82475	0.93180	4.105	39.94	96.5	21.1	46.63	±0.07
1200	3.68327	0.89679	4.107	26.51	97.3	20.3	46.66	±0.07
1300	1.15564	0.28286	4.085	3.35	95.3	6.4	46.42	±0.07
Total Gas			4.090				46.47	±0.11
Sample AR77-184; Biotite: Measured $^{40}Ar^{36}Ar_a$=298.9; J=0.004624±0.1% (1-sigma)								
600	0.03793	0.01191	3.185	3.29	19.3	0.3	26.38	±2.22
700	0.16122	0.04045	3.986	6.70	54.4	1.0	32.95	±0.31
800	1.34943	0.23559	5.728	13.97	66.4	5.9	47.16	±0.07
850	0.75942	0.13328	5.698	18.58	88.8	3.3	46.91	±0.33
900	1.22066	0.21329	5.723	18.48	93.4	5.3	47.12	±0.11
950	1.04585	0.18496	5.654	17.35	93.8	4.6	46.56	±0.07
1000	1.57164	0.27460	5.723	13.58	92.2	6.9	47.12	±0.13
1050	2.98429	0.52373	5.698	15.27	95.1	13.1	46.92	±0.07
1100	6.45204	1.14710	5.625	25.72	96.3	28.6	46.32	±0.07
1150	5.49668	0.98214	5.597	35.06	96.5	24.5	46.09	±0.07
1300	1.48435	0.26119	5.683	6.59	95.3	6.5	46.79	±0.10
Total Gas			5.629				46.36	±0.10
Sample AR76-120; Hornblende: Measured $^{40}Ar^{36}Ar_a$=298.9; J=0.004051±0.1% (1-sigma)								
700	0.10292	0.01638	6.284	2.79	20.1	0.9	50.32	±0.63
800	0.43162	0.07514	5.744	1.11	34.4	4.2	46.05	±0.40
900	0.17102	0.02913	5.870	1.17	65.8	1.6	47.05	±0.97
950	0.05433	0.00868	6.259	0.79	62.9	0.5	50.12	±2.96
1000	0.03927	0.00695	5.650	0.58	50.6	0.4	45.30	±2.78
1050	0.12363	0.02057	6.011	0.25	68.0	1.1	48.16	±0.81
1100	0.73248	0.12581	5.822	0.17	84.5	7.0	46.67	±0.43
1125	1.19561	0.20905	5.719	0.16	90.7	11.6	45.85	±0.07
1150	2.52563	0.44733	5.646	0.16	94.2	24.8	45.27	±0.07
1175	1.88304	0.33571	5.609	0.16	94.3	18.6	44,98	±0.08
1200	0.92173	0.16290	5.658	0.16	93.6	9.0	45.37	±0.10
1250	1.46451	0.25901	5.654	0.15	95.7	14.4	45.34	±0.14
1450	0.63177	0.10710	5.899	0.10	91.5	5.9	47.27	±0.11
Total Gas			5.698				45.68	±0.17

Appendix A. (Continued) $^{40}Ar/^{39}Ar$ analytical data for samples from the Absaroka volcanic province, northwest Wyoming and southwest Montana.

Temperature °C	$^{40}Ar_R$	$^{39}Ar_K$	$^{40}Ar/^{39}Ar$	$^{39}Ar/^{37}Ar$	$\%^{40}Ar_R$	$\%^{39}Ar$	Apparent Age (Ma ±1 sigma)	
Sample 71-0-13; Sanidine: Measured $^{40}Ar^{36}Ar_a$=299.7; J=0.005320±0.1% (1-sigma)								
550	0.15476	0.04311	3.590	979.52	32.1	0.5	34.13	±0.67
650	0.38783	0.08083	4.798	1732.48	52.0	1.0	45.47	±0.59
700	0.64821	0.13156	4.927	2524.13	85.6	1.6	46.68	±0.18
750	0.87046	0.17545	4.961	2247.15	94.4	2.1	47.00	±0.21
800	1.22527	0.24728	4.955	1542.66	96.5	3.0	46.94	±0.07
825	1.24249	0.25034	4.963	2494.59	96.6	3.0	47.02	±0.10
850	1.40161	0.28504	4.917	3520.36	95.8	3.4	46.58	±0.18
875	1.61373	0.32644	4.943	3395.40	96.4	3.9	46.83	±0.08
900	1.75813	0.35729	4.921	3563.92	95.2	4.3	46.62	±0.14
925	2.13665	0.43274	4.937	4844.46	97.6	5.2	46.77	±0.09
950	2.44047	0.49420	4.938	2089.01	97.9	6.0	46.78	±0.16
975	2.24177	0.45293	4.949	5328.71	98.0	5.5	46.89	±0.07
1000	2.91800	0.58924	4.952	10128.3	98.1	7.1	46.91	±0.07
1050	4.18990	0.84470	4.960	8384.92	98.8	10.2	46.99	±0.07
1100	6.60332	1.33047	4.963	13138.4	99.1	16.1	47.01	±0.07
1150	7.59076	1.52868	4.966	7105.52	99.1	18.5	47.04	±0.12
1350	3.43583	0.68873	4.989	4609.25	98.0	8.3	47.25	±0.08
1450	0.10166	0.01850	5.497	212.93	71.4	0.2	51.99	±0.81
Total Gas			4.948				46.88	±0.11
Sample AR76-115; Biotite: Measured $^{40}Ar^{36}Ar_a$=298.9; J=0.004665±0.1% (1-sigma)								
600	0.53341	0.07248	7.359	4.88	60.8	1.9	60.89	±0.49
700	0.35578	0.05035	7.067	5.46	71.1	1.4	58.51	±0.09
800	0.23534	0.03763	6.254	6.69	31.4	1.0	51.88	±0.32
850	0.35107	0.06115	5.741	15.15	80.4	1.6	47.68	±0.07
900	0.55347	0.10003	5.533	26.37	89.2	2.7	45.98	±0.32
950	0.59336	0.10846	5.471	22.80	91.0	2.9	45.46	±0.36
1000	1.13075	0.21051	5.371	26.32	93.0	5.7	44.65	±0.09
1050	2.87580	0.53450	5.380	17.99	85.9	14.4	44.72	±0.08
1100	6.95439	1.28762	5.401	2.59	97.1	34.6	44.89	±0.07
1150	3.96931	0.73507	5.400	2.15	96.8	19.8	44.88	±0.07
1200	2.14097	0.39408	5.433	4.16	97.0	10.6	45.15	±0.12
1250	0.43686	0.08051	5.426	1.47	95.4	2.2	45.10	±0.29
1400	0.23998	0.4516	5.314	0.52	88.1	1.2	44.18	±0.67
Total Gas			5.480				45.53	±0.11
Sample AR76-121; K-Feldspar: Measured $^{40}Ar^{36}Ar_a$=298.9; J=0.004567±0.1% (1-sigma)								
700	0.17629	0.02858	6.167	5.66	29.2	1.1	50.11	±0.21
800	3.378993	0.68985	5.494	13.81	85.9	26.9	44.70	±0.07
850	2.17729	0.40578	5.366	15.73	98.0	15.8	43.67	±0.07
900	1.51935	0.28231	5.382	14.88	98.2	11.0	43.80	±0.07
950	1.59882	0.29832	5.359	17.19	98.0	11.6	43.62	±0.12
1000	1.09053	0.20367	5.355	23.85	96.8	7.9	43.58	±0.10
1050	0.80555	0.14966	5.383	31.47	96.4	5.8	43.81	±0.23
1100	0.63950	0.11924	5.363	32.73	95.8	4.6	43.65	±0.37
1150	0.53857	0.09948	5.414	31.69	98.4	3.9	44.06	±0.12
1200	0.87515	0.16186	5.407	33.37	98.1	6.3	44.00	±0.17
1400	0.70193	0.12694	5.529	23.88	94.5	4.9	44.99	±0.27
Total Gas			5.423				44.13	±0.12

Appendix B. $^{40}Ar/^{39}Ar$ age spectra for samples from the Absaroka volcanic province, northwest Wyoming and southwest Montana.

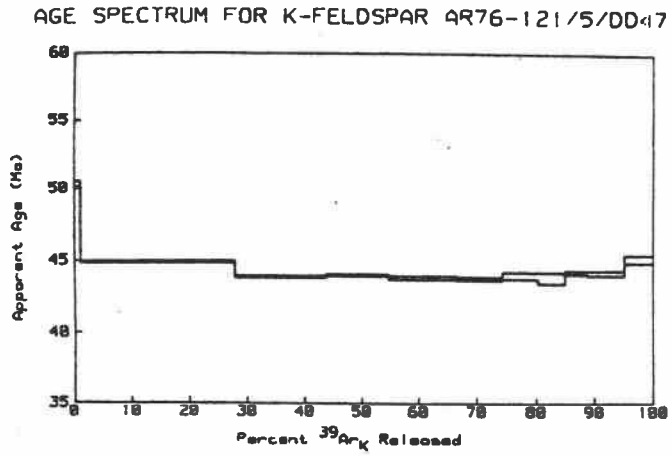

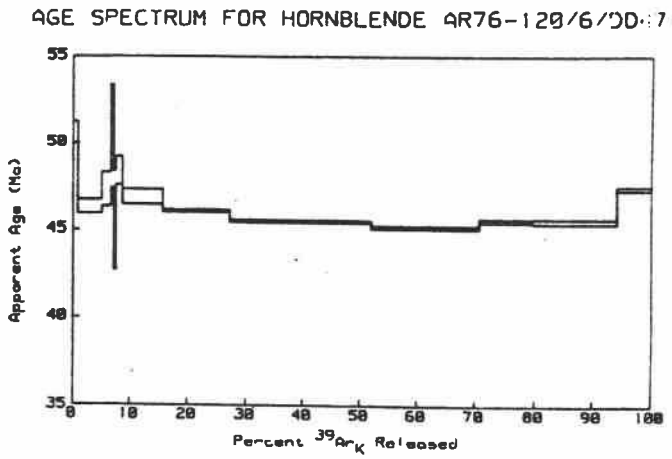

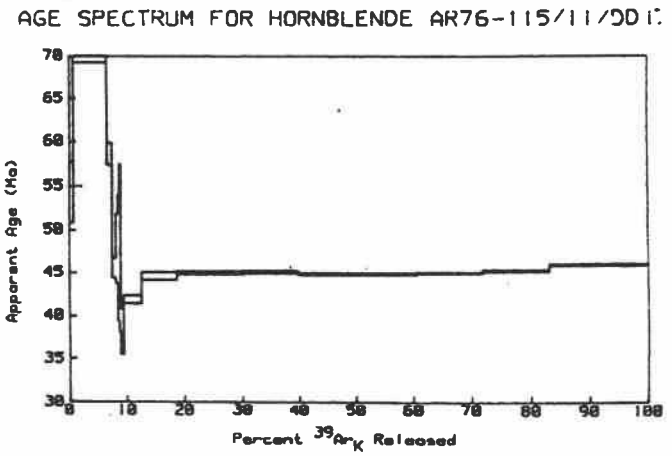

Appendix B. (Continued) $^{40}Ar/^{39}Ar$ age spectra for samples from the Absaroka volcanic province, northwest Wyoming and southwest Montana.

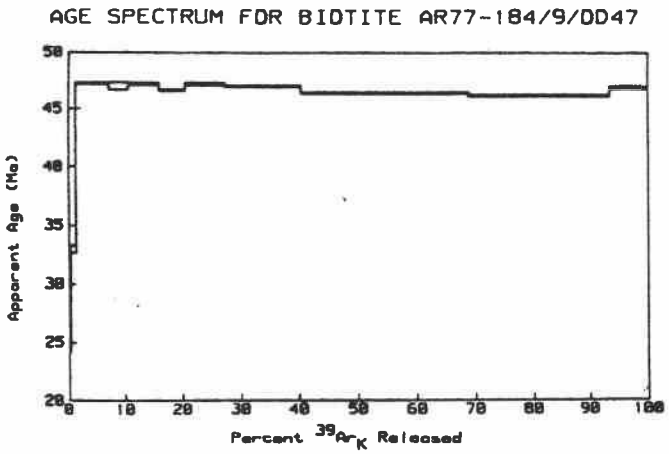

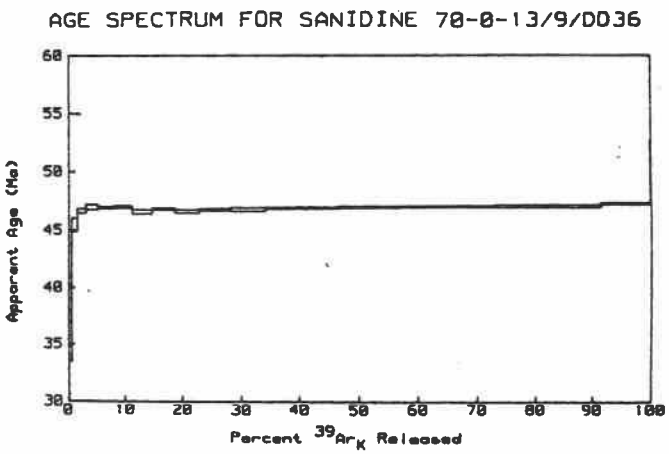

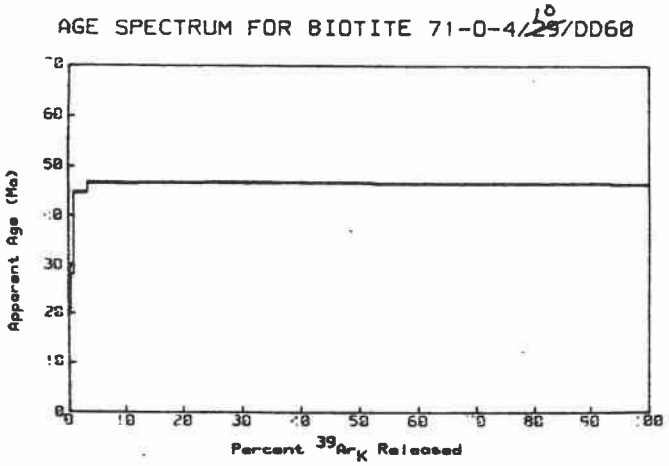

Appendix B. (Continued) $^{40}Ar/^{39}Ar$ age spectra for samples from the Absaroka volcanic province, northwest Wyoming and southwest Montana.

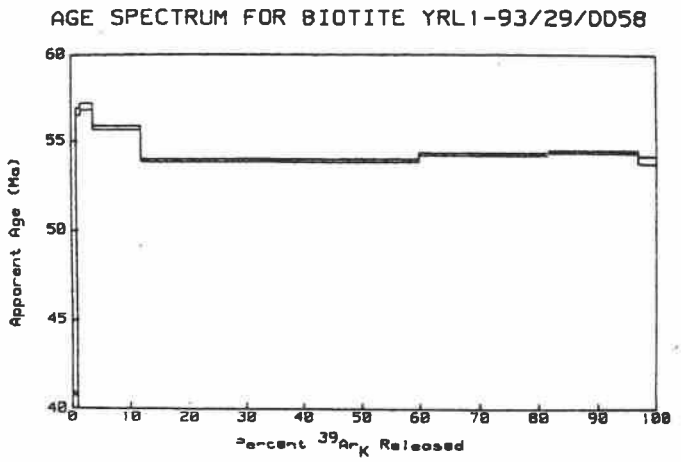

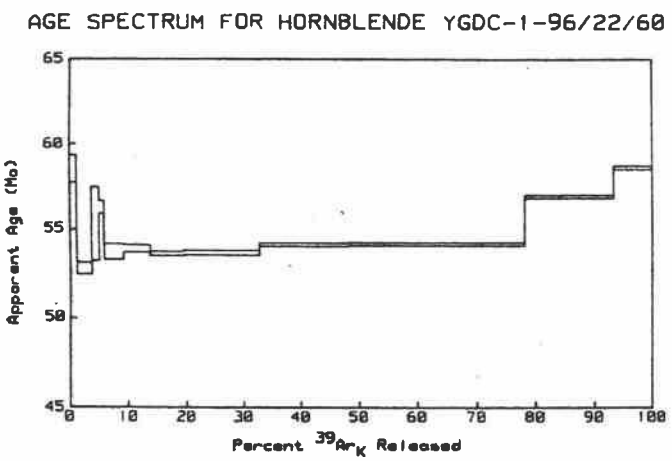

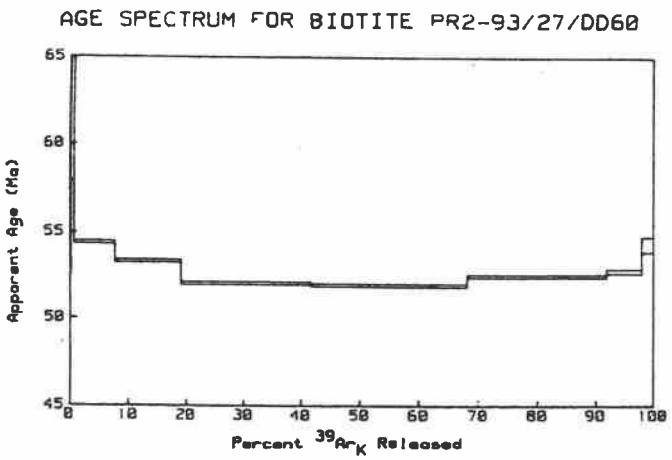

Appendix B. (Continued) $^{40}Ar/^{39}Ar$ age spectra for samples from the Absaroka volcanic province, northwest Wyoming and southwest Montana.

AGE SPECTRUM FOR BIOTITE P306/2/DD36

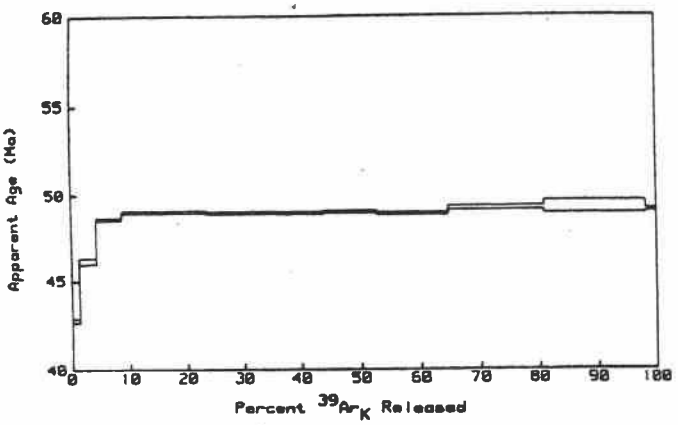

AGE SPECTRUM FOR FELDSPAR 3497/34/DD58

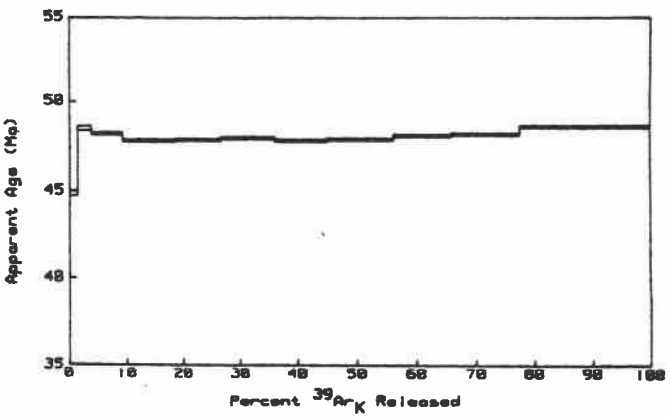

AGE SPECTRUM FOR HORNBLENDE 68-0-51/7/DD36

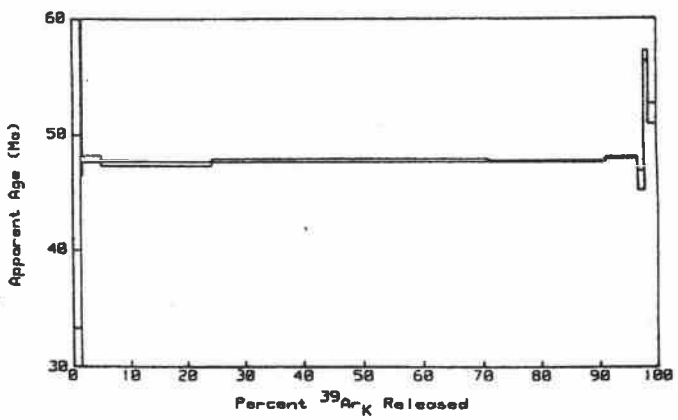

Appendix B. (Continued) $^{40}Ar/^{39}Ar$ age spectra for samples from the Absaroka volcanic province, northwest Wyoming and southwest Montana.

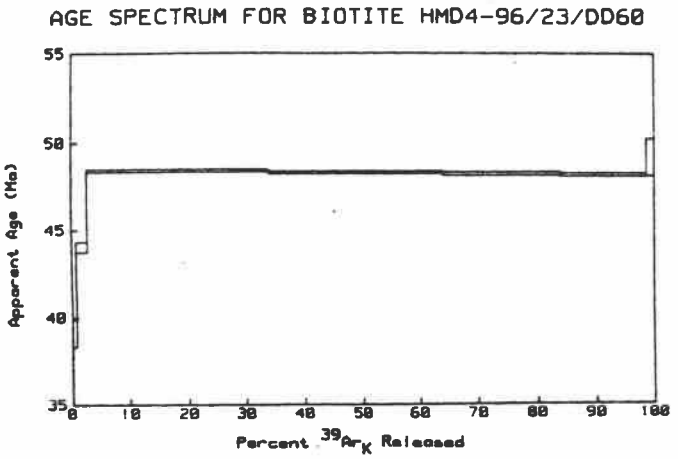

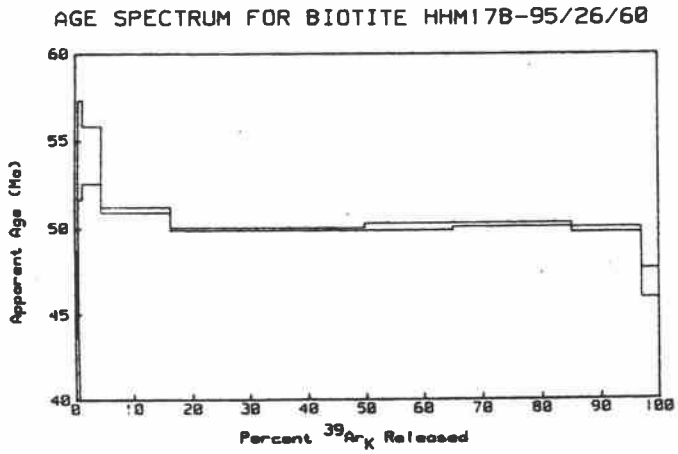

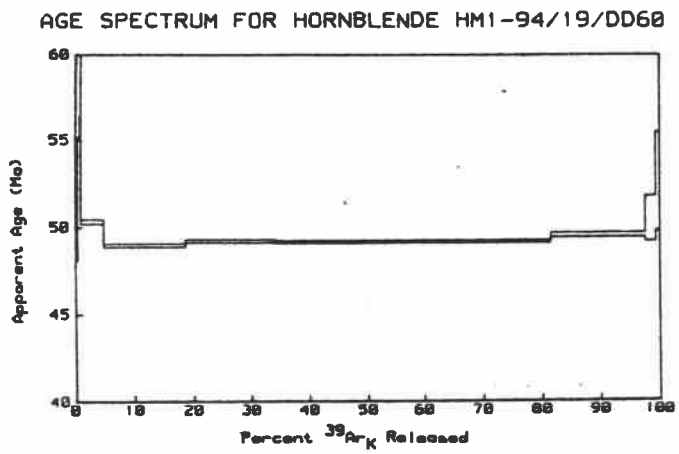

Appendix B. (Continued) $^{40}Ar/^{39}Ar$ age spectra for samples from the Absaroka volcanic province, northwest Wyoming and southwest Montana.

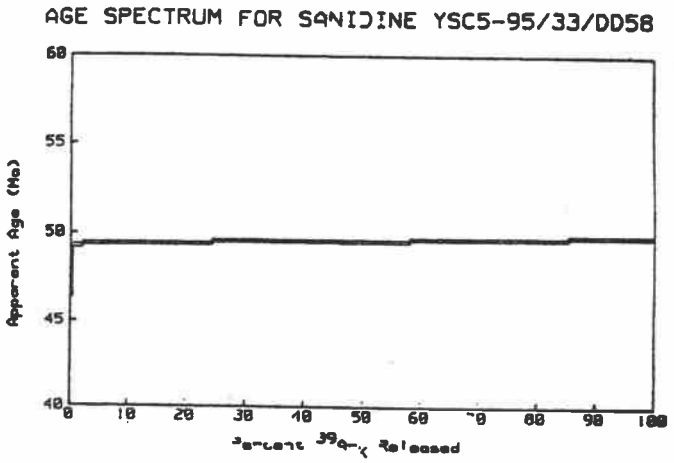

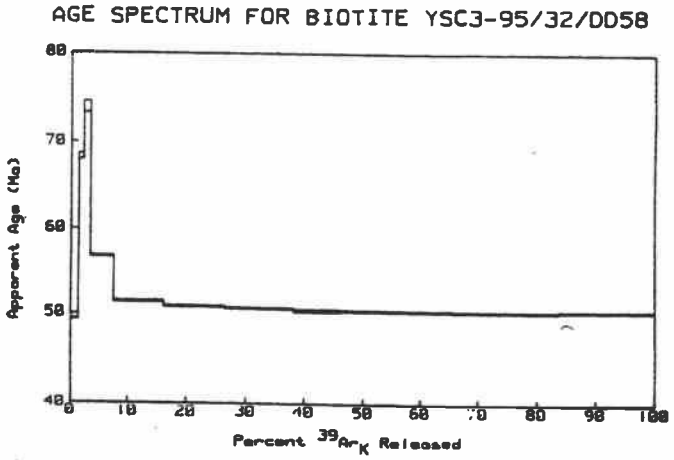

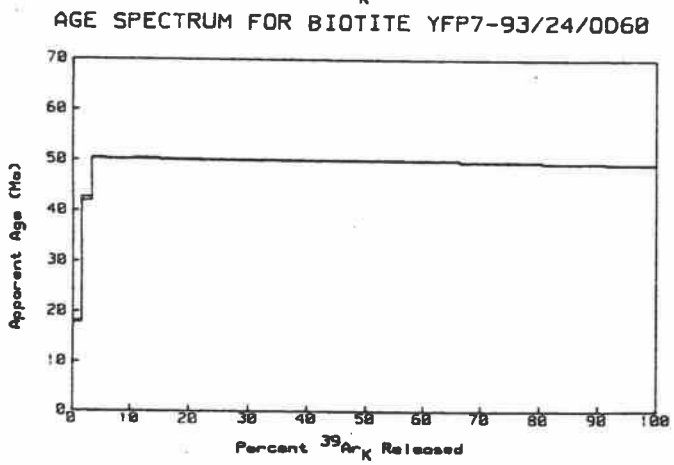

Appendix B (Continued) Linear isochrons for selected age data. (Samples with well-defined plateaus.)

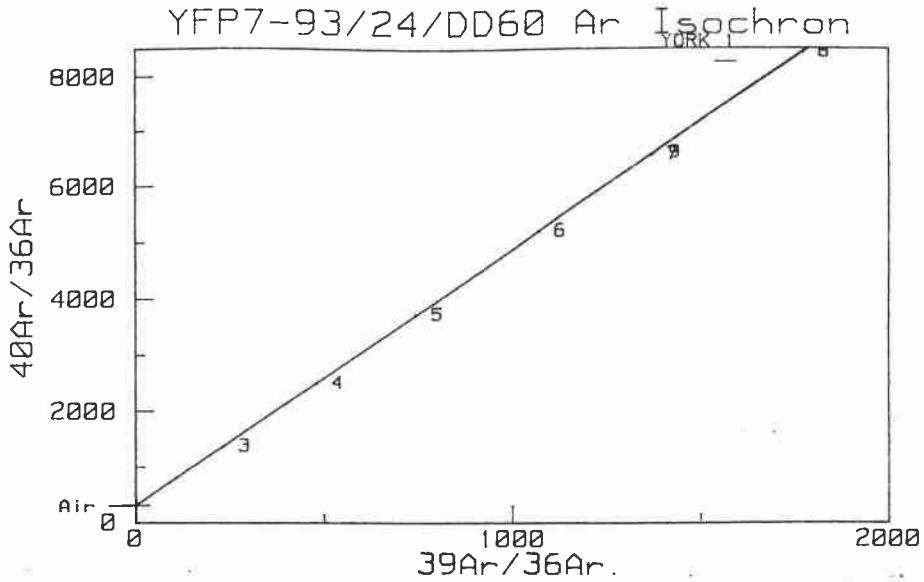

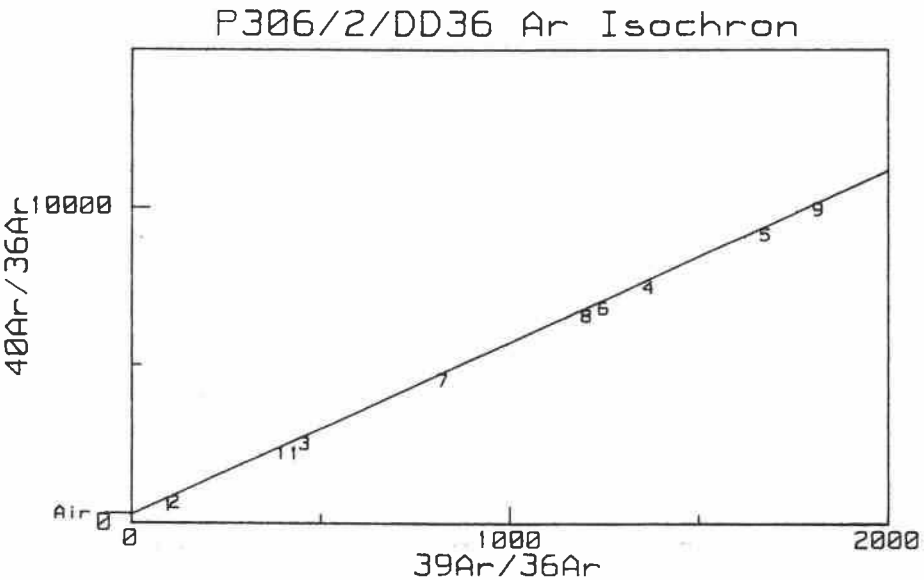

Appendix B (Continued) Linear isochrons for selected age data. (Samples with excess Ar.)

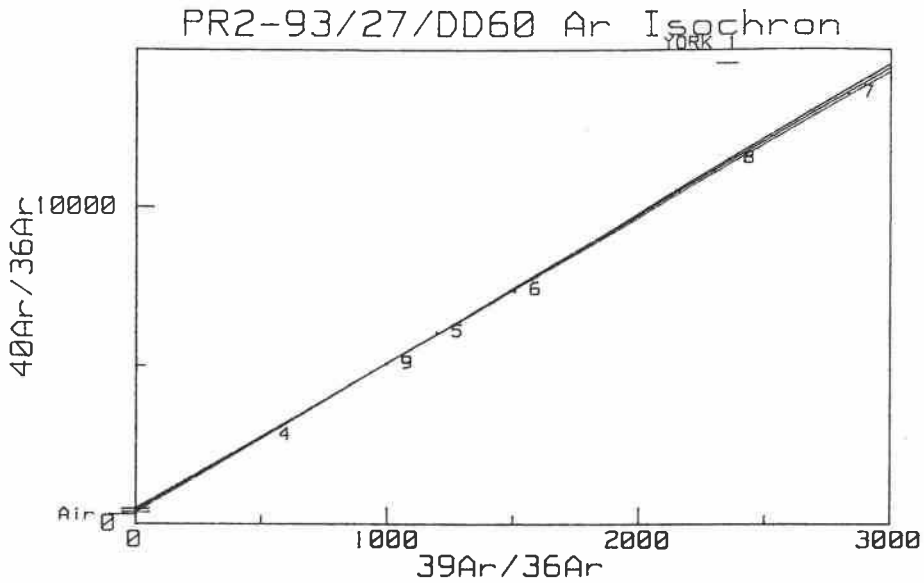

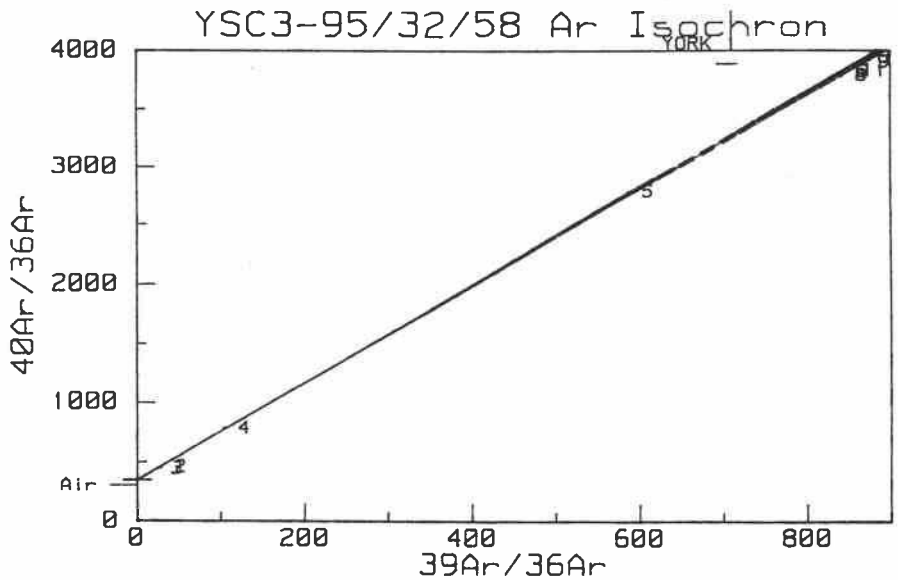

Appendix C. Electron microprobe analyses of feldspar compositions from ash-flow tuffs.

Pacific Creek

	YPC 95.3c	YPC 95.3r	YPC 95.1r	YPC 95.1c	YPC 95.2r	YPC 95.2c	YPC 95.4r	YPC 95.4c	YPC 95.5c	YPC 95.5r
SiO_2	61.902	60.935	64.378	644.431	61.017	64.692	64.987	64.969	62.241	59.24
Al_2O_3	23.726	24.805	18.048	18	21.863	18.152	17.563	17.481	19.347	19.458
Fe_2O_3	0.1576	0.2362	0.4306	0.5582	0.5754	0.4177	0.1533	0.0438	0.1469	0.1463
MgO	0.0025	0.0093	0.0025	0.0024	0.0444	0.0024	0.01	0.0025	0.0025	0.0025
CaO	5.0258	6.1112	0.6781	0.6457	3.9679	0.4836	0.2688	0.2444	0.223	0.3884
Na_2O	7.6927	6.9065	1.9448	1.5468	4.7754	1.4067	0.7234	0.5559	2.9145	3.0489
K_2O	1.2747	1.213	12.498	12.968	5.7339	13.628	14.764	15.174	10.536	9.9418
TiO_2	0.0165	0.0112	0.0827	0.1161	0.0282	0.1759	0.0032	0.0103	0.0012	0.0012
BaO	0.0219	0.07	0.2481	0.2023	0.363	0.1175	0.1412	0.0596	3.9529	4.7329

Lost Creek Tuff

	YLC 1-95.6.c	YLC 1-95.6.r	YLC 1-95.7c	YLC 1-95.7r	YLC 1-95.9.c	YLC 1-95.9r	YLC 1-95.12r	YLC 1-95.12c	YLC 1-95.1c	YLC 1-95.1c
SiO_2	64.891	65.245	64.457	63.871	61.929	63.902	64.897	65.709	61.036	62.818
Al_2O_3	19.177	19.313	18.996	18.797	19.506	19.676	18.274	18.362	19.733	19.283
Fe_2O_3	0.0803	0.0968	0.084	0.1279	0.1254	0.0012	0.3962	0.1315	0.0816	0.12
MgO	0.0025	0.0105	0.0025	0.0025	0.0025	0.0026	0.085	0.0025	0.0025	0.0027
CaO	0.3008	0.2584	0.3483	0.3461	0.4541	0.4946	0.5383	0.6027	0.4071	0.3767
Na_2O	3.1797	3.0631	3.3424	3.4328	3.108	3.1069	2.0531	2.4155	2.9685	2.9455
K_2O	11.658	12.058	11.452	11.442	10.906	11.321	12.464	12.266	10.574	11.215
TiO_2	0.0119	0.0076	0.0023	0.015	0.0012	0.0012	0.0167	0.0167	0.0012	0.0012
BaO	0.3779	0.2413	0.1459	0.0849	2.0803	1.2183	0.0773	0.0538	3.1719	1.9915

Slough Creek Lamar River

	YSC 3-95.1c	YSC 3-95.1r	YSC 3-95.3c	YSC 3-95.3r	YSC 3-95.4c	YSC 3-95.4r	YSC 3-95.2c	YSC 3-95.2r	YSC 4-95.5c	YSC 3-95.5r
SiO_2	58.584	57.871	57.92	57.462	57.228	58.517	58.209	58.801	58.225	55.456
Al_2O_3	25.499	25.759	25.334	25.409	25.888	25.481	26.028	25.012	25.686	27.007
Fe_2O_3	0.2489	0.2561	0.2617	0.2653	0.2963	0.2909	0.2873	0.3019	0.4043	0.2689
MgO	0.0135	0.0195	0.0076	0.0207	0.0079	0.0025	0.039	0.0086	0.0344	0.0148
CaO	7.2732	7.539	7.3965	7.5488	7.8797	7.0747	7.7166	6.7984	7.4613	9.0938
Na_2O	6.6182	6.4056	6.5466	6.7266	6.367	6.3441	6.0919	6.0737	6.4032	5.7452
K_2O	0.9983	0.8657	0.9311	0.9085	0.8903	1.0023	0.912	1.7241	0.9213	0.6332
TiO_2	0.0059	0.0012	0.0038	0.0012	0.0155	0.0091	0.0131	0.0012	0.0142	0.0121
BaO	0.2077	0.2437	0.2043	0.2304	0.2618	0.3294	0.2225	0.14	0.2054	0.125

Appendix C (Continued). Electron microprobe analyses of feldspar compositions from ash-flow tuffs.

Slough Creek Lamar River (continued)

	YSC 3-95.20c	YSC 3-95.20r	YSC 3-95.6c	YSC 3-95.6r	YSC 3-95.7c	YSC 3-95.7r
SiO_2	55.154	59.103	54.047	55.296	57.302	57.638
Al_2O_3	27.108	26.015	27.512	26.045	25.059	26.29
Fe_2O_3	0.2982	0.2416	0.3292	0.2908	0.3001	0.2141
MgO	0.0044	0.0109	0.0325	0.0097	0.0165	0.0243
CaO	8.8469	7.3621	9.9396	8.5271	7.3709	8.1673
Na_2O	5.7982	6.2611	5.5219	6.3206	6.3362	6.0158
K_2O	0.638	0.8988	0.5462	0.698	1.0526	0.735
TiO_2	0.0114	0.0119	0.0241	0.0085	0.0089	0.0038
BaO	0.1113	0.2017	0.1144	0.1923	0.1949	0.1102

Slough Creek Hildan

	YSC 6-95.24r	YSC 6-95.24c	YSC 6-95.4A.r	YSC 3-95.4A.c	YSC 6-95.r	YSC 6-95.c	YSC 6-95.5r	YSC 6-95.5c	YSC 6-95.3r	YSC 6-95.3c
SiO_2	64.369	64.638	64.264	63.882	64.593	63.896	64.874	64.51	64.623	64.367
Al_2O_3	19.046	19.037	19.163	19.315	19.024	18.809	19.524	19.292	19.044	64.367
Fe_2O_3	0.0381	0.0572	0.0742	0.0933	0.1144	0.1029	0.118	0.1124	0.122	0.1201
MgO	0.0025	0.0025	0.0025	0.0066	0.0025	0.012	0.0025	0.0025	0.0025	0.0025
CaO	0.37	0.383	0.3448	0.3739	0.3946	0.3872	0.4632	0.3836	0.3262	0.3637
Na_2O	3.6539	3.9038	3.5591	3.6949	3.9222	3.6552	3.7339	3.6148	3.6992	3.6061
K_2O	20.56	10.646	10.659	10.673	0.3946	10.871	10.198	10.685	10.636	0.889
TiO_2	0.0137	0.013	0.0084	0.0278	0.0069	0.1029	0.0167	0.0144	0.0015	0.0012
BaO	0.4947	0.4048	0.9489	1.0348	0.382	0.3709	0.9973	0.807	0.2853	0.4424

	YSC 6-95.2r	YSC 6-95.2c	YSC 6-95.1c	YSC 6-95.1r
SiO_2	64.695	64.788	64.305	65.457
Al_2O_3	19.294	19.219	19.051	19.379
Fe_2O_3	0.1487	0.0514	0.0343	0.1068
MgO	0.0025	0.0224	0.0025	0.0025
CaO	0.4957	0.4258	0.4387	0.4431
Na_2O	4.1645	3.5592	3.9332	3.9625
K_2O	10.214	11.094	10.636	10.091
TiO_2	0.0012	0.019	0.008	0.0015
BaO	0.4215	0.5323	0.41	0.3728

Appendix C (Continued). Electron microprobe analyses of feldspar compositions from ash-flow tuffs.

Slough Creek Aslan

	YSC 4-95.4c	YSC 4-95.4r	YSC 5-95.2r	YSC 5-95.2c	YSC 5-95.12c	YSC 5-95.12r	YSC 5-95.3r	YSC 5-95.3c	YSC 5-95.5r	YSC 5-95.6r
SiO_2	63.766	64.023	64.678	64.103	64.775	64.827	64.508	63.768	64.523	63.774
Al_2O_3	19.052	19.248	19.427	19.424	19.303	19.449	18.77	18.925	18.523	18.524
Fe_2O_3	0.1428	0.1808	0.1371	0.1028	0.0877	0.0991	0.0362	0.1353	0.0781	0.0838
MgO	0.0025	0.0025	0.0143	0.017	0.0025	0.0025	0.0038	0.0077	0.0025	0.0033
CaO	0.4056	0.4035	0.432	0.3903	0.4428	0.4625	0.369	0.3689	0.3515	0.3807
Na_2O	3.6081	3.6399	3.5602	3.5782	3.6996	3.6132	4.0052	3.729	3.6798	4.2152
K_2O	10.685	10.574	10.899	10.862	10.944	10.676	10.497	10.951	11.063	11.119
TiO_2	0.016	0.0106	0.0243	0.0243	0.0202	10.676	0.0122	0.0339	0.0251	0.0076
BaO	0.9257	1.1051	0.9385	1.0682	0.4428	0.533	0.3473	0.4195	0.3825	0.4407

	YSC 5-95.6c
SiO_2	65.068
Al_2O_3	19.267
Fe_2O_3	0.0572
MgO	0.0033
CaO	0.3735
Na_2O	3.6972
K_2O	10.992
TiO_2	0.0427
BaO	0.5175

Appendix D: Petrographic description of analyzed samples.

Hyalite Volcanic Center Samples

Presented in stratigraphic order, oldest to youngest:

GHP2-93: (Shoshonite Flow) Fine-grained seriate porphyritic, glomerocrysts of Ti-magnetite, augite(5%) and hypersthene with corroded or oxidized rims (<3%)± plagioclase in hypocrystalline groundmass of plagioclase, sanidine and opaque oxides. Plagioclase phenocrysts (10%) consist of two populations, 2-5mm An_{60-70} with sieve-texture interiors, and smaller (≤ 1mm) euhedral An_{50} plagioclase.

HGB12-95: (Shoshonite Flow) Fine-grained with (1-2 mm) twinned subhedral augite phenocrysts (15%) in holocrystalline groundmass of plagioclase, with small (<1 mm) phenocrysts of olivine (<5%).

HGB13-95: (Shoshonite Flow) Fine-grained with (1-2 mm) twinned euhedral augite phenocrysts (15%) in holocrystalline groundmass of plagioclase, with small (<1 mm) phenocrysts of iddingsitized olivine (<5%). Rare (<1%) hypersthene rimmed with augite.

HGB14-95: (Shoshonite Flow) Fine-grained with (2-3 mm) anhedral augite phenocrysts (≤10%) in holocrystalline groundmass of Ti-magnetite, microlitic plagioclase, with small (<1 mm) phenocrysts of olivine altered to bowlingite (<5%). Rare (<5.

HGB15-95: (Shoshonite Flow) Fine-grained with (1-5 mm) anhedral augite phenocrysts (12%) plagioclase (5%) with sericitic alteration in hypocrystalline groundmass of Ti-magnetite, microlitic plagioclase, with small (<1 mm) phenocrysts of olivine altered to bowlingite (<5%).

HGB18-95: (Shoshonite Flow) Fine-grained, sparsely porphyritic with augite (5%) glomerocrysts of augite, hypersthene rimmed with cpx, and plagioclase (5%) in a hypocrystalline groundmass containing plagioclase an Ti-magnetite.

HGB19-95: (Shoshonite Flow) Fine-grained, sparsely porphyritic with 4-10 mm phenocrysts of anhedral augite (5%) and hypersthene (<5%), together with plagioclase with corroded rims (5%) in a hypohyaline groundmass containing plagioclase.

HGB20-95: (Shoshonite Flow) Fine-grained, sparsely porphyritic with augite (1-2%) hypersthene (1-2%), and plagioclase (5%) with some calcite replacement in a hypohyaline groundmass containing plagioclase an Ti-magnetite.

HGB21-95 (Shoshonite dike, 10 cm from margin) Very-fine-grained, with 1.0 -0.5 mm trachytic plagioclase laths and augite, calcite replacement of olivine and some clinopyroxene.

HGB9-95: (Shoshonite Flow) Fine-to medium-grained with glomerocrysts of augite and plagioclase with inclusion-rich rims in a cryptocrystalline groundmass.

HGB7-95: (Shoshonite Flow) Fine-grained with a hypohyaline groundmass, and pilotaxitic phenocrysts of anhedral plagioclase (10%) and augite (5%).

HGB6-95: (Shoshonite Flow) Fine-grained with a hypohyaline groundmass, and pilotaxitic phenocrysts of anhedral plagioclase (5-10%) and augite (5%).

HGB3-95: (Shoshonite flow with vesicular segregations) Fine-grained with glomerocrysts of augite and magnetite and sparse (1-2%) hypersthene in a holocrystalline groundmass of feldspars with skeletal sanidine (?) and anhedral augite.

HGSC7-95: (Dike) Microcrystalline with 5% phenocrysts of hypersthene and resorbed plagioclase in a felty groundmass of magnetite and feldspars.

Ishawooa Volcanic Center Samples
(Presented in stratigraphic order:)

HISH50B-95 (Absarokite Flow) Sparsely porphyritic with euhedral olivine with iddingsite (1-2%) with inclusions of euhedral apatite, euhedral augite (5-7%), and apatite phenocrysts (1-2%) in a groundmass of sanidine, plagioclase and spinel.

HISH50-95 (Shoshonite Flow) Porphyritic with euhedral olivine with iddingsite (5-7%) with inclusions of euhedral apatite, euhedral augite (10%), and apatite phenocrysts (3%) in a groundmass of sanidine, plagioclase and spinel.

HISH49-95 (Shoshonite Flow) Euhedral aegerine-augite (5%), and apatite phenocrysts (1-2%) in a groundmass of sanidine, plagioclase and spinel.

HISH47-95 (Shoshonite Flow) Euhedral aegerine-augite (<5%), and apatite phenocrysts (1-2%) in a groundmass of sanidine, plagioclase and spinel.

HISH46-95 (Shoshonite Flow) Euhedral aegerine-augite (<5%), some replaced by opaque oxides, and apatite phenocrysts (1-2%) in a groundmass of sanidine, plagioclase and spinel.

HISH9-95 (Absarokite Flow)Porphyritic, with phenocrysts from 0.5 to 0.8 mm, of olivine (10%) commonly replaced by calcite and opaque oxides, and augite (8-10%) in a holocrystalline groundmass of sanidine and plagioclase.

HISH8-95 (Shoshonite Flow) Sparsely porphyritic, with augite (5-8%) and opx? rimmed with augite (<1%) in a holocrystalline microlitic groundmass of opaque oxides and feldspar.

HISH7-95 (Dike) Sparsely porphyritic, containing plagioclase (5-7%) with secondary growth rims, enstatite phenocrysts rimmed or as inclusions in augite (10%), groundmass augite and altered olivine phenocrysts in a fine-grained trachytic groundmass.

HISH6-95 (Shallow intrusion) Porphyritic granular texture, containing plagioclase (25-30%) quartz (5%), amphibole (10-15%) and biotite (7-10%) with chlorite alteration.

HISH29-95 (Shallow intrusion) Glassy and sparsely porphyritic with 4-6 mm olivine phenocrysts (<5%) orthopyroxene (enstatite?) with augite rims, secondary phenocrysts of augite and biotite, and rare (<1%) amphibole.

HISH36-95 (Shallow intrusion) Porphyritic granular texture, containing plagioclase (25-30%) quartz (<2%), amphibole (15-18%) and biotite (10%) with chlorite alteration, amphibole and pyroxenite phenocrysts common.

HISH37-95 (Shallow intrusion) Porphyritic granular texture, containing plagioclase (25-30%) quartz (5%), amphibole (10-15%) and biotite (7-10%) with chlorite alteration, commonly contains pyroxenite and rare granulite xenoliths

Rampart Volcanic Center

(Presented in stratigraphic order:)

HPt1-96 (Shoshonite flow) Porphyritic vitrophyre with anhedral to skeletal plagioclase laths 5-15 mm long (8-10%), subhedral augite (5%) and sparse euhedral olivine (3 %) and apatite (2-3%) in red-brown glass.

HPt2-96 (Absarokite Flow) Porphyritic with euhedral olivine with iddingsite (5-7%) with inclusions of euhedral apatite, euhedral augite (12%), and apatite phenocrysts (1-2%) in a groundmass of sanidine, plagioclase and spinel.

HPt3-95 (Basaltic Andesite Flow) Porphyritic anhedral augite (10%), plagioclase with calcic rims, embayed and skeletal orthopyroxene (enstatite?, < 5%) and olivine altered to bowlingite (<5%) with groundmass phases of anhedral augite and amphibole (<1%) in a holocystalline groundmass of plagioclase and spinel.

HPt4-95 (Flow) Porphyritic with euhedral augite (15%), orthopyroxene (5%), some with incomplete rims of augite in a hypohyaline trachytic groundmass of plagioclase and spinel.

HPt6-95 Crystal-rich dacitic tuff with phenocrysts of plagioclase (30%), hornblende (20%) and quartz (5%), minor cpx (<1 %) in oxidized, densely welded glass.

Crandall Volcanic Center
(Presented in stratigraphic order:)

HM9-95 (Flow) Fine-grained with 1-2 mm inclusion rich augite phenocrysts in trachytic to hypocrystalline groundmass of magnetite and feldspars.

HM13-95 (Flow) Fine-grained with 1 mm augite phenocrysts (10%) in hypocrystalline groundmass of magnetite and feldspars.

HM12-95 (Flow) Fine-grained with 1-2 mm euhedral augite phenocrysts (15%) in trachytic to hypocrystalline groundmass of magnetite and feldspars.

HM8-95 (Flow) Fine-grained, with inclusion-rich euhedral augite, 1-5 mm An_{60} plagioclase with skeletal interiors, and small abundant anhedral olivine in a holocrystalline microlitic groundmass.

HM17b-95 Fine-grained crystal-poor tuff, with recrystallized texture in thin section, 2-3 mm plagioclase and sanidine (1-2 %), 2-4 mm amphibole (2-3%) and glomerocrysts of augite and plagioclase (1-2%).

HM5-94 (Flow) Porphyritic, with augite glomerocrysts (8%) in granular groundmass of plagioclase and glass.

HM6-94 (Ring Dike) Intersertal to trachytic plagioclase-rich groundmass with partially recrystallized anhedral augite.

HM7-94 (Ring Dike) Plagioclase 2-5 mm, An_{70} (5%) and anhedral augite (<5%) in plagioclase-rich groundmass.

HM2-94 (Flow) Fine-grained with 1 mm augite phenocrysts (10%) and small euhedral olivine (<5%) in a hypocrystalline groundmass of plagioclase and magnetite.

HM18-94 (Flow) Phenocrysts consist of zoned augite (10%) and anhedral olivine(1%), in a holocystalline pilotaxitic groundmass of plagioclase and magnetite.

HM15-94 (Flow) Subhedral augite (10%) in hypohyaline groundmass with An_{60} plagioclase in a trachytic texture.

HM11-95 (Dike) Anhedral to skeletal An50 plagioclase (10%, 0.5-1.0 cm), anhedral augite (<5%) in holocrystalline groundmass of plagioclase and magnetite.

HM1-94 (Shallow intrusion) Amygdaloidal with holocrystalline recrystallized groundmass, plagioclase ghosts, anhedral augite, alkali feldspar replacing leucite (?), and 2-5 mm phenocrysts of amphibole.

HM9-94 (Dike) Phenocrysts consist of augite , olivine replaced by serpentine, small anhedral orthopyroxene, and complexly zoned plagioclase with calcic rims, in a holocystalline groundmass of plagioclase and magnetite.

HM11-94 (Dike) Phenocrysts large anhedral skeletal plagioclase (2-4 mm), augite , and olivine replaced by serpentine, in a granular groundmass of plagioclase and magnetite.

HM18-95 (Dike) Ophitic to intersertal texture with euhedral phenocrysts of augite (12%) and plagioclase (5%)

HM19-95 (Sill) Euhedral phenocrysts of augite (8%) and large plagioclase phenocrysts (1-3cm) plagioclase (10%) with an intersertal texture with glomerocrysts of cpx and olivine.

HM22-95 (Dike) Seriate porphyritic with euhedral augite 1-2 mm and skeletal laths of plagioclase in granular groundmass.

Appendix E. Pyroxene compositions from electron microprobe analyses.

Clinopyroxene sample	SiO2	TiO2	Al2O3	MgO	Fe2O3	CaO	Na2O	MnO	CrO
BHMcpx1	48.84	1.59	8.67	13.37	8.2	19.26	1.3	0.15	0.09
BHMcpx2	48.63	1.64	8.98	13.18	8.19	19.11	1.35	0.12	0.08
BHM1cpx3	48.54	1.66	8.94	12.62	7.41	20.55	1.36	0.15	0.03
BHM1cpx4	48.27	1.6	9.09	13.03	8.19	19.22	1.28	0.13	0.07
BHMcpx5	48.95	1.49	8.63	13.29	8.06	19.6	1.17	0.16	0.08
BHM1cpx7	48.71	1.66	8.37	12.6	7.54	21.66	1.21	0.12	0.11
BHM1cpx8	48.85	1.59	8.21	12.73	7.31	21.06	1.31	0.13	0.16
ISH50Bcpx1	50.25	0.93	3.87	14.16	8.02	22.23	0.58	0.2	0.04
ISH50Bcpx2	50.5	0.96	4.08	14.11	8.1	22.29	0.5	0.17	0.03
ISH50Bcpx3	50.4	0.97	3.9	14.19	8.16	22.21	0.53	0.17	0.02
ISH50Bcpx4	49.93	0.96	4.15	14.13	7.95	22.01	0.54	0.19	0.02
ISH50Bcpx5	50.46	0.93	3.77	14.31	8.04	22.03	0.51	0.18	0.05
ISH50Bcpx6	49.95	0.98	4.18	14.07	8.16	22.09	0.51	0.19	0.1
ISH50Bcpx7	49.86	1.07	4.29	13.91	8.41	22.45	0.54	0.18	0.04
ISH50Bcpx8	50.44	0.98	4.01	14.11	8.3	22.15	0.51	0.21	0.03
ISH50Bcpx9	50.82	0.93	3.36	14.08	8.43	22.13	0.55	0.22	0
HPT2cpx1	50.02	0.93	3.83	14.05	8.21	21.94	0.55	0.24	0.06
HPT2cpx2	50.5	0.78	3.53	14.12	8.17	21.79	0.59	0.23	0.03
HPT2cpx3	49.79	0.91	3.56	14.18	8.2	21.98	0.57	0.23	0.04
HPT2cpx4	50.87	0.82	3.28	14.19	7.95	22.24	0.54	0.19	0.02
HPT2cpx5	49.88	0.98	4.42	13.94	8.31	21.97	0.57	0.2	0.03
HPT2cpx6	48.92	1.12	4.74	13.46	8.53	22.05	0.55	0.24	0.04
HPT2cpx7	49.97	0.99	3.82	13.84	8.05	22.08	0.56	0.24	0.03
HPT2cpx8	49.67	0.95	3.89	13.77	8.13	22.1	0.54	0.24	0.04
HPT2cpx9	50.3	0.93	3.93	13.9	8.33	21.89	0.56	0.18	0.01
HPT2cpx10	50.35	0.91	3.9	13.91	8.23	21.91	0.55	0.17	0.04
HPT2cpx11	50.35	0.94	4.09	13.89	8.26	21.92	0.56	0.24	0.02
HPT1cpx1	49.18	1.03	4.21	14.11	7.84	22.38	0.48	0.21	0
HPT1cpx2	48.46	1.27	4.98	13.44	8.32	22.54	0.48	0.24	0.07
HPT1cpx3	49.74	1.02	4.29	13.91	7.9	22.28	0.47	0.2	0
HPT1cpx4	48.19	1.38	5.36	13.04	8.53	22.31	0.5	0.22	0
HM2-94cpx1	47.84	0.92	4.76	13.47	7.79	22.48	0.41	0.17	0.17
HM2-94cpx2	49.56	0.74	4.3	14.4	6.12	23	0.38	0.1	0.2
HM19cpx1	51.79	0.92	2.77	15.56	8.56	20.95	0.34	0.23	0.15
HM19cpx2	51.46	0.92	2.6	15.6	7.97	21.36	0.31	0.24	0.14
HM19cpx3	51.34	0.94	2.83	15.5	8.1	21.22	0.32	0.2	0.19
HM19cpx4	50.52	0.95	2.91	15.63	8.6	20.74	0.34	0.2	0.16
HM19cpx5	51.07	0.95	2.82	15.65	8.18	21.41	0.26	0.22	0.16

Appendix E (Continued). Pyroxene compositions from electron microprobe analyses.

Clinopyroxene sample	SiO2	TiO2	Al2O3	MgO	Fe2O3	CaO	Na2O	MnO	CrO
HM11cpx1	50.91	0.76	2.93	15.81	8.04	20.35	0.32	0.17	0.21
HM11cpx2	51.66	0.7	2.57	16.02	7.64	20.79	0.3	0.16	0.14
HM11cpx3	51.68	0.69	2.43	16	7.97	20.47	0.32	0.17	0.12
HM11cpx4	51.44	0.66	2.59	15.92	7.97	20.44	0.34	0.18	0.12
HM11cpx5	51.52	0.74	2.68	15.86	8.36	20.21	0.32	0.19	0.12
HM11cpx6	51.37	0.78	2.66	15.88	9.01	19.7	0.44	0.24	0.9
HM11cpx7	51.7	0.69	2.46	16.07	8.2	20.22	0.33	0.16	0.9
HM11cpx8	51.34	0.75	2.64	15.81	8.26	20.39	0.34	0.16	0.15
HM11cpx9	50.98	0.82	3.31	15.58	9.4	19.18	0.46	0.25	0.08
HM11cpx10	51.47	0.72	2.53	15.91	8.56	20	0.34	0.23	0.1
HM11cpx11	51.37	0.75	2.9	15.77	7.85	20.6	0.33	0.19	0.18
HM11cpx12	50.54	0.81	3.25	15.84	8.36	19.43	0.32	0.21	0.13
HM11cpx13	50.74	0.67	2.55	15.98	8.09	20.14	0.33	0.19	0.17
HM11cpx14	50.48	0.78	2.52	15.27	9.87	19.07	0.5	0.23	0.9
HM11cpx15	50.32	0.69	2.7	15.21	10.15	18.49	0.55	0.27	0.04
HM11cpx16	49.92	0.85	3.24	15.03	10.39	18.32	0.57	0.24	0.07
HBG21cpx1	50.91	0.73	3.27	14.89	10.94	18.96	0.43	0.3	0.04
HBG21cpx2	50.72	0.81	3.97	15.29	9.74	19.44	0.34	0.16	0.05
HBG21cpx3	51	0.63	2.44	14.56	11.9	18.28	0.39	0.34	0.05
HBG21cpx4	50.35	0.76	3.02	14.81	9.8	20.52	0.27	0.25	0.06
HBG21cpx5	50.72	0.65	2.46	15.48	9.85	18.92	0.26	0.26	0.04
HBG21cpx6	49.69	0.97	3.31	14.51	10.32	19.53	0.28	0.19	0.01
HBG21cpx7	49.91	1.16	2.93	14.04	11.37	19.22	0.35	0.29	0.01
HGB13cpx1	50.35	0.78	4.25	14.49	11.33	18.62	0.42	0.25	0.07
HGB13cpx2	50.88	0.57	3.78	14.85	9.5	19.83	0.5	0.28	0.14
HGB13cpx3	51.51	0.45	2.39	13.59	11.84	19.87	0.46	0.39	0
HGB6cpx1	51.11	0.62	2.99	14.47	12.21	18.72	0.46	0.28	0.02
HGB6cpx2	50.76	0.66	2.78	14.49	11.99	18.75	0.43	0.34	0.02
HGB6opx1	52.4	0.35	1.19	20.97	24.19	1.77	0.04	0.55	0.03
HGB6opx2	53.73	0.26	0.84	23.52	20.85	1.75	0.03	0.47	0
HGB6opx3	52.71	0.31	0.95	20.58	24.45	1.96	0.05	0.64	0
ISH29cpx1	53.19	0.25	3.16	16.35	6.3	20.7	0.68	0.09	0.32
ISH29cpx2	52.65	0.47	2.26	16.11	8.42	20.91	0.37	0.2	0.04
ISH29cpx3	54.61	0.21	2.03	17.69	6.77	20.11	0.36	0.21	0.21
ISH29cpx4	52.71	0.4	3.69	16.46	6.57	21.02	0.42	0.1	0.37
ISH29opx10	55.55	0.14	2.51	30.07	12.77	1.14	0.01	0.14	0.18
ISH29opx11	55.65	0.13	2.28	30.24	12.87	1.04	0	0.21	0.07
Orthopyroxene									
ISHopx1	55.43	0.19	0.85	28.02	15.52	1.68	0	0.28	0.01
ISHopx2	54.43	0.34	1.63	27.68	15.89	1.86	0	0.32	0.02
ISHopx3	52.84	0.07	3.4	26.11	18.43	0.34	0	0.19	0.31
ISHopx4	54.56	0.05	1.63	26.88	18.08	0.39	0	0.23	0.12
ISHopx5	55.26	0.09	2.08	29.03	14.39	0.99	0.01	0.21	0.15
ISHopx6	55.53	0.1	1.63	29.18	14.65	0.92	0	0.3	0.05
ISHopx7	54.27	0.1	2.16	27.05	17.22	0.76	0.01	0.37	0.05
ISHopx8	53.51	0.04	3.23	26.77	17.43	0.46	0.01	0.38	0.03
ISHopx9	56.34	0.09	1.1	30.66	12.75	1	0	0.23	0.12

Appendix F: AFC Calculations -
For Basanite and Phlogopite:

Element	Co bas	F	f	CA	DOl	Dcpx	DMg	BulkD	r	CL/Co	CL
Rb	30.6	0.95	1.053	3869	0.0049	0.048	0	0.0529	0.1	1.8382	56.25
Sr	996	0.95	1.053	194	0.0007	0.002	0	0.0028	0.1	1.0538	1050
Ba	594	0.95	1.053	5189	0.0005	0.001	0	0.002	0.1	1.1038	655.7
La	49.3	0.95	1.053	7.7	0.0003	0.001	0	0.0013	0.1	1.0535	51.94
Zr	286	0.95	1.053	7	0.0006	0.002	0.02	0.0224	0.1	1.0528	301.1

Element	Co	F	f	CA	DOl	Dcpx	DMg	BulkD	r	CL/Co	CL
Rb	56	0.95	1.053	3869	0.0049	0.048	0	0.0529	0.1	1.4819	82.99
Sr	1050	0.95	1.053	194	0.0007	0.002	0	0.0028	0.1	1.0537	1106
Ba	656	0.95	1.053	5189	0.0005	0.001	0	0.002	0.1	1.099	720.9
La	52	0.95	1.053	7.7	0.0003	0.001	0	0.0013	0.1	1.0535	54.78
Zr	301	0.95	1.053	7	0.0006	0.002	0.02	0.0224	0.1	1.0528	316.9

Element	Co	F	f	CA	DOl	Dcpx	DMg	BulkD	r	CL/Co	CL
Rb	83	0.95	1.053	3869	0.0049	0.048	0	0.0529	0.1	1.3423	111.4
Sr	1106	0.95	1.053	194	0.0007	0.002	0	0.0028	0.1	1.0537	1165
Ba	721	0.95	1.053	5189	0.0005	0.001	0	0.002	0.1	1.0948	789.4
La	55	0.95	1.053	7.7	0.0003	0.001	0	0.0013	0.1	1.0535	57.94
Zr	317	0.95	1.053	7	0.0006	0.002	0.02	0.0224	0.1	1.0528	333.7

Element	Co	F	f	CA	DOl	Dcpx	DMg	BulkD	r	CL/Co	CL
Rb	111.4	0.95	1.053	3869	0.0049	0.048	0	0.0529	0.1	1.2684	141.3
Sr	1165	0.95	1.053	194	0.0007	0.002	0	0.0028	0.1	1.0536	1227
Ba	789	0.95	1.053	5189	0.0005	0.001	0	0.002	0.1	1.0912	860.9
La	58	0.95	1.053	7.7	0.0003	0.001	0	0.0013	0.1	1.0534	61.1
Zr	333	0.95	1.053	7	0.0006	0.002	0.02	0.0224	0.1	1.0528	350.6

Element	Co	F	f	CA	DOl	Dcpx	DMg	BulkD	r	CL/Co	CL
Rb	141	0.95	1.053	3869	0.0049	0.048	0	0.0529	0.1	1.2231	172.5
Sr	1227	0.95	1.053	194	0.0007	0.002	0	0.0028	0.1	1.0536	1293
Ba	861	0.95	1.053	5189	0.0005	0.001	0	0.002	0.1	1.088	936.7
La	61	0.95	1.053	7.7	0.0003	0.001	0	0.0013	0.1	1.0534	64.26
Zr	350	0.95	1.053	7	0.0006	0.002	0.02	0.0224	0.1	1.0528	368.5

APPENDIX F: AFC Calculations (Continued)
OIB and Phlogopite

element	Co	F	f	CA	DOI	Dcpx	DMg	BulkD	r	CL/Co	CL
Rb	29.4	0.95	1.0526	3869	0.0049	0.048	0	0.0529	0.1	1.8703	54.986
Sr	718	0.95	1.0526	194	0.0007	0.0021	0	0.0028	0.1	1.0542	756.93
Ba	511	0.95	1.0526	5189	0.000495	0.001485	0	0.00198	0.1	1.1121	568.31
La	45	0.95	1.0526	7.7	0.000335	0.001005	0	0.00134	0.1	1.0536	47.414
Zr	255	0.95	1.0526	7	0.0006	0.0018	0	0.0224	0.1	1.0528	268.46

Element	Co	F	f	CA	DOI	Dcpx	DMg	BulkD	r	CL/Co	CL
Rb	55	0.95	1.0526	3869	0.0049	0.048	0	0.0529	0.1	1.4897	81.933
Sr	757	0.95	1.0526	194	0.0007	0.0021	0	0.0028	0.1	1.0541	797.98
Ba	568	0.95	1.0526	5189	0.000495	0.001485	0	0.00198	0.1	1.1062	628.31
La	51	0.95	1.0526	7.7	0.000335	0.001005	0	0.00134	0.1	1.0535	53.729
Zr	268	0.95	1.0526	7	0.0006	0.0018	0	0.0224	0.1	1.0528	282.15

Element	Co	F	f	CA	DOI	Dcpx	DMg	BulkD	r	CL/Co	CL
Rb	82	0.95	1.0526	3869	0.0049	0.048	0	0.0529	0.1	1.3458	110.35
Sr	798	0.95	1.0526	194	0.0007	0.0021	0	0.0028	0.1	1.0541	841.14
Ba	628	0.95	1.0526	5189	0.000495	0.001485	0	0.00198	0.1	1.1011	691.46
La	54	0.95	1.0526	7.7	0.000335	0.001005	0	0.00134	0.1	1.0535	56.887
Zr	282	0.95	1.0526	7	0.0006	0.0018	0	0.0224	0.1	1.0528	296.88

Element	Co	F	f	CA	DOI	Dcpx	DMg	BulkD	r	CL/Co	CL
Rb	110	0.95	1.0526	3869	0.0049	0.048	0	0.0529	0.1	1.2712	139.83
Sr	841	0.95	1.0526	194	0.0007	0.0021	0	0.0028	0.1	1.054	886.4
Ba	691	0.95	1.0526	5189	0.000495	0.001485	0	0.00198	0.1	1.0966	757.78
La	57	0.95	1.0526	7.7	0.000335	0.001005	0	0.00134	0.1	1.0534	60.045
Zr	297	0.95	1.0526	7	0.0006	0.0018	0	0.0224	0.1	1.0528	312.67

Element	Co	F	f	CA	DOI	Dcpx	DMg	BulkD	r	CL/Co	CL
Rb	140	0.95	1.0526	3869	0.0049	0.048	0	0.0529	0.1	1.2243	171.41
Sr	886	0.95	1.0526	194	0.0007	0.0021	0	0.0028	0.1	1.0539	933.77
Ba	758	0.95	1.0526	5189	0.000495	0.001485	0	0.00198	0.1	1.0928	828.31
La	60	0.95	1.0526	7.7	0.000335	0.001005	0	0.00134	0.1	1.0534	63.203
Zr	313	0.95	1.0526	7	0.0006	0.0018	0	0.0224	0.1	1.0528	329.52

APPENDIX F: AFC Calculations (Continued)
Basanite and lower crust (mafic granulite)

LC-88-3-5

element	Co	F	f	CA	Dplag	DOl	Dcpx	DMg	BulkD	r	CL/Co	CL	HGB13
Rb	30.6	1	1.03	18.8	0.071	0.01	0.32	0	0.082	0.8	1.1587	35.455	40.3
Sr	996	1	0.76	430	1.83	0.014	0.014	0	1.283	0.8	0.8348	831.47	594
Ba	594	1	1.01	313	0.23	0.01	0.01	0	0.162	0.8	1.1183	664.27	1360
Th	5.19	1	1.05	0.42	0.01	0	0.03	0	0.01	0.8	1.067	5.5375	4.47
U	1.63	1	1.05	0.05	0.01	0.002	0.04	0	0.011	0.8	1.0561	1.7214	1.02
La	49.3	1	1.02	11	0.19	0.007	0.007	0	0.134	0.8	1.0632	52.418	31.5
Nd	43.6	1	0.93	14	0.09	0.006	0.31	2	0.494	0.8	0.9908	43.197	27.5
Sm	8.85	1	0.97	3.9	0.072	0.007	0.5	1	0.301	0.8	1.0637	9.4142	5.8
Yb	1.81	1	0.97	3.26	0.056	0.049	0.62	1	0.304	0.8	1.3384	2.4226	2.08
Zr	286	1	1.02	202	0.048	0.012	0.012	0.4	0.115	0.8	1.1684	334.17	168
Hf	5.93	1	0.84	2.14	0.051	0.013	0.263	4	0.863	0.8	0.9118	5.407	3.62
element	Co	F	f	CA	Dplag	DOl	Dcpx	DMg	BulkD	r	CL/Co	CL	HGB13
Rb	35.5	1	1.03	18.8	0.071	0.01	0.32	0	0.082	0.8	1.141	40.505	40.3
Sr	831	1	0.76	430	1.83	0.014	0.014	0	1.283	0.8	0.8502	706.48	594
Ba	664	1	1.01	313	0.23	0.01	0.01	0	0.162	0.8	1.1069	734.95	1360
Th	5.5	1	1.05	0.42	0.01	0	0.03	0	0.01	0.8	1.066	5.863	4.47
U	1.7	1	1.05	0.05	0.01	0.002	0.04	0	0.011	0.8	1.0558	1.7949	1.02
La	52.4	1	1.02	11	0.19	0.007	0.007	0	0.134	0.8	1.0605	55.571	31.5
Nd	43	1	0.93	14	0.09	0.006	0.31	2	0.494	0.8	0.9916	42.641	27.5
Sm	9.4	1	0.97	3.9	0.072	0.007	0.5	1	0.301	0.8	1.0585	9.9502	5.8
Yb	2.4	1	0.97	3.26	0.056	0.049	0.62	1	0.304	0.8	1.2488	2.9971	2.08
Zr	334	1	1.02	202	0.048	0.012	0.012	0.4	0.115	0.8	1.1474	383.22	168
Hf	5.4	1	0.84	2.14	0.051	0.013	0.263	4	0.863	0.8	0.9185	4.9598	3.62

En88-11

element	Co	F	f	CA	Dplag	DOl	Dcpx	DMg	BulkD	r	CL/Co	CL	HGB13
Rb	30.6	1	1.03	7.2	0.071	0.01	0.32	0	0.079	0.8	1.0806	33.068	40.3
Sr	996	1	0.78	250	1.83	0.014	0.014	0	1.192	0.8	0.8209	817.64	594
Ba	594	1	1.01	300	0.23	0.01	0.01	0	0.151	0.8	1.1169	663.45	1360
Th	5.19	1	1.05	0.25	0.01	0	0.03	0	0.01	0.8	1.0602	5.5024	4.47
U	1.63	1	1.05	0.3	0.01	0.002	0.04	0	0.011	0.8	1.0885	1.7742	1.02
La	49.3	1	1.02	6.8	0.19	0.007	0.007	0	0.125	0.8	1.0481	51.673	31.5
Nd	43.6	1	0.93	8.4	0.09	0.006	0.31	2	0.49	0.8	0.9665	42.138	27.5
Sm	8.85	1	0.98	2.4	0.072	0.007	0.5	1	0.297	0.8	1.0303	9.1186	5.8
Yb	1.81	1	0.97	2	0.056	0.049	0.62	1	0.301	0.8	1.1983	2.1689	2.08
Zr	286	1	1.02	202	0.048	0.012	0.012	0.4	0.113	0.8	1.1691	334.36	168
Hf	5.93	1	0.84	1.8	0.051	0.013	0.263	4	0.86	0.8	0.9016	5.3462	3.62

element	Co	F	f	CA	Dplag	DOl	Dcpx	DMg	BulkD	r	CL/Co	CL	HGB13
Rb	33	1	1.03	7.2	0.071	0.01	0.32	0	0.079	0.8	1.0771	35.544	40.3
Sr	817	1	0.78	250	1.83	0.014	0.014	0	1.192	0.8	0.8309	678.83	594
Ba	663	1	1.01	300	0.23	0.01	0.01	0	0.151	0.8	1.1061	733.33	1360
Th	5.5	1	1.05	0.25	0.01	0	0.03	0	0.01	0.8	1.0596	5.828	4.47
U	1.8	1	1.05	0.3	0.01	0.002	0.04	0	0.011	0.8	1.0848	1.9527	1.02
La	51.7	1	1.02	6.8	0.19	0.007	0.007	0	0.125	0.8	1.0468	54.12	31.5
Nd	42	1	0.93	8.4	0.09	0.006	0.31	2	0.49	0.8	0.9679	40.653	27.5
Sm	9.1	1	0.98	2.4	0.072	0.007	0.5	1	0.297	0.8	1.0288	9.3624	5.8
Yb	2.2	1	0.97	2	0.056	0.049	0.62	1	0.301	0.8	1.1586	2.5489	2.08
Zr	334	1	1.02	202	0.048	0.012	0.012	0.4	0.113	0.8	1.148	383.45	168
Hf	5.3	1	0.84	1.8	0.051	0.013	0.263	4	0.86	0.8	0.9084	4.8143	3.62

element	Co	F	f	CA	Dplag	DOl	Dcpx	DMg	BulkD	r	CL/Co	CL	HGB13
Rb	36	1	1.03	7.2	0.071	0.01	0.32	0	0.079	0.8	1.0733	38.639	40.3
Sr	678	1	0.78	250	1.83	0.014	0.014	0	1.192	0.8	0.8422	571.05	594
Ba	733	1	1.01	300	0.23	0.01	0.01	0	0.151	0.8	1.0972	804.21	1360
Th	5.8	1	1.05	0.25	0.01	0	0.03	0	0.01	0.8	1.0591	6.143	4.47
U	1.95	1	1.05	0.3	0.01	0.002	0.04	0	0.011	0.8	1.0821	2.1101	1.02
La	54.1	1	1.02	6.8	0.19	0.007	0.007	0	0.125	0.8	1.0456	56.566	31.5
Nd	40.6	1	0.93	8.4	0.09	0.006	0.31	2	0.49	0.8	0.9693	39.353	27.5
Sm	9.36	1	0.98	2.4	0.072	0.007	0.5	1	0.297	0.8	1.0274	9.616	5.8
Yb	2.5	1	0.97	2	0.056	0.049	0.62	1	0.301	0.8	1.1365	2.8413	2.08
Zr	334	1	1.02	202	0.048	0.012	0.012	0.4	0.113	0.8	1.148	383.45	168
Hf	4.8	1	0.84	1.8	0.051	0.013	0.263	4	0.86	0.8	0.915	4.3922	3.62

APPENDIX G: Equations used in calculations.

AFC calculations use the following equation of DePaolo (1981):

$C_L/C_0 = f' + r / (r - 1 + D) \times C_A/C_0 (1 - f')$

C_L = Average concentration of a trace element in a mixed melt
C_0 = Initial concentration in the parental liquid
f' = A function of F (fraction of melt remaining) in AFC
C_A = Concentration of trace element being assimilated from wallrock
D = Bulk distribution coefficient of fractionating assemblage
r = Assimilation rate/ fractionation rate

Binary mixing calculation for basanite (BHM195) and lithospheric mantle end-member HM6A94, using equation of DePaolo (1979a):

$$f = \frac{R^X_A X_A(f) + R^X_B X_B(1-f)}{X_a f + X_B(1-f)}$$

For Nd:

$$\frac{(0.511624)\ 60\ \text{ppm Nd}(0.25) + (0.512784)\ 43.6\ \text{ppm Nd}(0.75)}{(60)(0.25) + (43.6)(0.75)}$$

$^{143}Nd/^{144}Nd = 0.51190$